Etude stratigraphique, pétrographique et diagénétique des grès d'âge Crétacé-Paléogène de la région ouest du bassin du lac Turkana, Kenya. Conséquences sur leurs caractéristiques réservoir et l'évaluation du potentiel pétrolier du nord-ouest du Kenya.

Peter Thuo

université de bretagne occidentale

THÈSE / UNIVERSITÉ DE BRETAGNE OCCIDENTALE
sous le sceau de l'Université européenne de Bretagne

pour obtenir le titre de
DOCTEUR DE L'UNIVERSITÉ DE BRETAGNE OCCIDENTALE
Mention : Géosciences Marines
École Doctorale des Sciences de la Mer

présentée par

Peter Thuo

Préparée à l'Unité Mixte de Recherche 6538
Domaines océaniques
Institut Universitaire Européen de la Mer

Stratigraphic, petrographic and diagenetic evaluation of Cretaceous/Paleogene potential reservoir sandstones of western Turkana, Kenya. Implications on the petroleum potential of northwestern Kenya.

Etude stratigraphique, pétrographique et diagénétique des grès d'âge Crétacé-Paléogène de la région ouest du bassin du lac Turkana, Kenya. Conséquences sur leurs caractéristiques réservoir et l'évaluation du potentiel pétrolier du nord-ouest du Kenya.

Thèse soutenue le 11 décembre 2009
devant le jury composé de :

Hervé Bellon
Professeur, UMR 6538 « Domaines Océaniques », IUEM, Université de Bretagne Occidentale / Examinateur
Sylvie Bourquin
Directeur de Recherche au CNRS, Géosciences Rennes / Examinateur
Martine Buatier
Professeur, Université de Besançon / Rapporteur
Philippe Duringer
Professeur, Université Louis Pasteur, Strasbourg / Rapporteur
Jean-Luc Potdevin
Professeur, Université de Lille 1 / Co-directeur de Thèse
Marina Rabineau
Chargée de Recherche au CNRS, UMR 6538 « Domaines Océaniques », IUEM, Université de Bretagne Occidentale / Examinateur
Jean-Jacques Tiercelin
Directeur de Recherche au CNRS, Géosciences Rennes,
Mathieu Schuster
Chargé de Recherche au CNRS, IPHEP, Université de Poitiers / Invité
Mwendia Nyaga
Managing Director, National Oil Corporation of Kenya / Invité

Stratigraphic, petrographic and diagenetic evaluation of Cretaceous/Paleogene potential reservoir sandstones of western Turkana, Kenya. Implications on the petroleum potential of northwestern Kenya.

Etude stratigraphique, pétrographique et diagénétique des grès d'âge Crétacé-Paléogène de la région ouest du bassin du lac Turkana, Kenya. Conséquences sur leurs caractéristiques réservoir et l'évaluation du potentiel pétrolier du nord-ouest du Kenya.

Summary

Introduction 3

Chapter I 19

1. Introduction 23

2. Regional geological setting 28

3. Field study, sampling and analytical methods 31

4. The Lapur Sandstone Formation 32

4.1. Chronological setting of LSF 36

4.2. Structural framework of LSF at the scale of the Turkana depression 43

4.3. Depositional environments of LSF 45

4.3.1. Facies description and depositional processes 45

4.3.1.1. Conglomerate facies. 45

4.3.1.2. Sandstone Facies 50

4.3.1.3. Claystone and silty claystone facies 52

4.3.1.4. Palaeosols and associated deposits 52

4.3.2. Facies associations and depositional environments 54

4.3.2.1. Distal alluvial fan facies associations 54

4.3.2.2. Braided stream facies associations 55

4.3.3. Vertical evolution of the LSF 55

4.3.4. Lateral variations of LSF 56

4.4. Post sedimentation evolution of the LSF 58

4.4.1. Detrital minerals 59

4.4.1.1. Polycrystalline quartz 59

4.4.1.2. Monocrystalline quartz 59

4.4.1.3. Feldspar 59

4.4.1.4. Other detrital grains 62

4.4.2. Cements 62

4.4.2.1. Zone I. Calcite cement 63

4.4.2.2. Zone II 63

4.4.2.3. Zone III 64

4.4.3. Porosity 67

4.4.4. Source of cements 67

4.4.4.1. Calcite cementation 67

4.4.4.2. Hematite cementation 69

4.4.4.3. Kaolin cementation 70

4.4.4.4. Feldspar alteration 70

4.4.4.5. Alteration of muscovite 71

4.4.5. Chronology of diagenetic events 71

5. Discussion. Importance of the Lapur Sandstone Formation for palaeogeographical and climatic reconstitutions, and implications for oil exploration 73

5.1. Palaeogeographical and climatic reconstitutions (from sedimentological data) 73

5.2. Climatic conditions from diagenesis data 75
5.3. Implications on the reservoir potential of LSF 76
6. Conclusions 77

Chapter II **79**
1. Introduction 81
2. Field study, sampling and analytical methods 81
3. Lithostratigraphy 82
4. Facies analysis 82
4.1. Conglomerate facies, Gcu 82
4.2. Sandstone facies 84
4.3. Facies associations 85
5. Post sedimentation evolution of the MSF 85
5.1. Detrital mineral composition 86
5.2. Cements 89
5.3. Paragenetic sequence 91
5.4. Porosity evolution and reservoir characteristics of MSF 93
5.5. Comparison with the Lapur Sandstone Formation 95
6. Conclusions 95

Chapter III **97**
1. Introduction 101
2. The Northern Kenya Rift Basins 103
2.1. The Lotikipi and Gatome Basins 103
2.1.1. Reservoir Rocks 104
2.1.2. Source Rocks 106
2.2. The Lokichar, North Lokichar and North Kerio Basins 107
2.2.1. Reservoir Rocks 110
2.2.2. Source Rocks 118
3. The Central Kenya Rift Basins 119
3.1. The Kerio and Baringo Basins 119
3.1.1. Reservoir Rocks 121
3.1.2. Source Rocks 122
Conclusions **123**
References **127**

Introduction

Introduction

Fifteen major sedimentary basins cover almost 30 % of the area of East Africa. They are distributed across the entire region extending from east to west and from north to south. These basins fall in 3 tectonostratigraphic settings namely Passive Margins, Rift Basins (the Central African Rift System (CARS)) and the East African Rift System (EARS) and Intracratonic Basins (Rubondo, 2003).

Geological and geophysical surveys together with exploration drilling has been intermittently undertaken to varying degrees in these basins over the last seventy years in an effort to search for oil and gas. Although this effort has been minimal given the size of the areas covered by these basins, it has so far yielded the discovery of a major oil field in the Albertine Graben and two gas fields of Songo Songo and Mnazi bay in the Ruvuma and Rufiji basins of Tanzania, respectively. Two other gas discoveries in Tanzania, the Kilawani and Mkuranga, are currently under appraisal.

In addition to the discoveries, all the basins of East Africa display good source rocks capable of generating oil and gas, together with good to excellent reservoir rocks and structures conducive for the accumulation of oil and gas. East Africa therefore offers definite opportunities for discovery of oil and gas. Its sedimentary basins are analogues to those in other parts of the world where large volumes of oil and gas are already being produced. Renewed exploration effort is required to realise the petroleum potential of East Africa.

The earliest efforts to establish the presence of economic reserves of oil in East Africa were first undertaken in the Albertine Graben during the 1930's. This was a follow up of the discovery of oil in the Graben during the 1920's. The first mention of oil seeps in Uganda was by Wayland (1925) who reported a total of 52 seeps. Five of the most prominent of these oil seeps are the Paraa, Kibiro, Kibuku, Hohwa and the fractured basement reservoir in the Kaiso Tonya area.

At Paraa, oil freely flows on to the surface of the water in the Victoria Nile River at several different spots and spreads over an area about half the size of a football field. At the Kibuku oil seep, drops of live oil seep from the cliff, producing a strong hydrocarbon odour and forms oil films in the small pools of water adjacent to the cliffs. In the Kibiro seep, oil saturated sands are present on the shores of Lake Albert. Coring these sediments revealed two meters of tarry sands overlying 4m of water wet sand through which asphaltic oil floated. Border-faulted gneisses and oil-impregnated sands have also been reported in the Kabyosi, Warwire and Hohwa river gorges in the Kaiso Tonya area on the shores of Lake Albert (PEPD, 2005; Kasande, 2007; Rubondo 2005).

Geochemical analysis of these oil seeps has yielded two different depositional environments for the source rocks in the basin. The presence of botryococcanes which are normally synthesized by the fresh water green alga Botryococcus brauni is indicative of a lacustrine type 1 algal-dominated source rock for the Kibiro oil seep. Sterane ratios and the presence of oleanane in the Kibuku seep are indicative of a significant contribution of higher land plants suggestive of deltaic depositional environments (PEPD, 2005).

Several shallow stratigraphic wells were drilled adjacent to these seepages. A deep well was drilled near Butiaba in 1938 by the African European Investment Company to a depth of over 1,200m. The well revealed several oil shows and recovered free oil on test but no economic reserves of oil were established. Subsequent geological surveys carried out in this area during the 1940's and 50 have established the presence of sedimentary sequen-

ces of shale and sandstones in outcrop. The discovery of gas at Songo Songo in Tanzania in 1974 by Agip and oil in the Sudan in 1979 by Chevron rekindled exploration interest in Uganda. During the 1983-1984 period, aeromagnetic surveys in the Albertine graben identified the presence of 3 major sub-basins with sufficient sediment thickness for oil generation (Rubondo, 2003).

The Albertine Graben is currently subdivided into 9 exploration areas (EAs), 5 of which have active production sharing agreements (PSAs) operated by 4 companies. EA-1 was licensed to Heritage Oil & Gas (Heritage) and Energy Africa (now Tullow) in 2004. EA-2 was licensed to Hardman Resources and Energy Africa in 2001, while EA-3A was re-licensed to Heritage and Energy Africa (Tullow) in 2004. In 2005, Neptune Petroleum (now Tower Resources) acquired exploration rights over EA-5, while EA-3B, 3C, 3D and 4A remain available for licensing (Fig. 1; PEPD, 2009).

Though the size of the Albertine Graben is in excess of 20,000 sq km in surface area, only a total of 2180km of onshore 2D, 2235 km of offshore (lake) 2D, 841 sq km of transition zone 3D, 404 km of transition 2D and 390 sq km of land 3D seismic data has been acquired to date. A total of 22 deep wells have been drilled to data (Fig. 1; Table 1). These wells drilled in the Turacco, Mputa, Waraga, Kingfisher, Ngassa, Nzizi, Jobi, Rii, Nsoga and Awaka prospects during the 2002-2009 period have confirmed the existence of a working petroleum within the Albertine Graben. The wells have confirmed the presence of multiple commercially exploitable accumulations of hydrocarbons, with flow testing of the Waraga, Mputa and Kingfisher prospects yielding flow rates of over

Well name	Exploration area	Well type	Year drilled	Total depth (m)	Status
Waki-1B	EA2	Exploration	1938	1237	Oil Shows
Turacco-1	EA3B	Exploration	2002	2488	Gas Shows
Turacco-2	EA3B	Exploration	2003	2963	Oil & Gas shows
Turacco-3	EA3B	Appraisal	2004	2850	Oil & Gas shows
Mputa-1	EA2	Exploration	2005	1187	Oil Discovery
Waraga-1	EA2	Exploration	2006	2010	Oil Discovery
Mputa-2	EA2	Appraisal	2006	1344	N/A
Kingfisher-1	EA3A	Exploration	2006	2125	Oil Discovery
Nzizi-1	EA2	Exploration	2006	1065	Oil & Gas Discovery
Nzizi-2	EA2	Appraisal	2007	982	N/A
Mputa-3	EA2	Appraisal	2007	973m	N/A
Mputa-4	EA2	Appraisal	2007	1082	N/A
Ngassa-1	EA2	Exploration	2007	1023	Gas Shows
Taitai-1	EA2	Exploration	2008	1006	Oil Shows
Ngege-1	EA2	Exploration	2008	640	Oil & Gas Discovery
Kingfisher-2	EA3A	Appraisal	2008	3906	N/A
Karuka-1	EA2	Exploration	2008	853	Oil Shows
Kasamene-1	EA2	Exploration	2008	866	Oil & Gas Discovery
Kigogole-1	EA2	Exploration	2008	616	Oil Discovery
Ngiri-1	EA1	Exploration	2008	911	Oil & Gas Discovery
Kingfisher-3 & 3A	EA3A	Appraisal	2008	3200	N/A
Jobi-1	EA1	Exploration	2008	637	Oil & Gas Discovery
Rii-1	EA1	Exploration	2009	705	Oil Discovery
Mputa-5	EA2	Appraisal	2009	1231	N/A
Karuka-2	EA2	Appraisal	2009	879	N/A
Nsoga-1	EA2	Exploration	2009	755	Oil Discovery
Awaka-1	EA2	Exploration	2009	684	Oil Discovery

Table 1. *Summary of wells drilled in the Albertine Graben, Uganda. Note some of the oil and gas discoveries occur in relatively shallow wells with depths between 600-700m (PEPD, 2009). The results of the appraisal wells are not reported due to commercial confidentiality.*

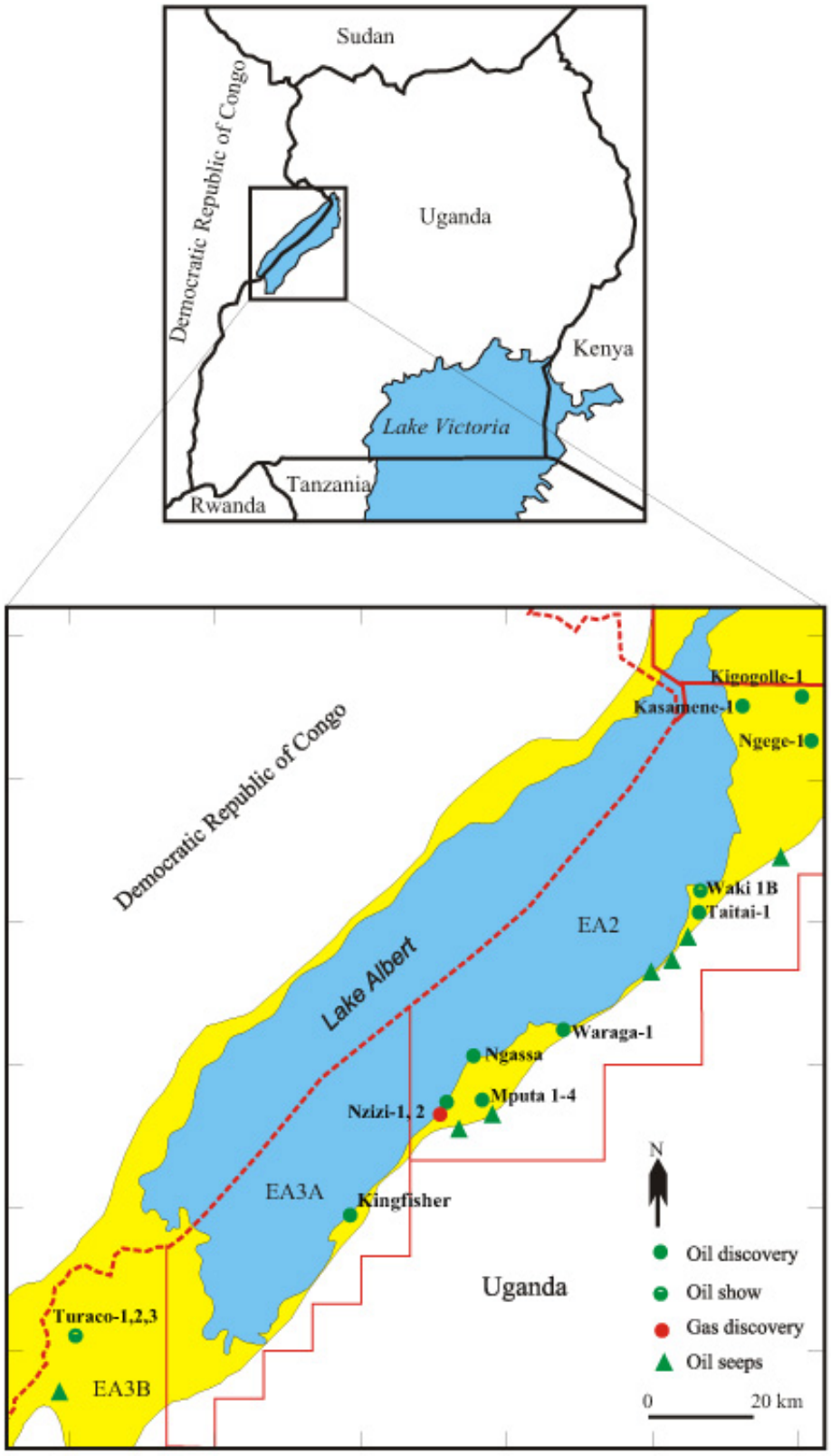

Figure 1. *Location of wells drilled in the Albertine Graben, Uganda. EA (Exploration Area) refers to the different exploration blocks (PEPD, 2009).*

12000, 2100 and 14000 barrels of oil per day. Estimated reserves are in the region of 20-25 billion barrels of oil in place (PEPD, 2009).

In the early 1950's, British Petroleum (BP) and Shell started exploration activities in the Lamu Basin and in the Coastal Basins of Zanzibar, Pemba and Mafia. This work culminated into the drilling of 8 exploration wells in the Lamu Basin and 4 wells in the Coastal Basins. None of those wells encountered hydrocarbons in sufficient quantities to justify further drilling (Rubondo, 2003; Alconsult, 1997; TPDC, 2009). In the Coastal Basins of Tanzania, Amoco joined Agip to drill 3 wells onshore and 3 wells offshore between 1973 and 1982. One of the offshore wells, Songo Songo 1, resulted in the discovery of the Songo Songo gas field. Another offshore well also resulted in the discovery of the Mnazi Bay gas field of similar size. Tanzania Petroleum Development Corporation (TPDC) drilled 8 wells around the Songo Songo (Fig. 2) discovery to delineate the field, which was found to hold one-two trillion cubic feet of gas.

The high oil prices of the early 1980's led to additional exploration activity in the region. This included funding of an aeromagnetic survey across the Albertine Graben by the World Bank. Shell, Esso, IEDC (International Economic Development Corporation) and BHP Billiton (Broken Hill Proprietary Company of Australia) also took licenses covering the Ruvu and Selous Basins where they acquired over 6,400 km of seismic data and drilled 5 exploration wells, none of which encountered economic reserves of oil (Rubondo, 2003; TPDC, 2009) (Fig. 2; Table 2).

During 1983, the international oil industry was drawn to the East African Rift System by the results of the aeromagnetic survey funded by the World Bank and the results of a seismic survey conducted over the Lake Malawi and Lake Tanganyika Basins by Duke University, as part of Project PROBE (Proto-Ocean and Basin Evolution) scientific study (Rosendahl, 1987; Rosendahl et al., 1986). The Rukwa Basin geometry was first established by a Petro-Canada gravity survey (Pierce and Lipkov, 1988). The studies confirmed the presence of thick sequences of sedimentary rocks in the basins and indicated good structures. These results together with the existence of oil seeps on Lake Tanganyika (Tiercelin et al., 1993; Morley, 1999; Simoneit et al., 2000) led Amoco to acquire acreage in the Rukwa Basin and drill two wells (Galula-1 and Ivuna-1) there; these two wells were also not successful (Rubondo, 2003; TPDC, 2009). Two wells (Buringa-1 and Rusizi-1) were also drilled in the onshore Lake Tanganyika (Rusizi Plain) (Morley and Wescott, 1999).

Oil prices collapsed in the mid 1980's and there was little additional acquisition of acreage by oil companies. Shell and Texaco which were still holding acreage in the Mandawa, Mafia and the Ruvuma Basins respectively continued to carry out work albeit at a slower rate. This work led to the drilling of an additional exploration well in each of these basins. Petro-Canada drilled an aid funded well on the Dar-es-Salaam Platform and another one on the Garissa High of the Lamu embayment. Exploration interest was low during the early 1990's mainly as a result of the low international prices of crude oil. These prices began to pick up in the late 1990's and this has led to renewed interest resulting in several companies being licensed in the different basins of East Africa.

In the southern Sudan, Chevron signed, in 1974, an agreement covering a block with an area of 516,000 sq km within the Melut and Muglad basins. Later in 1979, the Sudanese government and Chevron signed an agreement which resulted in the addition of the Bagarra and Blue Nile blocks to the concession area. Exploration commenced in 1975 with the acquisition of 80,000 sq km of aeromagnetic data followed by a reconnaissance seismic survey. The data confirmed the existence of a northwest-trending as well as north-trending basinal areas. During the 10 years that Chevron operated in southern Sudan, 58,000 km of 2D data plus one 3D survey were acquired. A total of 86 wells were drilled during this 10-year period (Schull, 1988) (Fig. 3). During the first period of exploration by Chevron between 1975 and 1980, efforts were concentrated in the Muglad basin where several discoveries were made, such as the Unity-1, Unity-2 and Abu Gabra-1 wells. In 1981, nine more wildcat wells were drilled, resulting in the discoveries in the Sharaf-1 well in north western Muglad. Other discoveries made in the same

Well Name	Operator	Lat. (S)	Long. (E)	TD (m)	TD Formation	TD Age	Spud Date	Completed	Status
Mafia-1	BP	07°52'40"	39°49'21"	3366	Ruaruke	Late Cret.	17/12/54	21/01/56	P&A with oil and gas shows
Zanzibar-1	BP	06°03'26"	39°13'02"	4353	Ruaruke	Late Cret.	10/05/56	17/03/57	P&A with gas shows
Mandawa-7	BP	09°24'58"	39°25'04"	4065	Nondwa	E. Jur.	23/03/58	31/01/59	P&A with oil and gas shows
Pemba-5	BP	05°16'11"	39°41'53"	3686	Ruaruke	Late Cret.	30/12/61	30/06/62	P&A with oil and gas shows
Ras Machuis-1	AGIP	06°00'56"	38°51'19"	3370	Ruaruke	Late Cret.	22/12/73	13/02/74	P&A with gas shows
Songo Songo-1	AGIP	08°28'38"	39°28'33"	4426	Mtumbei	Late Jur.	16/02/74	21/05/74	Gas discovery
Kisangire-1	AGIP	07°29'09"	28°32'42"	3296	Ngerengere	E. Jur.	22/10/75	25/02/76	P&A
Kisarawe-1	AGIP	07°00'19"	39°03'32"	4057	Bagamoyo	Late Jur.	10/03/76	9/07/76	P&A
Songo Songo-2	TPDC	03°31'00"	39°31'00"	990	Mafia	Eocene			P&A Gas blow out
Songo Songo-3	TPDC	08°31'19"	39°29'46"	2286	Kipatimu	E. Cret.	27/02/77	28/07/77	Gas well
Songo Songo-4	TPDC	08°31'01"	39°29'30"	2011	Kipatimu	E. Cret.	3/05/78	22/08/78	Gas well
Kizimbani-1	AGIP	09°02'25"	39°22'30"	2687	Basement	Precambrian	20/07/79	30/09/79	P&A
Songo Songo-6	TPDC	08°31'26"	39°30'04"	2048	Kipatimu	E. Cret.	23/01/81	29/04/81	P&A with gas shows
Songo Songo-5	TPDC	08°31'18"	39°28'53"	2978	Mtumbei	Late Jur.	25/05/81	8/10/81	Gas well
Songo Songo-7	TPDC	08°31'56"	39°29'15"	3377	Mtumbei	Late Jur.	15/10/81	31/03/82	Gas well
Kimbiji East-1	TPDC	06°59'16"	39°32'40"	3582	Ruaruke	Late Cret.	4/12/81	12/06/82	P&A with gas shows
Songo Songo-8	TPDC	08°33'08"	39°30'56"	3268	Mtumbei	Late Jur.	9/04/82	12/06/82	P&A
Mnazi Bay-1	AGIP	10°19'45"	40°23'28"	3489	Ruaruke	Late Cret.	26/06/82	16/11/82	Gas discovery
Songo Songo-9	TPDC	08°30'54"	39°28'45"	2057	Kipatimu	E. Cret.	19/11/82	27/01/83	Gas well
TanCan-1	PCIAC	06°56'58"	39°36'40"	4685		Paleogene	30/11/82	5/03/83	P&A with gas shows
Kimbiji Main-1	TPDC	06°58'19"	39°28'31"	4408	Makonde	E. Cret.	5/12/82	23/06/83	P&A with gas shows
Makarawe-1	IEDC	05°33'10"	38°52'11"	3821	Tanga	Triassic	7/08/84	9/11/84	P&A with oil and gas shows
Ruaruke North-1	SHELL	07°43'10"	39°10'16"	2000	Kipatimu	E. Cret.	10/08/84	25/09/84	P&A
Liwale-1	SHELL	09°25'53"	37°31'16"	1762	Karroo	Permo-Trias.	4/07/85	25/08/85	P&A
Kiwangwa-1	IEDC	06°21'43"	38°32'56"	3514	Tanga	Triassic	4/09/85	4/01/86	P&A with gas shows
Lukuliro-1	SHELL	08°21'32"	38°25'42"	2367	Madaba	Jurassic	18/09/85	12/11/85	P&A with gas shows
Galula-1	AMOCO	08°33'34"	32°54'24"	1524	Red Beds	(Jurassic?)	23/10/87	3/08/87	P&A
Ivuna-1	AMOCO	08°15'25"	32°18'27"	2316	Basement	Precambrian	23/08/87	4/09/87	P&A
Mbuo-1	SHELL	09°26'41	39°15'51"	3313	Basement	Precambrian	4/02/90	15/05/90	P&A
Lukuledi-1	TEXACO	10°09'56"	39°39'58	1941	Basement	Precambrian	30/08/90	30/10/90	P&A
Dira-1	SHELL	07°32'32"	39°33'58"	3529		E. Miocene	14/10/91	23/11/91	P&A
Mitagamma-1	DUBLIN	08°54'56"	39°09'53"	2390	Basement	Precambrian	30/10/96	11/12/96	P&A with oil shows
East Lika-1	DUBLIN	09°16'26"	39°04'04	2002	Basement	Precambrian	23/12/96	22/01/97	P&A
Mbate-1	DUBLIN				Basement	Precambrian			P&A
Nyuni-1A	NDOVU	08°22'55.7"	39°34'25.8"	3905	Kipatimu	Top Jurassic	26/08/03	12/12/04	
	/AMINEX								
Mnazi Bay-2	ARTUMAS								Gas Well
Mnazi Bay-3	ARTUMAS							17/12/06	Gas Well
Mnazi Bay-IX	ARTUMAS							17/12/06	Gas Well
Mkuranga-1	MAUREL &								
	PROM								
Mbezi-1	MAUREL &	07°11'53"	39°14'38"						
	PROM								
Minangu-1	MAUREL &	07°20'30"	39°07'46"						
	PROM								
Mihambia-1	MAUREL &	09°17'39.4"	39°13'12.7"						
	PROM								
Mafia Deep ST-1	MAUREL &	07°53'05"	39°45'09"						
	PROM								

Table 2. *Summary of the wells drilled in Tanzania (TPDC, 2009). The number of wells is increasing rapidly due to the appraisal programmes for the Mnazi Bay, Mkuranga and Kilawani gas discoveries.*

year included the Talih-1 well near the Unity field and the Adar-1 and Adar-2 wells in the Melut Basin. In 1982, 18 wells were drilled, mainly in the Muglad and Blue Nile Basins while in 1983, 24 wells were drilled including the discoveries in the Heglig-1 and Toma south-1 wells in the Heglig field in the Muglad Basin.

Currently in the Sudan, there are exploration activities in 20 onshore blocks, carried out by 10 operating companies, with development activities in 7 blocks. Crude oil production in the Sudan currently stands at approximately 500,000 barrels of oil per day (www.sudapet.sd).

Exploration in the sedimentary basins of Kenya

Kenya has 4 sedimentary basins, namely the Lamu Embayment, the Anza Graben, the Mandera Basin

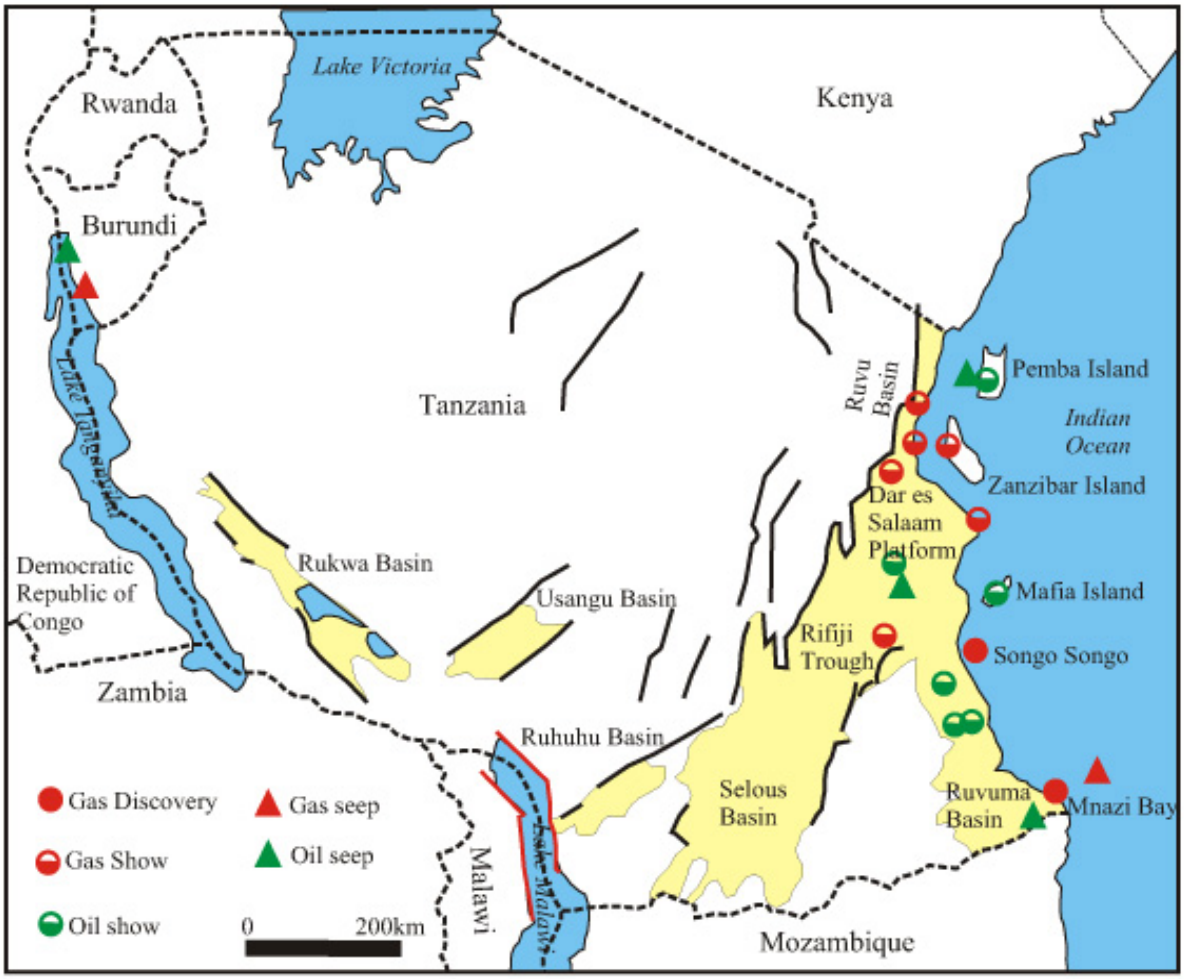

Figure 2. *Basins and wells location map showing the gas discoveries and surface oil seeps in Tanzania (TPDC, 2009). Not shown on the map are the recent discoveries in Kilawani north and Mkuranga. The gas discovery in Songo Songo has already been commercialized and is used mainly for power generation as well as in industries in the Dar es Salaam area.*

and the Tertiary Rift Basins (Fig. 4). The total area sedimentary cover in the country is approximately 317,000 square km. The total surface area of Kenyan territory is 582,646 square km (Kenya Bureau of Statistics, 2005) and which means more than half of Kenya is composed of sedimentary basins. Exploration for oil and gas in these basins has been going on sporadically since the early 1950's. To date, 31 exploration wells have been drilled in these basins, with the most recent well being drilled in during December 2006 to February 2007. The exploration activity has been subdivided into four phases pre-1996 (Alconsult, 1997) and a fifth phase can be added to incorporate current and recent activity (2000-2007). The earlier phases of exploration have been classified as 1954-1971, 1971-1976, 1976-1985 and 1985-1996 (Alconsult, 1997).

The exploration phases are closely related to shifting interest shown by oil exploration companies in different basin settings as dictated by prevailing regional and global trends and how these trends shift with time. Exploration interest in Kenyan acreage is also a encouraged by favourable fiscal and regulatory terms offered by the government, as well as positive drilling results from past exploration and also by discoveries in adjacent countries such the Sudan, Tanzania and recently, Uganda. These exploration phases have also been in response to prevailing trends in world oil prices, with high prices generally resulting in increased exploration activity (Alconsult, 1997).

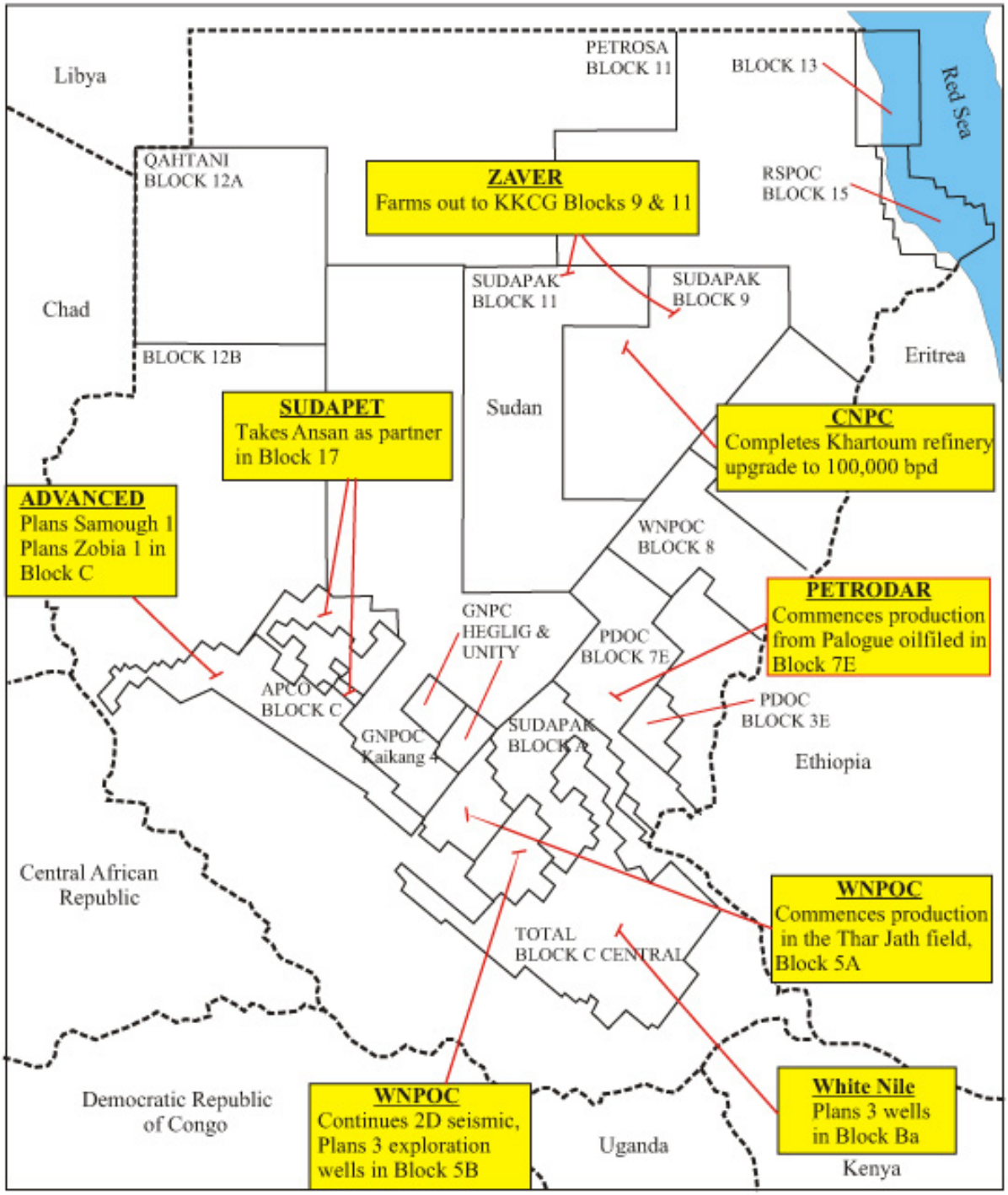

Figure 3. *Activity map showing the various concession holders in Southern Sudan (from EIA, 2007). Following US sanctions, there are hardly any western oil companies operating in Sudan. The bulk of the companies are from the east, led by China, Malaysia, India and Pakistan, who have taken advantage of the US boycott to position themselves for a share of the almost 500,000 barrels of oil per day production. Exports are mainly through pipelines that connect the producing fields to Port Sudan on the Red Sea coast.*

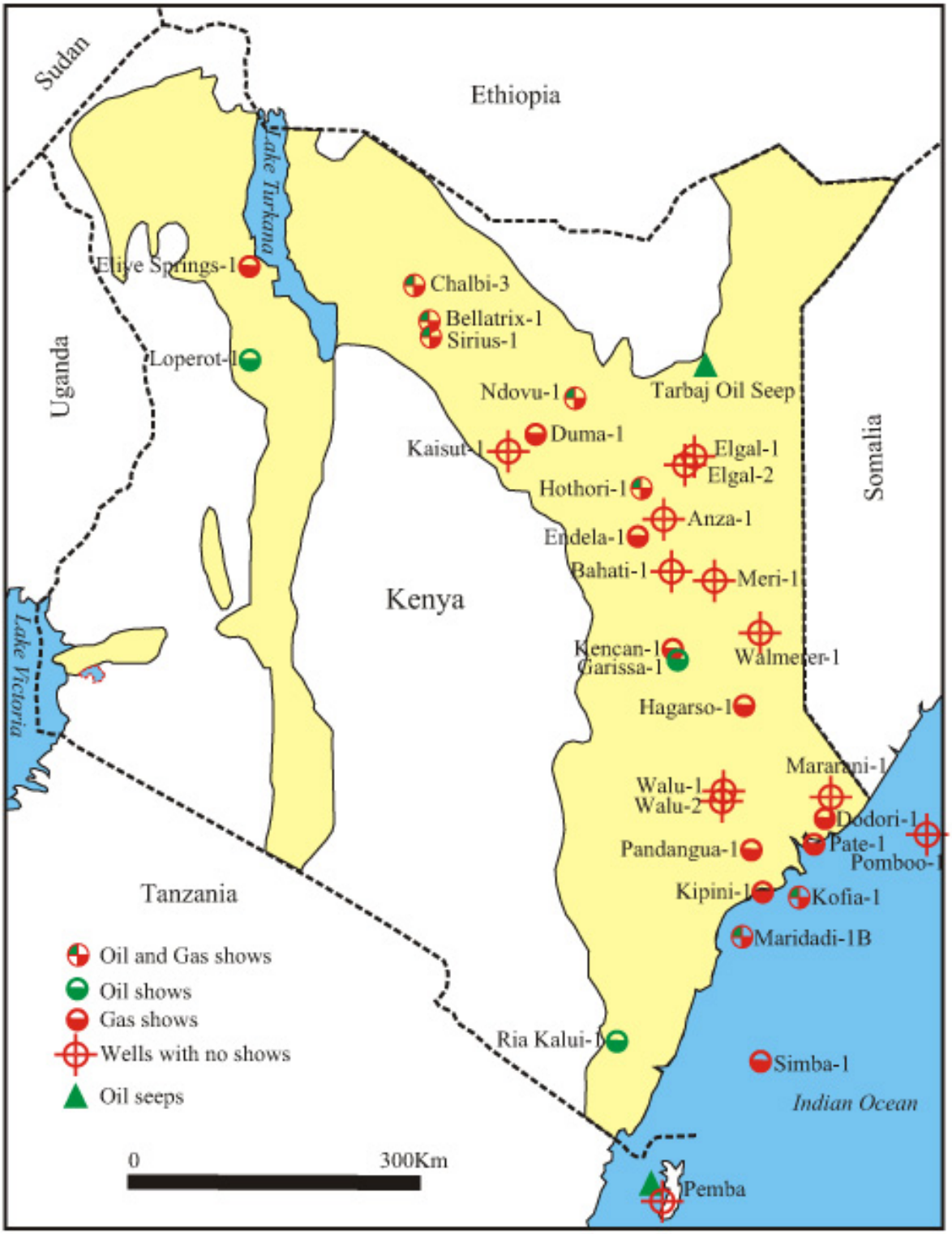

Figure 4. *Well location map of Kenya with hydrocarbon shows and sedimentary basins (NOCK, 2009). Several of these wells had oil and gas shows, one (Pate-1) was reported to have had a gas kick but no commercial hydrocarbons have been discovered while in two wells, Loperot-1 and Sirius-1, small amounts of oil were recovered during testing and reverse circulation, respectively.*

	Outer Continental Shelf Project	2008	4351		
	PGS Non-exclusive 2D survey	2008	3300		
LAMU (Onshore)	British Darcy	1955/56			3115
	BP Shell	1959/63	3831	7615	3814
	Bp Shell	1966/71	7071	22110	
	Whitestone	1974/75	498		83
	Sun Oil	1975	186		
	Texas Pacific	1975	73		250
	Wainoco & Anchutz	1975	50	3539	
	Ministry of Energy	1977		12941	
	Cities Services	1980	3080		
	Ministry of Energy	1983		3539	
	NOCK/ PetroCanada	1984	1208		
	CNOOC	2008			2734
ANZA		1973/75	3437	16412	3579
	Whitestone	1975	50		
	Ministry of Energy	1982		47649	
	Amoco & Shell	1985/87	6716		10732
	Total	1986/87	4169		785
	Lundin	2007			4000
	CNOOC	2008	916		
TERTIARY RIFT	Amoco		356		
	Shell				
	Duke		1135		
	CGG				
	Nyanza Trough		50		
	Kerio Valley		49		
	University of Leicester				8708
	Camec	2007			4000

Table 3. *Geophysical data acquired by various operating companies within Kenya sedimentary basins (NOCK, 2009). All the seismic data has been 2D, the first 3D data to be acquired in Kenya is in the final stages of preparation and is scheduled to be acquired before the end of the year 2009..*

Early 1950's to early 1970's period

BP-Shell was the first company to explore for oil in Kenya starting in 1954 and continuing until 1971. This work was concentrated in the northern parts of the Lamu Basin and by the end of this exploration phase; a total of 10 exploration wells had been drilled. The first exploration wells drilled by BP-Shell include Walu-1, Pandangua-1 and Meri-1 (Fig. 4; Table 3). These wells had total depths of about 2000 m and one terminated in the Upper Cretaceous while two terminated in Lower Tertiary. All the three wells were unsuccessful. The wells drilled later by BP-Shell (Walu-2, Mararani-1, Dodori-1, Garissa-1, Walmerer-1, Pate-1 and Kipini-1) penetrated deeper stratigraphic intervals down to the Jurassic.

The Dodori-1 well flowed gas at the rate of 3.1 thousand cubic feet per day from Paleocene sands while the Pate-1 well kicked, flowed wet gas, mud and water from Eocene sands near total depth. Also during the BP-Shell exploration phase, the Ria-Kalui-1 well was drilled by a plantation owner (Mehta & Co.) in the Permian Karroo group of southeastern part of the Lamu Basin. This well was drilled without any structural justification but purely on surface geological observations and it reached a total depth of 1537m. It was reported to have encountered some oil-stained sands in the Karroo but this cannot be confirmed since there are no cuttings or cores preser-

Well Name	Operator	Latitude	Longitude	TD (m)	TD Age	Year Completed	Status
Walu-1	BP/Shell	01o38'04"S	40o15'09"E	1768	Late Cret.	1960	P&A
Pandangua-1	BP/Shell	02o05'51"S	40o25'15"E	1982	Early Tertiary	1960	P&A with gas shows in Tertiary
Meri-1	BP/Shell	0o20'36"N	40o11' 00"E	1941	Early Tertiary	1961	P&A
Mararani-1	BP/Shell	01o34'57"S	41o14'10"E	1991	Early Tertiary	1962	P&A with oil shows in the Tertiary
Ria Kalui-1	Mehta & Co.			1538	Permo-Trias.	1962	P&A with oil staining in Karroo
Walu-2	BP/Shell	01o 38'02"S	40o15'10"E	3729	Early Cret.	1963	P&A with oil shows in Cretaceous
Dodori-1	BP/Shell	01o48'53.7"S	44o11'04"E	4311	Late Cret.	1964	P&A with oil and gas shows in
							Tertiary and Cretaceous
Walmerer-1	BP/Shell	0o05'35"S	45o35'05"E	3794	Early Cret.	1967	P&A with gas shows in Cretaceous
Garissa-1	BP/Shell	0o22'04"S	39o48'43"E	1240	Mid. Jurassic	1968	P&A
Pate-1	BP/Shell	02o03'53.98"S	41o04'52"E	4188	Early Tertiary	1971	P&A with gas shows in the Eocene
Kipini-1	BP/Shell	02o29'23.57"S	40o35'51"E	3663	Late Cret.	1971	P&A with oil and gas shows in
							Tertiary and Cretaceous
Hagarso-1	Texas Pacific	0o 47'43.5"S	40o26'40.5"E	3092	Early Cret.	1975	P&A with gas shows in Cretaceous
Anza-1	Chevron	0o55'10.864"N	39o41'42.761"E	3662	Late Cret.	1976	P&A with oil stain in Cretaceous
Bahati-1	Chevron	0o26'32.913"N	39o47'5.077"E	3421	Late Cret.	1976	P&A with oil stain in Cretaceous
Simba-1	Total	04o00'06.60"S	40o34'03.68"E	3604	Late Cret.	1978	P&A with gas shows in Tertiary and
							Cretaceous
Maridadi-1B	Cities Services	2o53'8.795"S	40o24'7.856"E	4198	Mid. Tertiary	1982	P&A with gas shows in the Tertiary
Kofia-1	Union	02o32'31.90"S	40o56'18.30"E	3629	Late Cret.	1985	P&A with oil and gas shows in
							Tertiary and Cretaceous
KenCan-1	PetroCanada	0o18'57.384"S	39o46'16.572"E	3863	Permo-Trias.	1986	P&A
Elgal-1	Amoco	01o22'47"N	39o53'09"E	1280	Permian	1987	P&A
Elgal-2	Amoco	01o27'32.708N	39o58'40.063"E	1908	Triassic	1987	P&A
Ndovu-1	Total	01o59'58"N	38o52'57"E	4269	Early Cret.	1988	P&A with oil and gas shows in
							Cretaceous
Sirius-1	Amoco	2o35'00.14"N	37o32'48.98E	2638	Lower Cret.	1988	P&A
Bellatrix-1	Amoco	2o42'12.98"N	37o32'22.34"E	3480	Lower Cret.	1988	P&A
Duma-1	Total	1o39'35.66"N	39o30'19.77"E	3333	Early Cret.	1989	P&A with gas shows in Cretaceous
Hothori-1	Amoco	01o11'16.8"N	39o29'37.8"E	4392	Late Cret.	1989	P&A with oil and Gas shows
							in Cretaceous and Tertiary
Chalbi-3	Amoco	3o01'50.81"N	37o24'43.09"E	3644	Lower Cret?	1989	P&A
Endela-1	Walter	0o45'20"N	39o28'52"E	2779	Early Tertiary	1989	P&A with gas shows in Paleogene
Kaisut-1	Total	1o31'03.82"N	38o16'28.89"E	1450	Early Tertiary	1989	P&A
Loperot-1	Shell	02o21'46.229"N	35o52'24.132"E	2950	Paleocene	1992	P&A with oil shows
Eliye Springs-1	Shell	03o13'50.62"N	35o54'40.19"E	2964	Upper Miocene	1992	P&A
Pomboo-1	Woodside	01o57'16.15"S	41o56'28.02E	4887	Late Cret.	2007	P&A

Table 4. *A summary of the deep exploration wells drilled in Kenya (NOCK, 2009). With only 31 wells drilled in an area of more than 300,000 sq km, the drilling density is so low (at about 1 well in every 10,000 sq km of sedimentary basin area) that no conclusions can be a regarding the full potential of the basins.*

ved at the National Oil Corporation of Kenya Core-Storage facility. During this period, Frobisher Ltd, Adobe Oil and Burmah Oil companies conducted extensive photogeological interpretation, field geological studies, gravity, aeromagnetic and seismic data acquisition that did not however mature into drilling programs (Alconsult, 1997).

Early to mid 1970's period

There was a hiatus of several years after BP-Shell withdrew from Kenya in 1971. The second phase of exploration activity which can be linked to the rising oil prices occasioned by the embargo imposed on the US and its allies during the Arab-Israeli Yom Kippur war was concentrated mainly in the northern part of the Lamu Basin. Texas-Pacific drilled the Hagarso-1 well (Fig. 4) in 1975, which encountered oil and gas shows in the Cretaceous. Other companies that were active during this period include Whitestone, Sun Oil, Canadian Superior, Wainoco and Anschutz. These companies acquired seismic, aeromagnetic and or gravity data (Table 3) but they did not drill any wells. In 1976, Chevron and Esso drilled the Anza-1 and Bahati-1 wells (Fig. 4) in the southern part of the Anza Basin, after an extensive seismic acquisition campaign. Both wells, which reached total depth in the Late Cretaceous, were abandoned as dry holes with oil stains in the Cenomanian horizon (Alconsult, 1997).

Mid 1970's to Mid 1980's

The period saw renewed interest in offshore Lamu Basin which resulted in the drilling of three deep wells. The first deep offshore well drilled in Kenya was Simba-1 which was drilled by Total in 1978 in 933 m water depth. The well reached total depth of 3604 m and terminated in the Late Cretaceous with gas shows in Tertiary and Cretaceous. The two other wells (Maridadi-1B and Kofia-1) were drilled by a consortium of Cities Services, Union and Marathon in 1982 and 1985 respectively (Fig. 4; Table 4). Although these wells were dry, seismic data acquired prior to their drilling indicated the presence of diapiric salt structures with potential to provide favourable hydrocarbon trapping mechanisms along the Kenyan continental margin (Alconsult, 1997).

Mid 1980's to early 1990's

The government of Kenya entered into a partnership with Petro-Canada International Assistance Corporation which resulted in the acquisition of new onshore seismic data and the drilling of the KenCan-1 well in the Anza Basin. During this period, discoveries by Chevron in southern Sudan together with the introduction of new legislative framework governing oil and gas exploration and production in Kenya resulted in renewed interest by international oil companies in exploration acreage. This interest focussed mainly in the Anza Basin which is believed to be the eastern termination of the Central African Rift System (CRAS) of which the southern Sudanese rift basins of Melut and Muglad are part (Schull, 1988; Alconsult, 1997).

In 1984, Project PROBE acquired 1,400km of reflection seismics onshore Lake Turkana while Amoco and later Shell acquired extensive onshore seismic data, a total of 5 wells were drilled. Total drilled Ndovu-1, Duma-1 and Kaisut-1 in the northern part of the Anza Basin while Amoco drilled Sirius-1, Bellatrix-1 and Chalbi-3 in the northwestern part of the Chalbi Basin. Although all these wells were plugged and abandoned as dry holes, they had good oil and gas shows. The first two wells ever to be drilled in the Mandera Basin were drilled by Amoco during this period. These wells (Elgal-1 and Elgal-2) were located on an upthrown horst of the Lagh Bogal fault which separates the Anza Basin from the Mandera Basin. They terminated at relatively shallow depths of 1280 and 1906 m respectively but penetrated Triassic and Permian stratigraphic horizons, indicating their location close to the edges of the basin (Alconsult, 1997).

In the Tertiary rift basins of northern Kenya, Amoco farmed out 50 % of its interest to Shell who drilled the first two wells (Eliye Springs-1 and Loperot-1) ever to be drilled in the Kenyan Tertiary rift. The Loperot-1

well penetrated a thick sequence of mature lacustrine source rock and recovered water and waxy crude from a Miocene sandstone interval. These wells were drilled in 1992, after which there was a hiatus of 14 years before the next well was drilled in Kenya (Alconsult, 1997). The Eliye Springs-1 well penetrated good reservoir quality fluvial and lacustrine sands with porosity from logs ranging between 20-35 %. The Tertiary sequence penetrated by the well is composed of terrestrial (fluvial to lacustrine environments) with interbedded volcanics. The lacustrine intervals had well established fresh water conditions with algal blooms in the clays. Geochemical analysis of these clays indicated the immature, marginal to good quality Type I/II source rock (Shell, 1993; Alconsult, 1997).

Mid 90's to present (2009)

The recent phase of exploration activity can be attributed to the successful completion of a basin study in the Lamu Embayment in which all past exploration data was integrated into a promotional report for sale to oil companies. This report was published in 1995 and it lead to a new shift of focus in oil exploration acreage to the offshore parts of the Lamu Basin. Among the companies that took up acreage in offshore Kenya include Star Petroleum and Dana Petroleum of United Kingdom and Pancontinental Oil and Gas of Australia which signed leases in the year 2000. Other companies which have since acquired farm-in interest in offshore Kenya include Woodside Energy, Origin Energy and Gippsland Offshore Petroleum, all of Australia. A total of 27,739 km of 2D seismic data was acquired during this phase of exploration and Woodside Energy drilled one deep offshore well, Pomboo-1 in 2300 m of water. The well did not encounter any hydrocarbons (NOCK, 2009) and Woodside has since relinquished their acreage.

In 2006, the Minister for Energy gazetted new exploration blocks in the country, with many blocks being subdivided into smaller acreages (Fig. 5). This was as a result of huge surge in interest shown by oil companies to acquire exploration acreage in Kenya. This can be attributed partly to the rising world crude oil prices and also to the recent discoveries in Uganda. The Ugandan discoveries have taken place in the Albertine Graben in the western arm of the East African Rift System. The environment is comparable to the Kenyan Rift, which belongs to the eastern arm of the EARS, and this has made exploration acreage in rift settings very popular with oil exploration companies. Oil companies that have taken up acreage recently include the China National Offshore Oil Corporation (CNOOC), Central African Mineral Exploration Company (CAMEC), Africa Oil Corp, East Africa Exploration, Vangold Resources, Platform Resources, Lion Petroleum and Anadarko Petroleum (NOCK, 2009).

Why undertake this study?

It is generally accepted that five elements must, of necessity, be in place for any accumulation of commercial petroleum to occur. These elements are organic matter-rich source rocks, porous and permeable reservoir rocks, migration pathway, trapping mechanism such as closed structures and a seal to prevent the accumulated hydrocarbons from escaping. It could also be added that the timing of development of these elements will also be critical in the formation of commercial accumulations of oil and gas. In the northern Turkana area of Kenya, an outcrop of potential reservoir sandstones has been known since the 1930's (Murray Hughes, 1933; Arambourg, 1935). There has however not been any detailed sedimentologic study of this potential reservoir to determine its value as far as the contributions to the overall petroleum potential of the area is concerned. There has been no systematic sampling, dating and interpretation of depositional environments for the Turkana Grits as they have been named in the past.

The aim of this study is therefore to conduct a detailed sedimentologic and diagenetic study of the major sedimentary formations of northwestern Kenya, named the Lapur, Muruanachok, Mount Porr and

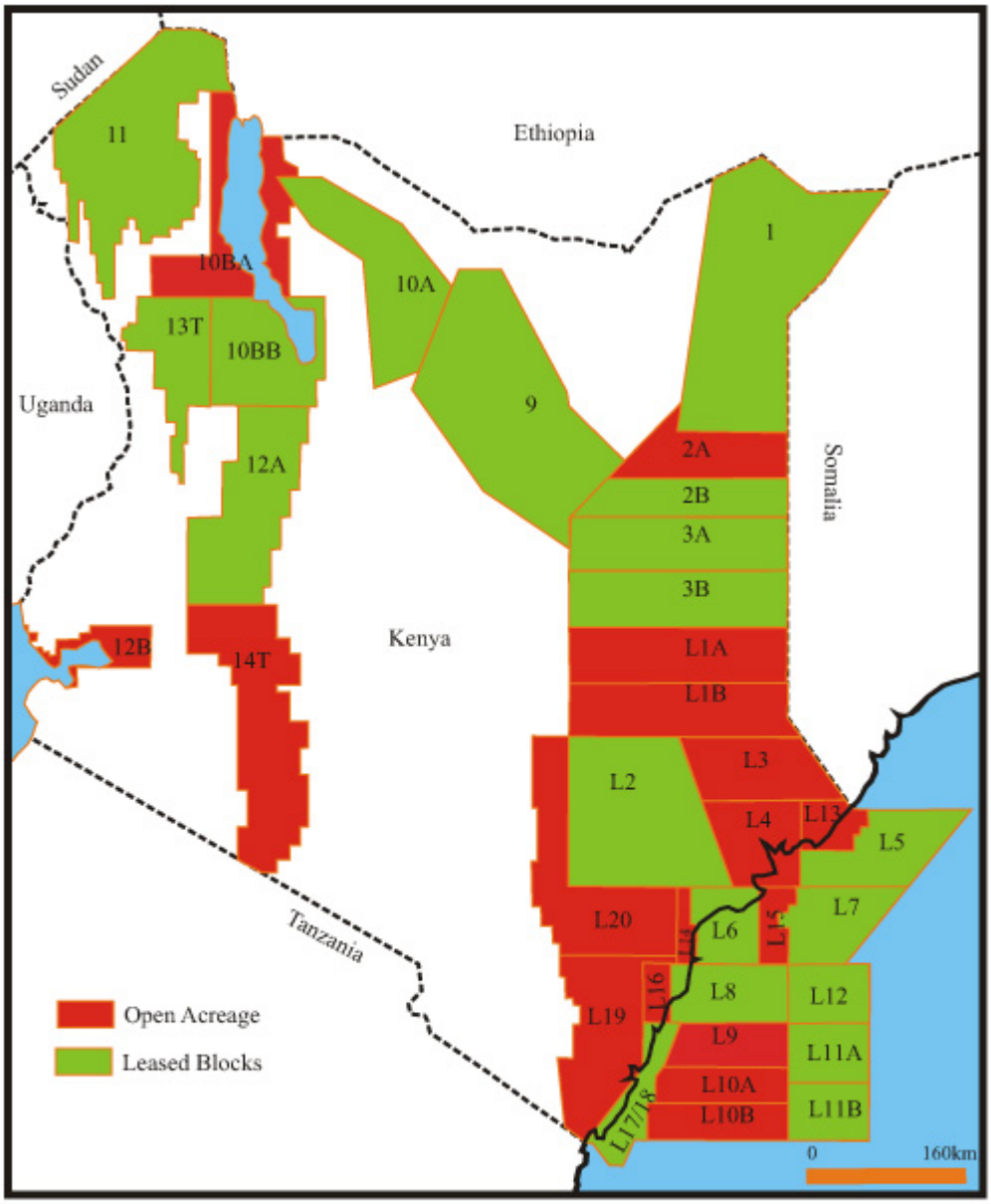

Block	Operator
1	East Africa Exploration (EAX)
2B	Lion Petroleum
3A, 3B	Vangold Resources
9, L2	Chinese National Offshore Oil Corporation (CNOOC)
10A, 10BB	Africa Oil Corp
11	Central Africa Mineral Exploration Company
12A, 13T	Platform Resources
L4, L13	Swiss Oil Holdings Inc.
L5, L7, L11A, L11B, L12	Anadarko Petroleum
L6	Gippsland Offshore Petroleum
L8	Origin Energy
L17/18	East Africa Exploration

Figure 5. *Kenya exploration acreage map showing exploration blocks status and operating companies (NOCK, 2009). A total of 21 exploration blocks are licensed to 11 companies, out of a total of 36 blocks, this being the highest number of blocks ever licensed in the history of exploration in the country.*

Lokichar/Lothidok Sandstone Formations which collectively form what has been referred to as the "Turkana Grits" (Murray-Hughes (1933). The study mainly comprises of field observations, sampling, measurement of stratigraphic sections and petrographic characterization to evaluate porosity, cementation and detrital composition with the ultimate aim of evaluating the reservoir potential of the different formations.

This study should form valuable basic data for oil exploration companies seeking to understand the petroleum geology of northwestern Kenya by providing a comprehensive study of the sedimentary units overlying basement. Brief descriptions of the volcanics covering the sediments have also been performed as they may have an effect on the post sedimentation alteration of the formations and hence their reservoir potential. Dating of these volcanics using radiometric methods allows the age of the essentially non-fossilifereous sedimentary formations to be constrained. Numerous dykes that have been intruded into the sedimentary formations have also been dated in order to estimate the timing of these events relative to the development of the potential reservoir facies.

The analytical methods used in this study include detailed stratigraphic logging and sampling where sections of the Lapur Sandstone Formation, the Muruanachok Sandstone Formation, the Lokichar/Lothidok and the Mount Porr Formations were performed in the field. In order to determine the sedimentologic and diagenetic evolution of the sandstones, selected representative samples were studied, both macroscopically and microscopically on the petrographic microscope. Cold cathode cathodoluminescence and scanning electron microscopy methods were used to complement the petrographic studies especially to understand the textural relationship between grains and the different cementing materials. The energy-dispersive x-ray analysis was used to study the chemical composition of the various cements and accessory minerals.

Presentation of results

The work is presented in three chapters:

Chapter I analyses the Lapur Sandstone Formation (LSF) which is given significant prominence because it forms the most vertically and laterally extensive outcrop of potential reservoir sandstones in the northern Turkana area. The LSF or equivalent sedimentary units are expected to form part of the basin fill in the Gatome/Lotikipi basins as well as the Lake Turkana basin. In this chapter, a review of the major sandstone formation of Cretaceous/Paleogene age in the wider eartersn abd central Africa region is presented. This is followed by a geological background of the LSF as one of the formations previously referred to as the "Turkana Grits" and its chronological setting, especially relating to the overlying Turkana Volcanics. The main body of this chapter contains a detailed facies, petrographic and diagenetic analysis of the LSF, leading to a climatic and paleogeographic reconstruction and in interpretation of the reservoir potential of the formation.

Chapter II deals with a petrographic and diagenetic evaluation of the Muruanachok Sandstone Formation (MSF), another formation of significant importance and forming part of the "Turkana Grits" outcropping in the southern part of the study area. The MSF or equivalent sandstones are expected to form part of the basin-fill and potential reservoir units in the north Lokichar basin and perhaps in the Lotikipi and Gatome basins to the north.

Chapter III is a synthesis of the overall hydrocarbon prospectivity of the northwestern Kenya sedimentary basins. It evaluates the reservoir potential of the LSF, MSF, the Loperot/Lothidok Sandstones and the Mount Porr Sandstones. On top of the reservoir potential, other aspects of hydrocarbon prospectivity such as the source rocks and traps in the basins have been evaluated.

Chapter 1

The Lapur Sandstone Formation of northern Kenya

The Lapur Sandstone Formation of northern Kenya.

Chronological setting, sediment characteristics and diagenetic evolution. Importance in terms of oil exploration for the Meso-Cenozoic Turkana Depression

La Formation Gréseuse de Lapur, Nord Kenya.

Contexte chronologique, caractéristiques sédimentaires et évolution diagénétique. Son importance en termes d'exploration pétrolière de la dépression Méso-Cénozoique du Turkana

Article soumis pour publication au «Journal of African Earth Sciences»

Auteurs : Peter Thuo[a, b],*, Jean-Luc Potdevin[c], Jean-Jacques Tiercelin[d], Sylvie Bourquin[d], Mathieu Schuster[e], Thierry Nalpas[d], Jean-Philippe Clément[b], Hervé Bellon[b], Hervé Guillou[f], Gilles Ruffet[d]

[a] *National Oil Corporation of Kenya, Aon Minet Building, Mamlaka Road Off Nyerere Road, P.O. Box 58567, 00200 Nairobi, Kenya*
[b] *UMR CNRS/UBO 6538 « Domaines Océaniques », Institut Universitaire Européen de la Mer, Place Nicolas Copernic, 292890 Plouzané, France*
[c] *Université de Lille 1, Sciences et Technologies, UFR des Sciences de la Terre, UMR 8157 CNRS Géosystèmes, 59655 Villeneuve d'Ascq Cedex, France*
[d] *UMR 6118 CNRS Géosciences Rennes, Université de Rennes 1, Campus de Beaulieu, Bât. 15, 35042 Rennes Cedex, France*
[e] *Institut International de Paléoprimatologie, Paléontologie Humaine: Evolution et Paléoenvironnements, UMR CNRS 6046, Faculté des Sciences de Poitiers, 40, avenue du Recteur Pineau, 86022 Poitiers cedex, France*
[f] *LSCE/IPSL, Laboratoire CEA-CNRS-UVSQ, Domaine du CNRS, Bât. 12, Avenue de la Terrasse, 91198 Gif-sur-Yvette, France*

Abstract

The northern Turkana region of northwestern Kenya forms the intersection between two important rift systems in Africa, the Cretaceous-Paleogene Central African Rift System (CARS) and the eastern arm of the Paleogene-Present East African Rift System (EARS). The southern Sudanese oil producing basins form part of the Cenomanian-Paleogene rifts and their extension into the Anza rift in northern Kenya makes the area of northern Turkana an important target for oil exploration. Reservoirs are an integral part of a petroleum system, the others being the mature source kitchens, effective migration pathways, competent seals, and trapping mechanisms. Limited past exploration activity in the area leaves the study surface outcrops as the main avenue for understanding the reservoir potential of the fluvial deposits of these rift systems. The outcrops of these potential reservoirs, collectively referred to as "Turkana Grits" in the past are represented, on the western side of Lake Turkana, by the Lapur Sandstone Formation in the north, the Muruanachok Sandstone Formation in the central part of the basin and by the Lariu Sandstones in the south. Equivalent grit outcrops on the eastern side of Lake Turkana are represented by the Mount Porr/Sera Iltomia Sandstone Formation.

Radiometric age determination on the basal parts of the Turkana Volcanics have enable the precise dating of the upper parts of the Lapur Sandstone Formation at between 33-37 Ma, while the base of the Formation has been dated as Cenomanian based on the presence of dinosaur bones near the contact with the underlying Precambrian basement. Field observations coupled with subsequent petrographic studies have enable the determination of the diagenetic evolution and the depositional environments for the Lapur Sandstone Formation. The basal and uppermost parts of the formation are interpreted as distal alluvial fan deposits while the middle part is composed of stacked braid channel deposits. The main cement material at the base of the formation is calcite while at the middle of the formation, hematite becomes the dominant cement and at the topmost section, kaolin cement dominates. This distribution of cements is consistent with the palaeoclimatic and palaeogeographic environments that prevailed during the deposition of the formation. During the deposition of the basal parts of the Lapur Sandstone Formation in the Cenomanian, the prevailing climatic conditions were mainly semi arid, which evolved to a predominantly humid conditions during the deposition of the upper part of the formation during Maastrichtian to Eocene/Oligocene. The lack of biostratigraphic data from the LSF however makes it difficult to precisely establish the chronology of the deposition of the formation. The diagenetic evolution of the sandstones has been favourable to the retention of adequate primary intergranular porosity and the creation of secondary intragranular dissolution porosity, mainly through feldspar dissolution and thus preserving the reservoir potential of the Lapur Sandstone Formation. The reservoir characteristics such as the porosity and cementation style of the Lapur Formation are comparable to those of the fluvial sandstone reservoirs of the southern Sudan oil fields and this should positively contribute to the overall petroleum potential of the northern Turkana region. Though the northern Turkana area has remained largely unexplored, it is hoped that the demonstration of the presence of reasonably good reservoir quality sandstones in the Lapur Sandstone Formation which are comparable and possible equivalents of the reservoirs in southern Sudan, will serve to encourage further interest in exploration for oil and gas in the Turkana area.

Keywords: Cretaceous; Eocene-Oligocene; Northern Kenya; Turkana depression; Anza and south Sudan Rifts; East African Rift System; Fluvial sandstone; Sandstone diagenesis; Reservoir potential

Mots-clés : Crétacé; Eocène-Oligocène; Nord Kenya; dépression du Turkana; Rifts d'Anza et du Sud Soudan; Système de Rift Est-africain; Grès fluviatiles; Diagenèse des grès; Potentiel réservoir.

1. Introduction

Thick piles of siliciclastic rocks characterise the northern, central and eastern parts of the African continent and relate to successions of eustatically and tectonically controlled depositional cycles that took place during Paleozoic and Mesozoic (Wycisk et al., 1990; Beauchamp, 1988; Khalifa and Catuneanu, 2008; Wolela, 2008), as well as early Cenozoic (Tiercelin and Lezzar, 2002). Among these periods, the Cretaceous is considered a crucial period for the geological evolution of northern and central Africa, with numerous active rifts linked to the break-up of western Gondwana and the opening of the south and equatorial Atlantic oceans (Guiraud et al., 2005). Thick series of continental deposits, associated with basins belonging to the Central African Rift System (CARS), covered a large part of northern and central Africa during this period (Whiteman, 1970; Prasad, 1971; Vail, 1974; Mateer et al., 1992; Bosworth and Morley, 1994; Morley et al., 1999b) (Fig. 6a). In Sudan, the main continental sedimentary formation of Mesozoic (late Jurassic to late Cretaceous) age is known as the "Nubian Sandstone" (Whiteman, 1970; Vail, 1974, 1982; Schull, 1988; Bussert, 1993) or as the "Nubian Cycles" (Klitzsch and Squyres, 1990) (Fig. 6b). This formation was interpreted as having accumulated in a large sag basin that evolved from isolated half-graben geometries belonging to the rift segments of northern, central and southern Sudan (Jorgensen and Bosworth, 1989; Bosworth, 1992) (Fig. 6b).

In northeastern Kenya, fluvial sandstones, lacustrine carbonates and shales as well as deepwater marine shales were investigated by seismic reflection surveys and several exploration wells drilled in the late 1980s. These deposits relate to the Anza Rift, a large multi-phase rift basin that was active from late Jurassic-Cretaceous to Paleogene time (Winn et al., 1993; Morley et al., 1999b) (Fig. 6b, c). In northern Kenya, at the northwest end of Lake Turkana, a ~500 m-thick pile of sandstones and conglomerates directly overlies the Precambrian basement and is capped by more than 500 m of lava flows designated the "Turkana Volcanics" (Bellieni et al., 1981, 1987; Zanettin et al., 1983) (Fig. 7). These sediments were originally described in the 1930's as part of the "Turkana Grits", a term first used by Murray-Hughes (1933) to refer to a series of hundreds of metres-thick immature siliciclastic sequences directly resting on an eroded and locally faulted surface of basement rocks. The sedimentary formations defined as "Turkana Grits" were identified at several locations in central and northwestern Kenya (Fig. 7):

- The Lubur (Lapur) Series at the northwest end of Lake Turkana (Arambourg, 1943);

- The Muruanachok Sandstone Formation to the west of the central part of Lake Turkana, near the town of Lodwar (Walsh and Dodson, 1969; Morley et al., 1992; Wescott et al., 1993; Morley et al., 1999b; Thuo et al., in prep.);

- The Lokichar and Lothidok Formations to the southwest of Lake Turkana (Boschetto et al., 1992; Morley et al., 1999b);

- The Lariu and Mount Porr-Sera Iltomia Sandstones at the southwest and southeast ends of Lake Turkana, respectively (Savage and Williamson, 1978; Williamson and Savage, 1986; Wescott et al., 1993; Tiercelin et al., 2004);

- The Kimwarer and Kamego Formations in the Kerio and Baringo Basins in the central Kenya Rift (Renaut et al., 1999; Tiercelin et al., 2004).

These "Turkana Grits" were at the time interpreted as having been deposited in lacustrine basins as shown by the presence of features such as current bedding, layers of well-rounded pebbles and calcareous claystones, grits and shales (Walsh and Dodson, 1969). Arambourg (1935) designated the grits occurring to the northwest end of Lake Turkana as the "Lubur Series" from their impressive exposure in the Lapur (Labur or Lubur) Range (Fig. 8). Paleontological evidence, both from vertebrate fossils and fossil wood of *Dryoxylon*

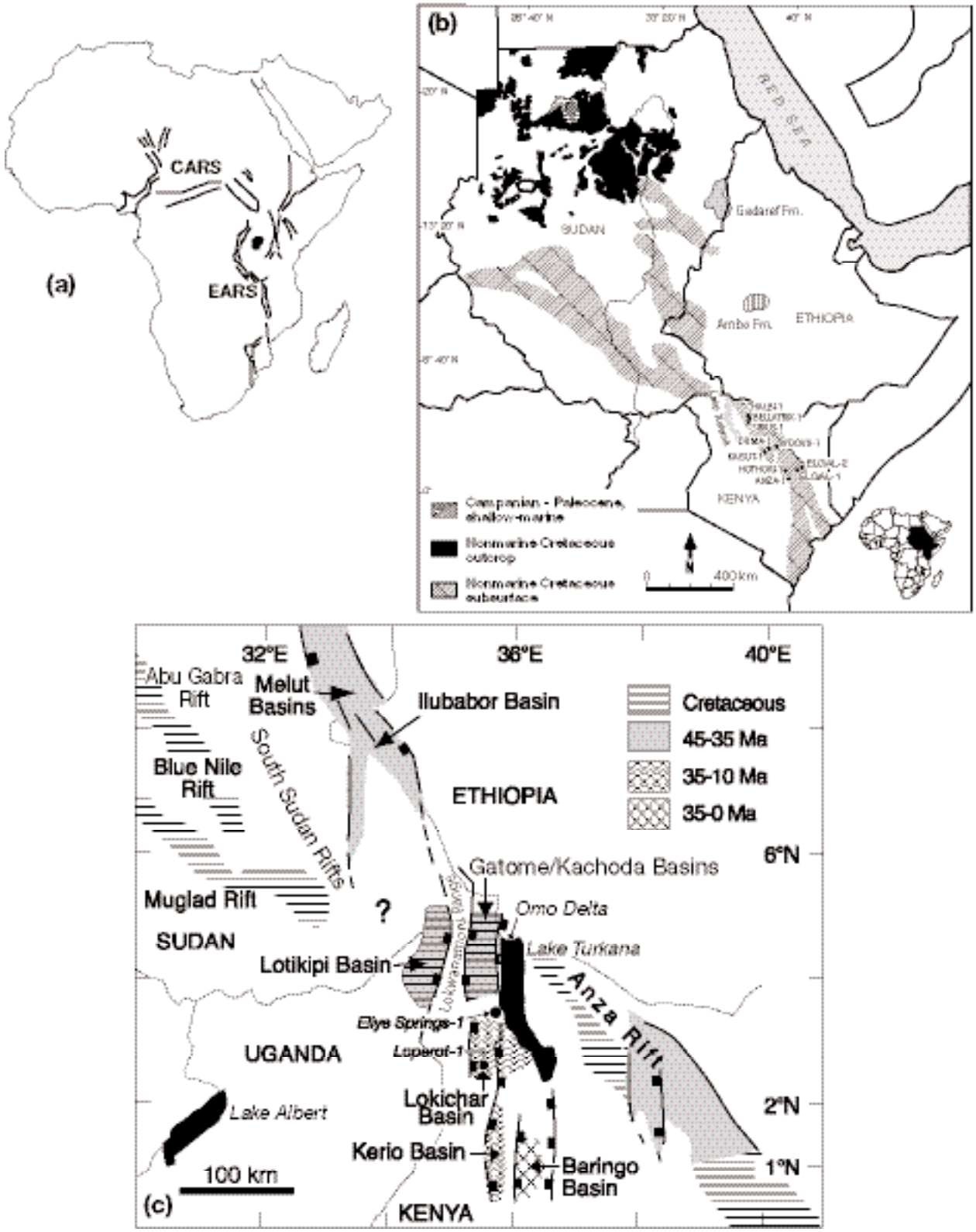
(a)
CARS
EARS
(b)
RED SEA
SUDAN
Gadaref Fm.
Amba Fm.
ETHIOPIA
KENYA
Campanian - Paleocene, shallow-marine
Nonmarine Cretaceous outcrop
Nonmarine Cretaceous subsurface
N
0
400km
32°E
36°E
40°E
Abu Gabra Rift
Melut Basins
Ilubabor Basin
Blue Nile Rift
South Sudan Rifts
ETHIOPIA
Cretaceous
45-35 Ma
35-10 Ma
35-0 Ma
6°N
Gatome/Kachoda Basins
Muglad Rift
?
Omo Delta
SUDAN
Lake Turkana
Lotikipi Basin
Lokwamamoni Basin
Anza Rift
Elye Springs-1
Loparot-1
UGANDA
Lokichar Basin
2°N
Lake Albert
Kerio Basin
Baringo Basin
1°N
100 km
(c)
KENYA

← ***Figure 6.*** *(a) Schematic map of Africa showing the major structures of the Central African Rift System (CARS) and the East African Rift System (EARS). (b) Distribution of surface and subsurface Cretaceous siliciclastic formations in central (Sudan) and eastern (Ethiopia, Kenya) Africa (from Vail, 1974; Beauchamp, 1988). Exploration wells drilled in the Anza Rift, showing occurrences of Cretaceous marine and non-marine sediments, are indicated (from Morley et al., 1999b). (c) Schematic map showing the distribution of Cretaceous(?) to Paleogene-Neogene rift basins in south Sudan and northern-central Kenya. The Loperot-1 well, drilled in the Lokichar Basin, and the Eliye Springs well, drilled in the Turkana/Lothidok Basin, respectively, are indicated (modified from Wescott et al., 1999; Ebinger and Ibrahim, 1994; Tiercelin et al., 2004).*

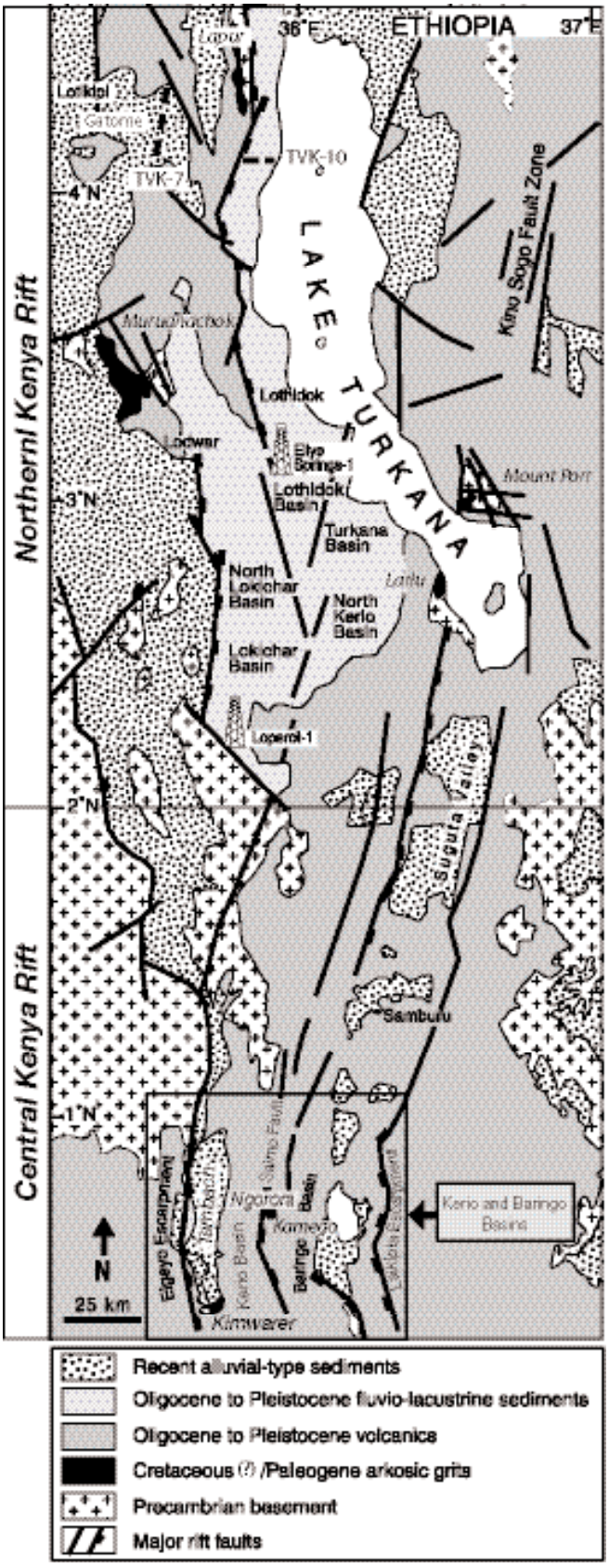

Figure 7. *Regional geology of the north, northwest and central parts of the Kenya Rift, showing the major faults and the metamorphic, volcanic and sedimentary terrains (compiled from Geological Map of Kenya, 1987; Walsh and Dodson, 1969; Wescott et al., 1999). The different "Turkana Grits" formations (Cretaceous(?)-Paleogene): Lapur Sandstone Fm., Muruanachok Sandstone Fm., Lokichar/Lothidok Sandstones, Lariu Sandstones, and Mount Porr Sandstones are indicated. The Loperot-1 and Eliye Springs-1 exploration wells drilled by Shell E & P Kenya B.V., and the seismic lines acquired by Amoco (TVK-7 and TVK-10) are shown.*

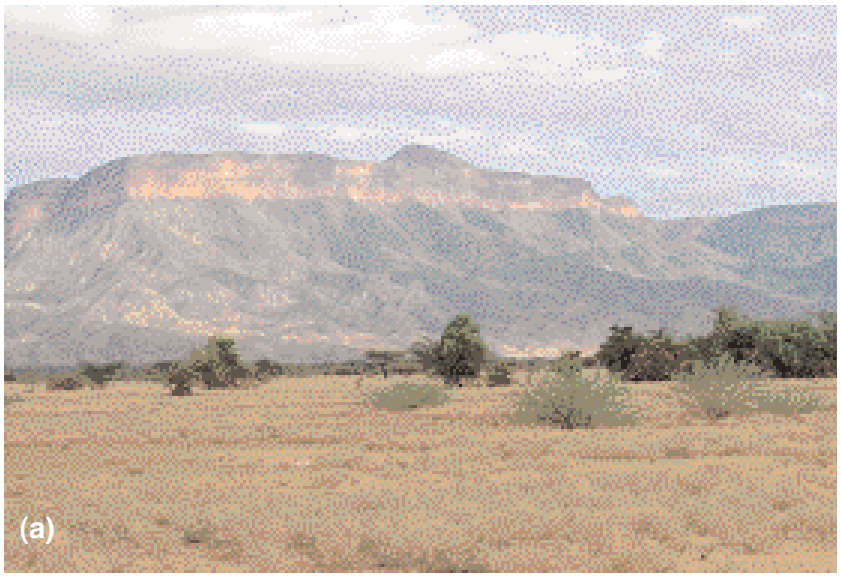
(a)


(b)


(c)


(d)

species, suggested an Eocene to early Miocene or even Cretaceous age for all these sediments (Murray Hughes, 1933; Fuchs, 1939; Arambourg, 1943; Shackleton, 1946). During the 1960's, the "Lubur Series" (named in this paper as the "Lapur Sandstone Formation" or LSF) were briefly described in reports by the Geological Survey of Kenya (Joubert, 1966; Walsh and Dodson, 1969; Dodson, 1971) but has been largely ignored as far as detailed studies are concerned, though mentioned in several papers (Beauchamp, 1977; Zanettin et al., 1983; Savage and Williamson, 1986; Handford, 1987; Morley et al., 1999a; Wescott et al., 1999; Tiercelin et al., 2004).

In the 1980's, following the discovery of large hydrocarbon accumulations in the Cretaceous-Paleogene rifts of southern Sudan (Schull, 1984; Peterson, 1986; Schull, 1988; Mohammed et al., 1999; Mohammed, 2002; Obaje et al., 2004), a phase of aggressive exploration was developed by Amoco Kenya Petroleum Company (AKPC) and later by Shell Exploration & Production Kenya B.V.(SEPK) in the western part of the Turkana Basin. An initial seismic acquisition campaign was conducted in 1984 under the auspices of the Project PROBE (Proto-Rifts and Ocean Basin Evolution) covering the offshore areas of Lake Turkana (Rosendahl et al., 1986; Dunkelman et al., 1988, 1989). Then, an intense onshore seismic reflection survey by AKPC (1985-1986) and the drilling of two exploration wells (Loperot-1 and Eliye Springs-1 by SEPK in 1990-1991) (Figs. 6c and 7) contributed to the imaging of the geometry and stratigraphy of a suite of Cretaceous(?)-Paleogene to upper Miocene half-graben basins to the immediate west of Lake Turkana. Sub-surface data indicated the existence of two deep half-graben basins, the Lotikipi and Gatome Basins (Fig. 6c), partly filled by thick piles of volcanics (up to 2,500 m) and sub-volcanic sedimentary rocks of possible Cretaceous or early Cenozoic age. These sedimentary formations were interpreted as possibly correlative with the "Lapur Sandstone Formation" outcropping to the east (Morley et al., 1999b; Wescott et al., 1999) or with the Muruanachok Sandstone Formation (MSF) that outcrops to the south-south-west (Wescott et al., 1999; Thuo et al., in prep.) (Fig. 7).

The possibility for a positive hydrocarbon potential in these basins (Morley, 1999) was confirmed by the drilling of the Loperot-I well that encountered high TOC potential source rocks and significant oil shows (Wescott et al., 1999; Talbot et al., 2004). This fact together with the proximity of these basins to the southern Sudanese oil-producing fields and the similarity in the structural trends of the two regions (Schull, 1988) (Fig. 6) makes the Lapur Sandstone Formation an important target for oil exploration, particularly in terms of its possible reservoir potential. It is indeed very surprising that a formation of such importance has until now received no more than a casual mention by oil exploration geologists. In this paper, we present the results of the first detailed chronostratigraphic, sedimentologic, petrologic and diagenetic study of a complete section, which is proposed as the "Type Section" of the Lapur Sandstone Formation, LSF. These results are significant as the LSF represents more than 60 million years (more history than, say, the entire East African Rift System) of the palaeogeographic and diagenetic evolution record of this area of northern Kenya. This study provides the necessary basic data set for any potential oil explorers in the Turkana region. It evaluates the depositional

← ***Figure 8.*** *Views of the Lapur Sandstone Formation. (a), (b) General views of the northern half of the Lapur Sandstone Formation, from east (Todenyang Plain) at 04°25'N. The LSF extends from lat. 04°14'N toward the north over more than 50 km, forming the Lapur Range. Almost all along the Lapur Range, the LSF sediments appear resting on a surface of basement rocks (gneiss, migmatites, and amphibolites of Precambrian age) with a tilt of one or two degrees to the south (Walsh and Dodson, 1969). This major range corresponds to the main border fault escarpment bounding the Turkana Rift Basin to the west. (c), (d) Views of the Lapur Range and the LSF from south and east at about 04°18'N. At the Lapur Peak, the LSF outcrops as a very impressive and abrupt cliff about one hundred of m high that culminates at 1620 m elevation. In this part of the Lapur Range, the LSF unconformably overlain the Precambrian basement, mainly formed with amphibolites which show characteristic erosion slope profiles. The whole formation shows a general tilt of 10-15° towards the west/southwest, and disapears rapidly below a thick accumulation of lavas forming the "Turkana Volcanics".*

setting of the LSF, its diagenetic evolution and the reservoir potential as well as the implications of the overall hydrocarbon prospectivity of the northern Turkana region. These results also contribute to a better understanding of the evolution of the Cretaceous-early Cenozoic continental basins in central and eastern Africa, in terms of associated palaeogeography and regional palaeoclimate.

2. Regional geological setting

The Turkana depression is a vast lowland lying at a mean elevation of ~400 m above sea level, where the main geographical feature is Lake Turkana, characterised at its northern end by a wide delta built by the Omo River (Fig. 7). This region has been described as the most important area in eastern Africa for studying a long-lived segment of the East African Rift System and how it interacted with the Cretaceous-Paleogene southern Sudan and Anza rifts (Fairhead, 1986; Morley et al., 1999b). The present-day Lake Turkana Basin is part of a string of major N-S oriented half-grabens that started to develop from Cretaceous(?) through Eocene-Oligocene to Plio-Pleistocene (Mugisha et al., 1997; Morley et al., 1999b; Hautot et al., 2000; Tiercelin and Lezzar, 2002; Tiercelin et al., 2004) (Fig. 6c). The northern end of this basin is a N-S trending half-graben that formed during middle to late Miocene times, following a major phase of volcanic activity dated late Eocene to middle Miocene, that resulted in the deposition of the 2.5 km-thick Turkana Volcanics (Bellieni et al., 1981, 1987; Zanettin et al., 1983; Clément, Bellon et al., work in progress). The structure of the northern half of the Turkana Basin has been partly imaged using offshore reflection seismic data of the PROBE Project (Rosendahl et al., 1986; Dunkleman et al., 1988, 1989) and few seismic lines acquired by Amoco Kenya Petroleum Company (Wescott et al., 1999). The major N-S oriented border faults that delineate to the west the Turkana Rift Basin (morphologically represented by the Murua Rith-Lapur (MRL) fault escarpment) are imaged on the onshore seismic line TVK-10 (Figs. 7, 8 and 9a). Exposed in the footwall of the MRL fault are the Lapur sandstones that overlie Precambrian basement and in turn are overlain by the Turkana Volcanics (Figs. 8 and 9b, sections 1, 2 and 3). The deep basin organization below the Turkana Volcanics is almost unknown because of the considerably degraded quality of seismic data below the subsurface volcanics (Morley et al., 1992; Wescott et al., 1999). Nevertheless, an alternative interpretation of the TVK-10 seismic line is proposed further in this work (see paragraph 4.2.).

To the west of the MRL escarpment, a gravity and seismic survey conducted in 1985 by Amoco Kenya Petroleum Company indicated the presence of two deep-buried, elongate (50 km long; 20 km wide) sedimentary basins, the Lotikipi Basin to the west, and the Gatome Basin to the east, separated by the Lokwanamoru structural high (Figs. 6c and 7). Depth to basement was interpreted to be 4 km and 6 km for the Lotikipi and Gatome Basins, respectively (Wescott et al., 1999; Desprès, 2008). Seismic data over the Gatome Basin revealed one major half-graben basin consisting of a late Eocene-Miocene volcanic sequence (Turkana Volcanics) and pre-volcanics sedimentary rocks overlying Precambrian basement. The structure of the Lotikipi Basin was interpreted either as a rift basin or a thermal sag basin, infilled by the late Eocene-Miocene Turkana Volcanics. Below the volcanics are possible Cretaceous-Tertiary sediments resting on Precambrian basement, resembling to the Lapur Sandstone Formation (Wescott el al., 1999). In terms of regional structure, the two Lotikipi and Gatome Basins appear to be on trend with the basins of the Abu Gabra, Blue Nile and Muglad Rifts in southern Sudan (Bosworth, 1992; Hendrie et al., 1994; Ebinger and Ibrahim, 1995; Wescott et al., 1999) (Fig. 6c). To the east of Lake Turkana, the presence of Cretaceous strata in the Sirius-1 exploration well (Fig. 6b) has suggested similarity between the Anza Rift and the southern Sudan rifts (Bosworth, 1992; Schull, 1988; Morley et al., 1999b). Nevertheless, no direct evidence relates the Lotikipi-Gatome rifting to the Cretaceous-Paleogene south Sudan-Anza rift systems or to the Paleogene northern Kenya-southern Ethiopia segment of the Eastern Branch of the East African Rift System.

3. Field study, sampling and analytical methods

A detailed lithostratigraphic log of the Lapur Sandstone Formation was measured in the field at the southern part of the Lapur Range immediately north of the Lokitaung Gorge (at lat. 04°17'17"N and long. 35°49'08"E) (Fig. 9a), starting near the base of the formation. The logging of the upper part of the formation up to the Turkana Volcanics was completed in the Lokitaung Gorge. A complementary section was measured in the Kerral Laga at lat 04°14'53''N; long. 35°47'54''E (top of the section), representing the upper part of the LSF and the details of the contact between the LSF and the overlying volcanics (Fig. 9a). It took approximately 10 working days in the field to complete the lithostratigraphic section, starting near the base on the first day and then climbing higher up in the section each day. Sampling was extensive and attempted to represent all major lithologies and sedimentary facies. An opportunity was availed to two of us (PT, JJT) when we were invited to be part of a helicopter-supported geological survey conducted in the northwest part of the Turkana depression by the Central African Mining & Exploration Company (CAMEC). The helicopter enabled easy access to the northernmost outcrops of the LSF at the steep cliffs near the Sudan-Ethiopia border at lat. 04°35'58.4"N and long. 35°47'03.9"E. CAMEC has been issued with a production sharing contract (PSC), a license by the Kenya Government to explore for oil in the area designated Exploration Block 11 in the northwestern corner of Kenya.

In order to determine the sedimentologic and diagenetic evolution of the LSF, 54 samples from the sections measured in the Lapur Range, Lokitaung Gorge and Kerral Laga have been studied. Macroscopic observations on hand specimens and microscopic studies on thin sections have been performed at the petrography laboratory of the UMR CNRS 8157 "Géosystèmes", University of Lille 1, France. The thin sections have been made to the standard thickness of 30 Ìm and they have all been impregnated with blue-dyed epoxy resin to allow easier visualization and highlight porosity. Twenty two of these thin sections were subsequently selected for study under SEM. The compositional percentages of the various components were visually estimated on the thin sections. Porosity on selected samples was measured using the Archimedes immersion method (as described in Potdevin and Hassouta, 1997). The thin sections were studied under optical microscopy, cathodoluminescence (CL) and scanning electron microscopy (SEM). We used an Olympus BX 60 petrographic microscope which allows polarized transmitted light and reflected light microscopic observation on the thin sections. A Technosyn cold cathode cathodoluminescence system model MKII 8200 operating at an accelerating voltage of 14.2 kV and a gun current of 220 ÌA, fitted on an Olympus BX40 microscope, was used to study selected samples, especially ones with carbonate cements. A digital Spot RT camera has been used to take photomicrographs of samples in CL and optical microscopic studies. SEM analyses have been conducted using a FEI Quanta 200 Environmental Scanning Electron Microscope (ESEM) fitted with an X-ray Energy Dispersive System (EDS). The tungsten electron source was at 20 kV. The spatial resolution of the EDS probe, a Roentec Single Drift Detector, is about 1 Ìm3. The ESEM has been used here under high vacuum conditions with carbon-coated thin sections to obtain better accuracy on the determination of mineralogical composition using the EDS system.

Isotopic dating was conducted on several lava samples belonging to the Turkana Volcanics, using three different techniques that are presented in the following "Chronological setting" paragraph 4.1.. Petrographic analyses were conducted on thin sections to identify the type of lava and determine the degree of alteration before dating. This process was completed by geochemical analyses using an inductively coupled plasma-atomic emission spectroscopy (ICP-AES) mainly conducted at UMR CNRS 6538 "Domaines Océaniques", Université de Bretagne Occidentale, Brest, France.

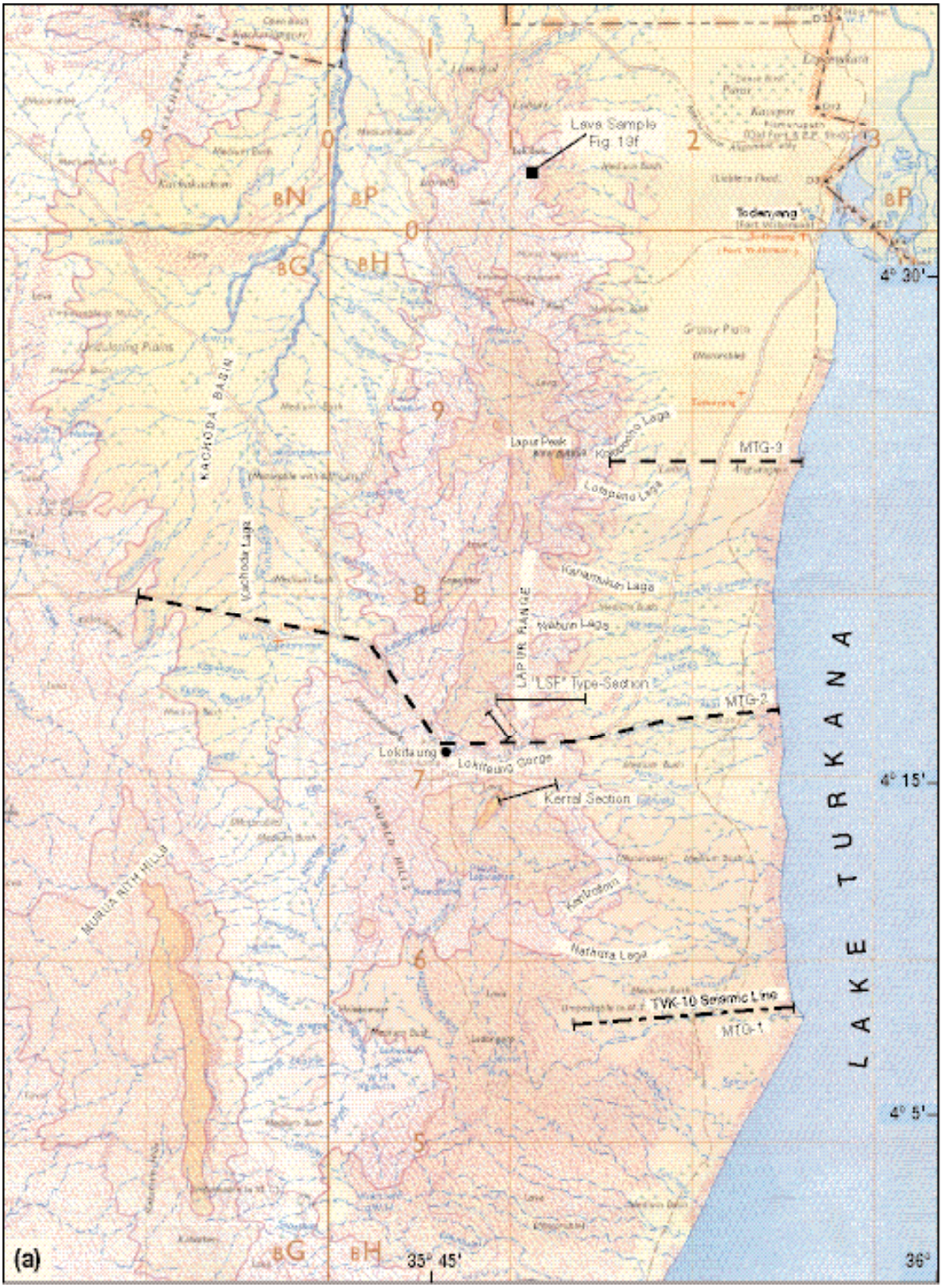

Figure 9. (a) *Topographic map (scale 1:250,000) of the northwest part of the Turkana Rift Basin showing the Murua Rith-Lapur Range, that corresponds to the western faulted border of the Turkana rift basin. On the west side of the map is the Kachoda Basin, which appears to be a small, N-S oriented faulted basin parallel to the main Lotikipi and Gatome Basins (see Fig. 6c). Names and location of major lagas (laga is the Turkana expression used for ephemeral streams) and sites/geological sections used in the text are indicated.*

(b)

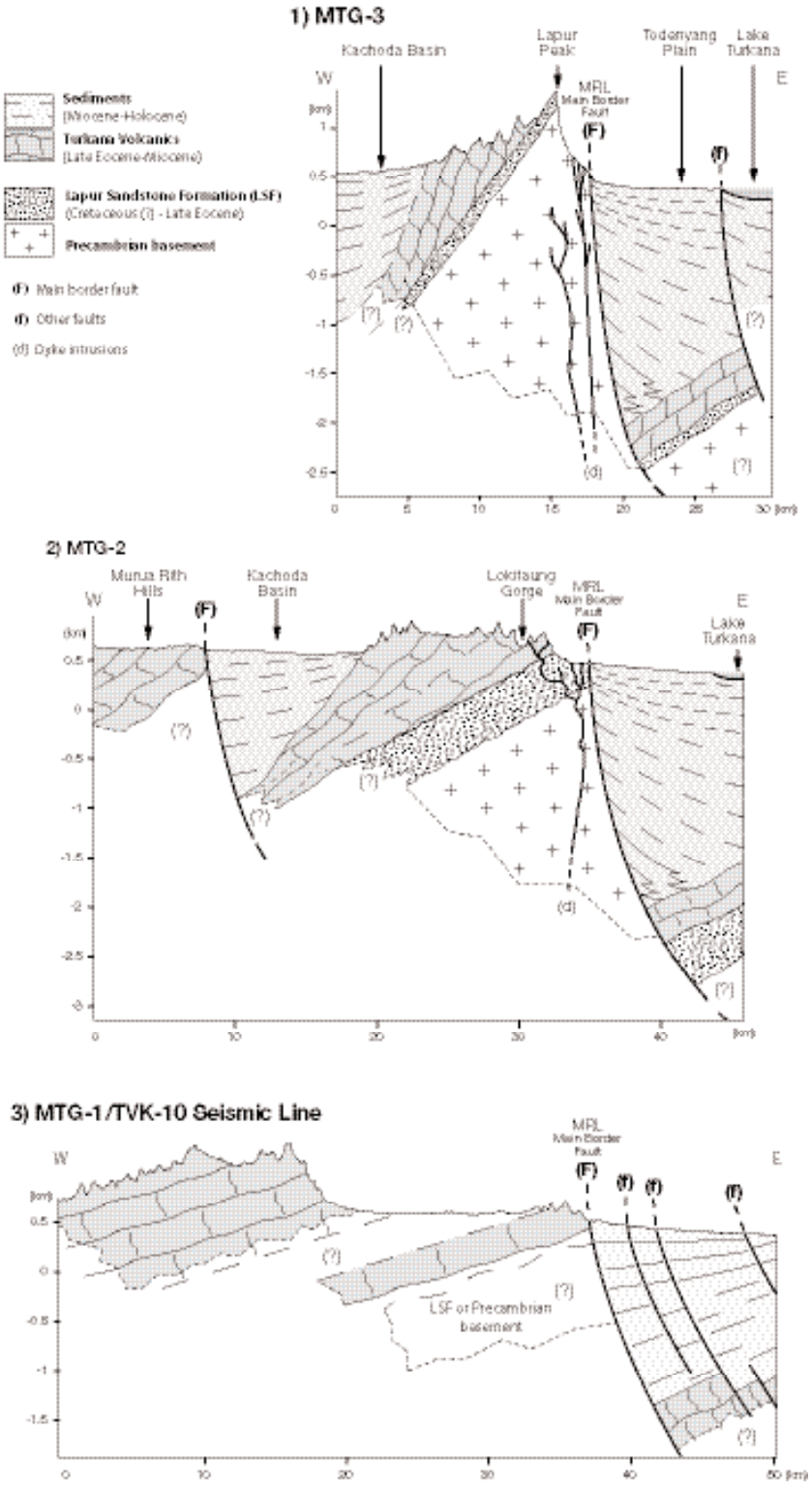

Figure 9. (b) *Schematic geological cross-sections, from south to north, across: (1) MTG-1 Profile: the Lapur Range and the western side of the Lake Turkana Basin, through the Todenyang Plain at 04°25'N; (2) MTG-2 Profile: the Kachoda Basin, the Lokitaung Range and Gorge, and the Lowarengak alluvial plain; (3) MTG-3 Profile: the Lake Turkana alluvial plain immediately west of the Murua Rith-Lapur Range. This cross-section strictly follows the trace of the TVK-10 seismic line (Amoco Kenya Petroleum Company). These sections have been constructed on the base on fieldwork (for the surface interpretation), and seismic (Wescott et al., 1999) and magnetotelluric and gravity data (Abdelfettah, 2009) for the subsurface interpretation of the MTG-2 and 3 lines. The subsurface interpretation of the MTG-1 line is in this figure only based on the interpretation of the TVK-10 seismic line by Wescott et al. (1999). An other interpretation is presented further on Figure 19b.*

4. The Lapur Sandstone Formation

The Lapur Sandstone Formation (LSF) forms impressive outcrops along the northern part of the Murua Rith-Lapur Range from Kerral and the Lokitaung Gorge at about lat. 04°17'N. In this area, the succession of strata forms steep hills with a gentle dip of 10-15° to the west, up to the region of the Lapur Peak to the north where it corresponds to the most prominent and impressive topographic feature, the Lapur Peak cliff, at about 04°25'N, that culminates at an altitude of ~1400 m and is not really accessible due to thick vegetation cover and the steepness of the valleys and gorges in front of the cliff as one approaches from Todenyang side (Figs. 8 and 9a). This abrupt change in morphology corresponds to an uplifted footwall block bounded to the east by the N-S-trending Murua Rith-Lapur (MRL) extensional faults that form the main western border of the Miocene Turkana Rift Basin. Small outcrops of sandstones, representing the southernmost occurrence of the LSF, occur further south, at Keniroliom (04°11'10"N; 35°49'41"E) (Fig. 9a). In this area, beds of conglomerate, sandstone and sandy claystone up to 10 m thick are strongly tilted (up to 40° to the west) or sometimes appear nearly vertical. They are affected by numerous faults with minor throw and they are intensely cut by volcanic dykes measuring up to 6-m in width (mainly oriented N0°, N30° and N160°) and also intruded by volcanic sills. Immediately north of the Lokitaung Gorge (04°17'18''N; 35°49'08''E), the LSF type-section outcrops prominently on steep hills, with beds dipping 10-15° to the SSW (Fig. 9a). The measured section commenced at lat. 04°17'18"N; long. 35°49'08"E, and terminated at lat. 04°17'10"N; long. 35°48'24"E, covering a total thickness of 485 m (Figs. 10 and 11a-e; North Lokitaung Gorge). The upper part of the section was completed in the Lokitaung Gorge at lat. 04°17'04''N; long. 35°48'36''E. This part of the section, was 90 m thick, and it terminated at the contact with lava flows of the Turkana Volcanics and is well exposed on the right bank of the Lokitaung Laga at lat. 04°15'02''N; long. 35°48'04"E (Lokitaung Gorge) (Figs. 10 and 11e). Complementary observations have been conducted a few km south, in the Kerral Laga (04°14'53''N; 35°47'54''E), where only the upper part of the LSF is visible as a result of the general SSW dip of the formation (Figs. 9a and 12; Kerral Section). In the area immediately north of the Lokitaung Gorge, the lowermost section of the LSF is intensely affected by minor faults mainly oriented N-S that are associated to the major MRL rift border fault. These faults delineate numerous small tilted blocks showing varying dip directions, from east to west or southwest. Here, the sandstones are also intruded by a large number of 1- to 10-m wide volcanic dykes, mainly oriented N60° to N110°.

Towards the north, at the Kanamukun and Nabuin lagas (04°20'00"N; 35°49'12"E), the LSF overlies a surface of Precambrian basement rocks (Figs. 8a-d and 9a). This contact is gently undulating and the surface of basement shows a tilt of one or two degrees to the south, which was interpreted as a pre-sedimentation tilting (Fuchs, 1939; Walsh and Dodson, 1969). Farther north, between Laga Kolobocho (04°23'23"N; 35°53'14"E) and Laga Lotapeno (04°24'39"N; 35°50'12"E) in the area of the Lapur Peak (Fig. 9), the Lapur sandstones unconformably overlie Precambrian amphibolites and migmatites (Walsh and Dodson, 1969) (Fig. 8c, d).

4.1. Chronological setting of LSF

The chronologic position of the Lapur Sandstone Formation has been up to now inferred from the facts that: 1) it overlies basement of Precambrian age; 2) it is overlain by the Turkana Volcanics which have been radiometrically dated; and 3) from the discovery in the lowest parts of the formation of silicified fossil

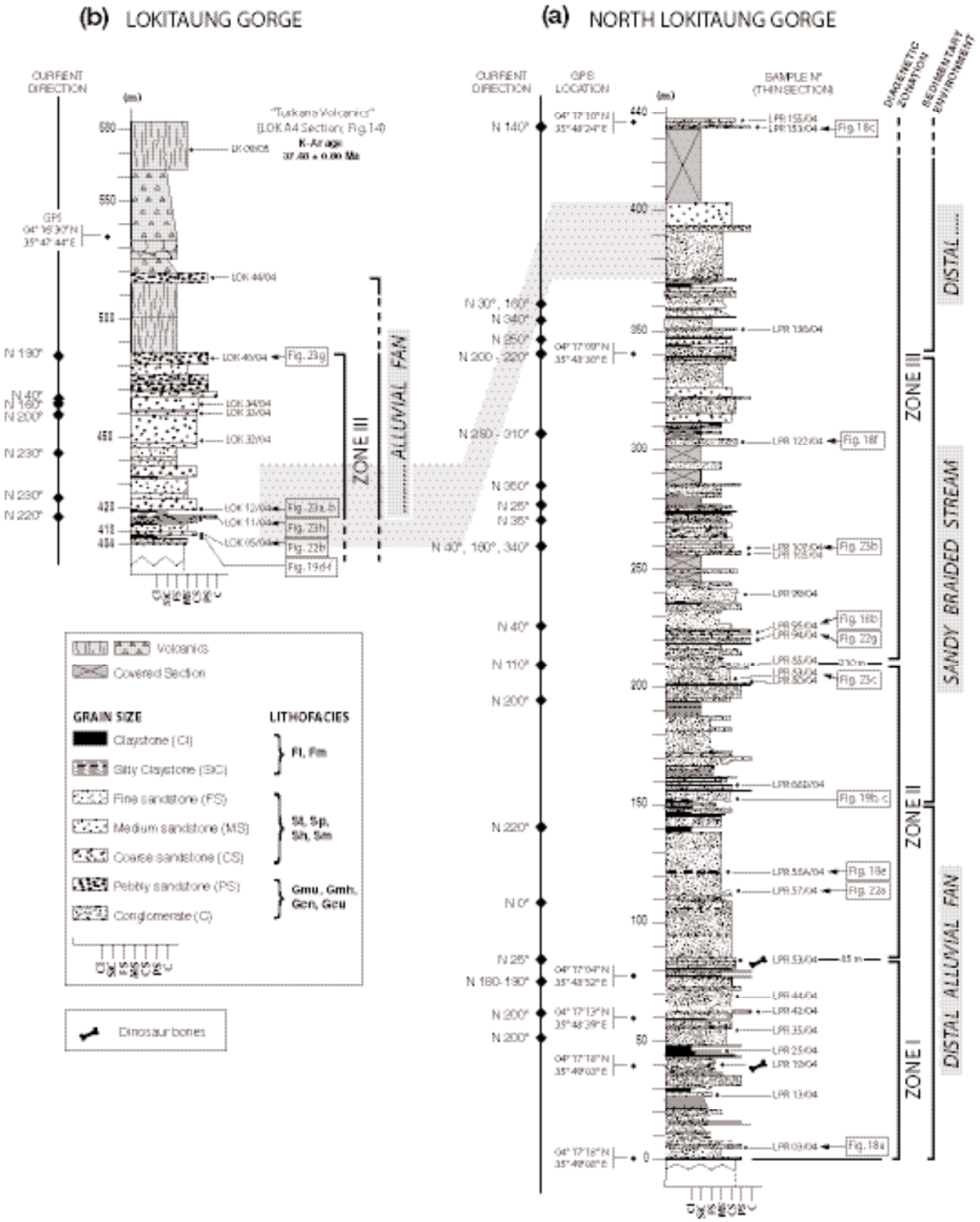

Figure 10 *. Lithostratigraphic logs of the Lapur Sandstone Formation: (a) immediately north of the Lokitaung Gorge (type-section); (b) the upper parts of the formation have been described in the central part of Lokitaung Gorge, up to the contact with the Turkana Volcanics (See Fig. 9a). The sedimentologic nomenclature follows standard granulometry scale from claystone as the finest to conglomerate as the coarsest.*

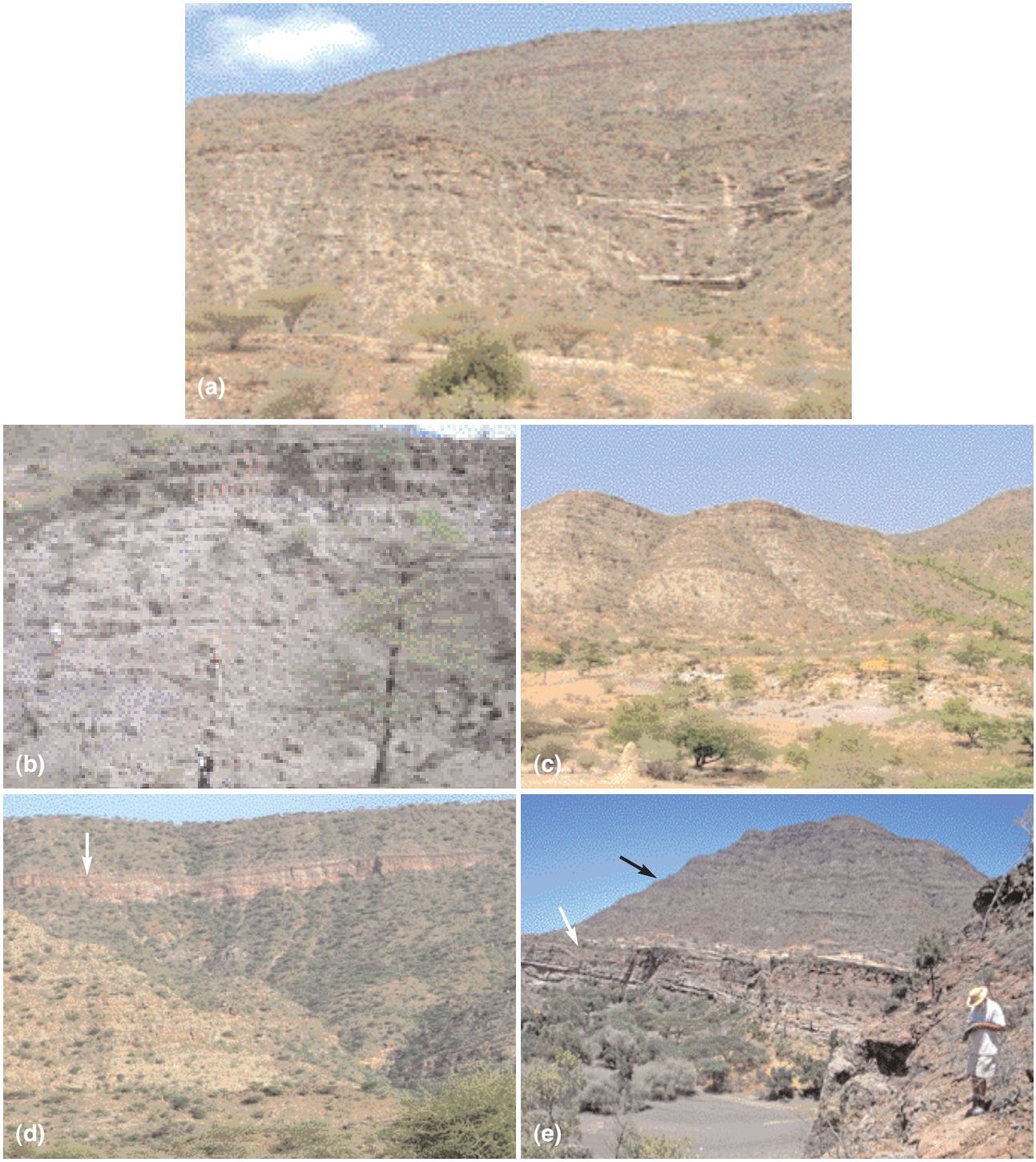

Figure 11 *. The Lapur Sandstone Formation at the type-section, immediately north of Lokitaung Gorge (See Fig. 9). (a) View of the middle and upper terms of the LSF from the 90 m mark up to the 440 m mark on the North Lokitaung section (See Fig. 10a). (b) Lowest terms of the LSF, formed by purple, white nad grey arkosic sandstones and conglomerates at base, overlain by (c) Yellow ochre fine sands that contain fragmented dinosaur remains. The steep slope of the hill is formed by alternating sandstone beds of metric to decametric size. (d) Near the top of the hill is visible the several tens of m thick sandstone and conglomerate bar that forms the "multicolour cliff" that can be followed over kms in the landscape (See black arrow on photo (a)). (e) View of the upper part of the LFS, in the Lokitaung Gorge, showing the multicolour cliff overlain by the 500 m thick pile of Turkana Volcanics.*

tree trunks and poorly preserved dinosaur bones. Understanding the chronology of the of the LSF, which has not been studied in detail before this work, will help in reconstructing the palaeogeography of the Turkana depression from Cenomanian to early Oligocene and this understanding is essential for evaluating the hydrocarbon potential of the region.

The first geologist to assign an age to the LSF was Murray-Hughes (1933), who considered the "Turkana Grits" to be of Jurassic age. Then, Arambourg (1935) correlated the Lapur Sandstone Formation with the Adigrat Sandstone of Ethiopia that range from upper Triassic to middle Jurassic (Dodson, 1971; Garland, 1980; Bosellini et al., 2001; Getaneh, 2002; Wolela, 2008) (Fig. 1a). On the basis of dicotyledonous fossil trees found in the area of the Lokitaung Gorge, Fuchs (1943) ruled out age older than Cretaceous and suggested an Oligocene-Miocene deposition. He also mentioned the discovery of remains

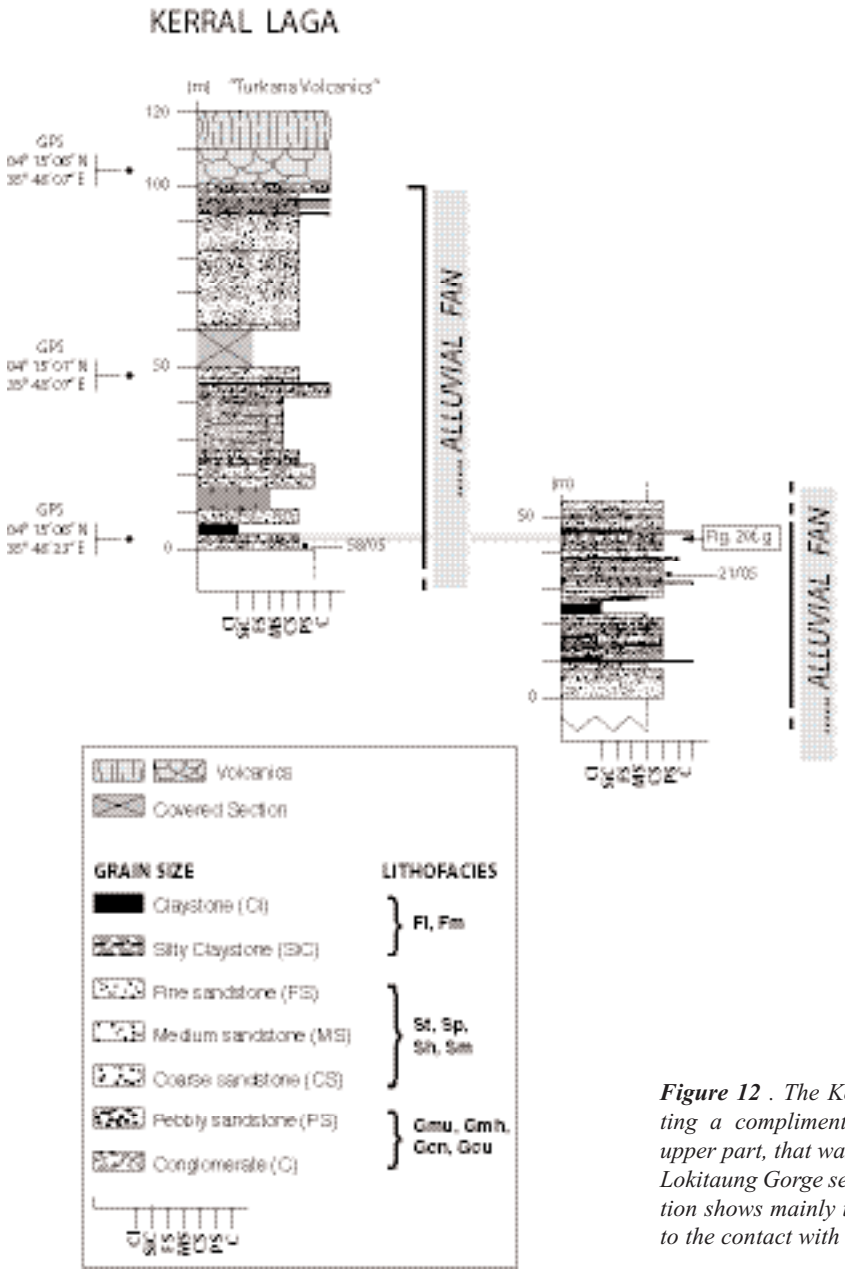

Figure 12 *. The Kerral Laga section, representing a complimentary log of the type-section, upper part, that was measured to the south of the Lokitaung Gorge section (See Fig. 11e) . The section shows mainly the upper parts of the LSF up to the contact with overlying Turkana Volcanics.*

of leaves, that were not identified because they were too fragmentary. Arambourg (1943) disagreed with this Oligocene-Miocene age and concluded later on the basis of fossil evidence "the discovery of dinosaur bones and angiosperm wood in the area of the Lokitaung Gorge" that the age of the Lapur Sandstone Formation was Cenomanian to basal Paleocene (Arambourg and Wolff, 1969). The dinosaur bones in the LSF have so far only been reported in the lower part of the formation at the type-section (Figs. 10a and 11c). The poor state of preservation of the bones may suggest reworking and, as a consequence, the age for the lower part of the formation cannot be defined as precisely Cenomanian. More recently, Beauchamp (1977, 1988) compared the Lapur sandstones to the fluvial Ambo Sandstone in central Ethiopia, which is dated upper Jurassic-Cretaceous on the basis of fossil wood. Another probable equivalent of the LSF is the "Nubian Sandstone Formation" of Sudan, locally identified to be early Cretaceous (Neocomian) (Edwards, 1926; Whiteman, 1970, 1971; Vail, 1974; Beauchamp, 1988; Schull, 1988; Salama, 1997) or Maastrichtian, e.g. the "Gedaref Formation" of eastern Sudan (Klitzsh and Squyres, 1990; Eisawi and Schrank, 2009) (Fig. 6b). In northwest Sudan, fluvial deposits of lower Cretaceous age conformably overlie Precambrian basement (Wycisk et al., 1990) and are unconformably overlain by fluvial deposits of Cenomanian to Santonian(?) age (Mateer et al., 1992).

From Kerral in the south to the area north of the Lapur Peak (Fig. 9a), the upper parts of the LSF are overlain by a 500-m thick pile of flood basalts, mainly quartz and olivine tholeiites, designated the Turkana Volcanics by Bellieni et al. (1981, 1987) and Zanettin et al. (1987) (Fig. 13a). At lat. 04°16'04"N, long. 35°47'34"E, on the right bank of the Lokitaung Gorge, basaltic flows overlie, in stratigraphic contact, the upper beds of the LSF (Figs. 9a, 12, 13a and 14a; see lithostratigraphic section LOK A). In the same area, other sections show lavas stratigraphically overlying LSF sandstones (Figs. 9a, 13b and 14a; see lithostratigraphic sections LOK A1 and A2) as well as alternating sandstone beds and lava flows (Figs. 9a and 14a-d; see lithostratigraphic sections LOK A3 to A7). At the LOK A3 section on the left bank of the Lokitaung Gorge (lat. 04°16'30"N; long. 35°47'44"E) (Fig. 14a), a 30-m thick basaltic flow overlies several metre-thick beds of yellow-beige sandstones. In the upper part of the lava pile occurs an interbedded 4-m thick dark grey, horizontally bedded conglomeratic sandstone. In the lower part of this conglomeratic sandstone bed, well-rounded pebbles and cobbles up to 20 cm in diameter of grey green basalt similar to the underlying lava are embedded, together with subangular to rounded clasts of quartz (Fig. 13c). The presence of basalt clasts within this conglomeratic sandstone indicates erosion and reworking processes of underlying lava flows by post-eruption fluvial dynamics. Similar observations of Lapur sandstones being interbedded with lavas forming the lower parts of the Turkana Volcanics have been made at different locations in the Lokitaung Gorge area (Fig. 14). This confirms earlier field observations by Walsh and Dodson (1969; page 14) who said that "deposition of the sediments continued sporadically after the onset of volcanism, and sandstones and sandy clays are intercalated in the lower-most lavas".

The contact between LSF and the Turkana Volcanics can be seen all along the Lapur Range (Figs. 9a and 13d, e) up to north of the Lapur Peak where only a few meters of volcanics (mainly a fine-grained basalt) are seen overlying reddish sandstones which rest on Precambrian basement (Figs. 9a and 13f). A slight angular unconformity between the upper parts of LSF and the lower flows of the Turkana Volcanics is visible at the field scale in the Lokitaung Gorge (Fig. 15a). This angular unconformity between the Turkana Volcanics and early rift sedimentary rocks of Paleogene or Cretaceous age can be tentatively interpreted on the TVK-7 reflection seismic line (Amoco Kenya Petroleum Company) that crosses the Gatome Basin to the immediate west of the study area (Wescott et al., 1999; fig. 6, p. 59) (Fig. 15b).

The base of the Turkana Volcanics was dated at around 33 Ma by Bellieni et al. (1981), based on one sample of trachyte collected north of Muruanachok. Two basalts sampled along the Lokitaung Gorge provided

K/Ar ages of 30.4 ± 1.5 and 29.6 ± 4.4 Ma, respectively (Bellieni et al., 1981; Zanettin et al., 1983) (Fig. 7). Other age measurements resulted from Amoco Kenya Petroleum Company field work and indicate values between 37 and 29 Ma (Morley et al., 1992; 1999b, fig. 2, p. 22). Several new K/Ar ages and one Ar-Ar age have been obtained on samples collected during successive field trips (2002, 2004, 2005, and 2008) at different sections in the Lokitaung Gorge and at the north end of the LSF (Figs. 13 and 14a). At section LOK A on the right bank of the Lokitaung Gorge (lat. 04°16'04"N; long. 35°47'34"E) (Figs. 13b and 14a), a 20-m thick quartz-tholeiite flow characterized by large columnar jointing (sample LAP 02/09B) (Clément, Bellon et al., work in progress) (Tables 5 and 6) immediately overlies the upper beds of the LSF. A second 20-m thick quartz-tholeiite flow (Table 5) showing large columnar jointing and tore cooling structures (sample LAP 02/09A; collected at 04°16'13.2"N; 35°47'18.8"E) (Tables 5 and 6) overlies the LAP 02/09B flow (sample collected at 04°16'06"N; 35°47'19"E). The contact between these two flows is undulating and underlined by a several m-thick malachite-rich breccia (Fig. 13g). These two lavas have been dated at 33.57 ± 1.88 Ma for the LAP 02/09B sample, and 32.77 ± 1.84 Ma for the LAP 02/09A sample (Table 7a). In the LOK A2 section (04°16'04"N; 35°47'34"E), up to 55 m of basaltic lavas and breccias overlie LSF sandstones. These sandstones can be correlated with the sandstones at the base of LOK A section. On top of this basaltic pile is the LAP 02/09B quartz-tholeiite flow dated 33.57 ± 1.88 Ma (Fig. 14a). In the LOK A3 section (04°16'30"N; 35°47'44"E) (Fig. 14a), a 10-m thick olivine tholeiite flow (sample LK 45/04) (Tables 5 and 6) occurs 5 m above the upper-most LSF bed. This lava has been dated 35.23 ± 0.74 Ma using the Cassignol Method (Table 7b). At section LOK A4, close to LOK A3, a 65-m thick pile of basaltic flows overlies the upper-most LSF bed described in section LOK A3 (Fig. 14a). The 20-m thick upper-most lava flow (sample LK 09/05) in this section is dated 37.48 ± 0.80 Ma (Table 7b).

A sample from a thin basaltic flow immediately overlying the upper beds of the LSF at the extreme north end of the Lapur Range was collected during the 2008 CAMEC fieldtrip at lat. 04°32'45"N; long. 35°46'35" (section LOK A8; Figs. 9a, 13f and 14a). This rock was dated at 35.60 ± 0.80 Ma (Ar-Ar) (Ruffet, unpublished report, 2008). According to these isotopic ages obtained from 4 geological sections in the Lokitaung Gorge and at the north end of the Lapur Range, the uppermost terms of the Lapur Sandstone Formation appear to have been deposited between 37 and 33 Ma (upper Eocene to lower Oligocene), contemporaneously with the early flows of the Turkana Volcanics. The tentative interpretation of stratigraphic correlation between the different sections presented Figure 14 demonstrates onlap-toplap relationships between the lowermost lava flows of the Turkana Volcanics and the upper LSF beds. With a possible Cenomanian(?) age at its base and an upper Eocene-lower Oligocene age at its top, the Lapur Sandstone Formation reflects a long (up to 60 millions years) and probably complex depositional history. Lithofacies, sedimentary structures and architectural element analysis presented farther on will help to differentiate successive depositional sequences.

Several non-stratigraphic contacts have also been observed between the upper terms of LSF and lavas. On the right bank of the Lokitaung Gorge, the LOK A7 section (Fig. 14b) shows a 14-m thick lava bed (sample LAP 02/05) interbedded between several metres thick sandstone beds forming the topmost part of LSF. This lava, which is interpreted as a sill, corresponds to a strongly altered basanite (with loss on ignition (LOI) of 4.87 %) showing 2-6 cm thick dykelets of amphibole-rich material (Tables 5 and 6). The upper sandstone beds are in turn overlain by up to 10-m thick lava flows showing rough columnar jointing or spheroidal weathering. To the south, in the Kerral Laga, the LOK A5 section (lat. 04°14'53"N; long. 35°47'54"E) (Figs. 9a and 14b) shows a 9-m thick lava bed interbedded between metre-thick sandstone beds that are in turn overlain by a succession of lava flows several tens of metres in thickness. The interbedded lava (sample KER 63/05), also interpreted as a sill, connects laterally to a 0.50-m thick lava dyke (sample KER 64/05) that crosscuts the lower sandstone beds (Fig. 16a, b). They both form a single intru-

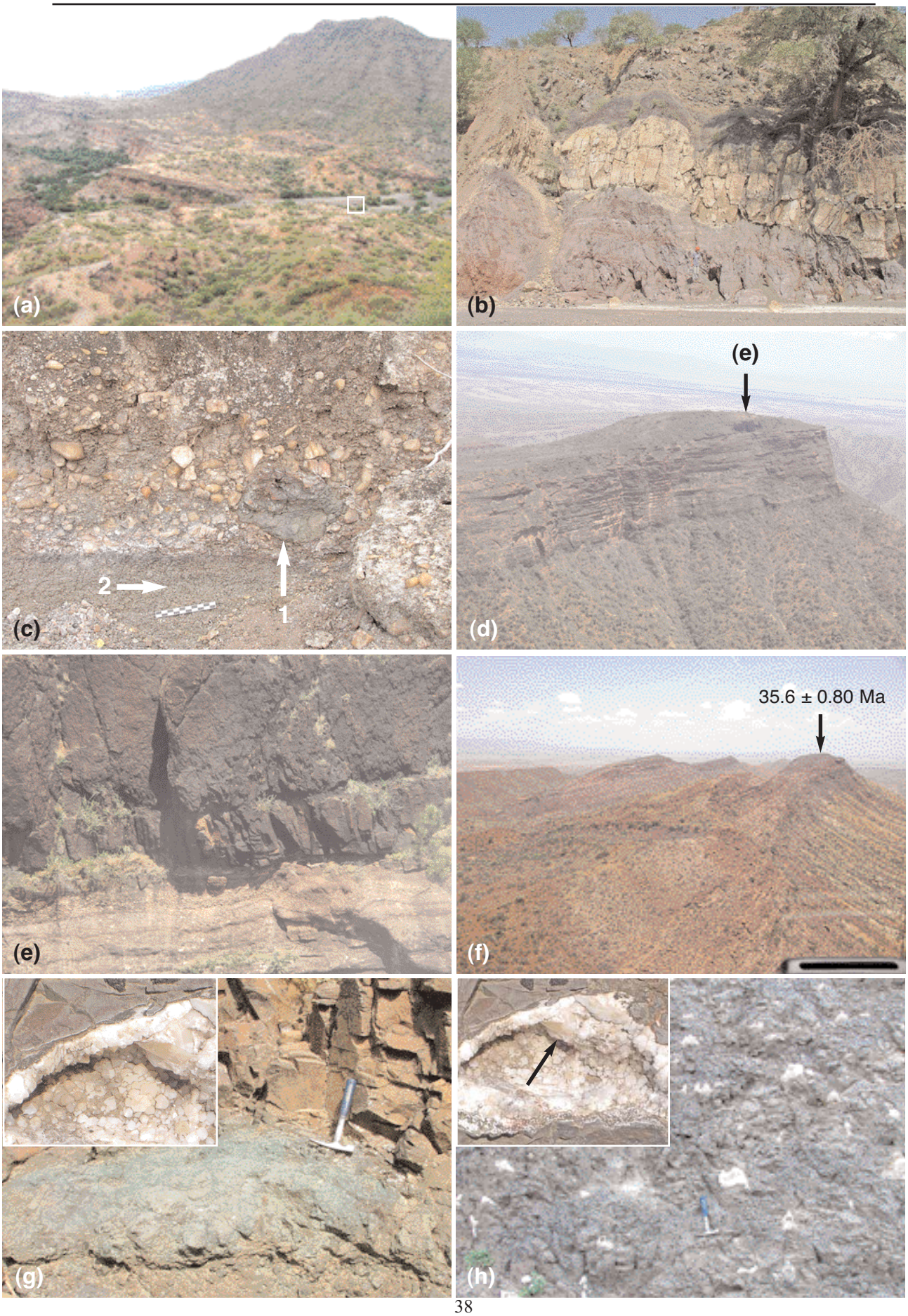
(a)
(b)
(c)
2
1
(d)
(e)
(e)
35.6 ± 0.80 Ma
(f)
(g)
(h)

sive system visible within the upper parts of the LSF. These two lavas are petrographically and geochemically similar. They are intensively altered basaltic rocks showing mainly secondary calcite and brown clays. Plagioclase, clinopyroxene and olivine phenocrysts can still be recognized within KER 63/05 sample whereas KER 64/05 is totally altered (Tables 5 and 6).

Many other dykes of various trends (N0°, N50-70°, N90°, N160°) and widths (from a few decimeters up to 10 m) as well as sills have been observed to crosscut the LSF and to intersect each other at Keniroliom, Kerral, Lokitaung Gorge areas (Fig. 16c-f). In the Lapur Peak area, a few narrow basaltic dykes (max. 0.80 m wide) were seen intruding the amphibolitic basement (Fig. 16g, h). Dating such dykes has been difficult because of the deep alteration of the rocks. Nevertheless, in the Kerral area, one of the largest dykes - ~10 m wide, several hundreds of m long, trending N60° - and which is seen crosscutting the middle and upper terms of LSF (Fig. 16c, d), is a relatively fresh lava (sample KER 65/05 collected at lat. 04°15'01"N; long. 35°48'23"E) which has been geochemically characterised as a tephrite. It has been dated 27.03 ± 0.57 Ma (Tables 5, 6 and 7b). This lava is of similar age to that of the 15-m thick tephrite flow sampled in the upstream part of the Lokitaung Gorge, near the town of Lokitaung at lat. 04°15'43"N; long. 35°45'23"E (sample LAP 02/13D), which is dated 27.81 ± 0.65 Ma (Fig. 14; section LOK A) (Tables 5, 6 and 7a). Other volcanics of similar age have been characterised within the Turkana Volcanics south of the Lokitaung Gorge (Nathura Laga section; lat. 04°10'02''N; long. 35°47'32''E; Fig. 9a), where they are represented by rhyolitic sills and dykes (samples NATH 08/04 and 09/04) that have been dated 28.73 ± 0.64 Ma and 27.40 ± 0.66 Ma, respectively (Clément, Bellon et al., work in progress) (Table 7a). These data suggest volcanic phases of upper Oligocene age marked by the emplacement at the base of Lapur sandstones of intrusive bodies (dykes and sills) and overlying lava flows, both characterised by silica undersaturated (tephrites) or silica supersaturated lavas. New geochemical studies will confirm whether or not those lavas may belong to the same magmatic phase (Clément, Bellon et al., work in progress).

4.2. Structural framework of LSF at the scale of the Turkana depression (Figs. 9b and 17)

The Lapur Range (Fig. 8), an impressive 50 km-long range, is the only place where, at outcrop level, the Lapur Sandstone Formation can be seen and its proper stratigraphic position identified. Due to its general dip to the W-SW, exposures of the LSF disappears rapidly below the overlying Turkana Volcanics (Figs. 8 and 9b). Farther to the west (Fig. 7), in the Gatome and Lotikipi Basins, poorly imaged sub-volcanic strata have

← ***Figure 13.*** *Photographs of various sites and geological sections showing the different types of contacts between the Lapur Sandstone Formation and the Turkana Volcanics. (a) General view from the left side of the Lokitaung Gorge of the upper parts of LSF (white arrow) overlain by a ~500-m thick pile of Turkana Volcanics (black arrow). The small white box on the right side of the photograph shows our Land-Rover, for scale. (b) Detailed view of the stratigraphic contact between the upper terms of the LSF and the lowermost flows of the Turkana Formation. Right bank of the Lokitaung Gorge at 04°16'04''N, 35°47'34''E (LOK A2 section; Fig. 14). (c) Detailed view of LOK A3 section (see Fig. 14). At the base of this conglomeratic sandstone bed, subangular to well-rounded pebbles and cobbles of grey green basalt (white arrow, 1) similar to the underlying lava (white arrow, 2) are seen to be reworked within quartz pebbles. (d)-(f) Residual basaltic flows (black arrows) unconformably overlying the upper terms of the Lapur Sandstone Formation at Lapur Peak and northward. The fine-grained basalt that unconformably overly the upper terms of LSF at the north end of the Lapur Range has been dated (Ar-Ar) 35.6 ± 0.80 Ma. (g) Malachite-rich breccia between the two first basaltic flows that overlain the upper-most terms of LSF, dated 33.57 and 32.77 Ma, respectively (See Fig. 14; LOK A section). (h) Quartz + calcite-rich (white arrow) geodes in basaltic lava, Lokituang Gorge section (See Fig. 14; LOK A section).*

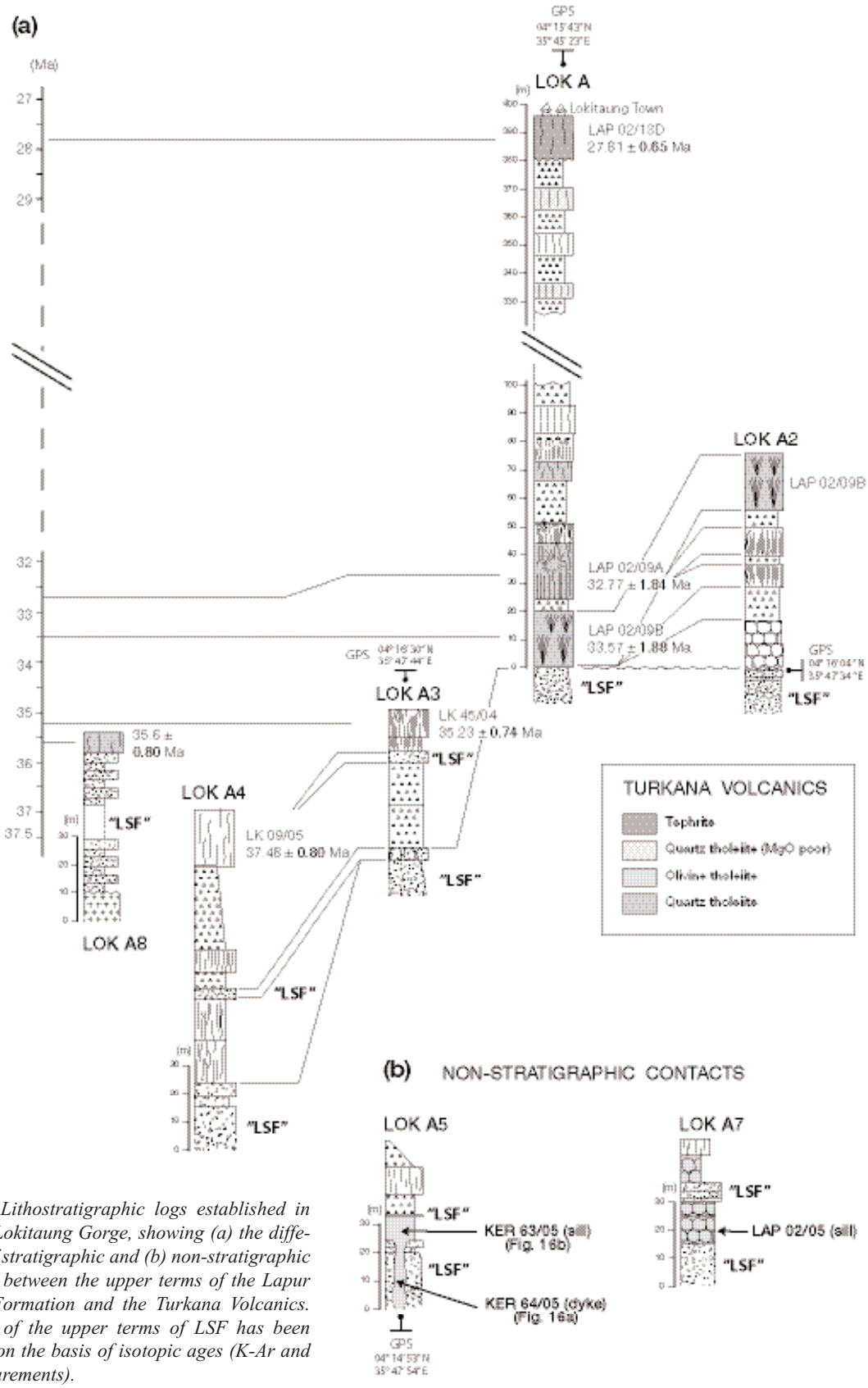

Figure 14. *Lithostratigraphic logs established in the central Lokitaung Gorge, showing (a) the different types of stratigraphic and (b) non-stratigraphic (b) contacts between the upper terms of the Lapur Sandstone Formation and the Turkana Volcanics. Chronology of the upper terms of LSF has been established on the basis of isotopic ages (K-Ar and Ar-Ar measurements).*

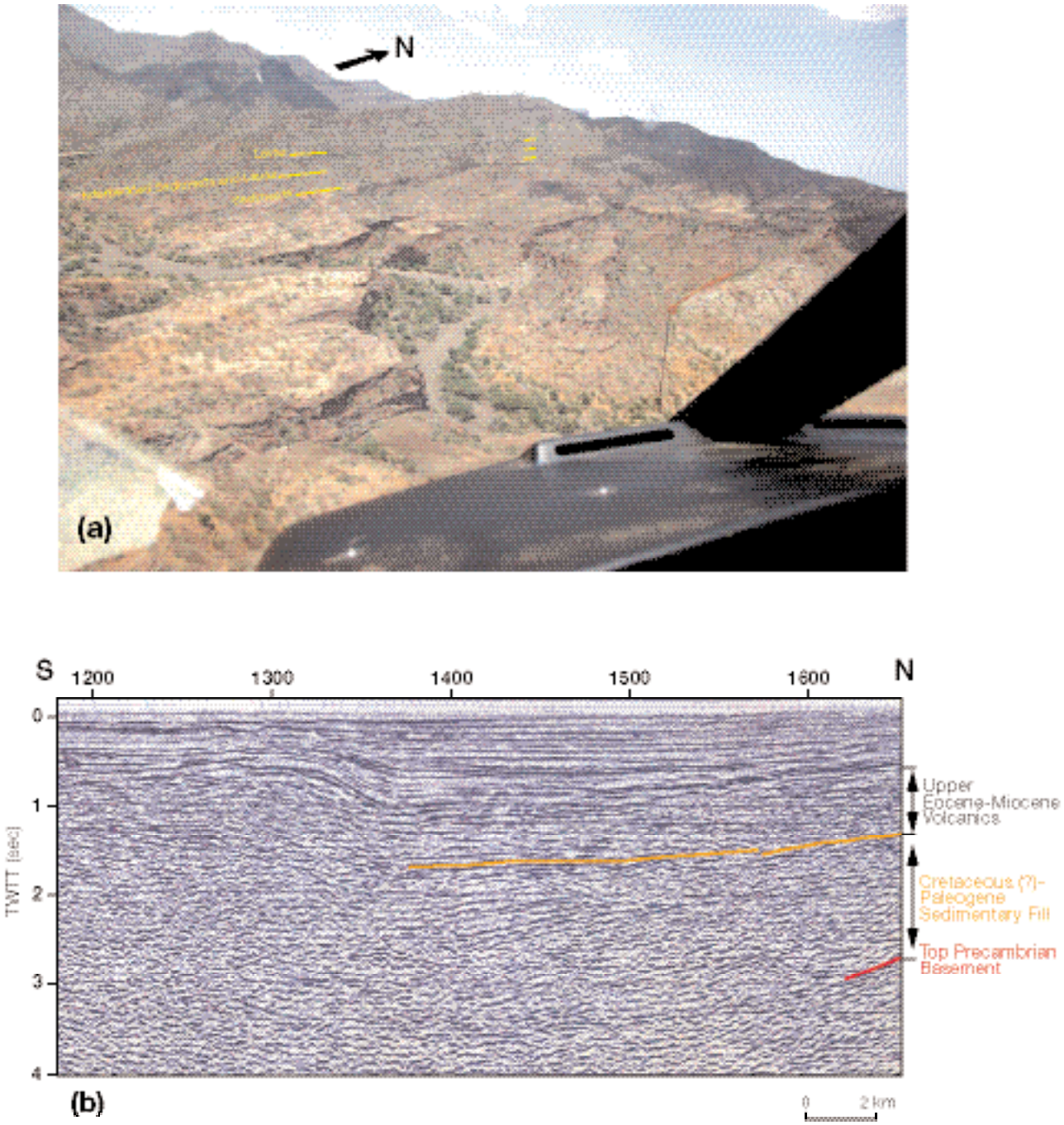

Figure 15. *(a) View from helicopter of the left bank of the Lokitaung Gorge (04°16'04"N; 35°47'34"E): slight angular unconformity (underlined by yellow marks) between the upper terms of LSF and the Turkana Volcanics. (b) Northern portion of seismic line TVK-7 (North Gatome Basin) showing possible angular unconformity between early rift sedimentary rocks (Cretaceous(?)-Paleogene; which can be interpreted as the Lapur Sandstone Formation(?)) and Turkana Volcanics (from Wescott et al., 1999). Orange mark: Unconformity. Red mark: Top Precambrian basement.*

Sample	*Sampling site*	*Strat. (m)*	*Nature a*	*Field notes*	*Microtexture*	*Phenocrysts b*	*Microcrysts b*	*Optical alterationc*
LAP 02-09B	LOK A	10	Q-Th	20 m-thick flow	microlithic, glomerophyric	Plg	Plg, Cpx, Fe-Ti ox	+
LAP 02-09A	LOK A	34	Q-Th	20 m-thick flow	microlithic, glomerophyric	Plg	Plg, Cpx, Fe-Ti ox	+
LAP 02-13D	LOK A	390	T	10 to 15 m-thick flow	microlithic, phyric	Plg, Cpx, Olv, Ap	Plg, Cpx, Fe-Ti ox	
LOK 45-04	LOK A3	44	Ol-Th	10 m-thick flow	microlithic		Plg, Cpx, Fe-Ti ox	+++
KER 63-05	LOK A5		B	altered 9 m-thick sill	microlithic	Plg, Cpx, Olv	unidentifiable	intense, carb.
KER 64-05	LOK A5			unidentifiable dyke	secondary recrystallization	unidentifiable	unidentifiable	intense
KER 65-05	LOK A5		T	N60°-trending, 9.50 m-thick dyke	microlithic, slightly phyric	Plg, Cpx, Olv	Plg, Cpx, Fe-Ti ox, Amp	+++, LTI
LK 09-05	LOK A6	60		20 m-thick flow	no data			
LAP 02-05	LOK A7	12	B	4 m-thick flow	coarsly microlithic, phyric	Cpx, Olv, Plg	Plg, Cpx, Fe-Ti ox, Amp, Bi, Ap	++, LTI

a Q-Th, quartz-tholeiite; Ol-Th, olivine-tholeiite; T, tephrite; B, basanite.
b Plg, plagioclase feldspars; Cpx, clinopyroxenes; Fe-Ti ox, Fe-Ti oxides; Olv, olivines; Amp, amphiboles; Bi, biotite; Ap, apatite. In the case of phenocrysts, minerals are listed in order of decreasing amounts.
c Alteration: number of crosses shows the clays alteration degree, from the almost fresh rocks (no cross) to the ones where clays reach to ca. 10 vol.% (3 crosses). The presence of secondary carbonates (carb.), and low temperature iddingsite (LTI) is also indicated.

Table 5. *Petrographical description of volcanic samples from the Turkana Volcanics associated to the Lapur Sandstone Formation.*

Sample	*Sampling site*	*Strat. (m)*	*Natureb*	*SiO2*	*TiO2*	*Al2O3*	*Fe2O3 c*	*MnO*	*MgO*	*CaO*	*Na2O*	*K2O*	*P2O5*	*LOI*	*Total*	*Q d*	*ne*	*hy*	*ol*
LAP 02-09B	LOK A	10	Q-Th	48.50	2.24	14.40	13.40	0.19	5.75	11.07	2.49	0.28	0.28	1.53	100.13	0.77		17.48	
LAP 02-09A	LOK A	34	Q-Th	48.15	2.24	14.30	13.40	0.19	5.75	11.10	2.44	0.25	0.27	1.71	99.80	0.77		17.41	
LAP 02-13D	LOK A	390	T	45.50	2.60	17.70	12.55	0.23	3.58	9.00	5.30	1.76	0.55	1.02	99.79		15.22		8.84
LOK 45-04	LOK A3	44	Ol-Th	47.78	2.72	13.47	14.02	0.21	6.03	10.51	2.65	0.72	0.37	1.21	99.69			12.82	3.71
KER 63-05	LOK A5		B	43.10	2.35	15.90	13.05	0.21	4.62	9.30	4.13	1.22	0.41	5.61	99.90		9.95		11.48
KER 64-05	LOK A5		no	38.60	2.25	15.00	12.55	0.29	4.63	11.00	3.40	0.44	0.35	10.74	99.25		10.43		9.53
KER 65-05	LOK A5		T	44.00	2.37	16.90	12.30	0.22	3.99	9.10	5.00	1.53	0.43	4.23	100.07		14.76		9.29
LAP 02-05	LOK A7	12	B	43.20	2.21	14.00	12.70	0.20	6.76	11.20	3.39	0.95	0.40	4.87	99.88		8.85		12.17

a The analyses were performed by ICP-AES (UMR 6538 "Domaines Océaniques", Université de Bretagne Occidentale, Brest, France). See Cotten et al. (1995) for the analytical procedure.
b Q-Th, quartz-tholeiite; Ol-Th, olivine-tholeiite; T, tephrite; B, basanite; no, intense alteration does not allow petrographical identification.
c Total Fe calculated as Fe2O3.
d CIPW norms calculated with Fe2O3/ Fe2O3* from Middlemost (1989). Q, quartz; ne, nepheline; hy, hypersthene; ol, olivine.

Table 6. *Chemical dataa (wt.% oxide) and CIPW norm on volcanic samples from the Turkana Volcanics associated to the Lapur Sandstone Formation.*

been estimated by Morley et al. (1992) and Wescott et al. (1999) to be arkosic sandstones (that may refer to the "Turkana Grits") and lacustrine deposits possibly similar to those identified in the rift basins at the south-west end of the Turkana Basin (such as the Lokichar and North Kerio Basins) (Fig. 7). A revised interpretation of the N-S oriented TVK-7 seismic line crossing the Gatome Basin (Fig. 17a) suggests the presence of a sedimentary unit (named Unit "A" in this work) with a total thickness of about 600 m, unconformably overlain by the Turkana Volcanics. One possible interpretation is that this sedimentary unit may relate to the Lapur Sandstone Formation, that outcrops in a similar stratigraphic manner 50 km to the east, in the Lapur Range (Fig. 9b). A gravity and magnetotelluric survey conducted across the Lapur Range at the latitude of the Lokitaung Gorge (04°17'N) (Abdelfettah, 2009), has allowed the identification to the immediate east of the Gatome Basin of a small N-S oriented half-graben basin named the Kachoda Basin (Fig. 9; MTG-2 profile). This basin was found to contain a thickness of 1.5 km of possible Mio-Pliocene(?) to Holocene sediments and below these, about 800 m of Turkana Volcanics. Below the volcanics, possible "basement" is interpreted to be at a depth of 2.3 km below the surface (Fig. 9b). Unfortunately, this combined gravity/magnetotelluric method did not authorize to establish a clear distinction between the Lapur Sandstone Formation, that is characterized by high values of resistivity (>100 ø.m), and the Precambrian basement that shows similar resistivity values.

Sample Code	Analysis number	Weight fused (g)	K* (wt.%)	40Ar* (%)	40Ar* (10-11mol/g)	Mean age	±	error
LAP 02/13 D	B 6507-6	1.0032	1.51	75.0	7.32			
	B 6256-2	0.7072		70.9	7.36	27.81	±	0.65
NATH 09/04	B 6742-2	0.4018	2.69	78.9	15.96	27.40	±	0.66`
NATH 08/04	B 6723-2	0.7042	3.18	89.5	12.87	28.73	±	0.64
NATH 02/09 A	B 6379-5	1.0095	0.23	42.8	1.31	32.77	±	1.84
LAP 02/09 B	B 6272-7	0.8002	0.26	46.0	1.51	33.57	±	1.88
LOK 45/04	B 6745-5	0.7035	0.23	55.7	1.57			
	B 6770-6	1.0025		55.9	1.61	39.09	±	2.18

Sample ID	*Exp.#*	*Weight molten (g)*	*K* (wt.%)*	*40Ar* (%)*	*40Ar* (10-11mol/g)*	*40Ar* weighted mean (±1s)*	*Age ± 2s Ma*
KER 65/05	7195	0.35711	1.174± 0.012	28.409	5.577± 0.028		
KER 65/05	7210	0.29287	"……..."	29.374	5.513± 0.028	5.545 ± 0.020	27.03± 0.57
LK 45/04	7165	0.62734	0.467 ± 0.005	50.132	2.846 ± 0.014		
LK 45/04	7180	0.51511		39.569	2.919 ± 0.015	2.881 ± 0.010	35.23± 0.74
LK 09/05	7179	0.63366	0.259± 0.003	9.087	1.754± 0.009		
LK 09/05	7194	0.40205	"……..."	13.845	1.650± 0.009	1.701±0.007	37.48± 0.80

Table 7. *(a) Conventional K-Ar ages and (b) K-Ar ages, Cassignol method, of lava flows and dykes belonging to the Turkana Volcanics. The flows dated immediately overlie the upper terms of the Lapur Sandstone Formation. Age calculations are based on the decay and abundance constants form Steiger and Jäger (1977).*

As a consequence, the presence of the Lapur Sandstones in the Kachoda Basin below the Turkana Volcanics cannot be firmly demonstrated but can be strongly suspected due to nearness of Lapur Sandstones outcrops. Lateral extension westward in the Gatome Basin is unsure.

Below Unit "A" on the TVK-7 seismic line (Fig. 7), is a "tilted block" palaeotopography that results from normal faulting affecting a "stratified basement", that could be interpreted either as a pre-middle Cretaceous sedimentary formation (if the "A" unit corresponds to the Lapur Sandstone Formation), or as the Precambrian basement (Fig. 17a). Such a normal faulting phase may thus relate to one of the lower-middle Cretaceous rifting events that affected southern Sudan and northern Kenya (Giedt, 1990; Genik, 1993; Salama, 1997; Wescott et al., 1999). The "A" sedimentary unit that can be compared to the Lapur Sandstone Formation or an equivalent sedimentary unit unconformably overlies the top of this palaeotopography (Winn et al., 1992; Bosworth and Morley, 1994; Morley et al., 1999). A re-interpretation of the TVK-10 seismic line (Fig. 9a) suggests the presence in the subsurface and below the "Turkana Volcanics" of a 300-m thick sedimentary unit that could be attributed to the Lapur Sandstone Formation (Fig. 17b)

4.3. Depositional environments of LSF

The depositional environments of the LSF were inferred from studying the lithology, sedimentary structures, and facies associations at the type-section as well as at complementary section at the Kerral laga.

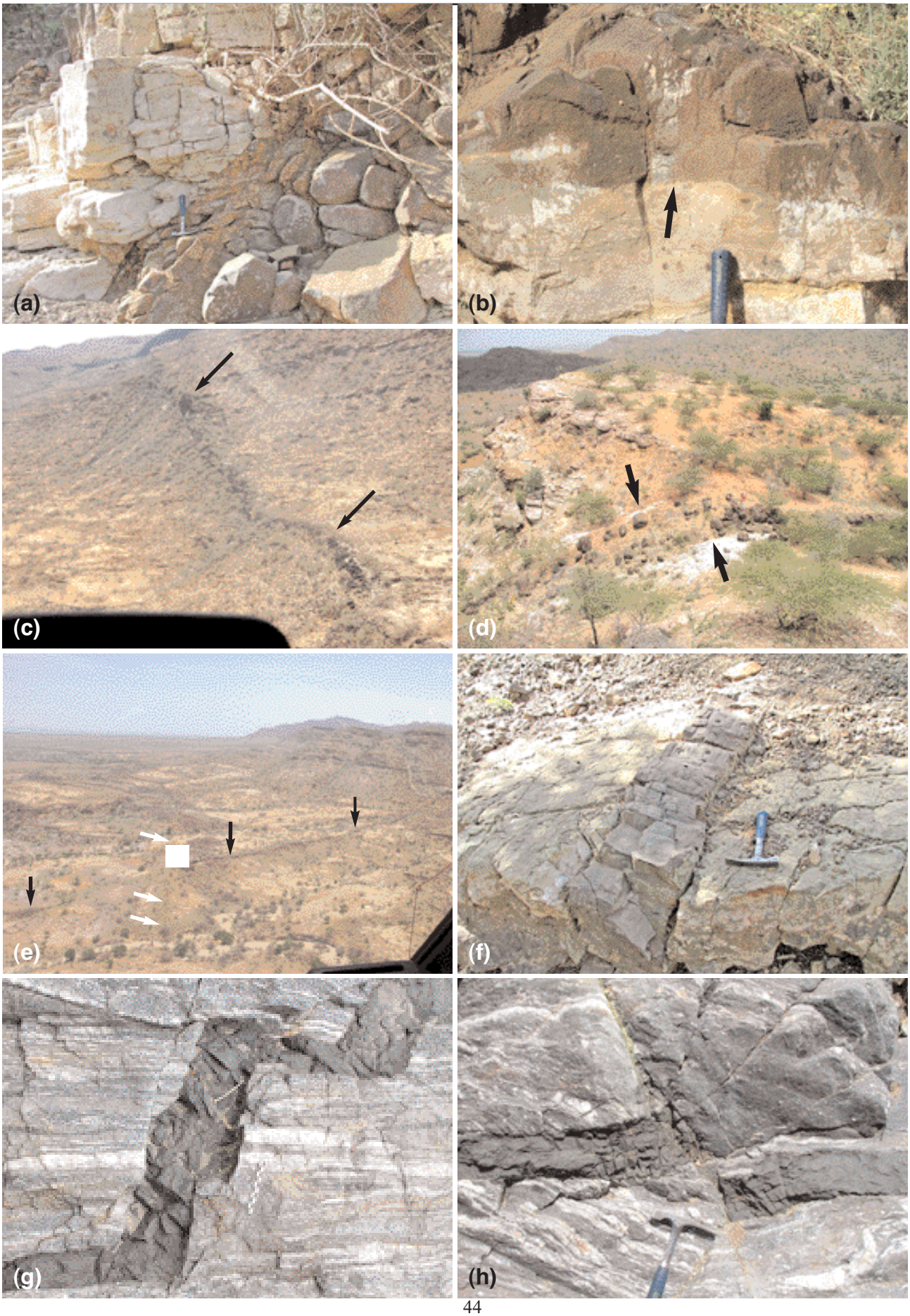
(a)
(b)
(c)
(d)
(e)
(f)
(g)
(h)

The basal contact with the underlying Precambrian basement was not seen at the location of the type-section but outcrops a few kilometers further to the north. The two sections were correlated using a prominent multi-coloured sandstone bed several tens of m thick and of wide lateral extension visible neat the top of the section (Figs. 10, 11a, d, e and 12).

4.3.1. Facies description and depositional processes

A total of 11 lithofacies have been identified in the LSF. These are based mainly on grain size, sedimentary structures, grading, and matrix content especially in the conglomerate facies. The facies codes have been adapted from Postma (1990), Horton and Schmitt (1996), and Miall (1996) (Table 8).

4.3.1.1. Conglomerate facies. Although the conglomerate facies is present throughout the vertical section of the formation, it is only abundant at the base and near the top of the formation, occurring with less abundance in the middle parts. A total of 4 different types of conglomerate facies have been identified in the LSF. They range in bed thickness from 0.5 to 2.5 m.

- **Facies Gmu**. This is composed of a massive, ungraded, matrix-supported, poorly sorted conglomerate lacking internal stratification. The facies is represented by granule-pebble conglomerates with planar to slightly erosive lower boundaries. Some of the beds are lenticular in shape. The pebbles, which are composed of mainly quartz with few metamorphic rock fragments, are subangular to subrounded and range in size between 3-5 cm in diameter. They are in a matrix of light grey and burgundy coarse to very coarse sandstone. This facies is represented by beds LPR 03/04 and LPR 42/04 in the lower parts of the LSF (Figs. 10a and 18a). This facies is interpreted as a non-tractional deposition of gravel attributed to cohesionless or plastic debris flows (Nielsen, 1982).

- **Facies Gmh**. This facies is composed of horizontally stratified, matrix-supported, conglomerate with subangular to rounded quartz pebbles up to 10 cm in diameter and few cobbles. The matrix is made of very coarse purple sandstone with horizontal beds. The facies is represented by bed LOK 34/04 near the top of the LSF in the section completed in the Lokitaung Gorge (Fig. 10b). A the base of this bed, the facies exhibit planar crossbeds with the pebbles aligned along the planes of the crossbeds. Bases are frequently subhorizontal. Maximum bed thickness is 2.5 m. This lithofacies is interpreted as the product of bedload traction carpets (Nilsen, 1982) of high-energy gravity deposits in a steep topographic gradient (Rohais et al., 2008).

- **Facies Gcn**. This facies is a normally graded, clast-supported conglomerate. It is uncommon in the LSF, the only identified representative bed being LPR 95/04 within the middle part of the formation (Figs. 10a and 18b). The representative bed thickness is 1.5 m thick and it grades into a coarse pebbly sandstone towards the top. The quartz pebbles are up to 8 cm in diameter, subangular to subrounded, whitish in colour and they occasionally have brown iron oxide staining. Normal grading developed where turbulence became the princi-

← ***Figure 16**. Dykes and sills intruding the Lapur Sandstone Formation. (a) On the right bank of the Kerral laga (04°14'53"N; 35°47'54"E; LOK A5 section; Fig. 14), this 0.50-m thick lava dyke (sample KER 64/05) is seen crosscutting sandstone beds of the LSF. (b) The KER 64/05 dyke connects laterally to a 9-m thick sill (sample KER 63/05) intruded between the two upper-most beds of the LSF and digesting the upper part of the lower sandstone. (c), (d) This 10-m wide, N60°-trending dyke (sample KER 65/05) is seen running over hundreds of m crosscutting the middle and upper parts of the LSF in the Kerral area (Fig. 6a). This dyke has been dated at 27.03 ± 0.57 Ma (see Table 7b).(e) Dykes running to the immediate north of the Lokitaung Gorge. One dyke (black arrow) is oriented N 40° and is intersected by an other dyke running N165°. (f) Subvertical dyke crosscutting the last sandstone bed of the LSF, left bank of the Lokitaung Gorge (04°16'5"; 35°47'26"). (g), (h) At Lapur Peak, N90°-100° to N340°-trending dykes are seen crosscutting Precambrian amphibolites. Some of these dykes are affected by minor normal or strike-slip faulting.*

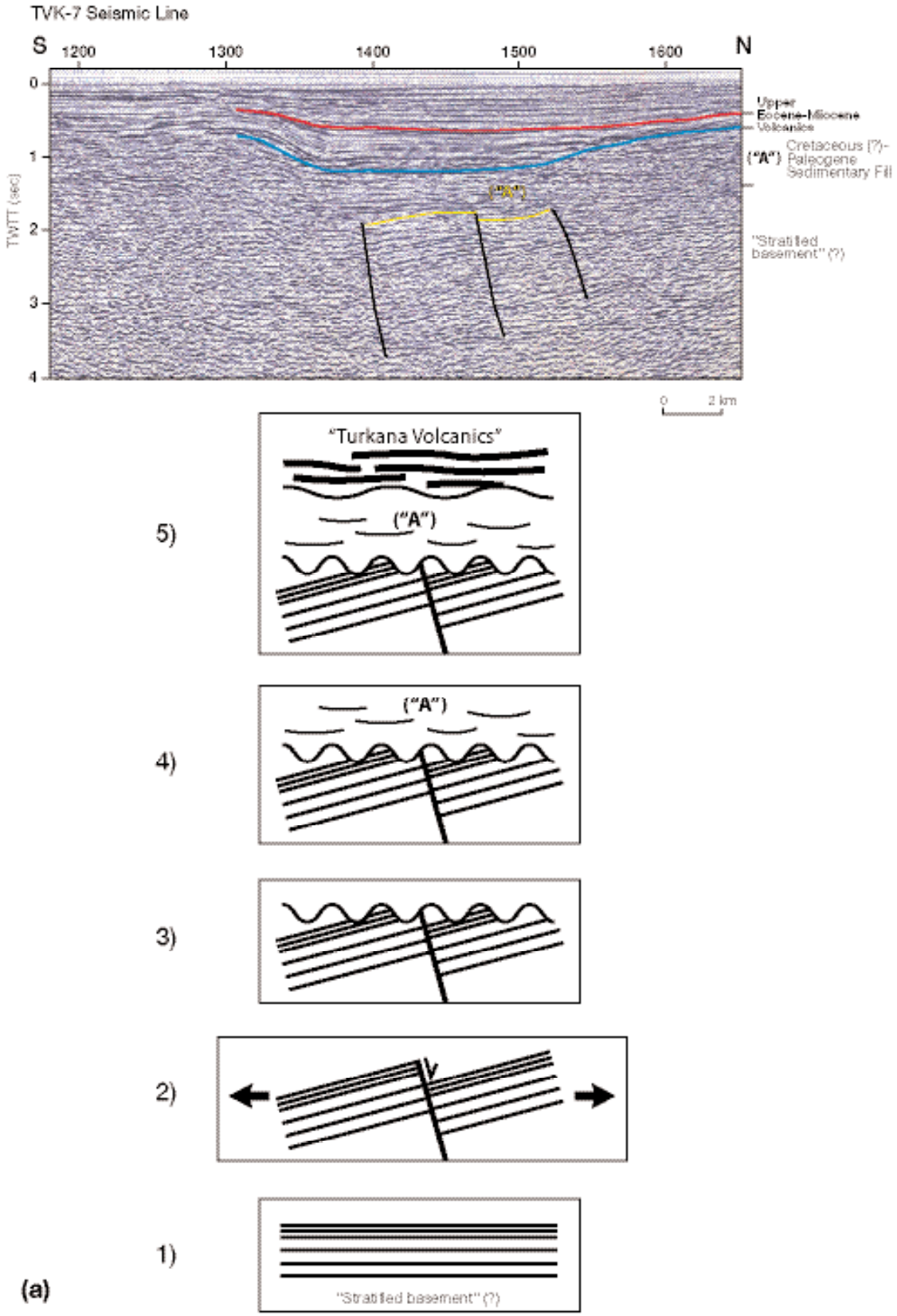
TVK-7 Seismic Line
S
1200
1300
1400
1500
1600
N
0
1
2
3
4
TWTT (sec)
Upper Eocene-Miocene Volcanics
("A") Cretaceous (?)-Paleogene Sedimentary Fill
"Stratified basement" (?)
0 2 km
"Turkana Volcanics"
("A")
5)
("A")
4)
3)
2)
1)
"Stratified basement" (?)
(a)

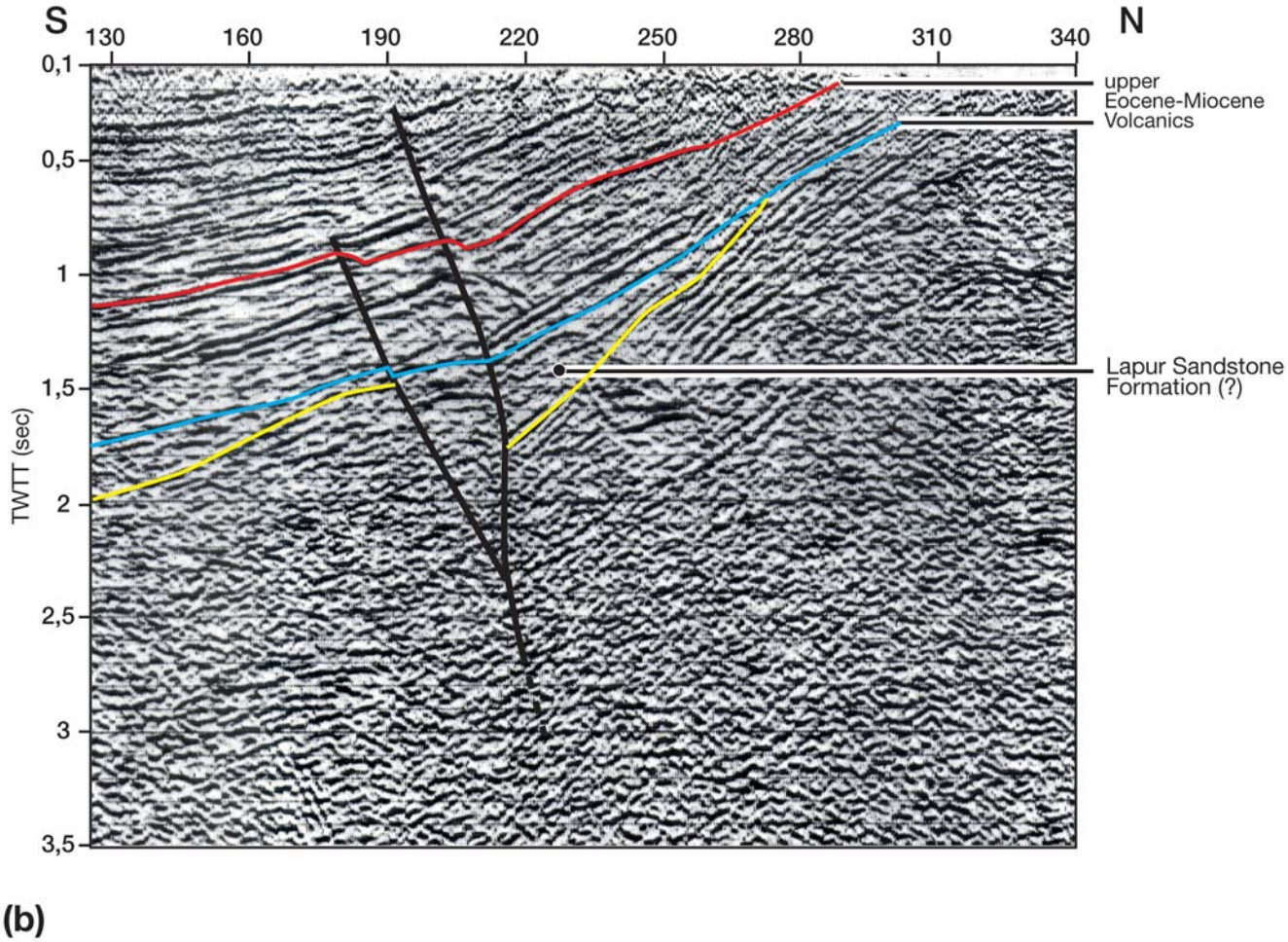

← ***Figure 17. (a) Structural framework of the Lapur Sandstone Formation deduced from a re-interpretation of the TVK-7 seismic line (Fig. 2) and oucrop data. 1) A "stratified basement" (that can also be interpreted as a stratified sedimentary series, or Precambrian(?) metamorphic basement, is visible at the base of the seismic line. 2) A first phase of deformation is attributed to a normal faulting episode that created a series of small north-dipping tilted blocks similar in geometries to those that are observed in the basins of the Sudan Rifts (Bosworth, 1992). This "tilted block" topography developed upon a "stratified basement" possibly during middle-late Cretaceous, prior to 3) A phase of erosion marked by a first angular unconformity affecting the top of the "tilted block" topography. 4) The deposition of a sedimentary unit ("A") that can be interpreted as the LSF (or a lateral equivalent) on top of this erosive unconformity. This geometry can be compared with the main geometry of the Lapur Sandstone Formation in the Lapur Range, that unconformably overlies an eroded basement surface. 5) A second angular unconformity is visible between the top of Unit "A" and the base of the "Turkana Volcanics". Variations in thickness of the lava pile can result of palaeotopographic effects (see Fig. 15). Nevertheless, the age of the lower sequences cannot be precisely determined without drilling as it was the case for the south Sudan Rifts (Bosworth, 1992). (b) A re-interpretation of the TVK-10 seismic line (See Fig. 9a) suggests the presence, below a package of well-marked reflectors that can be interpreted as the "Turkana Volcanics", of a sedimentary unit about 300 m thick, that can be attributed to the Lapur Sandstone Formation. This interpretation supports the presence of the LSF in the subsurface, farther south than the main outcrops of the Lokitaung Gorge. The previous interpretation published by Wescott et al., (1999, page 57, Figure 2) was only showing a thick (up to 2 seconds TWTT) pile of sediments attributed to late Miocene-Pliocene, overlapping a not very well defined seismic facies unit interpreted as representing the upper part of the Turkana Volcanics.***

Facies	Description	Depositional process
Gmu	Massive, ungraded, matrix-supported, poorly sorted, granule to pebble conglomerate	Cohesionless or plastic debri flow, high strength, viscous
Gmh	Horizontally-stratified, matrix supported conglomerate	Traction carpets driven by stream flow or high density turbulent flow
Gcu	Massive, ungraded, clast-supported, conglomerate	Pseudoplastic debri flow, inertial bedload in turbulent flow
Gcn	Normally graded, clast- supported conglomerate	Pseudoplastic debri flow, low strength, or lag deposit
Sm	Massive, fine to very coarse sandstones with no sedimentary structure	Sedimentary gravity flow deposits, rapid suspension fall-out
Sh	Horizontally laminated, fine to coarse-grained sandstone	Plane-bed flow, critical flow regime
St	Trough cross-laminated, fine to very coarse-grained sandstone	Sinuous-crested and linguoid, 3-D dunes migration, lower flow regimes
Sp	Planar cross stratified fine to very coarse sandstone	Transverse and linguoid bedforms, 2-D dune migration
Fm	Massive, structure-less mudstone	Low energy flow deposition from suspension, overbank or floodplain
Fl	Laminated mudstone	Overbank, abandoned channel or waning flood deposits

Table 8. *Lithofacies analysis and classification for the Lapur Sandstone Formation. The facies codes are adopted from Postma (1990), Miall (1996), and Horton and Schmitt (1996).*

Figure 18. *(a) Matrix-supported conglomerate (facies Gmu), massive, ungraded, poorly sorted subangular gravels and pebbles (quartz and rare elements of basement max. diameter 3-5 cm). Matrix made of coarse sand, immature grains. (b) Normally graded clast supported conglomerate, (facies Gcn), maximum pebble size 8 cm diameter, mainly subrounded pebbles composed predominantly of quartz. (c) Massive ungraded clast supported conglomerate (facies Gcu), composed of rounded to well rounded pebbles, maximum diameter 5 cm, with abrupt bed terminations, the facies is overlain by reddish-brown coloured coarse grained pebbly sandstone with faint planar cross stratification (facies St). (d) Huge beds of faintly trough-cross bedded sandstones (facies St) with large scale troughs. (e) Trough cross-laminated sandstone (facies St), Lokitaung Gorge, middle part of the LSF. Boxed image shows planar cross-stratified sandstone (facies Sp), very coarse-grained sandstone, with individual cross beds measuring 4-6 cm thick, which occurs associated with facies St. (f). Medium grained sandstones with interbeds of planar cross stratified facies (Sp) and horizontally bedded facies (Sh) occurring in the middle parts of the type-section. (g) Horizontally laminated sandstone (facies Sh), occurring in fine to medium sandstone, lower parts of the Kerral section. This facies occurs commonly interbedded with low angle planar cross-laminated sandstone, facies Sp.* →

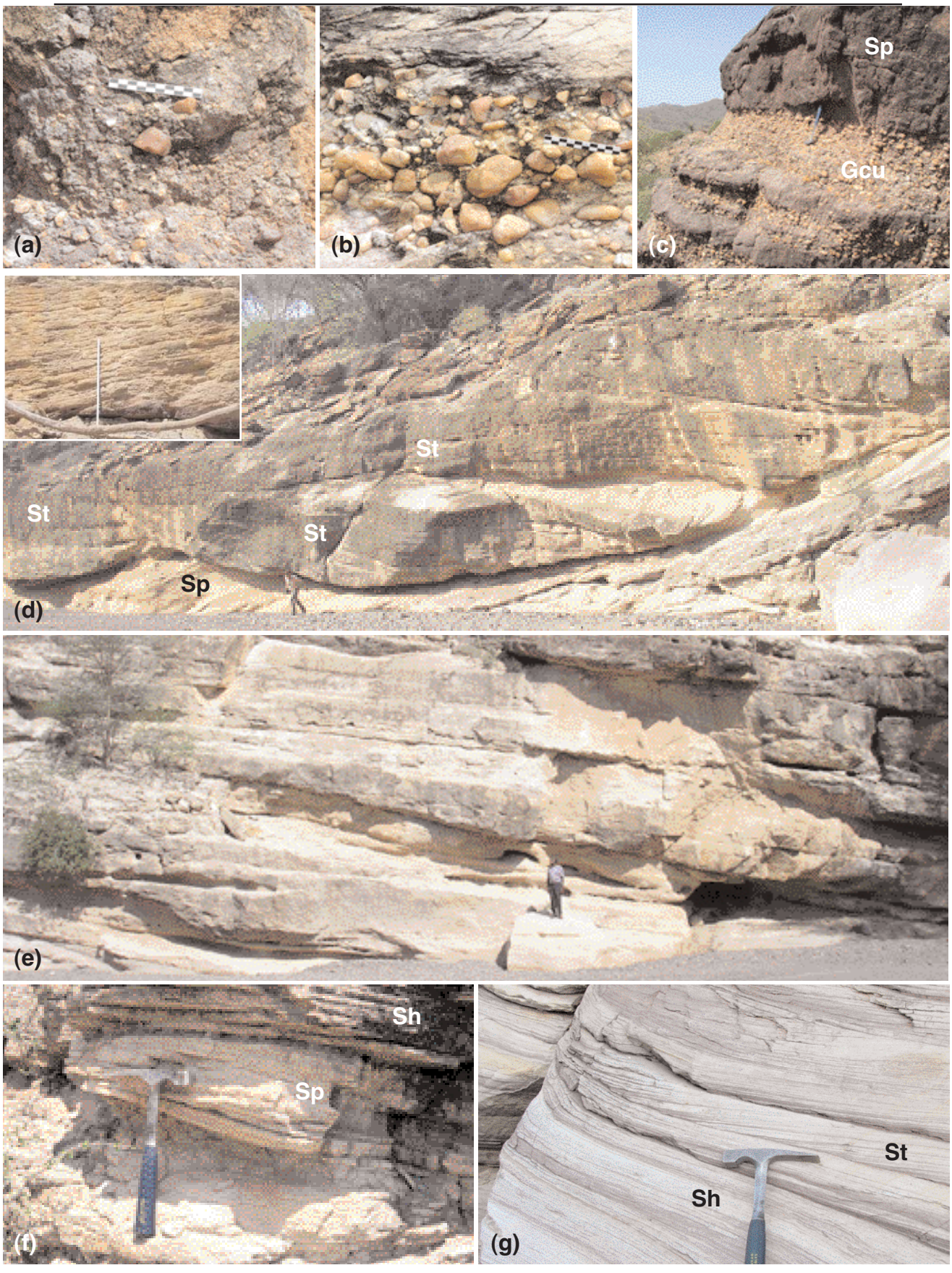
(a)
(b)
Sp
Gcu
(c)
St
St
St
Sp
(d)
(e)
Sh
Sp
(f)
St
Sh
(g)

pal clast-support (Nemec and Steel, 1984). This facies represents low strength pseudoplastic grain flows or lag deposit (Miall, 1977; Horton and Schmitt, 1996; Miall, 1996).

- **Facies Gcu.** This is a facies composed of ungraded, clast-supported gravel-pebble conglomerate containing a matrix of coarse, dark-brownish grey sandstone. The quartz pebbles are rounded to surrounded and are 3 to 10 cm in diameter. The facies is represented in the LSF by bed LPR 80/04 which occurs in the middle of the formation and in the bed LPR 153/04 towards the top of the type-section (Figs. 10b and 18c). In

← ***Figure 19.*** *(a) Massive, fine to coarse grained sandstone (facies Sm). The beds are structureless and measure up to 6 m in thickness. Upper beds terminations are marked by the presence of iron crusts. (b) Several m-thick bed of massive coarse sandstone showing faint horizontal bedding and a prominent erosive base (see Fig. 11b; North Lokitaung Gorge section, 150 m mark). (c) Same bed as in (b) above showing a well-marked erosive base developped on dark grey claystone facies, and horizontally-aligned holes that contained clay clasts which have been removed by differential weathering. (d) Dark grey silty laminated claystone (facies Fl) conformably overlying massive medium-grained sandstones, and unconformably overlain by planar and horizontally stratified medium-grained sandstone (facies Sp and Sh). Kerral Laga section, upper part. (e) Same facies (Fl) as in (d) above, this time overlain by ungraded matrix supported conglomerate facies Gmu and underlain by coarse-grained sandstone. Note well-preserved wave ripple developed on top of (Fl) facies. (f) Squashed clay pebble, 20 cm in diameter, within coarse-grained pebbly sandstone, upper part of the LSF within the multi-colour cliff in Lokitaung Gorge section.*

LPR 153/04, the bed is lenticular in shape with a thickness of 0.5 m increasing laterally to 1 m towards the south and it is bounded at the top and base by iron oxide crusts measuring 5-50 mm in thickness. This facies is deposited by the process of low strength pseudoplastic debris flows by the action of viscous, laminar or turbulent flow within high energy regimes (Nilsen, 1982).

4.3.1.2. Sandstone Facies. This lithofacies is the most prominent in the LSF and is represented throughout the formation. It has been subdivided into 4 based on the dominant sedimentary structures.

- **Facies St**. This facies is well represented though not very abundant in the LSF and is present mainly at the base and near the middle of the formation. It is composed of coarse to granular sandstone with trough cross-bedding. The facies is represented by beds LPR 08/04, LPR 44/04, LPR 85/04 and LOK 44/04 (Figs. 10a and 18d, e). In most cases the facies is interbedded with facies Sp (planar cross-bedded sandstone) and occasionally with facies Sh (horizontally stratified sandstone). Colour ranges from grey to brown. Bed thickness varies between 1.0 and 4 m. Almost all bed contacts with underlying units are erosive to strongly erosive. Trough cross-stratified facies is interpreted as the product of three-dimensional dunes migrating in channels under the conditions of the upper part of the lower flow-regime, transporting coarse bedload of material along the deeper parts of the channel (Miall, 1996; Hjellbakk, 1997; Gosh et al., 2006).

- **Facies Sp.** This facies consists of fine, medium to coarse and very coarse gravely sandstone with planar cross-stratification. The facies is more common in the upper part of the formation. The colour of the sandstones ranges from greyish white to reddish brown. Beds range in thickness from 1.4 m to 4 m, with the exception of one bed (bed LPR 58A/04 is 25 m thick) (Fig. 10). Most bed terminations are horizontal to subhorizontal and abrupt. The orientation of the planar cross-beds range from N25°, N40°, N140°, N180° and N340°. Nodular horizons occur in some beds (e.g. LPR 58A/04). This facies commonly occurs in close association with the trough cross-stratified facies (St) (Fig. 18e) and in many instances, the two facies grade into each other vertically and also laterally. Sp facies are formed by the migration of 2D dunes where sand is transported up the flanks of the bedforms by traction and intermittent suspension and deposited at the crest, in such channel locations as the base of longitudinal bars or at the intersection of channels (Miall, 1977; Horton and Schmitt, 1996; Miall, 1996; Khalifa and Catuneanu, 2008).

- **Facies Sh.** This facies is made of coarse to very coarse, occasionally pebbly, horizontally stratified sandstone. It is more abundant towards the top of the formation, and totally lacking in the units at the base. The facies is represented in the LSF by beds LPR 99/04, LPR 105/04, LPR 107/04, LPR 122/04 and LPR 155/04 (Figs. 10 and 18f, g). Bed thickness varies between a minimum of 1.7 m to a maximum of 4.5 m. The beds exhibit individual horizontal stratifications up to 4 cm thick and sometimes have planar cross-bedded facies (Sp) at the base or in the middle which bounds the horizontally stratified horizons. They occasionally show a strongly erosive basal contact (Fig. 18f, g). They range in colour from greyish white to reddish brown. Most are interpreted as the deposits of large, flat, simple bars resulting from the action of vigorous currents.

Sh can be attributed to planar bed flows of shallow high velocity (Miall, 1978; Harms et al., 1995) or traction carpets (Postma, 1990).

- **Facies Sm**. This facies is composed of fine to very coarse-grained sandstone lacking sedimentary structures. The facies is evenly distributed within the LSF although they are more abundant towards the base of LSF. The beds vary in thickness from a minimum of about 0.2 m to a maximum of between 3 and 6 m on average. Nodular horizons are common, mostly occurring at the base or the top of the respective beds. This facies is most common in the lower parts of the LSF represented by beds LPR 13/04, 19/04, 25/04, 35/04 and 68D/04 (Fig. 10a). The sandstones show a variety of colours ranging from whitish grey, grey-purple, to yellowish orange and brown. Clasts of 2-3 cm of grey argillaceous material are present in the massive units (See § 4.3.1.3.). Massive sandstone beds are interpreted as sand rapidly deposited directly from turbulent suspension by hyperconcentrated mass flows or subaqueous high-density turbidity currents (Ghibaudo, 1992).

4.3.1.3. Claystone and silty claystone facies. Claystone and silty claystone facies occur more commonly in the lower part of the LSF than in the upper section, where they only appear as thin beds (few tens of cm in thickness) or as reworked clay pebbles. Attempts to recover organic debris such as pollens or plant remains from these claystones that could be used for palynological and palynofacies investigation were unsuccessful. Plant remains are however present at several levels in sandstones, in the form of silicified tree trunks that locally are up to 7 m long.

- **Facies Fl**. This facies is made of laminated or thinly bedded claystones and is not very common in the LSF, though it is represented in the lower part of the type-section (sample LPR 65/04; Fig. 10a), and in the upper part of the formation at the Kerral section (sample KER 21/05; Figs. 12 and 19d, e). In LPR 65/04, the facies passes downwards into the massive claystone (Fm) facies. In the type section of the LSF, there are several horizons made of unexposed sections buried under screes (Fig. 10) and it is suspected that such horizons may be made of fine-grained facies (either Fl or Fm) that have been selectively weathered.

- **Facies Fm.** This facies is composed of claystone and silty claystone and is not evenly distributed in the formation, being confined mainly in the lower section. The colour of the claystones ranges from reddish to violet, grey green, and dark grey to black. Bed thickness is quite variable with minimum of 0.2 m to a maximum of 10 m. Other occurrences of this facies are in the beds LPR 59/04 in the middle of the formation and LPR 133/04 near the top of the type-section (Fig. 10). The contact with overlying beds is almost always strongly erosive (Fig. 19b-e). Clay pebbles are locally incorporated in coarser facies overlying the claystones (Fig. 19c, f), perhaps as rip up clasts indicating erosion of flood-plain deposits accompanied by sediment bypass. Facies Fm is interpreted as overbank or abandoned channel deposits that accumulate in from stagnant pools of water during low stage channel abandonment, including deposits of distal parts of the flood-plain ponds (Miall, 1996).

4.3.1.4. Palaeosols and associated deposits. Palaeosol horizons are common in the lower and upper parts of LSF, both at the Lokitaung Gorge (type-section) and the Kerral sections (Figs. 9a, 10 and 12). They

Figure 20. *(a) Vertical burrows within the lower parts of the LSF at the north Lokitaung Gorge section. The lower bed is in an erosive contact with the overlying massive sandstone bed. (b) Burrows, plan view, within a purple palaeosol horizon of the lower part of the LSF, right bank of the Karamukun Laga (Fig. 9a). They occur as white-grey sediment within a predominantly purple sandstone. This bed possibly correlated with similar facies observed at the type–section (photo (a)). (c) (d) Several palaeosol horizons showing alternating red and grey zonation within the upper parts of the LSF. (e) Plan view of root traces within the upper part of the LSF at the very north end of the Lapur Range. (f), (g) Large columnar pipes within the palaeosol zone of the multi-coloured cliff in the upper Lokitaung Gorge and Kerral sections. These pipes occur within medium to coarse grained sandstones and can be interpreted as fluid conduits or water escape features. (h), (i) Crusts of hematite that are common especially within the middle part of the LSF in the north Lokitaung Gorge section. They form bed terminations within the sandstone unit of the braided river deposit.* →

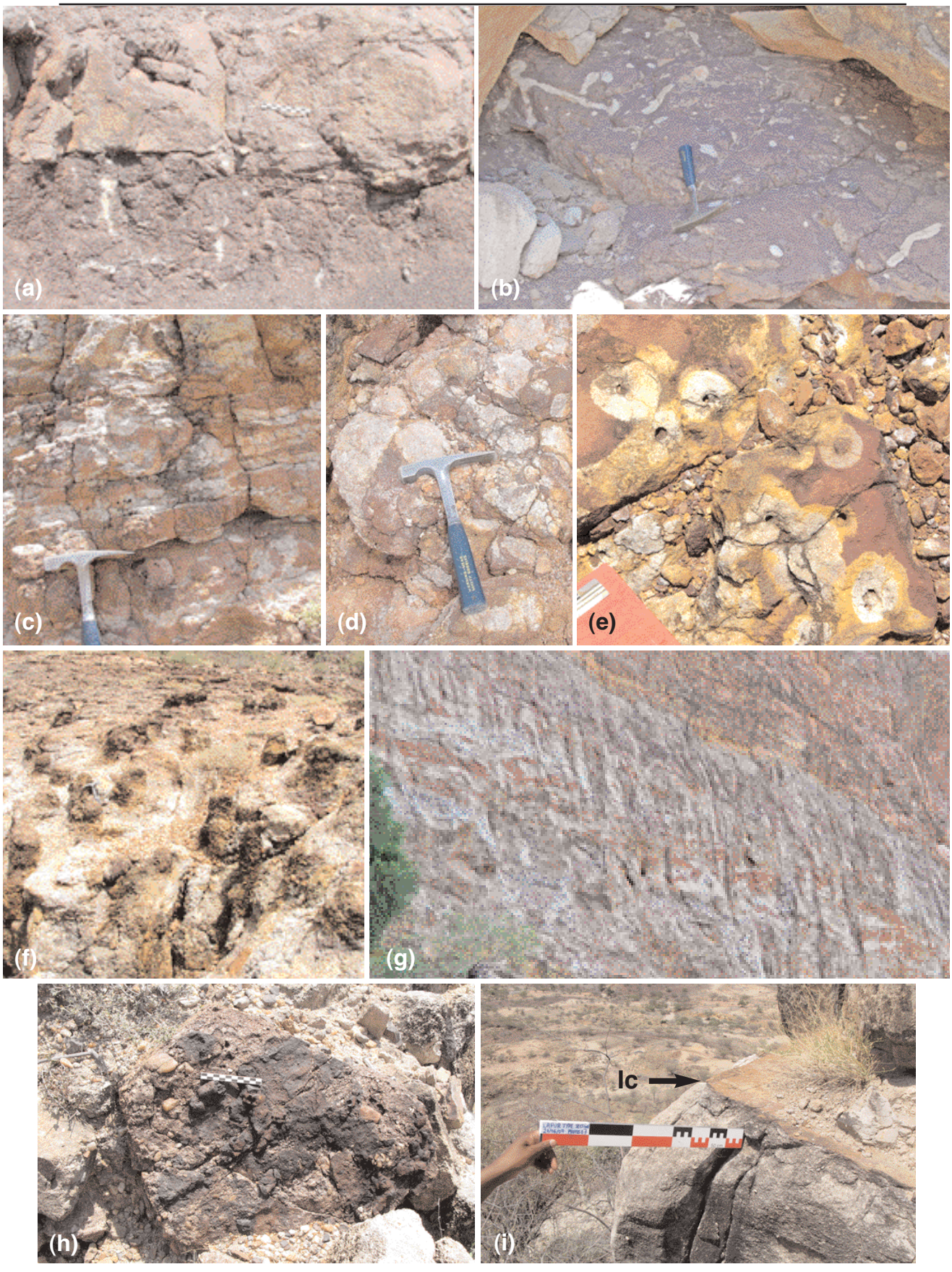
(a)
(b)
(c)
(d)
(e)
(f)
(g)
(h)
lc
(i)

occur mainly in the silty claystone facies, and are marked by extensively burrowed horizons (Fig. 20a, b) or by distinctly mottled levels with alternating burgundy and grey colours and abundant root traces (Fig. 20c-e). Large columnar pipes form an especially prominent zone within the palaeosol zone of the multi-coloured cliff in the upper Lokitaung Gorge and Kerral sections (Figs. 11a, d, 12 and 20f, g). These pipes occur within medium to coarse grained sandstones. Similar cylindrical columns were observed in the Jurassic sandstones of southeastern Utah and can be explained in terms of permeability heterogeneities, presence of nuclei for precipitation, followed by a self organization process or the influence of microbes. Where the sandstone within the pipes is more permeable than the host sandstone thereby acting as conduits for fluid flow, this creates areas of preferential cementation (Chan et al., 2000; Beitler et al., 2005; Parry et al., 2009). Fluid flow is more efficient in the vicinity of faults and in the case of the LSF, the formation outcrops in the vicinity of the main Lapur-Murua Rith boundary fault which should serve as a main conduit of groundwaters.

The colours visible in such types of facies are indicative of the drainage prevailing within the flood-plain or abandoned channel environments where the sediments lay exposed for extended periods without deposition, the red representing good drainage and an oxidising early diagenetic environment, while grey beds suggest water-logged and reducing pore water environments (Collinson, 1996). Red hematite-rich palaeosols are interpreted as having developed under semi-arid to arid conditions (Reed, 1991; Khalifa and Catuneanu, 2009).

The “ferruginous crust” facies is concentrated around the level 150 to 300 m above the base of the type-section (Fig. 10a; north Lokitaung Gorge, type-section). These crusts are generally thin, normally measuring between 1 and 2 cm with a maximum of 5 cm, and occur at the top of sandstone beds and occasionally in the middle. They are dark reddish-brown to black-brown in colour and are very well indurated (Fig. 20h, i).

4.3.2. Facies associations and depositional environments

The LSF is characterized by a predominantly coarse-grained facies association with only few and laterally discontinuous fine-grained facies. The most common facies association consists mainly of bedload deposits, predominantly sands and gravels being the main grain sizes, though pebbles are sometimes abundant. The facies associations observed in the type-section of the LSF have been attributed to 2 depositional environments:

1) Distal alluvial fan environments represented by the lower and upper parts of the LSF; and 2) Sandy braided river depositional environments represented by the middle part of the LSF (Fig. 10).

4.3.2.1. Distal alluvial fan facies associations. Facies assemblages associated with distal alluvial fans are dominated by massive ungraded gravely conglomerates with trough cross-bedded (St) and planar cross-bedded (Sp) sandstone facies with minor amounts of horizontally stratified sandstone (Sh), planar cross stratified conglomerates and massive claystone (facies Fm) (Miall, 1977; Collinson, 1996). The conglomerate facies are both clast-supported (facies Gcu) and matrix-supported (facies Gm). Grading may be present (facies Gcn), suggestive of deposition from dilute and turbulent flows, while the presence of horizontal stratification in the conglomerates may represent deposition either at the top of braid bars or as lags on channel floors (Collinson, 1996).

This facies association was observed to be the dominant association in the lowermost (the basal 150 m) and the uppermost (above the 340 m mark) parts of the LSF in the type-section as well as the top part of the Lokitaung Gorge section (Fig. 10). In the basal parts of this section, thin beds of medium- to coarse-grained and pebbly sandstones as well as silty claystones occur. The coarse-grained sandstones are

generally thin-bedded, around 0.5 m thick with maximum bed thickness of 2.5 m while the fine- and medium-grained sandstones (facies St and Sp) form beds that are 2-6 m in thickness. Silty claystones (facies Fm) occur in beds that up to 10 m in thickness. Higher up in the basal section, coarse-grained sandstones (facies Sp) up to 25 m thick occur with conglomerate beds (Gmu facies) ranging between 0.5-1 m in bed thickness occur. Towards the top of this basal section of the LSF, the main facies are the medium-grained sandstones with tabular cross beds, facies St, composed of beds that are 1-25 m thick.

The dominant facies in this association include the conglomerate facies Gmu, Gcu and Gmh as well as the sandstone facies St, Sp, Sm and Sh. Both the upper and lower parts of the formation also show the presence of abundant root traces which is consistent with flood-plain and overbank depositional environments. These are preserved as bleached zones having distinctive colour contrasts of grey in a predominantly red background (Fig. 20c-e), interpreted as diagenetic alteration of the sediment in alternating reducing and oxidizing environments. The columnar structures which have been observed in the multi-coloured cliff at Kerral and in the Lokitaung Gorge are possibly interpreted as water escape features (Fig. 20f, g).

4.3.2.2. **Braided stream facies associations.** Braided river environments are dominated by bedload transport and are therefore associated predominantly with sand grade or coarser material (Miall, 1977; 1996). Mean and maximum grain size depend on stream power and decrease downstream. Gravel bars are commonly longitudinal in form and are characterised by massive or crudely horizontal stratification. Few beds representing the facies Gmu (massive ungraded matrix-supported) are commonly present and are regarded as products of cohesive debris flows (Miall, 1977; Collinson, 1996; Einsele, 2000) while facies Gcu and Gcn (clast-supported ungraded and clast-supported normally graded conglomerates, respectively) result from high-energy flow that transports coarse bedloads while keeping sand in suspension in stream flows. These may develop also as lag deposits which may become subsequently partially eroded and thus preserve little structure such as graded bedding. Facies Gmh (matrix-supported horizontally-stratified conglomerate) are deposited as channel bottom-load traction carpets (Collinson, 1996). The conglomerate facies form very few thin beds within this section near the base of the LSF.

Sand bars within braided river environments are typically linguoid and they contain abundant planar cross-bedding (Miall, 1977). The facies Sm (massive sandstones) and Sp (planar cross-stratified sandstones) form the bulk of the sandy facies in the LSF. The association indicates deposition in a laterally aggrading channel system where facies Sp were deposited as 2D migrating bars within an incised channel while Sm facies could have been the result of channel bank collapse within the sandy braided river environment (Miall, 1977, 1996). Sm facies are also likely to result from channel overflow deposits produced by flooding events. During such events, water overflows the channels and deposits massive structureless sands in sheets as the water loses energy quickly (Miall, 1996; Neves et al., 2005). Trough cross-bedded facies St is present in the LSF but it is less abundant. These are the product of migrating 3D dunes under the low flow regime conditions (Miall, 1977; Horton and Schmitt, 1996). Horizontally laminated sandstone facies Sh is more abundant towards the top of the formation. Horizontal lamination can occur during floods and also shallow water. During floods, plane bed conditions develop in the upper flow regime creating traction carpets on the channel floor, depositing poorly sorted laminated sands (Miall, 1977). These facies are present in the middle of the LSF, approximately between the 150 m and the 340 m mark from the base in the type-section (Fig. 10a). This part of the formation is characterized by presence of thinner beds (average 2 m thickness) of fine to coarse sandstones, mainly composed of facies St, Sp and occasionally Sh, together with thin beds of conglomerate (1 m thick) facies Gcu and Gcn. Several ferruginous crusts up to 1-2 cm thick mark the bed terminations (Fig. 20h, i).

4.3.3. Vertical evolution of the LSF

The basal section of the LSF, extending from the base of the type-section to the 150 m level, shows an abundance of thin conglomerates, with more massive sands towards the top and prominent palaeosol horizons nearer the base. The coarse pebbly sandstone beds are generally thin (0.50 m) with maximum bed thickness of 2.5 m. The fine and medium sandstones form beds that are between 2 to 6 m thick with an average bed thickness of about 3 m. The claystones and silty claystones have bed thicknesses of up to 2 m and are dark grey or greyish brown to violet coloured and commonly contain root moulds and burrows. These associations of facies can be attributed to the distal parts of an alluvial fan. The top of this lower part is marked by a prominent erosive discontinuity at the level of 150 m from the base of the type-section (at the lower boundary of bed LPR67/04; Fig. 10a) that separates the lower dark grey claystones from the overlying sandstones marked by the first prominent cliffs on the type-section (Figs. 10a and 19b, c).

This evolves vertically into a section from 150 m to 370 m (Fig. 10a) which is dominated by sand deposition with very few thin conglomeratic beds and virtually no claystones or silty claystones. The sandstones are mainly fine- to coarse-grained, trough cross-bedded, planar cross-bedded and occasionally horizontally stratified. This represents a more channeled depositional system dominated by thinner bedded with abundant ferruginous crusts marking bed terminations. This section represents a shift from the distal alluvial fan to a sand-dominated braided river environment. In the field, this section is marked by the sandstone beds (metric to decametric in thickness) that occur between the major erosive discontinuity at the top of the claystones (150 m from base of the type-section) of the lower alluvial fan and the base (370 m) of the multicolour cliff (Fig. 11a, d).

The top part (above 370 m) (Fig. 10b), reflects a return to distal alluvial fan environments with the re-appearance of more thin-bedded conglomerates and prominent palaeosol horizons. Thin claystones and silty claystones also occur in this section, representing overbank deposition. In the field, this section occurs between the multicolour cliff and the top of the LSF which is marked by the interfingering with the Turkana Volcanics (Fig. 11d, e).

4.3.4. Lateral variations of LSF

At the type-section north of the Lokitaung Gorge (Fig. 10a), the contact between the lowest parts of the Lapur Sandstone Formation and the basement is not visible (Fig. 21a). However, further north, at the Kanamukun Laga (at about lat. 04°20’47’’N) (Figs. 9a and 21b), the LSF is observed to have been deposited on a surface of basement rocks having a tilt of 1-2° to the south, thus individual units of the LSF appear progressively higher stratigraphically toward the north than those at the basal contact near the Lokitaung Gorge (Walsh and Dodson, 1969). At about 10 km to the north, in the Kanamukun Laga (Fig. 9a), sediments typical of the lower part of LSF are unconformably overlain by plurimetric beds of yellow-beige massive sandstone that are similar to the sandstones beds above 150 m in the type-section. This important erosive unconformity is visible at the type-section as well as in the Kanamukun Laga, and marks the transition from the alluvial fan environment represented by the lower terms of the LSF, to the braided river environment that characterises the middle part of the formation. Farther north, in the Nabuin and Kanamukun Lagas (lat. 04°20'00"N; long. 35°49'12"E) (Fig. 9a), a succession of individual sandstone beds 10- to 20-m thick characterise the LSF. Two main sedimentary units can be defined on the right bank of the Kanamukun Laga (Fig. 21c): - a lower unit is formed by a succession of massive sandstone beds of metric thickness, forming 5- to 10-m thick packages with numerous

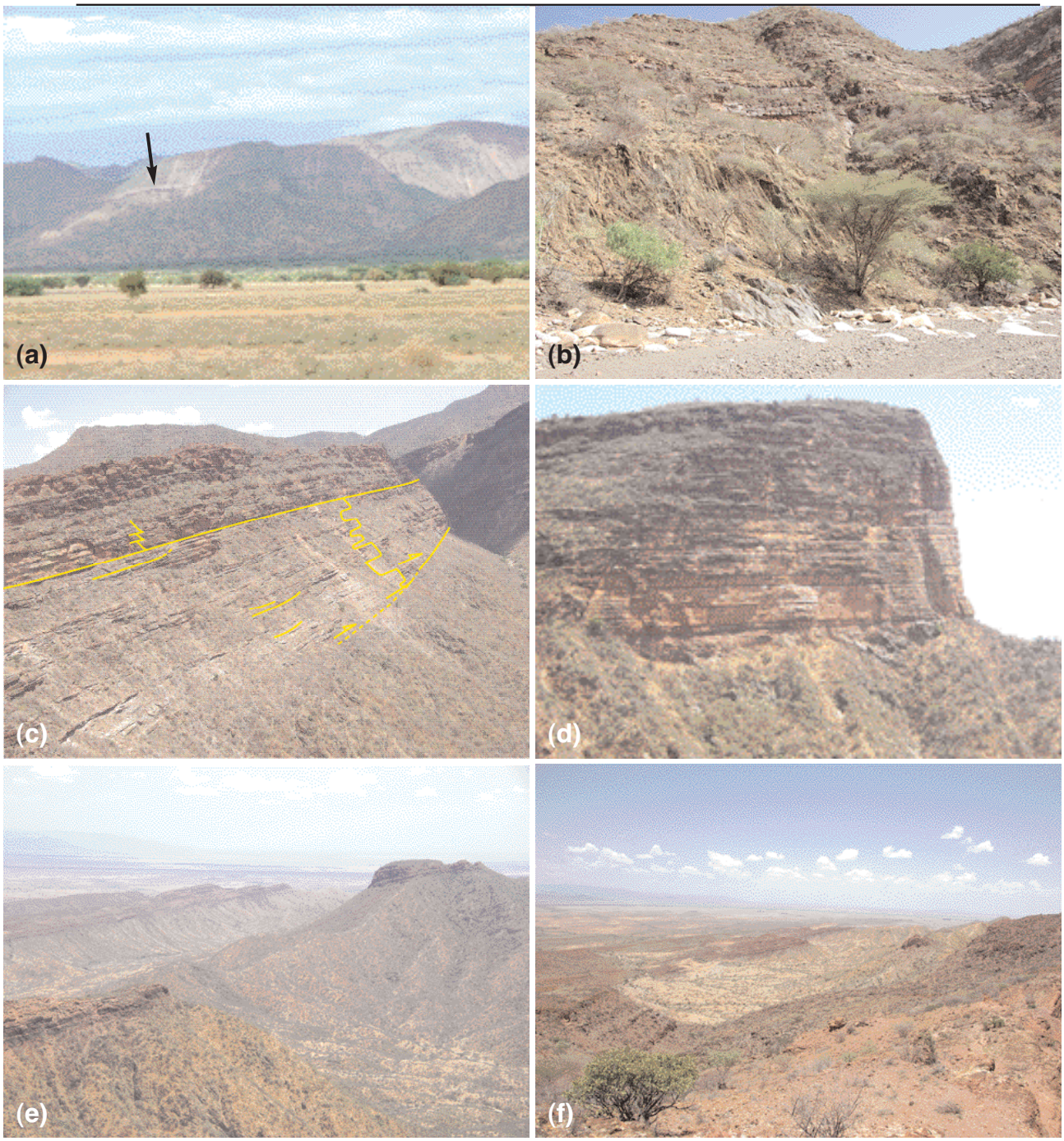

Figure 21. *Lateral variations of the LSF, from the north Lokitaung Gorge type-section northward. View toward the west, from the Todenyang Plain. (a) Panoramic view of the upper parts of the LSF in the area of Nabuin Laga (Fig. 9a). The multicolour cliff, which represents the upper alluvial fan environment in the LSF, is seen disappearing northward. (b) Left bank of the Kanamukun Laga: the lowest parts of the LSF are seen unconformably overlying amphibolitic rocks of Precambrian age. (c) Upstream Kanamukun Laga, view of the middle part of the LSF. The lower unit is seen onlapping, toward the north, the Precambrian basement surface. This unit, which is made up of a succession of channel sandstone bodies, disappears quite rapidly to the North. The upper unit is formed by a several tens of metres thick accumulation of individual sandstone bodies which are metre- to decametre-thick. (d) View from helicopter of the 100-m thick cliff in the area of Lapur Peak. This unit corresponds to the upper unit seen on photo (c). (e), (f) The northernmost end of the Lapur Range, the upper parts of the LSF are formed by alternating metre-thick sandstones and silty claystones that look very similar to the facies observed at the top of the type-section in the Lokitaung Gorge. These deposits, which are only 50 m thick, overlie the Precambrian basement and dip 10-15° toward the west. They are locally overlain by small patches of basalts belonging to the "Turkana Volcanics".*

channel features, that alternate with beds of similar thickness possibly formed by silty mudstones; - an upper unit formed by stacked stratal sandstone units of plurimetric thickness forming an abrupt cliff several tens of metres thick. At the Lapur Peak (at about lat. 04°25'N in the Lapur Range) (Fig. 9a), the LSF is in the form of an impressive cliff overlying the Precambrian basement, with a total thickness not exceeding 100 to 120 m and individual massive sandstone beds from 4 to 10-20 m thick (Fig. 21d). This implies a major decrease in the total thickness of the Lapur Sandstone Formation from the "type-section" at the north Lokitaung Gorge, where the measured total thickness was 500 m, up to the Lapur Peak where the LSF is only 100-120 m thick, this drastic decrease in thickness happens over a relatively short horizontal distance of no more than 15 km. At the extreme end of the Lapur Range, the Lapur Sandstone Formation forms low hills showing sandstone beds dipping west toward the Kachoda Basin (Figs. 9a and 21e, f). Piles of burgundy coloured, metre-thick beds overlie the Precambrian basement, with a total thickness not exceeding 50 m. The upper beds correspond to Fe-coated sandy gravels and purple siltstones showing numerous root marks (Fig. 21e). Here, the top of the cliff is overlain by basaltic lava flows several metres thick belonging to the "Turkana Volcanics" (fine-grained basalt dated 35.6 ± 0.8 Ma; see § 4.1.) (Figs. 9a and 13d-f). At the extreme north end of the Lapur Range, the landscape is formed by very low hills that merge from the wide and flat Todenyang Plain (Fig. 9a). These hills appear to be only formed by small outcrops of LSF sandstones overlying the basement. This is not in agrement with the geological map published by Walsh and Dodson (1969) that shows only patches of volcanics overlying basement forming the last reliefs of the Lapur Range. Sedimentary facies observed in this area look very similar to the ones observed at the upper part of the LSF type-section in the Lokitaung Gorge section and at Kerral. This suggests that at the north end of the Lapur Range, only the upper terms of the LSF measuring no more then 50 m, are represented.

The Lapur Sandstone Formation illustrates a quite long time interval from about 99 Ma up to 37-33 Ma. Only a few unconformities have been identified in the type-section at the Lokitaung Gorge (See § 4.3.3.). In the absence of other detailled lithostratigraphic sections over the 50 km long LSF outcrops, and the lack of biostratigraphic markers (to the exception of the fragmented dinosaur bones discovered in the lower terms of the formation), only a rough description of the lateral stratigraphic and environmental variations of the LSF can be made. Our present knowledge indicates that only the upper terms of LSF, that are interpreted as representative of an alluvial fan environment, dominate the landscape from Kerral/Lokitaung Gorge up the north end of the Lapur Range. The lower terms, that also are representative of alluvial fan environment, seem to disappear rapidly at the Nabuin Laga (Fig. 9a). The intermediate "braided stream" environment is well represented from the type-section at the Lokitaung Gorge up to the immediate north of the Lapur Peak, and is characterised by a strong variation in thickness, from more then 220 m at the type-section up to 100 m at Lapur Peak, and less than 50 m farther north. Such decrease in thickness is particularly well illustrated along the right bank of the Kanamukun Laga where the lower sandstone units representative of the braided system are seen progressively disappearing toward the north on the basement surface. Therefore, detailled lithostratigraphic logging focussing on the recognition of major and minor unconformities (based on sedimentary and chronological gaps) as well as the search for essential biostratigraphic markers have to be planned for a comprehensive knowledge of the Lapur Sandstone Formation.

4.4. Post sedimentation evolution of the LSF

The major aim of the diagenetic study is to unravel the post-sedimentation alteration of the sediment, the sequence of events causing this alteration and the implications of these changes to the overall reservoir potential of

the LSF. Understanding the initial mineralogical composition of the sediment and its original porosity and later cementation profile is of fundamental importance in deciphering the reservoir characteristics of the sandstones. The depositional mineralogical composition of the formation is that of a feldspathic sandstone with sediment sourced from metamorphic basement. The main diagenetic features observed in these sandstones are mechanical compaction and cementation by calcite, kaolin and hematite. All three cements are present from the base to the top of the LSF series but their relative distribution distinguishes three main diagenetic zones (Fig. 10):

- Zone I, which forms the basal section 0 to 85 m in the measured section;
- Zone II, which forms the middle part of the measured section between 85 to 210 m;
- Zone III, which forms the uppermost 285 m of the formation.

The diagenetic evolution of the Lapur Sandstone Formation has been deciphered from ordinary petrographic and scanning electron microscope (SEM) observation of detrital components, cements and porosity.

4.4.1. Detrital minerals

The main detrital minerals in the LSF are, in order of relative abundance, polycrystalline quartz, monocrystalline quartz, feldspars, and accessory minerals such as muscovite, zircon, apatite, rutile, ilmenite and biotite. Other detrital grains include metamorphic rock fragments and sedimentary rock fragments composed of detrital claystones and siltstones. The chemical composition of some of the cements and detrital minerals are given in Table 9.

4.4.1.1. Polycrystalline quartz. This is the most abundant type of detrital grains in the LSF. Together with monocrystalline quartz, it constitutes between 30 and 80 % of total sample thin section area by visual estimation. The grains vary in size from about 0.2 mm to a maximum of 20 mm and the number of micro-crystals varies from 2-3 to more than 100 per polycrystalline grain. Grain shapes vary from subrounded to elongate, and grain boundaries within the polycrystalline grains vary from straight regular polygonal shapes to slightly sutured ones (sample LPR 19/04) (Fig. 22a). These structures result from intracrystalline deformation rather than intercrystalline deformation i.e., pressure solution. Indeed quartz overgrowth are absent and indented contacts are very rare. On the other hand planar grain to grain contacts are common, suggesting the existence of significant mechanical compaction but no chemical compaction such as by pressure solution.

Grains with etched boundaries are present in some samples and inclusions, sometimes of authigenic brown iron oxides and kaolin (sample LPR 19/04), suggesting the filling of pre-existing grain fractures. Grain shattering is very common and produces irregularly oriented micro-fractures which are commonly filled by iron oxide or calcite cements. Grain corrosion, occurring as elongate or irregular holes (sample LPR 107/04) with brown edges is a common phenomenon and in certain instances appears to contribute to secondary intragranular porosity. This corrosion perhaps occurred during oxide and calcite cementation because theses cements filled the hole produced by corrosion.

4.4.1.2. Monocrystalline quartz. This is less abundant than the polycrystalline variety in most samples throughout the studied section. It is more abundant in the finer grained samples and grains range in shape from subangular to subrounded, measuring up to a maximum of 10 mm, but on average between 1 and 3 mm in diameter. The grains are relatively inclusion-free but show a straight to moderately undulose extinction suggesting a significant intracrystalline deformation in the source rock.

Sample	LPR126/04	LPR136/04	LPR68/04	LPR74/04	LPR35/04	LOK05/04
Na2O		0,41		0,65	11,23	0,01
MgO						0,36
Al2O3	45,93	40,51	18,17	18,18	19,43	25,6
SiO2	54,07	46,99	63,54	63,64	69,43	65,91
K2O		12,09	18,29	17,52	0,53	2,62
FeO						1,7
Total	100,00	100,00	100,00	99,99	100,62	96,20
Na		0,05		0,06	0,94	0,00
Mg						0,03
Al	2,00	3,02	1,00	1,00	0,99	1,84
Si	2,00	2,98	2,97	2,97	3,01	4,01
K		0,98	1,09	1,04	0,03	0,20
Fe						0,09
Oxygen	7	11	8	8	8	11
Total Cations	4,00	7,03	5,07	5,08	4,98	6,17
XNa	0	0	0	0	0	0
XMg	0	0	0	0	0	0
XAl	1	1	1	1	1	1
XSi	2	2	2	2	2	2
XK	0	0	0	0	0	0
XFe2+	0	0	0	0	0	0
S Oxygen	3	3	3	3	3	3
Fact K	2	4	3	3	3	4

Table 9. *SEM-EDX chemical analysis and the computed structural formulae on selected detrital minerals and cements of the LSF. The elemental ratios used for the calculation of structural formulae are based on a total of 7, 11, 8, and 8 oxygen atom(s) per analysis formula unit of kaolin, muscovite, microcline and albite respectively.*

Figure 22. *Petrographic micrographs of the studied sandstones (LP = polarised light; LPA = cross polarized light). (a) Detrital grains in the LSF include polycrystalline quartz, monocrystalline quartz and feldspars. Well preserved feldspar grains (such as the microcline showing characteristic crosshatched twinning), are not common in the LSF. The cement in this sample is poikilotopic calcite (sample LPR 19/04, LPA). (b) Most K-feldspars have undergone various stages of dissolution, resulting in the creation of secondary intracrystalline porosity, here visible in blue (sample LOK 05/04, LPNA). (c) Some microcline grains have undergone a certain amount of albitization. This is however only evident under SEM-EDX element mapping (sample LPR 74/04, SEM-EDX mapping, MAG: magnification, HV: high voltage, WD: working distance). (d) Metamorphic rock fragments (MRF) contribute a significant amount of framework grains in the LSF (sample LOK 05/04, LPA). (e) Cathodoluminescence (CL) shows the presence of at least two zones of luminescence in calcite cements of the LSF; a thin bright orange outer zone and a thicker, dull orange zone towards the pore centre. Quartz grains (Qtz) are very dark (very low luminescence) while feldspar (Kfs) luminesces deep blue. CL photograph. Sample LPR 25/04. (f) Late fracture-filling calcite (Cal) cement occurring towards the top of the LSF. Note the fracture cuts across kaolin (Kln) cements as well as hematite (Hem) cements, indicating it is a late cement (sample LPR 132/04, LPNA photograph). (g) Relationships between hematite and kaolin precipitation and K-feldspar dissolution. A first type of hematite cement (Hem-1) is a rather continuous rim of euhedral grains which grew around the detrital minerals toward the center of the primary pores. The detrital grains of feldspar show an extensive dissolution resulting in secondary intragranular porosity which is posterior to Hem precipitation. Vermicular kaolin cement filled the remaining primary porosity after Hem precipitation and could be contemporaneous to the K-feldspar dissolution. A later type of opaque oxide cement (MnOx) filled partially the secondary porosity in the feldspar grain. This later cement is manganiferous (LPA, Sample LPR 94/04). (h) Vermicular pore-filling kaolin and the abundant microporosity associated with it. Polarised non-analysed light LPNA. Sample LPR 119/04. LPA = Polarised analysed light; LPNA = Polarised non-analysed light; Mc = microcline, Ms = muscovite, Kln = kaolin, Hem = hematite, Ab = albite, Qtzp = polycrystalline quartz, Qtzm = monocrystalline quartz, Cal = calcite, Ês = secondary porosity (mineral abbreviations adapted from Kretz, 1983).* →

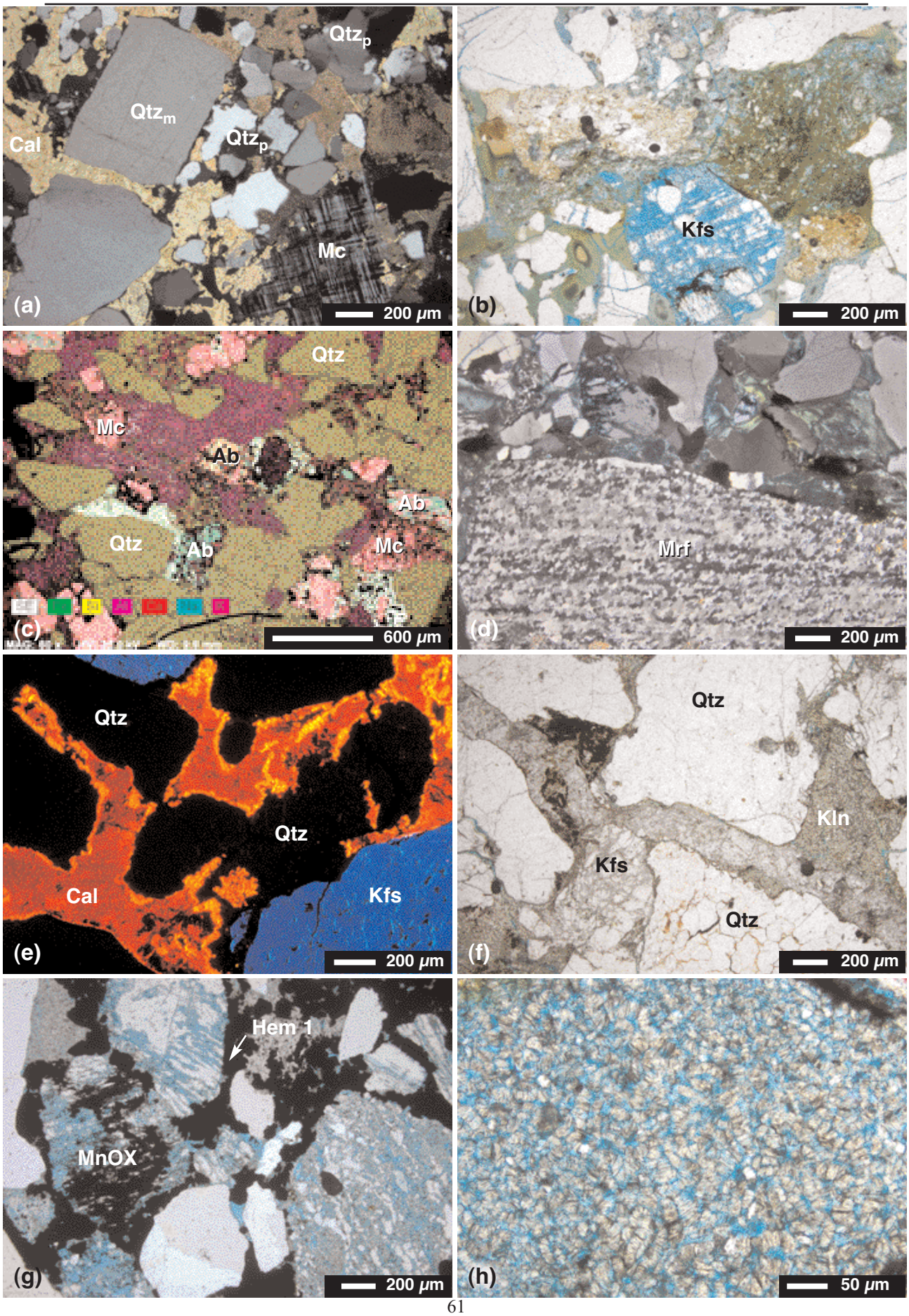
Qtz$_p$
Qtz$_m$
Cal
Qtz$_p$
Mc
(a)
200 μm
Kfs
(b)
200 μm
Qtz
Mc
Ab
Ab
Qtz
Ab
Mc
(c)
600 μm
Mrf
(d)
200 μm
Qtz
Qtz
Cal
Kfs
(e)
200 μm
Qtz
Kln
Kfs
Qtz
(f)
200 μm
Hem 1
MnOX
(g)
200 μm
(h)
50 μm

4.4.1.3. Feldspar. Feldspars are the second most important detrital grains in abundance and they make up to 30 % of the total components in some samples. Only potassium and sodium feldspars are present in the studied sample. The typical structural formula for these alkali feldspars calculated from SEM-EDS data (Table 9) is very close to the theoretical composition of the pure end member of the solid solution. The potassium feldspars are more abundant than sodium feldspars (albite) which, in some samples, are totally lacking.

Some alkali feldspars, where well preserved, show the characteristic cross-hatched twinning of microcline (sample LPR 19/04; Fig. 22a). These feldspar grains forms mostly coarse elongate grains measuring in some cases up to 25 mm in long diameter. The state of preservation of feldspar grains varies and in almost all cases, there has been some amount of alteration, ranging from minor to severe, where the grain has been almost completely dissolved (sample LOK 05/04; Fig. 22b). Alteration, in some cases, appears to have proceeded through a progressive local replacement of the feldspar by calcite or hematite cement along the cleavage planes of the feldspar grain. In many cases, the total dissolution of the feldspar generates moldic secondary porosity while partial dissolution feldspar leaves secondary dissolution porosity.

Albite has also been identified in a few samples on the SEM. The typical structural formula computed from SEM-EDS chemical analysis (sample LPR 74/04; Fig. 22c and Table 9) is very close to the theoretical composition of pure albite. Some of the albite apparently is diagenetic in origin resulting from the partial albitization of K-feldspar. There are almost always some remnants of the original grain that allows its identification as a feldspar but in rare cases, only the shape of the outline of the now secondary moldic dissolution pore space enables one to deduce that originally, the grain was that of a K-feldspar grain.

4.4.1.4. Other detrital grains. Other detrital grains in the LSF that occur only in small amounts, as trace or accessory minerals, include metamorphic rock fragments (MRF), sedimentary rock fragments (SRF), heavy minerals such as zircon, apatite, rutile, ilmenite, undifferentiated manganese-minerals and micas such muscovite or biotite. These are important as they give an idea of the nature of the sediment source rock and the source of the elements that make up the cement. The MRF are relatively more abundant in the upper part of the formation represented by the LOK series of samples (from the Lokitaung Gorge type-section) and are generally elongate grains composed of tiny sometimes elongate and aligned crystals of quartz, muscovite and iron oxides. Most of the MRF's are quartzitic in nature (sample LOK 05/04; Fig. 22d). The SRF are mainly claystone clasts with minor amounts of siltstones and they comprise up to 10 % of some samples and they appear squashed, showing evidence of sediment compaction in most cases. They appear to be more abundant just above the base of the formation and towards the top. Some SRF have undergone replacement by authigenic kaolin cement as shown by the kaolin being enclosed within an envelope of dust of precursor clay clast. The rim is made of an insoluble residue of the replacement process.

The heavy minerals were identified on the SEM. Zircon is a well distributed accessory heavy mineral in the LSF and it occurs in samples from all units of the formation, sometimes in very well preserved crystalline shapes. Apatite, rutile, ilmenite and manganese minerals (perhaps pyrolusite and psilomelane) are present only in trace amounts and in few samples. Their occurrence or abundance does not appear to be restricted to any specific horizons within the formation. Micas, especially muscovite, are present in most parts of the LSF but appears to be more frequent towards the top of the formation, where almost all samples contain a few flakes. Biotite is much less common and occurs only in very few samples, where it is in most cases altered. The source of the biotite could be basement-derived sediment material since the metamorphic rocks in the area of Lapur Range consist of among other types, biotite migmatites. Pyrite was observed on only one sample LOK 40/04 at the very top of the LSF (Fig. 10b), perhaps associated with the overlying volcanic flows.

4.4.2. Cements

The most important cements in the LSF are calcite, kaolin and hematite. Calcite cements are more abundant at the base and towards the top of the formation, hematite cements are most abundant in the numerous Fe-crusted zones which are concentrated within the middle part of the formation (Fig. 10a), while the kaolin is most abundant in the upper parts of the formation. On the basis of the predominant cement type, the Lapur Sandstone Formation has been subdivided into three diagenetic zones as presented above (Fig. 10).

4.4.2.1. Zone I. Calcite cement. Calcite is the most abundant cement in Zone I and it occurs most abundantly in the lowermost 85 m of the formation (Fig. 10a). In this zone, the calcite occurs in abundances ranging from 10 % up to 40 % (by visual estimation). The SEM-EDS gives the typical composition of a very pure calcite grain with only trace amounts of iron and magnesium in some of the samples. Calcite occurs mainly in poikilotopic textures where one large optically continuous crystal of calcite cements together several individual detrital grains. The heterogeneous colours of theses crystals as observed under CL (sample LPR 25/04) (Fig. 22e) suggest that the calcite is actually cement precipitated into empty pore space and that the poikilotopic textures results from recrystallization. The cement is made up of two luminescent zones: an outer brightly luminescent zone that follows the outline of the pore space and measures 20-50 μm on average, and an inner zone of dull orange luminescence formed by the pore-filling cement measuring up to 200 μm.

The cement is apparently pore-filling as there is no evidence of dissolution of previous minerals as these would be expected to leave relics which are not observed in the samples. It also occurs in places as a partial replacement of feldspar, this is observed in CL where the feldspar or more precisely, its remains, luminesces deep blue while the calcite cement luminesces orange. The feldspar is microcline, based on SEM petrography. The calcite cement is usually so pervasive that the primary intergranular porosity is often completely filled. Presence of a rim of hematite cement around detrical grains followed by calcite cement suggests that hematite is earlier than calcite and the presence of planar grain to grain contacts indicates that the sediment had undergone some mechanical compaction prior to cementation. The high amount of calcite cement filling primary porosity suggests a rather early diagenetic episode, only preceded by some early mechanical compaction and the precipitation of a rim of hematite cement. Another phase of calcite which is non luminescent (i.e. very dark) made of a succession of irregular rims of small crystals of calcite which grew around some detrital grains is observed in a few samples. This cement is also interpreted as having been precipitated early after sediment deposition.

A later phase of calcite cementation within this zone took place after the fracturing of quartz grains as indicated by the presence of calcite within the fractured grains (sample LPR 19/04) (Fig. 22a). This phase of calcite cementation is less significant volumetrically compared to the earlier poikilotopic cement. Other cements in Zone I include early-generation hematite and kaolin resulting from the dissolution of feldspars as well as from the kaolinization of detrital clays which are most developed in the other zones (see below). Nevertheless, Zone I is also characterized by rare occurrences of silica-rich clay cements.

Silica-rich clay cement. This has been identified in a few of the samples studied under SEM by its high Si/Al ratio (?2) on the EDS. It occurs as a more homogeneous clayey material adjacent to more crystalline vermicular kaolin (samples LPR 19/04, LPR 35/04 and LOK 13/04; Fig. 10). Some EDS analyses are close the theoretical structural formula of pyrophyllite Al2Si4O10(OH)2 (sample LPR 35/04; Table 9) with minor amounts of potassium and iron. Nevertheless other analyses show higher Si/Al ratio (?4) and various low contents of Fe, K, Mg, Na or Ti. It is characterised by lack of observable structure as opposed to the ver-

micular texture of kaolin crystals with which it is commonly associated. Its identification is based purely on chemical analysis (Table 9) and it was not possible to distinguish it from pore-filling clay minerals. It could be a mixture of amorphous silica, silica rich clay like pyrophyllite, potassium clay and iron oxide.

4.4.2.2. Zone II. This zone is characterised by the presence of abundant hematite cements, the presence of distinct ferruginous crust horizons with very high concentration of hematite and the marked decrease in or the total absence of carbonate and clay mineral cements. This zone has a thickness of approximately 125 m, staring at the 85 m mark and terminating at the 210 m mark on the measured type-section (Fig. 10a).

Hematite cements. These are widely distributed within the vertical section studied and range in percentages between trace (less than 3 %) to a maximum of 40 %. On average, all the samples contain between 5 and 10 % hematite cement (visual estimation). It occurs as dark red to brown-black and is commonly a pore-lining cement, starting out at the fringes of pore space and increasing inwards towards the pore centre. The depth of the colour depends on the thickness of the cement crust, as it was noted to be darker at the pore edges than at the centre of the pore. Where the hematite is very abundant, the rock acquires a reddish colour and locally, these are associated with ferruginous crusts which are common especially near the middle of the formation. In sample LPR 94/04 (Figs. 10 and 22g), the earlier hematite cement is a pore-lining cement with crystals growing towards the center of an open pore space. This cement is reddish-brown in reflected light. That the early cement predates feldspar dissolution is evidenced by the existence of sharp contact between grains of partially dissolved feldspar containing no cement (see arrows Fig. 22g) and hematite-cemented pore space. A later generation of manganiferous cement (MnOx in Fig. 22g) in the sample LPR 94/04 was precipitated in the secondary intragranular pore space of partially dissolved feldspars. This second-generation cement, whose manganiferous nature was identified under SEM analysis remains black under reflected light.

4.4.2.3. Zone III. This zone, which forms the top (285 m) of the LSF and was described in the type-section exposure and completed at the Lokitaung Gorge (Fig. 10b), is characterised by the presence of abundant kaolin cementation and a notable decrease in the amount of hematite and calcite cementation.

Kaolin cement. Kaolin is the most widely distributed cement in the LSF and it occurs in virtually all samples throughout the section, varying only in abundance from trace amounts (generally less than 5 %) in the basal parts of the section to a maximum of 30 % (in samples LPR 126/04 and LPR 140/04) towards the top of the formation. SEM-EDS analysis gives the typical structural formula for kaolin Al2Si2O5(OH)4 (sample

Figure 23. *Petrographic micrographs of the studied sandstones. (a), (b) Kaolin crystals with a booklet shape and various crystallographic orientations. Intercrystalline microporosity remains between the crystals. The general shape of the whole kaolin grains and the presence of a faint brown film of an insoluble residue suggest the kaolinization of a detrital clay clast which suffered mechanical compaction. The kaolin precipitation succeeded an early hematite (Hem) cement. (Sample LOK 12/04, LP). (b) is an enlargement of white box in photograph (a) where the black arrows show the insoluble residue of the kaolinized clay clast. (c) A typical mixture of platy and vermicular crystals in kaolin cement (sample LPR 83/04, SEM photograph). (d) Bent and partially kaolinized muscovite (Ms) grain, kaolinization results in frayed grain edges as it is converted into kaolin (Kln), (LPA; sample LPR 107/04). (e) Three different types of cement are seen in this photograph where the sequence of cementation from the pore edges towards the pore center is a thick pore-lining hematite (Hem) cement followed by a layer of cryptocrystalline quartz and finally in the pore center, kaolin cement (LP, sample LOK 11/04). (f) is an enlargement of the white box in photograph (e). (g) Bioclastic grains are very rare in the LSF; the only occurrence noted are algal grains found in the topmost bed (sample LOK 40/04) of the LSF just below the contact with the Turkana Volcanics (h) Floating grains of detrital quartz in a predominantly carbonate matrix; possibly detrital in origin (LP, sample LPR 136/04). In CL, some dark bioclastic grains are still visible cemented or replaced by a late luminescent calcite cement. (LP, sample LOK 11/04). (LP = Polarised light; LPA = Cross polarized light). Ms = muscovite; Kln = kaolin; Hem = hematite; Qtz = quartz; Cal = calcite (mineral abbreviations from Kretz, 1983).* →

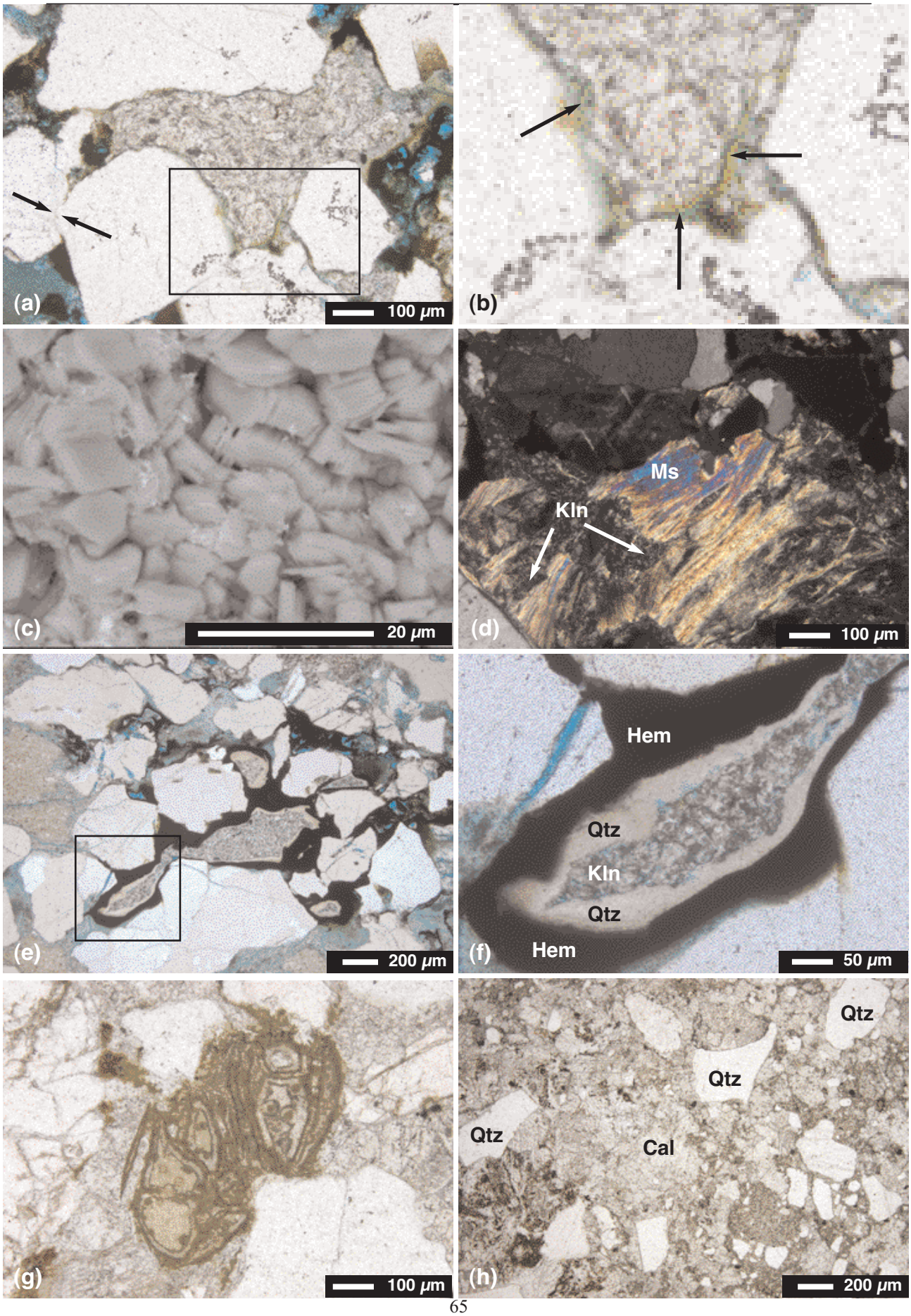
(a)
100 μm
(b)
(c)
20 μm
(d)
Ms
Kln
100 μm
(e)
200 μm
(f)
Hem
Qtz
Kln
Qtz
Hem
50 μm
(g)
100 μm
(h)
Qtz
Qtz
Qtz
Cal
200 μm

LPR 126/04) (Table 9). On average the kaolin content is between 10 and 20 % on all samples throughout the vertical section studied (visual estimation). Vermicular kaolin occurs in close association with detrital clay clasts (sample LOK 12/04) (Fig. 23a, b) and leached feldspars which may be indicative of the alteration of detrital clays and dissolution of feldspars to be replaced by vermicular kaolin. It also occurs commonly as a pore-filling cement forming at the centre of pores with other cements such as hematite and remnants of detrital clays fringing the pores. Kaolin occurs mainly in vermicular textures (e.g. in sample LPR 83/04; Fig. 23c) where the crystals are stacked and arranged in characteristic worm-like structures. Under the SEM, kaolin was observed to form both platy and vermicular textures. Some muscovite grains show a certain degree of kaolinization (sample LPR 107/04) (Fig. 23d) especially at the ends, producing radial fibrous kaolin. Generally kaolin crystals appear to develop preferentially at the ends of the muscovite elongate crystals between the muscovite cleavage planes where the muscovite seems to be destabilized, resulting in a fibrous "horse-tail" appearance. Kaolin cement was not observed to cause complete occlusion of primary intergranular porosity or even secondary dissolution porosity within pore space and a certain amount of microporosity remains within the kaolin-cemented pores (Fig. 23e, f).

Hematite cements. In Zone III, the hematite cements are particularly common in the section measured within the Lokitaung Gorge, and they are clearly early cements; as they occur as pore-lining cements followed, in many instances, by later generations of siliceous and kaolin cements (sample LOK 11/04) (Fig. 23e, f). This type of cementation is very common within this zone and the different cements and their relative timing of generation are clearly distinguishable.

Siliceous cements. These occur only in the top zone of the LSF and they are amorphous non-crystalline in texture (sample LOK 11/04) (Fig. 23e, f), identifiable only through SEM-EDS analysis. This type of cement is predated by the reddish-brown hematite cement and post dated by pore-filling vermicular kaolin cements.

Calcite cement. The only significant calcite cementation is at the very top of the formation, observed in the last sedimentary bed (pebbly sandstone) which is interbedded within the first flows of the “Turkana Volcanics” (Figs. 10 and 23g; sample LOK 40/04). In the upper parts of the LSF, the calcite cement is different in texture from the cement in the lower parts. Some of the calcite in upper units occurs as fracture-filling cements with drusy-mosaic textures cutting across pre-existing kaolin as well as hematite cements. Sizes of individual calcite crystals increases progressively from the edge of the pore inwards. In sample LPR 136/04 (Fig. 23h), there appears to be more calcite than detrital grains and the latter grains appear to be floating in a matrix of sparry micro-crystalline calcite with a sucrosic texture. These grains are probably reworked pre-existing carbonate that has subsequently between re-cemented together by recrystallized calcite. The recrystallized calcite occurs in poikilotopic textures while the detrital calcite occurs as distinct granular textures, indicative of detrital origin for some of the cement, where pre-existing carbonate is reworked, recrystallized and included into the rock as detritus, with later cementation by late-generation calcite cement. Recrystallized calcite is recognized by its appearance as patchily distributed coarsened crystals lacking the precipitational variations in crystal size seen in drusy carbonates which increase in crystal size from pore wall to pore centre (Morad, 1998).

At the very top of the Lokitaung Gorge section (Fig. 10b), there occurs what appears like the remains of a bioclastic grain (sample LOK 40/04) (Fig. 23g), perhaps an algal fragment which could have provided the substrate onto which poikilotopic crystals developed. The sample has both poikilotopic and sparry calcite textures. In CL, some dark bioclastic grains are still visible cemented or replaced by a late luminescent calcite cement. Localized lacustrine environment could also have contributed to the source of Ca, evidence for this is in the presence of bioclastic grains which have been seen only at the top of the LSF.

Hematite cements. In Zone III, the hematite cements are particularly common in the section measured within the Lokitaung Gorge, and they are clearly early cements; as they occur as pore-lining cements followed, in many instances, by later generations of siliceous and kaolin cements (sample LOK 11/04) (Fig. 23g, h). This type of cementation is very common within this zone and the different cements and their relative timing of generation are clearly distinguishable.

Siliceous cements. These occur only in the top zone of the LSF and they are amorphous non-crystalline in texture (sample LOK 11/04) (Fig. 23g, h), identifiable only through SEM-EDS analysis. This type of cement is predated by the reddish-brown hematite cement and post dated by pore-filling vermicular kaolin cements.

4.4.3. Porosity

Porosity measurements were performed on a total of 24 samples taken from the LSF type-section (Fig. 24). The present total porosity in the samples is the net porosity after the original porosity at deposition has been reduced by diagenetic processes. These processes include mechanical compaction and the precipitation of cements. From the samples studied, the LSF has total porosity values ranging from a minimum of 3 % to a maximum of 25 %. While this porosity appears to be evenly distributed, it is markedly less abundant in the lower-most parts and the top-most parts of the LSF (which are cemented by poikilotopic calcite). This is as would be expected that the presence of pervasive cementation by poikilotopic calcite would drastically reduce the amount of primary intergranular porosity and this is what is observed in the LSF samples at the base of the formation. The percentage of calcite cement in the samples is close to the assumed original intergranular porosity of about 40 %. A significant part of the remaining porosity can be attributed to microporosity inside the kaolin cements and to K-feldspar dissolution.

4.4.4. Source of cements ad diagenetic reactions

This discussion attempts to postulate the possible sources of the major cement types in the LSF in view of the important role these cements play in the determination of the reservoir quality of any sandstone unit.

4.4.4.1. Calcite cementation. In the basal section of the LSF, calcite cements were probably precipitated prior to any significant sediment compaction. The main diagenetic events in this section were the deposition of grain-coating hematite cement, the formation of kaolin cements mainly from the alteration of feldspars and the precipitation of poikilotopic calcite cement. Assuming that the sandstones had 45 % initial intergranular porosity and the present residual porosity is less than 5 %, and the amount of cement is approximately 40 %, this suggests that there has been no appreciable loss of porosity through compaction. There is no evidence of a significant mechano-chemical (pressure-solution) compaction; most of the compaction is therefore mechanical and it involves ductile deformation, re-arrangement and fracturing of grains. In other parts of the formation that do not have calcite cement, there is evidence of a higher amount of compaction with the presence of broken muscovite grains. Early calcite cement may have greatly inhibited sediment compaction and the mechanical compaction is assumed to have been early.

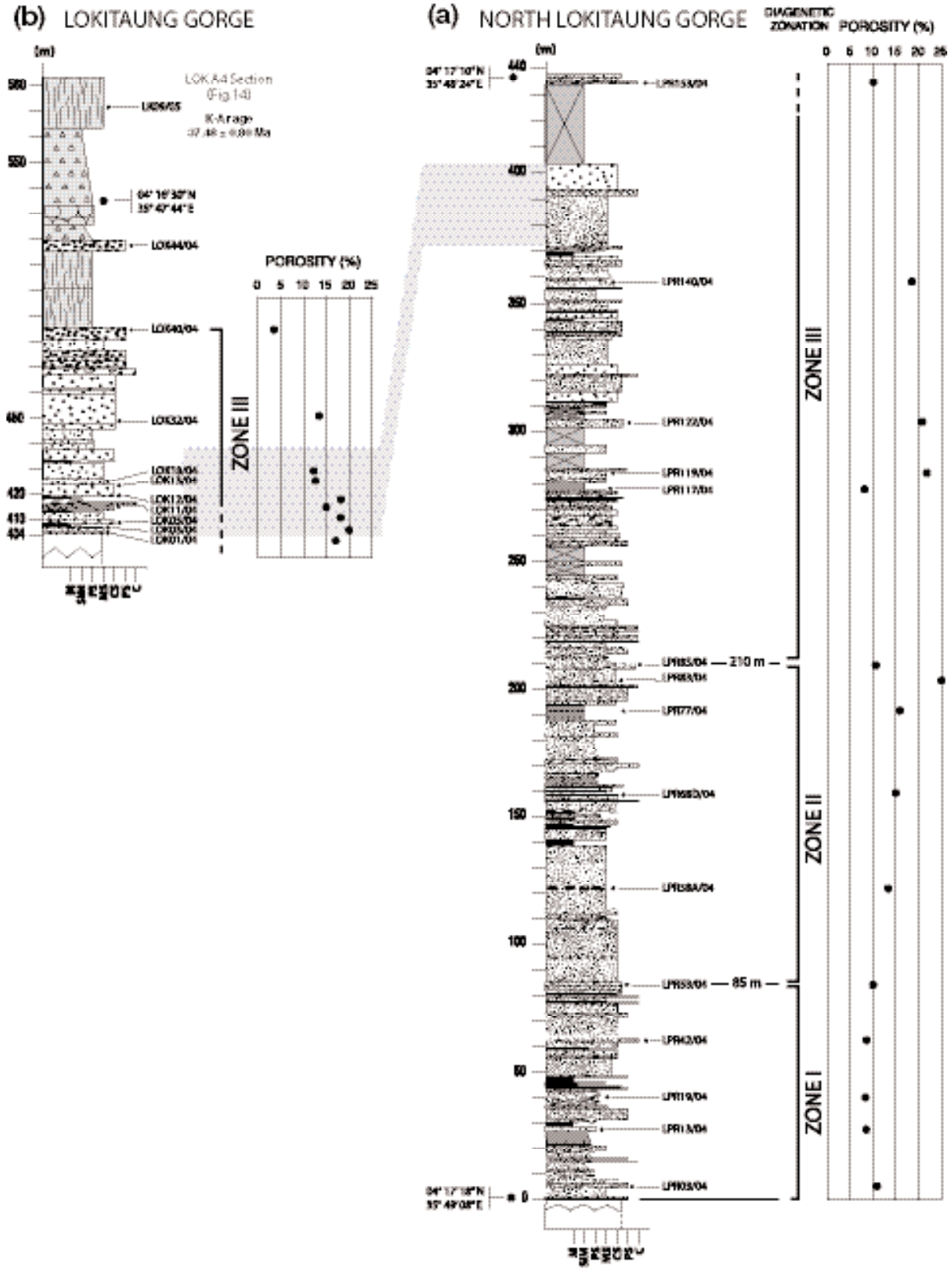
(b) LOKITAUNG GORGE
(m)
LOK A4 Section
(Fig.14)
K-Ar age:
POROSITY (%)
0 5 10 15 20 25
ZONE III
(a) NORTH LOKITAUNG GORGE
DIAGENETIC ZONATION
POROSITY (%)
0 5 10 15 20 25
ZONE III
ZONE II
ZONE I
210 m
85 m

Calcite cement in this zone is therefore considered early cement and the product of shallow burial diagenesis. Poikilotopic calcite (Fig. 22a) is a common early diagenetic primary cement in sandstones calcretes, especially in fluvial channels (Morad, 1998). In continental sediments with low organic matter, dissolved carbon is derived from the decay of plant remains within the soil horizons and from atmospheric CO2. Calcretes occur as concretions and laterally extensive cements in flood-plains and also develop in fluvial channel sandstones and they dominate in the coarse grained proximal facies. Sources of calcium for calcretes may include windblown dust, pyroclastic material, or groundwater may bring carbonate ions from carbonate terrains to siliclastic sequences. Additional sources include Ca dissolved in rainwater and dissolution of Ca-plagioclase (Morad, 1998). In the LSF case, the source of carbonate ions may be from groundwater enriched with Ca2+ ions picked up by fluid circulating through the Cretaceous sediments deposited during the marine transgression whose limit is to the east of Lake Turkana (Bosworth and Morley, 1994; Morley et al., 1999). Nevertheless a marine source is may be more realistic to explain the large amounts of carbonate cement observed (approximately 5.5 cubic km based on average of 20 % calcite content in a LSF outcrop measuring 4.4 km wide, 63 km long and 0.1 km thick calcite cemented zone). Other sources may include carbonate-rich lavas overlying the LSF, which can be used to account for the calcite-cemented zone at the top of the formation where the cement occurs as fracture filling calcite. Indeed numerous calcite geodes are present in the overlying Turkana volcanics (Fig. 13h), attesting to the fact that the lavas are calcium-rich and that calcite is mobile. Geochemical analysis of samples of lavas indicate that the calcium values, measured as % CaO, range between 9.1 and 11.1 (Table 6).

The numerous dykes that cut across the LSF could be a potential calcium source for calcite cementation (See § 4.1.). Their alteration by late magmatic fluids or most probably by diagenetic fluid circulations activated by the thermal effect of this magmatic phase could mobilize calcium by intensive alteration of magmatic minerals (Daoudi and Potdevin, 2002). Field evidence has noticed the presence of well indurated, tightly cemented sandstone units in the proximity of dyke and sill intrusions in the lower parts of the LSF. The overlying Turkana Volcanics are likely sources of some of the calcium that forms calcite cement as evidenced by presence of horizons with abundant calcite geodes within the lower parts of the volcanics (Fig. 13h).

Late generations of replacive calcite occur in some cases especially in the middle and top section of the formation where the calcite replaces all types of older grains (including quartz and feldspars) and cements such as hematite and kaolin. This late generation cement was most likely precipitated as a result of chemical stability differences between mineral phases with respect to the prevailing circulating pore waters.

4.4.4.2. Hematite cementation. Hematite cementation is associated with ferricrust development and is most pronounced in the middle section of the LSF. When deposition areas, especially alluvial flood-plains, are starved of sediment supply for extended periods, in situ alteration of sediment may take place. This alteration commonly takes the form of pedogenesis and the development of red hematite pigments through the weathering of ferromagnesian minerals and the infiltration of weathering products into the sediment (Collinson, 1996). Hematite is the main cement in the middle section of the LSF. At least 2 generations of dark coloured oxide cements were observed, where the early first generation of hematite cement is succeeded by precipitation of kaolin and later by the dissolution of K-feldspar. The dissolution of feldspar is in turn followed by the precipitation of a second generation of a manganiferous variety and finally in some cases, the depo-

← ***Figure 24.*** *Lithologic log of the LSF with a porosity plot, showing measured porosities ranging from 3 to 25 %. The trend of the porosities follows what is expected in view of the cementation profile of the LSF. Low porosities are generally associated with cementation by calcite while kaolin cemented zones retain higher porosity values.*

sition of a grain- and cement-replacive calcite. The fact that some of the hematite cement in the LSF occurs as grain coating early cement preceding all other cements, it is proposed that this may be primary in origin and that the grains may already have been coated with hematite at the time of deposition (Levandowski et al, 1973; Tucker, 2001). Subsequently, other generations of hematite and manganiferous cements were formed by direct precipitation at or near the soil surface from fluids enriched in Fe-Mn as a result of dissolution of ferromanganese minerals. Textural discontinuities such as the jump from a coarse underlying sandstone into an overlying claystone can induce short range changes in redox potential which is higher in the coarse sediment and lower in the finer one. Any ferrous ions in circulating fluids are oxidized on reaching the Eh jump (where the redox potential suddenly changes from a high to low value at the bed interface) resulting in their immobilization as a crust of ferric oxide (Schwertmann and Cornell, 2000).). In the LSF, such terminations are not uncommon, where a lower sand body is capped by ferric crust that separates it from the overlying claystone beds.

Outcrops of Precambrian basement rocks composed mainly of amphibolites occur along the eastern part of the Lapur Range. These are believed to be metamorphic derivatives of intrusions into the basement system and are composed of mainly andesine feldspar, diopside, hornblende and epidote as well as ilmenite, sphene and apatite as accessory minerals (Walsh and Dodson, 1969). Weathering of these amphibolites as well as amphibolites-sourced sediments could be the source of substantial amounts of iron that can be attributed to the large amounts hematite cements in the LSF. Lateratization can occur in well drained uplands with alternating dry and wet seasons at temperatures above 16 °C and rainfall above 1000 mm annually (Jones, 1965). Though the average annual rainfall (present-day) in the Lokitaung area is approximately 500 mm (Walsh and Dodson, 1969) it sometimes exceeds 1000 mm (for example in 1961 it was 1081 mm) and with the average temperatures of 34 °C, conditions for the formation of period laterites can easily be attained. Conditions similar to these present-day ones could have been achieved in the past allowing for the formation of laterites. Hematite-rich crusts could be the result of episodic lateritization. Hematite in the sandstones of the LSF was probably originally derived from ferrous silicates in the underlying crystalline basement rocks as well as from the dehydration of other ferric oxides after deposition as in the case of the Cretaceous Bima Sandstone of Nigeria (Jones, 1965).

4.4.4.3. Kaolin cementation. Kaolin is the predominant cement in the top section of the LSF. The term kaolin is used to refer to kaolinitic cements in the formation since it has not been possible to differentiate between the different possible polytypes of kaolin cements such as dickite, nacrite and kaolinite proper (Buatier et al., 1997; 2000). The general sequence of cementation towards the top of the LSF is the precipitation of early hematite followed by the formation of an amorphous siliceous cement and finally a pore-filling kaolin cement. Several possible sources of kaolin have been suggested and they include the alteration products of K-feldspars, the alteration of muscovite and the kaolinization of detrital clays (Hassouta et al., 1999). Weathering of iron minerals followed by meteoric leaching of detrital clays and feldspars can create supersaturated fluids with respect to amorphous silica in the upper part of LSF (Zone III) resulting in the precipitation of amorphous silica cements. In the lower parts (Zone I) by contrast, the fluids would be supersaturated with respect to silica-rich clays (pyrophilite) which would then be precipitated. Following the precipitation of silica-rich clays and silica in the lower and upper zones respectively, the fluids would become progressively under saturated with respect to silica and thus result in the precipitation of kaolin.

In order to allow for the precipitation of kaolin, the diagenetic fluids need to have low concentrations of Si and K and also to become enriched in Si and Al. Chemical composition of meteoric water (very low concentration of silica and potassium) which has evolved to silica-aluminium rich concentration by leaching of K-feldspars which allow precipitation of kaolin.

Since in order that amorphous silica precipitated, the point of silica saturation must be reached and there must be either K-feldspar or silica-rich clays co-precipitation with amorphous silica. The silica rim cement may also be due to some kind of evaporation process will allow supersaturation of circulating waters with respect to silica. This kind of evaporative processes may also explain the precipitation of hematite cements. Seasonal dry and hot spells could create conditions conducive for such processes.

4.4.4.4. Feldspar alteration. The samples from the LSF perhaps contained up to 30 % feldspars during their deposition since a few of them still have such a high abundance of residual feldspars at present. These feldspars have undergone varying degrees of dissolution and are considered to be the main source of the kaolin cements within the LSF. Alteration of feldspars is inevitable since their detrital grains are commonly in disequilibrium with diagenetic pressure, temperature and pore fluid chemistry and are therefore prone to diagenetic processes that help them reach equilibrium. The main processes of feldspar alteration are dissolution, replacement by clay minerals (e.g. kaolinization) and albitization (Worden and Morad, 2000). For instance, the dissolution of feldspar and precipitation of kaolin can be related by a reaction like the following:

$$\underset{\text{K-feldspar}}{2KAlSi_3O_8} + 2H^+ + H_2O = \underset{\text{Kaolin}}{Al_2Si_2O_5(OH)_4} + 4SiO_2 + 2K^+$$

Due to the higher Si/Al ratios of feldspars compared to the clay minerals that replace them, reactions that involve production of clays at the expense of feldspars lead to the release of Si and thus creates potential for quartz or amorphous silica cementation. This reaction in many instances is accompanied by co-precipitation of carbonate cements such as calcite (Worden and Morad, 2000). In the LSF, there is no quartz overgrowth cementation. The released silica may have been transported in solution to other sites of silica precipitation. This silica was perhaps the source of the amorphous silica cements observed as part of pore-filling cements in the LSF if the conditions allowed the saturation point with respect to silica were attained. Where present these amorphous quartz post-date hematite cements and pre-date kaolin cementation.

Some kaolin crystals are enclosed in poikilotopic calcite indicating that the kaolin must have formed prior to the calcite cement. Kaolinization of feldspars leaves a thin outline in completely replaced grains; sometimes there are identifiable remains of the detrital grain. Replacement of detrital clays by kaolin is identified by the presence of vermicular authigenic kaolin completely surrounded by remains of clay clasts. Albitization of feldspars is common in deep burial diagenesis and it is not considered a major pathway of feldspar alteration within the LSF, though there are a few grains of albite present. These grains are considered detrital in origin but there is also evidence of albitization of K-feldspar. The dissolution of micas, feldspars, clay clasts and the formation of kaolin are attributable to near-surface, meteoric water diagenesis (El Ghali et al., 2006). During various time, conditions of pH and ionic equilibria have favoured the side-by-side precipitation of both kaolin and silica-rich clays.

4.4.4.5. **Alteration of muscovite.** Where muscovite has suffered diagenetic alteration, the grains expand into and fill primary porosity (Fig. 23d), suggesting that this alteration may have happened prior to major reduction in porosity by compaction or intergranular cementation. This alteration is replacive in nature and where the grain is in contact with open pore space, the flow of under-saturated acidic waters allow the dissolution of muscovite accompanied by removal of the reaction products in solution (Crowley, 1991). Since the solubility of Al is low at high Si saturation, pore waters available to react with muscovite quickly exceed the solubility of kaolin resulting in the precipitation of kaolin in place of or adjacent to dissolved muscovite grains. These altered grains act as nucleation centres for additional precipitation of kaolin, the formation of splayed and expanded textures being attributable to the displacive growth of kaolin

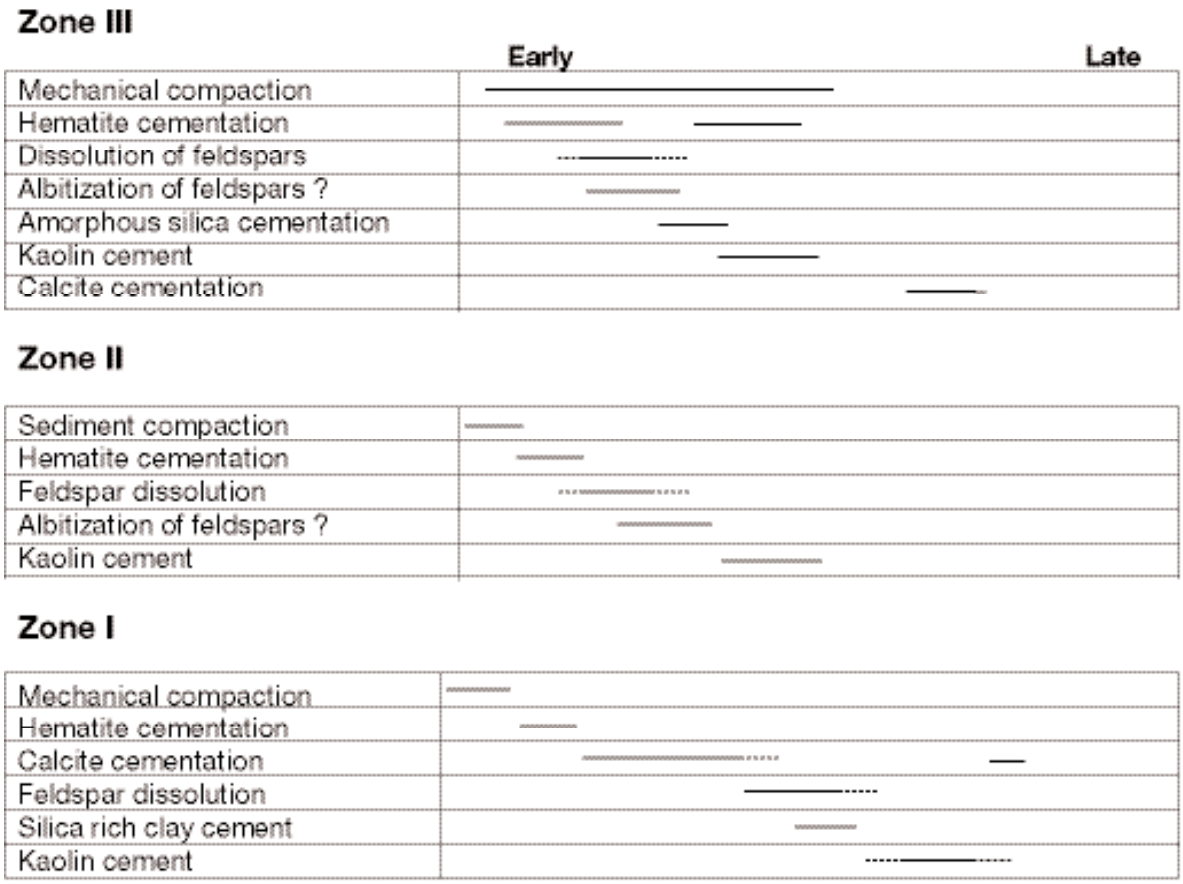

Figure 25. The paragenetic sequence within the three main diagenetic zones in the LSF. Zone I represents the bottom 90 m, Zone II the middle 120 m and Zone III the top 275 m (including the section completed in the Lokitaung Gorge section) of the formation. Relative timing and duration of the various events is indicated by the position within the early to late time domain. Dotted lines indicate high levels of uncertainty.

between the cleavage sheets of muscovite (Crowley, 1991). The reaction for the alteration reaction has been suggested as follows (Bjorkum et al., 1988; Hassouta et al., 1999):

$$2\ KAl_3Si_3O_{10}(OH)_2 + 2\ H^+ = 3Al_2Si_2O_5(OH)_4 + 2\ K^{++}$$
Muscovite — Kaolin

Though this alteration was observed to occur frequently, the amounts of muscovite available for the alteration is generally quite small, the abundance of muscovite in the LSF is only in trace amounts. The resulting kaolin is therefore expected to be volumetrically small.

4.4.5. Chronology of diagenetic events

The major diagenetic events and cements types that characterize the different zones are shown in Figure 25 and are described below.

The early diagenetic events in all the three zones of the LSF involved a certain amount of mechanical compaction of the sediment attributed to the overburden weight. Hematite cementation took place early as

discerned from the relationship between the detrital grains and the cement in relation to its exact position with the pore system. Most of the hematite appears as pore-lining cement with the later cements occurring as pore-filling varieties. In Zone I, some of the calcite cementation which is the main diagenetic feature, is early cement where it is predated only by cementation by hematite. A later generation of calcite cement in this zone may have been initiated by the effects of hydrothermal fluids during the emplacements of the numerous dykes that cut the sandstones in this zone. A later phase of calcite cement is seen at the top of Zone III in the form of fracture filling and pore filling poikilotopic cement. These cements are likely to be associated calcium ions sourced from the overlying Turkana volcanics. Kaolin cementation in this zone is partly a product of feldspar dissolution. In Zone III, there are clearly at least two episodes of hematite cementation, where an early phase predates feldspar dissolution followed by a later manganiferous phase which post-dates dissolution of feldspars and is emplaced within the secondary intragranular pores resulting from the dissolution (Figs. 17g and 20). Zone III also gives a clear sequence of cementation between the emplacement of hematite which predates the fine cryptocrystalline siliceous cement which is in turn post-dated by pore-filling kaolin cement (Fig. 18g, h).

5. Discussion.

Importance of the Lapur Sandstone Formation for palaeogeographical and climatic reconstitutions, and implications for oil exploration

Exploration for oil in the northern Turkana area of Kenya by Amoco Kenya Petroleum Company and later by Shell Exploration and Production Kenya BV in the mid 1980s was to search for the Cretaceous basins similar to the ones that had been discovered in southern Sudan by Chevron (Schull, 1988; Giedt, 1990; Morley et al., 1999). The Lapur Sandstone Formation being an exposed Cretaceous(?)-Paleogene potential reservoir unit therefore gives the exploration geologist the opportunity to study what may be expected to be present in the subsurface of the different Mesozoic-Tertiary basins in the region. Surface sampling and petrographic and diagenetic studies may enable the prediction of various reservoir parameters, such as porosity evolution, as they may be expected to be at depth within the basins.

Palaeogeographic reconstruction together with an interpretation of palaeoclimatic conditions have significant control on the sedimentological characteristics of any sedimentary formation. Palaeogeography controls sediment production and also determines the mode of sediment transport as well as its final resting place in terms of erosion, transport and deposition. Sediment source material, whether it is basement derived or sourced mainly from volcanics or has significant volcanic input determines to a large extent whether its diagenetic alteration will retain significant amounts of the desirable reservoir characteristics of effective porosity and permeability. The LSF is composed predominantly of arkoses made of quartz and feldspars derived from basement with no volcanic input. Diagenesis of the LSF involves mainly sediment compaction, dissolution of unstable grains such as feldspars and the cementation by calcite, hematite and kaolin. The prevailing climatic conditions determine the products of diagenesis. Hot and dry conditions where evaporation greatly exceeds precipitation produce evaporites while semi-arid conditions accompanied by humid seasonality with higher precipitation than evaporation produces dolocretes and calcretes. Where conditions are seasonally dry and its mainly hot and humid with precipitation just exceeding evaporation, laterites and ferricretes form. In the use of clays as sedimentological markers, kaolin which is an important cement in the LFS, normally forms under semi-arid conditions with a seasonally dry period where overall, precipitation only just slightly exceeds evaporation (Sellwood and Price, 1993).

5.1. Palaeogeographical and climatic reconstitutions (from sedimentological data)

Much of the drainage of the eastern-central part of Africa is relatively young. Major changes in river courses were linked to tectonic (doming and occurrences of volcanic plumes) and climatic changes. During middle-late Cretaceous, drainage in northern and eastern Africa was dominated by rivers flowing to the north-west (Sirte River) and to the south-east (Sudan Rift Rivers and Anza River), respectively (Burke, 1996; Burke et al., 2003). Rift-controlled rivers, flowing through the south Sudan rift basins, deposited huge amounts of sandstones such as the Nubian sandstones along the way. The course of the Anza River toward the south-east was in the same way controlled by the Anza Rift structure, feeding the Lamu Delta and draining into the Indian Ocean (Reeves et al., 1987; Burke, et al., 2003) (Fig. 26). Sandstones that belong to the LSF can be linked to such fluvial network palaeogeographies (Mateer et al., 1992).

Chronological data obtained in this work indicate an early Paleogene age for the very top of the LSF, suggesting that fluvial palaeogeographies that characterised the northwest part of the Turkana Depression from middle Cretaceous may have existed until this period (late Eocene-early Oligocene). Measured palaeocurrent

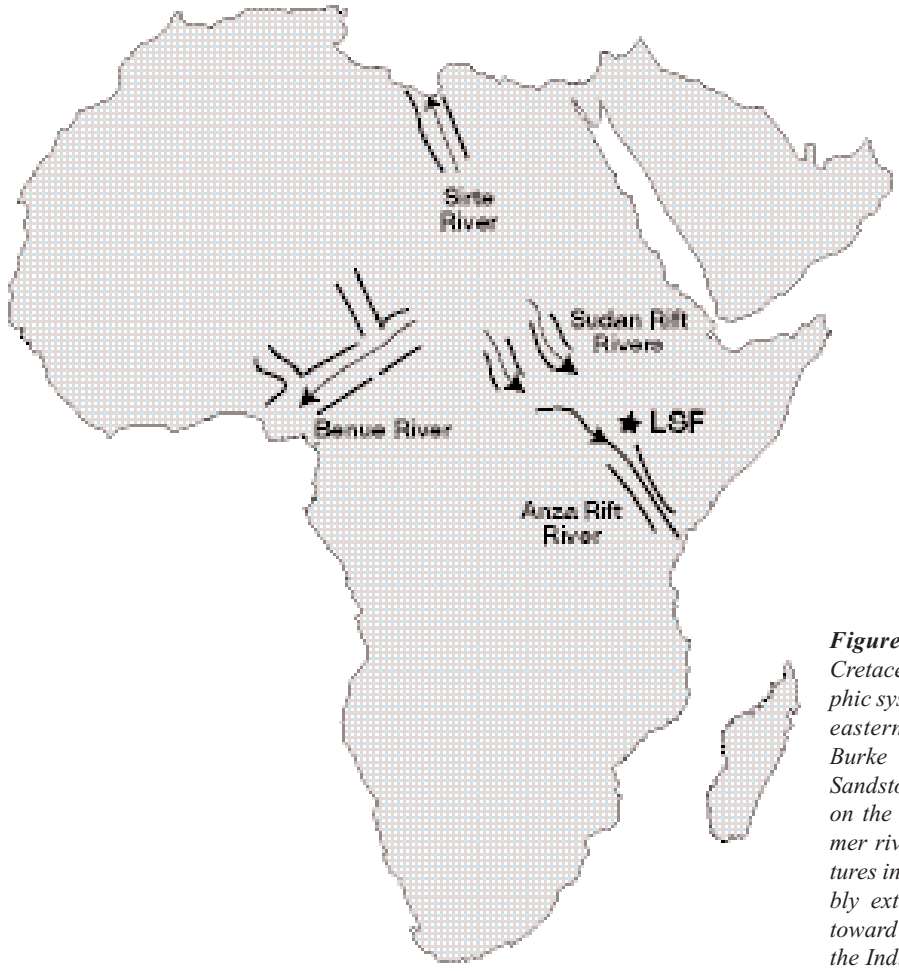

Figure 26. *Schematic map of Cretaceous-Paleogene hydrographic system in central (Sudan) and eastern (Kenya) Africa (from Burke et al., 2006). The Lapur Sandstone Formation (black star on the map) may represent a former river controlled by rift structures in southern Sudan and possibly extending into the Anza Rift toward the Lamu embayment and the Indian Ocean.*

directions in the type-section especially within the braided system, show significant scatter but there is a tendency to favour the south-southwest direction (Fig. 10). While the number of measurement and their distribution with respect to the whole of the LSF outcrop from south to the north may not be adequate to base a conclusion on, McGuire et al. (1985) reported two sets of current directions for the LSF, an east-trending set in the south while in the north, the trend was reported as typically west-southwest. The lower and top parts of the LSF were deposited in distal alluvial fan environment while the middle part corresponds to a more channelized, sandy braided stream environment. As shown in paragraph 4.3.4., there is dramatic thinning of sediment thickness from south to north. This was attributed by McGuire et al. (1985) to both depositional causes (onlap towards the north) and erosional truncation of the sedimentary sequence underlying the volcanics.

The lower part of the Lapur Sandstone Formation is interpreted as representing an alluvial fan environment that could be related to the tilted block structure that is illustrated in the subsurface at the northern end of the Gatome Basin (TVK-7 seismic line; Fig. 15). Such alluvial fan deposits, of possible Cenomanian(?) age, may have accumulated during the phase of extension leading to the formation of this half-graben geometry as it exists in different basins of south Sudan. The abrupt change observed in the LSF (150 m mark in the type-section; Figs. 11a and 19b, c) from an alluvial fan system toward a braided river system could relate to the end of this phase of extension, possibly associated to a major change in climate. This major change may have been preceded by a important stratigraphic gap, with strong erosion resulting in the disapearance of fault scarps associated with the alluvial fan environment, and a large part of the fan deposits previously accumulated.

The quite abrupt disappearance of the LSF fluvial system may have coincided with the first volcanic eruptions linked to the shallow-plume generated volcanism that reached the area west of Lake Turkana at around 35 Ma (Burke, 1996; George et al., 1988; Burke et al., 2003). Our results in this work indicate an age of between 37-35 Ma for the earliest lavas belonging to the Turkana Volcanics, with intermittent minor sandstone deposition within the earliest lava beds. This age can be compared with the shallow-sourced plume igneous activity whose age has been reported to be between 45 Ma and 35 Ma in southern Ethiopia (George et al., 1998).

5.2. Climatic conditions from diagenesis data

The diagenetic process that a sediment goes through after deposition is dependent on, among other factors, the humidity or aridity of the prevailing climatic conditions. The products of diagenesis will therefore be closely related to the climatic changes that have taken place since the deposition of the sediment. In order therefore to understand the diagenetic evolution of the LSF, it is necessary to understand the climatic conditions that prevailed between the upper Cretaceous and the Eocene-Oligocene boundary, the period during which the formation was deposited.

The clay mineral assemblages can be used as sedimentological markers where the preference of kaolinite to smectite is indicative of a shift from predominantly arid to humid, with precipitation exceeding evaporation (Sellwood and Price, 1993). During the Cenomanian period (99-93 Ma), the climate for the northern Kenya as well as for the rest of central Africa was semi-arid. This period corresponds to the time of deposition of the lower part of the LSF and the diagenetic minerals to be expected (Sellwood and Price 1993) in this part of the formation include calcite and hematite, which indeed is the case. The climatic situation remained the same for the Coniacian-Santonian period (89-83 Ma) but changed during Maastrichtian (70-65 Ma) when the region became humid, and the major product of diagenesis from this period should be kaolinite (Sellwood and Price, 1993). The upper half of the LSF may have been deposited during the period when the climate was predominantly humid and therefore

the abundance of kaolinite as the main cement is to be expected. On the basis of cement stratigraphy, a relative chronology can be established, especially for the middle and upper parts of the formation, which have dominant palaeoclimate-sensitive cementation products of hematite and kaolin. Possible correlation of climatic periods and ages to diagenetic zones is as follows:

Eocene (55.8-33.9 Ma)	Humid	Kaolin (Zone III)
Paleocene (65.5-55.8)	Humid	Kaolin (Zone III)
Maastrichtian (70.6-65.5)	Humid	Hematite/kaolin (Zone II/Zone III)
Campanian (83.5-70.6)	Semi-arid	Calcretes (Zone I)
Santonian (85.8-83.5)	Semi-arid	Calcretes (Zone I)
Coniacian (89.3-85.8)	Semi-arid	Calcretes (Zone I)
Cenomanian (99.5-93.5)	Semi-arid	Calcretes (Zone I)

(From Guillocheau, personal communication).

There must be gaps which can only be clarified by future work to study the nature of the bounding surfaces to identify unconformities and determine their significance in terms of how much time they may represent.

Palynological data from the black shales found in the Loperot-1 exploration well drilled in the Lokichar Basin (southwest Turkana) (Fig. 7) indicate that tropical conditions with >1000-1500 mm rainfall existed in this region of Africa from Oligocene up to early Miocene times (Morley et al., 1992; Wescott et al., 1999; Vincens et al., 2006). A rich mammal fauna of late Oligocene age (27-28 Ma) was recently discovered in the Lokone area of the Lokichar Basin (Ducrocq et al., 2009). Such mammal fauna as well as abundant fishes and reptiles also suggest a palaeogeography dominated by a freshwater lake environment, suggesting a wet period during which a freshwater lake may have existed. Humid conditions with seasonal dry periods support the generation of kaolin as the main diagenetic product, which fits well with the observation that kaolin is the main cement material in the upper half of the LSF.

During the late Cretaceous period, the African continent was low-lying, and large areas were frequently and extensively inundated, particularly on its eastern coast where the Lamu Embayment was invaded by waters from the Indian Ocean (Markwick, 1998; Burke et al., 2003). Marine incursions have been identified in the Anza Basin exploration wells as far west as the Ndovu-1 well (Fig. 6b) located in the central parts of the Anza Basin to the east of Marsabit where hundreds of metres of Cenomanian marine shales have been encountered (Bosworth and Morley, 1994; Morley et al., 1999c). This extent of marine transgression is currently unknown, but may have been even further to the west, covering the whole of the Anza Basin (Guillocheau, personal communication). Marine connections through the Anza River or inundations from the middle Cretaceous Indian Ocean can support the theory of marine-influenced source for the carbonate cements of the LSF. Another possible source of calcite cements of marine origin could be the postulated Miocene link between southern Turkana area and the Indian Ocean coast, through the Anza Basin and Lamu embayment (Bosworth and Morley, 1994). One evidence for this connection is in the discovery of a late Burdigalian (20.5-16 Ma) fossil whale in fluvial grits near Loperot in the Lokichar Basin (Mead, 1975) (Fig. 7). This author suggested that the whale must have strayed into a large river system somewhere east of the Turkana area. This Miocene river system could possibly relate to the Cretaceous-Paleogene Anza River draining into the Indian Ocean as described by Burke (2003). As the upper parts of LSF were deposited (upper Eocene-early Oligocene), there was a change to warmer, wetter climate with the increased temperatures and rainfall favouring chemical weathering and erosion (Weissert et al., 1998; Donnadieu et al., 2006; Sellwood and Valdes, 2006). These climatic conditions are conducive for the development of hematite and kaolin cements which are the predominant cements in the middle and upper parts of the LSF.

5.3. Implications on the reservoir potential of LSF

The reservoir potential of a sandstone can be directly correlated to the amount of porosity and permeability which depend on both depositional as well as diagenetic controls. The depositional controls include mineralogy, grain size and sorting while diagenetic ones include compaction and cementation (Selley, 1978; Schmid, 2004). The original detrital composition of the LSF composed predominantly of polycrystalline quartz grains with mainly K-feldspars sourced from metamorphic basement. Arkosic facies of sandstones such as the ones deposited in LSF tend to undergo marked reduction in permeability following the diagenetic breakdown of feldspars (Morley, 1999). The main control on reservoir quality is cementation by calcite (lower 85 m), hematite (middle 125 m) and kaolin (upper 275 m). The initial depositional porosity of the LSF may have been as high as 40 % as is common with many sandstones during deposition (Selley, 1978; McBride et al., 1996), which has since been reduced to values ranging from 3 to 25 %. The initial mineralogical composition of quartz, feldspar and ferromagnesian minerals is composed of relatively high amounts of stable grains and the main agent of porosity reduction is cementation. In the lower part of the formation, cementation mainly by poikilotopic calcite has reduced porosity to between 7 and 11 %. The lowest porosity measured in the LSF is reported from the top of the formation which is also cemented by poikilotopic calcite. In terms of hydrocarbon reservoir potential, the low porosity values and the corresponding low permeability values expected to be associated with lower part of the LSF make it a less prospective horizon. This would hold true unless there is, at depth, porosity enhancing processes such as dissolution of calcite which can improve reservoir potential. In terms of secondary or enhanced recovery from hydrocarbon reservoirs, carbonate cemented ones can benefit immensely from acid treatments resulting in increased permeability and hence in improved flows of produced fluids (Griffith and Nelson, 1988).

The middle 100 m of the LSF is characterized by the abundance of hematite cements associated with locally abundant ferruginous crusts measuring up to 20 mm that occur at the tops of various beds. The effects of the abundant hematite has been to reduce the porosity of this section of LSF to between 11 and 25 %. Kaolin cements are also present within the section where it occurs as a later cement after hematite. Though the measured porosity values are fair to good, the presence of iron crusts, if these are laterally continuous in reservoir scale, could create possible reservoir heterogeneities resulting in compartmentalization and hence production difficulties. Acid fracturing of hematite-containing reservoirs can result in the formation of insoluble iron compounds causing reservoir damage (Smith et al, 1966; Crowe, 1985; Griffith and Nelson, 1988).

In the top zone of the LSF, the most prominent cement is kaolin with subordinate amounts of hematite (except for the topmost calcite-cemented beds). Porosity in this zone has been relatively well-preserved, with values ranging from 12 to 22 % (Figs. 11 and 24). Secondary dissolution porosity from the dissolution of feldspars and secondary intragranular porosity from partial dissolution of feldspars are important contributors to the total porosity. It has however been noted (Schmid, 2004) that secondary porosity is not in most cases of real benefit to reservoirs since it is redistributional in nature, where the material from dissolved minerals is re-precipitated as new cement elsewhere.

Microporosity is significant within the vermicular variety of the pore-filling kaolin. Due to its generally small size, however, the microporosity is unlikely to contribute significantly to permeability of the reservoir. Kaolin associated with kaolinization of detrital clays does not appear to produce significant amounts of microporosity. From a production point of view, the high amounts of microporosity associated with kaolin cements causes high residual water saturation and the small kaolin crystals can easily be moved from pore centers to pore throats by the moving fluids resulting in the clogging of pore throats and thus reducing the permeability of the reservoir (McBride et al., 1996). Overall, the top half of the LSF constitutes a more prospective reservoir zone than the lower half.

6. Conclusions

The age of the uppermost parts of the LSF has been conclusively fixed, from stratigraphic field work and numerous radiometric age determinations using K/Ar and Ar/Ar methods, as ranging from 37 to 33 Ma (upper Eocene-early Oligocene). We do not have new ideas on the age of the base of the LSF, since no new fossil evidence was obtained from the field, apart from the strongly fragmented dinosaur bones encountered near the base of the type-section north of the Lokitaung Gorge. This basal part of the formation will therefore continue to be considered as Cenomanian in age, in agreement with previous authors. The environments of deposition of the basal and the topmost parts of the LSF have been interpreted as distal alluvial fans while the middle part of the formation corresponds to a braided stream system. There must be many stratigraphic gaps which were not evaluated in the field due to the fact that the one lithologic section measured in the field was not adequate to identify such gaps and further field studies are recommended in order to fully understand the gaps within the sedimentary unit. Diagenetic evolution of the formation has shown that the dominant cement material changes from dominant calcite at the base to hematite within the middle zones of the formation to kaolin towards the top. This is consistent with climatic conditions prevailing in the central-eastern Africa region during the deposition of various zones which evolved from mainly semi-arid during the Cenomanian (99.6-93.5 Ma) to a more humid environment starting from the Maastrichtian (70.6-65.5 Ma).

Reservoir potential of the LSF, based on results of porosity measurements which have yielded values ranging from a minimum of 3 % to a maximum of 25 %, is generally fairly good. The top zone of the formation has the best preserved porosity values (12-22 %) and therefore represents the best potential reservoir section. These values compare well with other observed porosity preservation in sandstones of similar depositional environments such as the ones in the southern Sudanese basins where porosities have been reported to be fairly good with values ranging from 8 to 38 % in the Unity Field of the Muglad Basin (Schull, 1988), where Giedt (1990) reported permeabilities in the range of 40 to more than 10,000 millidarcies in the main reservoir horizons which are mainly in the kaolin-cemented horizons. For the reservoirs of the Lokichar basin, the Lomerimong sandstones have a residual porosity of ranging from 1-15 % (Tiercelin et al., 2004), the low values are caused by the cementation by calcite as well as due to the presence of micritic and clay matrix. Subsurface samples from sidewall cores obtained from the Loperot-1 well show drastic reduction of porosity due to laumontite and quartz cementation. The porosity values at the same time show a discrepancy between point count values and wireline log-calculated values, the later being much higher than the former due to the presence of microporosity attributed to the abundant detrital and authigenic clays (Visser, 1993). Considering the fact that the reservoirs of southern Sudan and other basins of the Central African Rift System (CARS) are confirmed oil-producing reservoirs and that the LSF reservoir appears to compare favorably with these known producers, the overall oil exploration potential of northern Kenya should be comparable to the other basins of the CARS, at least from a reservoir point of view. Even with the expected reduction of porosity with depth of burial due to diagenetic alteration of the sandstones, residual porosity can be expected to remain of reasonable reservoir quality between 12-14 % (Morley, 1999). Source rocks have been confirmed in the Turkana area in the Loperot-1 well (Lokichar Basin) where total organic carbon (TOC) values are reported to be as high as 17 %, with an average of 4.5 % (Morley et al., 1999b; Talbot et al., 2004). On the outcrop level, the claystones identified within the LSF (lower and upper terms) were not subjected to geochemical analysis to determine their organic matter richness and hence their source rock potential. Palynofacies studies conducted on a restricted number of samples did not demonstrate the presence of organic debris. This could be an interesting target for future work, perhaps engaging proper methods of sampling in the field. However, due to the lack of adequate well data with only two wells drilled in the entire north-western Turkana area, these ideas can only be confirmed after further exploration drilling. With the area having been licensed to oil exploration companies, this may be expected to happen in the not too distant future.

Chapter 2

The Muruanachok Sandstone Formation of northwest Kenya

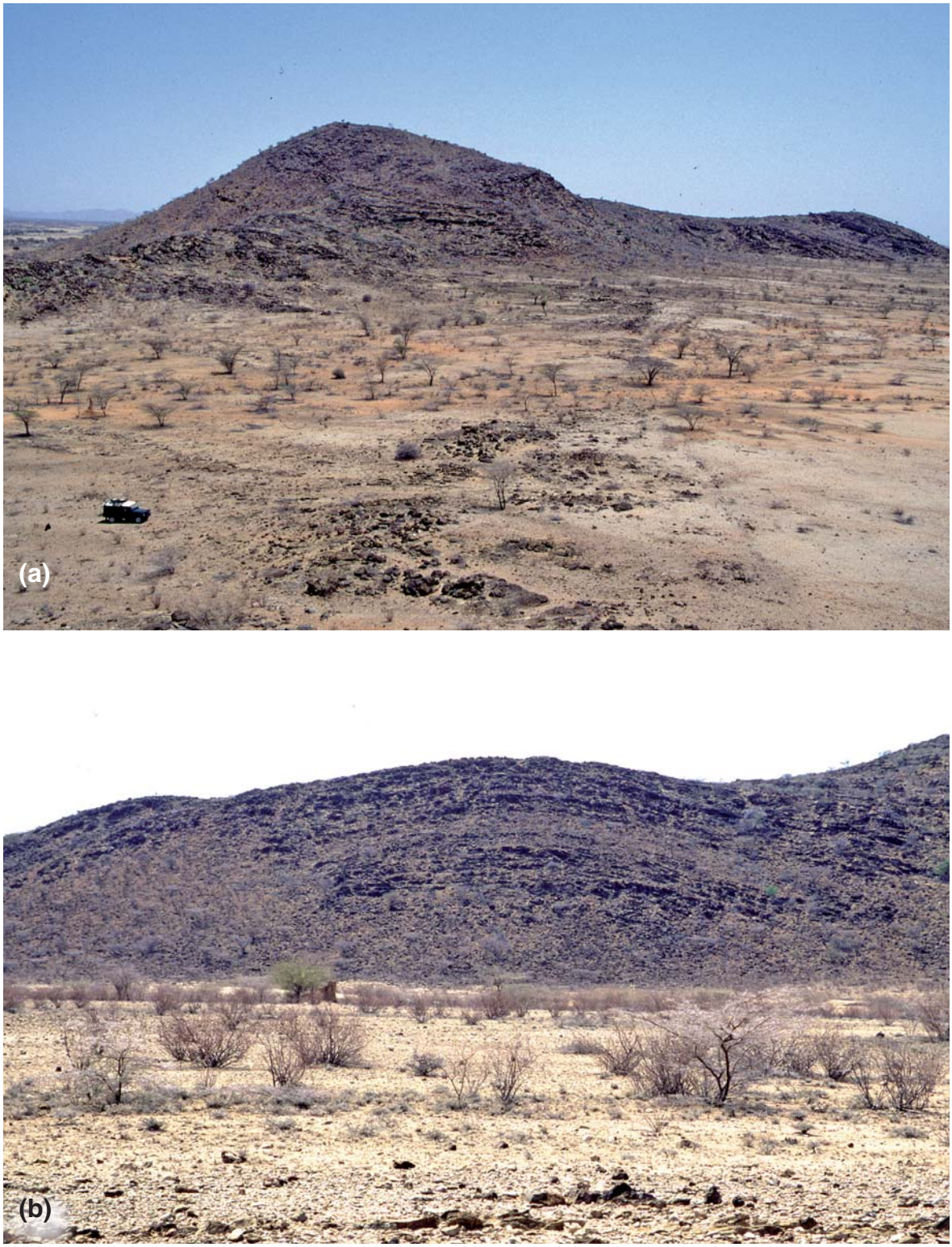

Figure 27. *The Muruanachok Sandstone Formation. (a) View of the main Muruanachok Hill. (b) Anticlinal attitude of the MSF beds, from northeast side of the main hill.*

Chapter II

The Muruanachok Sandstone Formation of northwest Kenya

1. Introduction

On the western side of Lake Turkana, the other possibly equivalent sedimentary unit to the Lapur Sandstone Formation is the Muruanachok Sandstone Formation. The Muruanachok area is a transitional area between the basins of western Turkana and the Lotikipi Plain containing coarse arkosic sandstones interbedded with minor red-brown siltstones and shales. The sedimentary units of Muruanachok Sandstone Formation (MSF) outcrop in isolated hills and gullies in the vicinity of the Muruanachok Hills about 45 km northwest of Lodwar (Fig. 7). They were considered part of the "Turkana Grits" of Murray-Hughes (1933). The sediments do not contain any definitive fossil evidence for dating purposes and they may be late Oligocene-early Miocene or older. They are intruded by early Miocene volcanics and are unconformably overlain by late Oligocene to Miocene volcanics (Morley et al., 1992; Morley et al., 1999c). The volcanics within the vicinity of the Muruanachok area are dated at 18.5-25.5 Ma (McGuire, 1985) and this can be taken to be the minimum age for the topmost parts of the formation.

Sediments of the Muruanachok Formation are estimated to be at least 350 m thick, which is taken to be a minimum estimate because neither the top nor the base is preserved. The type exposure at the Muruanachok Hills has been reported as having a thickness of approximately 100 m where the section shows basalts capping an eroded surface of coarse soft grits with no obvious thermal alteration of the grit, which is underlain by fine red clay (Walsh and Dodson, 1971; McGuire, 1985). The original shape of the Muruanachok Formation has been lost. At the Muruanachok Hills, the formation is exposed in a series of 2 small hills and one main hill, just off the main Lodwar-Lokichoggio road. One small hill is adjacent to the road while the other two are further inland. The two form a doublet with a common base and two different peaks. The doublet expresses a faint anticlinal attitude on the beds observable at about halfway up the smaller of the two peaks (Fig. 27). The well-developed trough-cross beds within the Muruanachok Formation show paleocurrent direction indicating a north-northwest trend (McGuire, 1985). Fossil wood is abundant in the sandstones but other than fossil leaf imprints with an argillaceous horizon, the Muruanachok Formation is fossil-poor.

2. Field study, sampling and analytical methods

A detailed stratigraphic log of the MSF was measured in the field during august 2004. The basal contact with the underlying basement was not seen at the location of stratigraphic section but outcrops a few hundred meters further to the northeast. Sampling was extensive and attempted to represent all major lithologic units within the section. In order to determine the sedimentologic and diagenetic evolution of the MSF, 19 samples of the main profile measured in the main Muruanachok Hill have been studied. Macroscopic observations on hand specimens and microscopic studies on thin sections have been performed, using a similar procedure to the one presented in Chapter I, Paragraph 3.

3. Lithostratigraphy

The Muruanachok Hills, which provide the type exposure for the formation, are easily accessible along the Lodwar-Lokichoggio road, 45 km northwest of Lodwar. The main outcrop is in the form of two small hills and one larger hill, all distinctly exposed on the left side of the road towards Lokichoggio from Lodwar. A stratigraphic section was measured on the main hill exposure whose base is at lat. 03°21'31"N and long. 35°24'03"E, with a total thickness of 104 m (Fig. 28). The underlying basement is not exposed here and the basal part is scree-covered up to around 15 m of vertical section. Lavas expected to stratigraphically overly the sandstones are also not exposed here.

4. Facies analysis

Five different facies were identified in the MSF based mainly on the sedimentary structures present in the beds and grain size of the dominant lithology (Table 10).

4.1. Conglomerate facies, Gcu

This facies is not very common in the MSF and it is represented by only three thin beds occurring near the base and towards the top of the formation; and they measure 10 cm and 80 cm in thickness. One bed (MUR 68B/04) is a laterally discontinuous conglomerate horizon within a 2 m thick sandstone bed near the top of the formation. The facies is made of clast-supported, ungraded conglomerates, with subangular to sub-rounded quartz pebbles measuring up to 5 cm in diameter. Subhorizontal, elongate clay clasts are abundant, giving the beds the faint horizontally bedded structure and they measure up to 20 cm in long diameter. This facies is interpreted as the results of deposition in longitudinal bars as channel lag deposits.

Facies code	*Description*	*Interpretation*
Gcu	Ungraded, clast-supported, conglomerates with abundant quartz pebbles and sub-horizontally bedded elongate clay clasts	Products of subaerial plastic or pseudoplastic flows
Sp	Planar cross stratified fine to very coarse sandstone	Transverse and linguoid bedforms, 2-D dunes, sand waves, lower flow regime
Sh	Horizontally laminated, fine to coarse-grained sandstone	Plane-bed flow, lower and upper flow regime
Sm	Massive, fine to very coarse sandstones with no sedimentary structure	Sedimentary gravity flow deposits, rapid suspension fall-out
St	Trough cross-laminated, fine to very coarse-grained sandstone	Sinuous-crested and linguoid, 3-D dunes, lower flow regimes

Table 10. *Facies analysis for the MSF. The facies codes are adapted from Postma (1990); Horton and Schmitt (1996), and Miall (1977, 1996).*

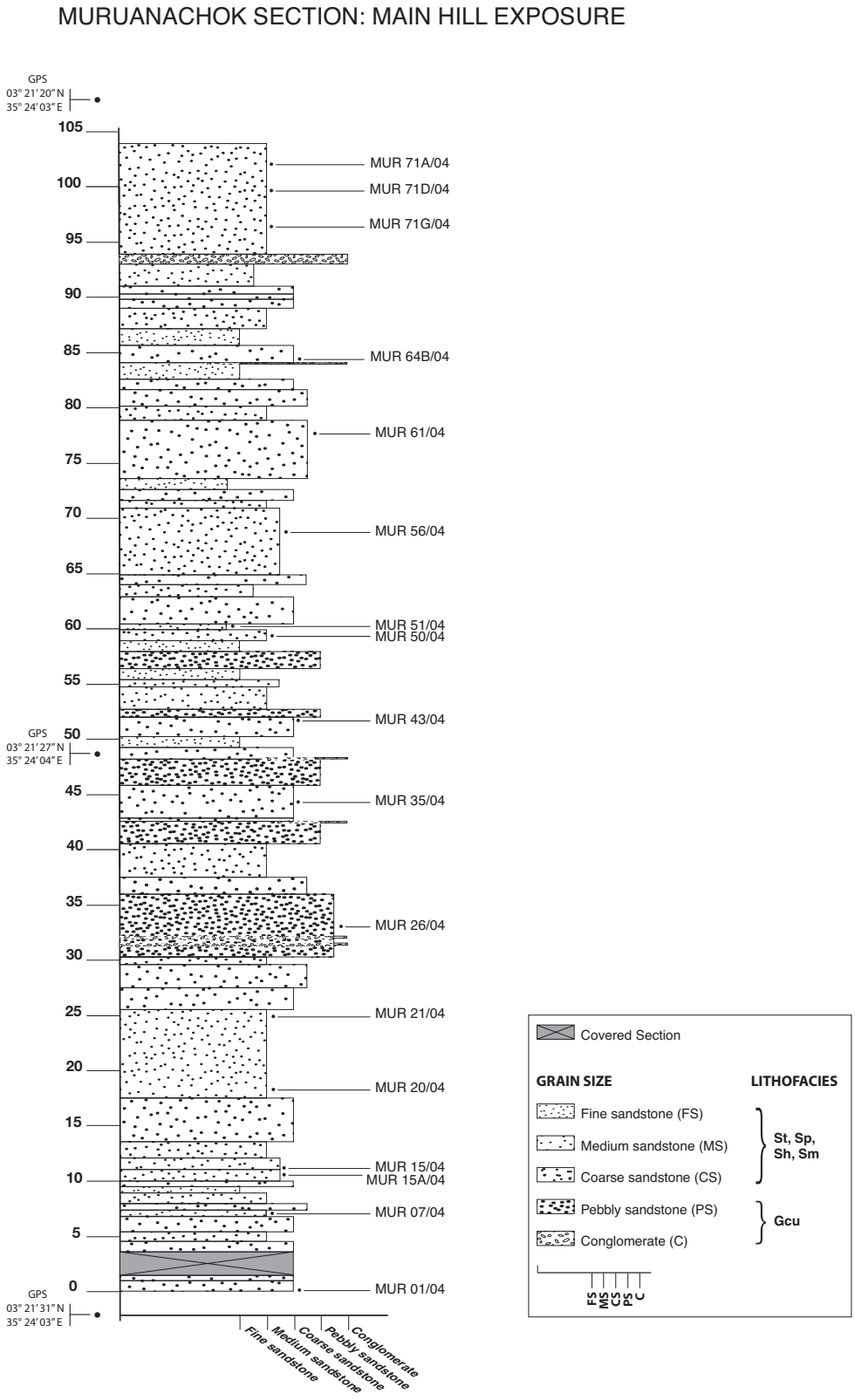

Figure 28. *Lithostratigraphic log of the Muruanachok Sandstone Formation, main Muruanachok Hill (See Fig. 27a).*

4.2. Sandstone facies

Sandstone forms the most abundant facies in the MSF. Based on the dominant sedimentary structures, 4 types of sedimentary facies were recognized in the formation (See Table 10). They are described below in order of relative abundance.

Facies Sm

Massive sandstone beds lacking sedimentary structures are the most abundant facies type in the MSF and it occurs throughout the vertical section measured. Due to its general lack of sedimentary structure the top 10 m quartzitic bed at the very top of the measured section has been classified as belonging to the Sm facies. Fine to medium sandstones are the dominant grain size range, while coarse and pebbly to conglomeratic sandstones also occur but in smaller proportions. The samples are well to very well indurated. They range in colour from white to light grey, yellow to purple and brown. The quartzitic bed at the top is highly silicified, it produces a metallic ring when struck with a hammer, it contains fossil wood fragments and it is highly jointed and faulted in places. Oxidation gives it a reddish-brown colouration. The white, pebbly, massive beds contain pebbles of quartz and clay clasts that are 2-4 cm in diameter. The clay clasts form subhorizontal layers towards the base of the beds. There is tendency for the beds to grade vertically from horizontally bedded facies Sh (marked in most cases by the presence of horizontally aligned elongate clay clasts) to massive beds of facies Sm. Transition from planar The sandstones range in granulometry from fine sandstones, medium to coarse and very coarse. Some sandstones show bimodal grain size distribution with medium grained sandstone in fine sand to silty matrix.

Facies Sm is interpreted as a deposit of subaerial hyperconcentrated flows or in subacqueous high-density turbidity currents. In this case, sand is deposited directly from turbulent suspension with insufficient time for development of bedfoms (Horton and Schmitt, 1996).

Facies Sp

This facies is composed of fine, medium, coarse, very coarse and occasionally pebbly and microconglomeratic sandstones, all with planar cross stratification. Clay clasts are present in the pebbly sandstones. Samples are commonly well indurated. It forms beds with thickness ranging from 0.7 to a maximum of 6 m, and their colour ranges from white, grey, to yellow with brown stains. Orientation of the planar cross stratifications are in the direction N40°, N80°, N90°, N100°, N130°, N180°, N220°, N230° and N300°.

Facies Sp is deposited by the action of 2-D dune generation and migration on non-cohesive sand beds (Miall, 1977). Lack of sigmoidal foresets signifies the absence of a strong separating eddy normally associated with high water stage; indicating that these beds were deposited at the low water stage (Miall, 1977).

Facies Sh

Sh facies is composed of horizontally stratified fine, medium and coarse grained sandstones, with clay clasts measuring up to a maximum of 20 cm in long diameter. Bed thickness varies from 80 cm to a maximum of 7 m. Colour of the sandstones ranges from grey through yellow to brown. This facies sometimes is association with the planar cross-stratified facies Sp and the massive sandstones facies Sm, where vertical gradations between one facies to another is observed within one bed. In most instances, the horizontal stratification is marked by zones containing abundant clay clasts that are elongated and aligned in a horizontal fashion.

The facies is most abundant in the lower parts of the MSF. This facies is interpreted as deposits of subaerial sheetfloods, wave-driven bedload traction and high and low density turbidity currents. Subhorizontal stratification in sheetflood deposits is the result of upper-flow regime plane bed conditions during the deposition of sand (Horton and Schmitt, 1996).

Facies St

This facies consists of fine, medium to coarse-grained pebbly occasionally conglomeratic sandstones with trough cross stratifications. The samples are well to very well indurated and have quartz pebbles measuring up to 2 cm in diameter. Bed thickness ranges from 80 cm to 6 m and their colour ranges from white to beige and yellow. It commonly occurs in association with facies Sp (planar cross-stratified sandstones) and facies Sm (massive sandstones). Individual sets of crossbeds are up to 1 m in thickness while sub-sets are several cm thick. Facies St is interpreted as the product of migration of 3-D dunes under low flow regime conditions (Miall, 1977; Horton and Schmitt, 1996).

4.3. Facies associations

The facies in the MSF are, in order of relative abundance, Sm, Sp, Sh, St and Gcu; occurring in frequencies of 39 %, 37 %, 12 %, 7.5 % and 4.5 % respectively. There is a pronounced deficiency in the facies Fl and Fm, normally associated with floodplain and overbank deposits, perhaps tending to indicate that the deposition of MSF took place outside the distal realms of alluvial fans. Conglomerate facies are also significantly absent in the formation with the exception of minor amounts of the facies Gcu. Lack of the poorly sorted matrix supported conglomerate facies is also suggestive of deposition outside the proximal and lower reaches of alluvial fans and the proximal braided environments which are generally more gravely. The most abundant facies in the MSF are the Sm and the Sp facies, with minor amounts of St, Sh and Gcu.

The facies associations for the MSF can therefore be attributable to sandy braided river depositional environments, gravel-rich perhaps indicating deposition in the middle to distal reaches of the braided environments (Einsele, 2000; Collinson, 1996; Miall, 1977; Miall, 1996). The significant amounts of massive sandstones Sm, products of subaerial hyperconcentrated flows, can be attributed to flash flood deposits in the distal parts of braided environments. The facies Gcu is attributed to small channel deposits brought into the channels during waning stages of higher energy phases flooding events capable of transporting some gravel material to the distal reaches of braided stream environments. Sh facies (12 % frequency) can be interpreted to have been deposited in association with the Sm facies during floods when plane bed conditions are likely to have developed in the upper flow regime. These conditions can occur where the channel floor becomes a traction carpet with continuous particle movement resulting in the deposition of poorly sorted sediments (Miall, 1977).

5. Post sedimentation evolution of the MSF

Reservoir characteristics have direct implications on overall hydrocarbon potential of the region under study. The mineralogic composition during the deposition of the formation is that of an arkosic sandstone with sediment sourced from metamorphic basement. The main diagenetic features observed in the MSF include cemen-

tation by calcite, kaolin and hematite. The diagenetic evolution of the Muruanachok Sandstone Formation has been deciphered from ordinary petrographic and SEM observation of detrital components, cements and porosity.

5.1. Detrital mineral composition

The main detrital components of the MSF include, in order of relative abundance, monocrystalline quartz, polycrystalline quartz, detrital clays and feldspars and trace accessory minerals whose chemical composition is given in Table 11.

Monocrystalline quartz

This is the most common type of detrital grain in the MSF; it is the predominant grain type in 13 out of 17 samples studied (visual estimation). Most grains are subangular to subrounded, and have slightly to moderately undulose extinction. Strongly undulose extinction is present in only one sample (MUR 43/04). The

Mineral	Kaolin	Muscovite	Microcline	Pyrophyllite			
Sample	MUR50/04	MUR20/04	MUR64B/04	MUR20/04	MUR20/04	MUR50/04	MUR56/04
Na2O			**0,13**	**0,29**		**1,50**	
MgO		**1,90**		**0,92**	**0,22**	**0,70**	**1,85**
Al2O3	46,01	31,98	18,19	26,44	30,83	28,48	26,28
SiO2	53,99	49,18	63,78	68,93	65,94	65,46	68,06
K2O		11,28	17,90	1,43	0,99	0,55	1,00
CaO						0,59	0,69
TiO2		0,34		0,50	0,35	1,83	
FeO		5,32		1,50	1,66	0,89	2,11
Total	100,00	100,00	100,00	100,01	99,99	100,00	99,99
Na			0,01	0,03		0,17	
Mg		0,18		0,08	0,02	0,06	0,16
Al	2,00	2,44	1,00	1,81	2,11	1,96	1,81
Si	2,00	3,18	2,98	4,01	3,83	3,82	3,97
K		0,93	1,07	0,11	0,07	0,04	0,07
Ca						0,04	0,04
Ti		0,02		0,02	0,02	0,08	
Fe2+		0,29		0,07	0,08	0,04	0,10

Table 11. *Quantitative SEM-EDX chemical analyses on the oxides of selected minerals from the MSF (%). The analysis was performed on both detrital grains and cements.*

maximum grain size is 6 mm. Grains occasionally have pitted surfaces. Shattering of grains is common, grain-to-grain pressure solution contacts are frequently observed.

Polycrystalline quartz

This forms the predominant detrital grain type in 4 out of the 17 samples that were examined petrographically. The grains are subangular to subrounded, with a maximum pebble diameter of 3 cm. Stretched appearance on some crystals in the polycrystalline is grains common as well as grain shattering and pressure solution on grain to grain contacts (figure 3a, sample MUR 64B/04). Severe compaction in certain cases has resulted in grain interpenetration in some samples (MUR 64B/04; Fig. 29a and MUR 15A/04; Fig. 29b). Some fractures in the fractured grains have been partially healed through the precipitation of calcite cement (sample MUR 64B/04; Fig. 29a). Corrosion of grains is common (MUR 56/04; Fig. 29c); resulting in mostly irregular, sometimes elongate cavities which, when not filled by kaolin or calcite cements, contribute secondary intragranular porosity.

Feldspars

The 17 samples analysed contain between 5 and 25 % feldspars (visual estimate). The feldspars are composed mainly of the alkali feldspar microcline as identified through chemical analysis under SEM-EDX (Table 11). The typical structural formula for the microcline is $K_{1.07}Al_{1.00}Si_{2.98}0_8$ (sample MUR 20/04). The feldspars are highly corroded (sample MUR 71G/04; Fig. 29d) resulting in significant amounts of secondary intragranular porosity. Trace amounts of plagioclase feldspar were observed under thin section microscopy. In some instances the feldspars are relatively well preserved (sample MUR 01/04; Fig. 29e).

Various stages of replacement of feldspar grains by calcite were observed in several samples such as MUR 50/04, MUR 61/04 and MUR 71D/04. This has the effect of reducing the secondary intragranular porosity created by the dissolution of feldspars.

Detrital clays

Samples of the MSF contain on average between 10 and 30% detrital clays, with the exception of two samples MUR 20/04; Fig. 29f) and MUR 21/04 which contain 40 and 60 % detrital clays respectively. The clay is light grey to yellowish brown in colour. Muscovite mica is widely distributed throughout the formation, in small quantities. The mica flakes are usually bent or broken (sample MUR 35/04; Fig. 29g), indicating the severity of sediment compaction. There is incipient kaolinization of the muscovite grains which has taken place along cleavage planes of the micas as well as along its ends which are flayed and altered (Fig. 29g). There are also rare cases of mica/quartz pressure solution with mutually interpenetrated and extensively dissolved grains (sample MUR 35/04; Fig. 29h). Other detrital accessory minerals present in very small quantities include rutile, ilmenite, psilomelane, zircon and sphene.

Iron oolites occur, concentrated especially in sample MUR 50/04 (Fig. 30a, b) and a few in samples MUR 56/04, MUR 61/04 and MUR 64B/04). These are normally in the form of composite oolitic grains with pseudo-concentric brown rings, deformed and partially infilled by calcite. It is not easy to identify the nuclei of these oolites but there in some instances small sand grains trapped within their framework. Where they are not completely cemented by calcite, the oolites have intragranular porosity within spaces between the iron oxide coatings.

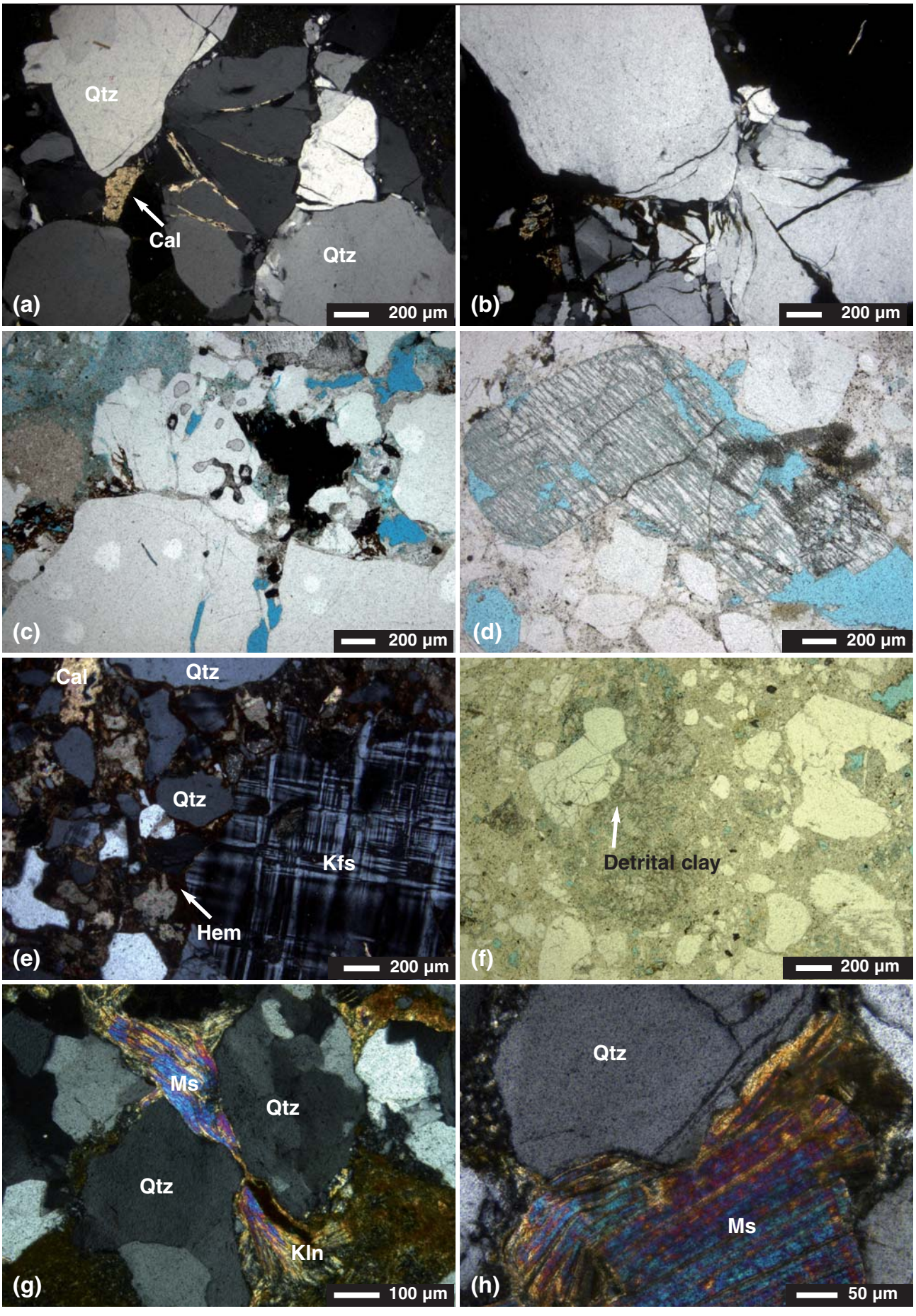
Qtz
Cal
Qtz
(a)
200 µm
(b)
200 µm
(c)
200 µm
(d)
200 µm
Cal
Qtz
Qtz
Kfs
Hem
(e)
200 µm
Detrital clay
(f)
200 µm
Ms
Qtz
Qtz
Kln
(g)
100 µm
Qtz
Ms
(h)
50 µm

5.2. Cements

The MSF is not generally a well-cemented formation. Total cement ranges in abundance between trace amounts to approximately 30 %, on average it is about 10 %. The three main cements in the MSF are kaolin, calcite and hematite. Kaolin occurs with abundances ranging between 5-10 %, calcite ranges between 5-10 % and hematite 5-10 %. Other cements which occur in unquantified amounts include pyrophyllite and quartz overgrowths. The top unit contains beds of quartzitic sandstones which have undergone post-depositional silicification. Faulting is extensive in the MSF and slickensides are common along fault planes.

Calcite

This cement is present in significant abundance at the base of the formation and towards the top. It occurs as pore-filling cement associated with brown clays in sample MUR 01/04 and as in-fill between concentric rings in the hematitic oolites (sample 50/04; Fig. 30a, b). In other samples, (MUR 71D/04; Fig. 30c) it occurs as a product of the replacement feldspars. The calcite is relatively pure and it has a typical chemical composition of $Ca_{1.00}CO_3$ (sample MUR 50A/04).

Kaolin

Kaolin occurs as vermicular pore-filling cement, well distributed throughout the vertical profile of the formation. Its abundance ranges from 5 to 10 %. Samples MUR 56/04 (Fig. 30d) and MUR 64B/04 contains a variety of kaolin containing stacked thin fibrous crystals forming coarse vermicular structures measuring about 60µm in width. The typical structural formula of the kaolin computed from SEM-EDX analysis is $Al_{2.01}Si_{2.00}O_5(OH)_4$ (sample MUR 50/04).

Hematite

This cement is well distributed throughout the formation but it always occurs in small quantities except in the samples containing hematitic oolites (MUR 50/04; Fig. 30a, b; MUR 56/04, MUR 61/04 and MUR 64B/04). Abundance in the samples studied ranges from 5 to 20 %. In certain instances it becomes difficult to distinguish which hematite is cement and which is detrital in origin. Hematite occurs as pore-lining cement (e.g. sample MUR 07/04 and MUR 20/04), pore-filling cement (sample MUR 26/04; Fig. 30e) and disseminated tiny grains in fine-grained matrix (MUR 20/04 and MUR 21/04).

← ***Figure 29.*** *(a) Compaction of grains and fault-related deformation is a common occurrence in the Muruanachok Sandstone Formation (MSF); resulting in pressure solution contacts (Psc) and extensive grains shattering (sample MUR 71A/04; LPA photo). The fractures have been partially filled by calcite cement (Cal). (b) Severe compaction in certain cases has resulted in grain interpenetration in some samples (MUR 64B/04; LPA photo). (c) Corrosion of quartz grains has resulted in the formation of secondary intragranular porosity (sample MUR 56/04; LPNA photo). (d) Alkali feldspars (Kfs) have undergone extensive dissolution resulting in secondary intragranular porosity (Êsi) (sample MUR 71F/04; LPNA photo). (e) Calcite (Cal) is an important cement in the MSF; the calcite is later generation than hematite (Hem) note coarse feldspar grain (Kfs) and smaller quartz grains (Qtz) in bimodal size distribution (sample MUR 01/04, LPA photo). (f) Some units especially in the lower parts of the MSF have samples containing abundant detrital clays (Sample MUR 20/04; LPNA photo). Note partially dissolved feldspar (Kfs) and secondary dissolution porosity Êsd. (g) Mica grains are normally good indicators of the intensity of compaction, here a grain of muscovite (MS) is squashed between two grains of polycrystalline quartz (Qtz), note incipient kaolinization (Kln) at edges of muscovite grain (sample MUR 35/04, LPA photo). (h) Pressure solution contacts are well developed between muscovite and quartz grains (sample MUR 35/04; LPA photo). LPA= Polarized analysed light; LPNA= Polarized non-analysed light.*

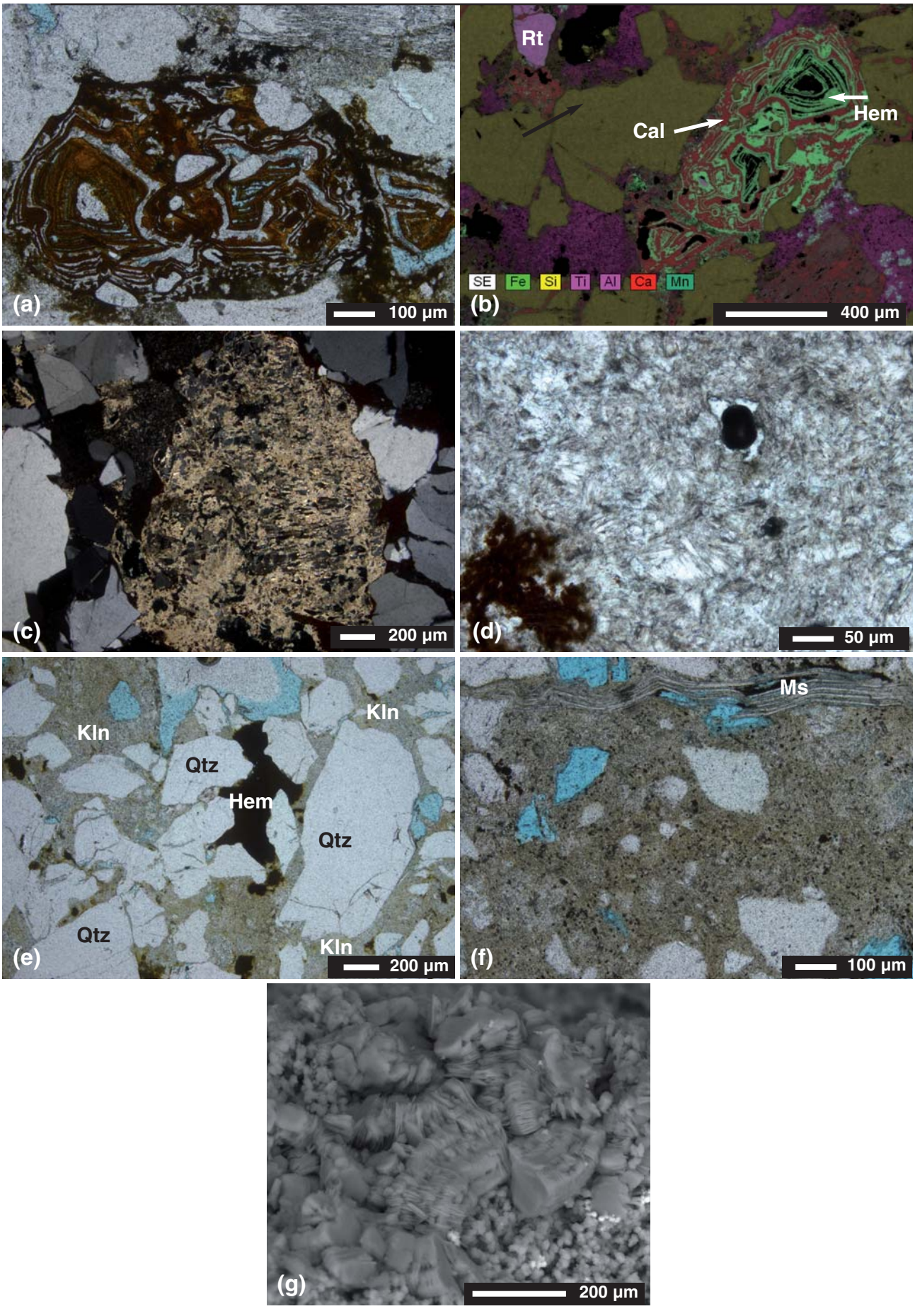
(a)
100 µm
Rt
Cal
Hem
SE
Fe
Si
Ti
Al
Ca
Mn
(b)
400 µm
(c)
200 µm
(d)
50 µm
Kln
Kln
Qtz
Hem
Qtz
Qtz
Kln
(e)
200 µm
Ms
(f)
100 µm
(g)
200 µm

Porosity

No actual measurements of porosity were carried out but visually estimated porosity from thin section ranges from 5 to 20 %. This is mainly in the form of residual primary intergranular porosity and secondary intragranular porosity within the partially dissolved feldspars (MUR 07/04, MUR 20/04 and MUR 64B/04). Primary intergranular porosity ranges from 2 to 20 %. Secondary grain dissolution and intragranular porosity ranges from 2 to 10 %. Total dissolution of feldspars has also created some amounts of secondary dissolution porosity. Microporosity is significant within samples (e.g. MUR 26/04 and MUR 43/04) which contain high amounts of kaolin. Intragranular fractures within quartz grains have been partially filled by calcite cements but they still contribute a certain amount of intragranular porosity (MUR 56/04, MUR 64B/04 and MUR 71A/04). Corroded quartz grains (such as in samples MUR 07/04 (Fig. 30g) and MUR 15/04) are very common in the MSF and they contain secondary intragranular porosity. Oolitic grains that are not completely cemented by calcite exhibit intragranular porosity (MUR 50/04) and feldspars that are partially dissolved sometimes show residual secondary intragranular porosity MUR 61/04; Fig. 30h).

5.3. Paragenetic sequence

The diagenesis that a particular rock undergoes depends on many factors, among them being provenance, depositional environment, texture, mineralogical partitioning, detrital mineralogy, porosity, permeability, tectonic setting, geochemical parameter, fluid flow and time (Hayes, 1979). The main cement materials in the MSF include hematite, calcite and kaolin.

Hematite cementation

Hematite cements were apparently precipitated throughout the entire diagenetic history, from early to late. The alteration of exposed sediment in tropical conditions commonly takes the form of pedogenesis and the development of red hematite pigments through the weathering of ferromagnesian minerals and the infiltration of weathering products into the sediment (Collinson, 1996). Weathering of detrital ferromagnesian minerals such as hornblende is a main source of ferrous ion for the formation of iron oxides. The presence of hematite included in both kaolin and calcite cements indicated that hematite precipitation preceded the formation of both kaolin and calcite. Occurrence of discrete disseminated hematite within mostly detrital clay matrix could be indicative of formation of hematite from weathering processes, perhaps involving ferromagnesian minerals derived from basement sources. Basement rocks in the region are rich in ferromagnesian minerals and include rich amphibolites (Walsh and Dodson, 1971).

← ***Figure 30.*** *(a) Iron oolites are concentrated in a zone near the middle of the MSF containing abundant hematite cement (Hem) in unit 3 of the MSF (sample MUR 50/04). The deformed pseudo-concentric rings are made of hematite with calcite cement and intragranular pore space within the framework of oolites (a and b are LPNA photos, g is an SEM-EDX element mapping photo). Rt is rutile, a common accessory mineral in the MSF). (c) K-feldspar replacement by calcite is common in the MSF (sample MUR 71D/04; LPA photo). (d) Vermicular kaolin commonly occurs as a pore-filling cement (sample MUR 56/04; LPA photo). (e) Hematite is another common pore-lining and sometimes pore-filling cement in the MSF (sample MUR 26/04; LPNA). (f) Hematite sometimes occurs as small discrete grains within detrital clay matrix (sample MUR 20/04; LPNA). Note deformed muscovite grain, Ms. (g) Corrosion of quartz grains contributes secondary intragranular porosity (Êsi) which, together with primary intergranular porosity (Êpi) and microporosity make total porosity in the sandstones (sample MUR 07/04; LPNA photo). LPA= Polarized analysed light; LPNA= Polarized non-analysed light.*

Calcite cementation

The precipitation of calcite cements occurred in at least two phases, one a relatively early event while the second one is late-generation, taking place after fracturing of quartz grains and partially healing the fractures. The reaction for the precipitation of calcite is:

$$Ca^{2+} + HCO_3^- = CaCO_3 + H^+$$

Poikilotopic calcite is common in early diagenetic primary cements in sandstones. In continental sediments with low organic matter, dissolved carbon is derived from the decay of plant remains within the soil horizons and from atmospheric CO2. Calcretes occur as concretions and laterally extensive cements in floodplains and also develop in fluvial channel sandstones and they dominate in the coarse grained proximal facies. Sources of Ca for calcretes may include windblown dust, pyroclastic material, or groundwater may bring carbonate ions from carbonate terrains to siliclastic sequences. Additional sources include Ca dissolved in rainwater and dissolution of Ca-plagioclase (Morad, 1998). In the case of the MSF, sources for the Ca may include younger carbonate-rich Oligocene Miocene lavas, though there was no direct contact between the two was observed in the field. Late generations of replacive calcite occur where the calcite replaces all types of older grains (including quartz and feldspars) and cements such as hematite and kaolin.

The proposed diagenetic evolution of the MSF can be summarized Figure 31 below. There are 5 main diagenetic events identified in the MSF. There are:

1. Precipitation of first generation of calcite cements.
2. Dissolution of feldspars.
3. Calcitization of feldspars.
4. Precipitation of kaolin cements.
5. Precipitation of hematite cements.

Minor events include compaction and precipitation of quartz overgrowth cements, corrosion of quartz grains, precipitation of pyrophyllite cements and fracturing of quartz grains associated with tectonic events.

Kaolinization of detrital grains

Several possible sources of kaolin suggested for the MSF include the alteration products of K-feldspars, the alteration of muscovite and the kaolinization of detrital clays. Alteration of feldspars is inevitable since their detrital grains are commonly in disequilibrium with diagenetic pressure, temperature and pore fluid chemistry and are therefore prone to diagenetic processes that help them reach equilibrium. The main processes of feldspar alteration are dissolution, replacement by clay minerals (e.g. kaolinization) and albitization (Worden and Morad, 2000). In the MSF, there was no evidence of albitization. Kaolinization reaction is in the form:

$$\underset{\text{K-feldspar}}{2KAlSi_3O_8} + 2H^+ + H_2O = \underset{\text{kaolin}}{Al_2Si_2O_5(OH)_4} + 4SiO_2 + 2K^+$$

Due to the high Si/Al ratios of feldspars compared to the clay minerals that replace them, reactions that involve production of clays at the expense of feldspars lead to the release of Si and thus creates potential for quartz cementation. This reaction in many instances is accompanied by co-precipitation of carbonate cements such as calcite (Worden and Morad, 2000).

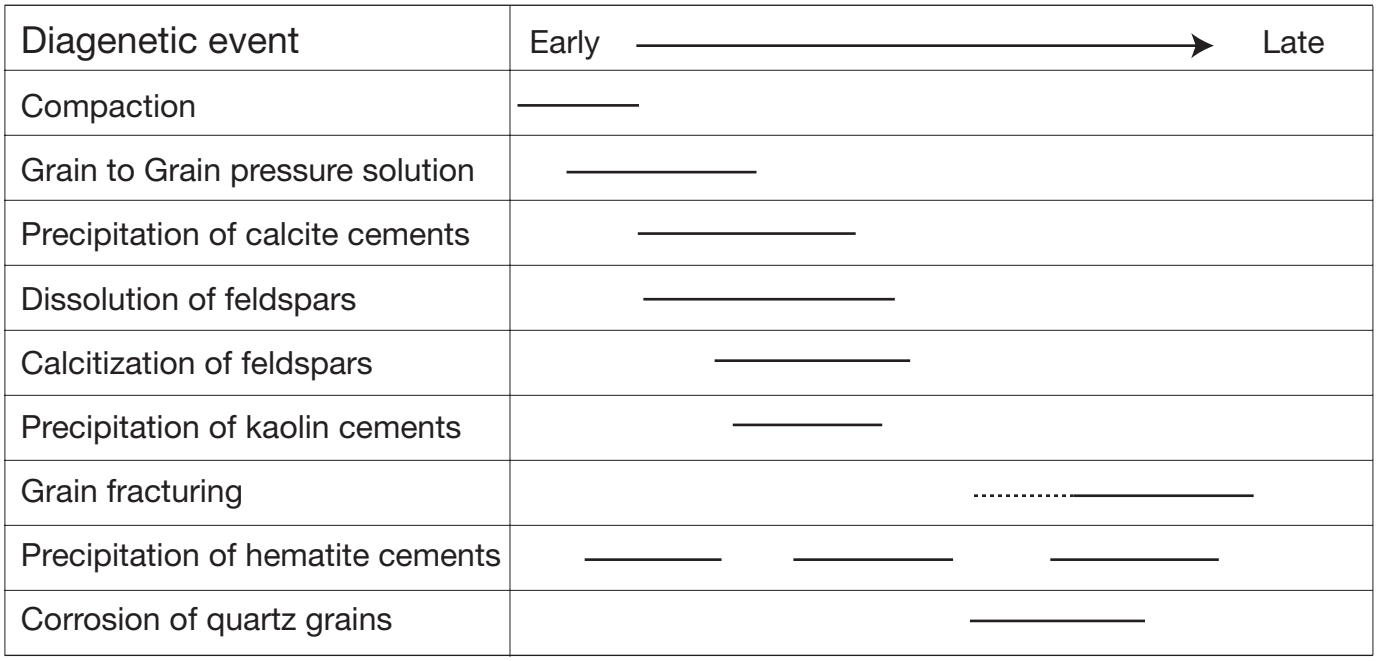

Figure 31. *Post-sedimentation evolution of the Muruanachok Sandstone Formation (MSF).*

Alteration of muscovite

The alteration of muscovite was observed frequently; though the amounts of muscovite available for alteration is generally quite small. The resulting kaolin from this alteration in the MSF is therefore expected to be volumetrically small. The reaction for the alteration reaction has been suggested as follows (Bjorkum & Gjelsvik, 1988; Al-Aboud, 2003):

$$2\ KAl_3Si_3O_{10}(OH)_2 + 2\ H^+ = 3Al_2Si_2O_5(OH)_4 + 2\ K^{++}$$

Muscovite Kaolin

The alteration of muscovite is evident along the cleavage planes and on the edges of the mica crystals.

5.4. Porosity evolution and reservoir characteristics of MSF

The porosity of sediments generally decreases with increasing depth of burial. This relationship has been widely studied especially concerning clays and shales as these can be hazardous to drilling operations. There exists an intimate relationship between porosity and sediment structural parameters such as sorting, grain size, packing arrangement and clay content. Primary depositional porosity increases with increased sorting, coarsening grain size, looser grain packing arrangements and decreasing clay content; the porosity of a sandstone at any given depth is therefore a function of both the porosity gradient and the primary depositional porosity (Selley, 1978). Porosity of a sand at a given depth can be predicted from the equation:

$$\phi^d = \phi^p - G.D.\phi$$

where ϕ^d is the porosity at depth, ϕ^p is the primary depositional porosity, D is the depth, and G is the porosity gradient. Pressure, mineralogy, geothermal gradient and fluid chemistry are the main factors that control the porosity gradients. As sediment becomes buried progressively deeper, its (geostatic) overburden pressure and hydrostatic (pore) pressure increases. Their effect on porosity is constant and depth dependent; however, abnormal pore pressures, where they occur, serve to preserve porosity. Quartzose sands can maintain economic porosity to depths below 6000 m while mineralogically immature sands may reach a porosity of 10% at a depth of just below 2400 m (Selley, 1978).

Calcite is the most important cementing agent within hydrocarbon reservoirs, and it is relatively stable at alkaline environments. In oil producing reservoirs, understanding the geochemical parameters of this mineral is imperative as potential for reservoir damage exits if incompatible fluids are introduced during reservoir stimulation attempts. Solubility of calcite decreases with increasing temperatures and increases with increasing pressure and decreasing pH conditions (Blatt, 1979; Pettijohn et al, 1973). Potential production problems associated with the introduction of hydrofluoric acid or fluoroboric acid into calcite-cemented reservoirs include the formation of insoluble fluorite (CaF_2), deposition of fluorosilicates and hexafluorosilicates.

Though kaolin cements are stable, the introduction of acids may result in the loosening of kaolin crystals in the pore systems, allowing east transportation of the kaolin booklets to the pore throats during turbulent flow. The relatively large crystals migrate to pore throats where they form brush heaps which can significantly reduce the permeability of a reservoir by acting as barriers to fluid flow. These brush heaps are quite difficult to treat once formed.

In the MSF, primary depositional porosity may be expected to have been approximately 40 %, in line with porosity measurements in modern surface sediments in the fluvial environments (Selley, 1978). These sandstones had an original mineralogy characteristic of arkosic sandstones containing up to 25 % feldspars. The alteration of these feldspars would create secondary intergranular porosity, enhancing the total porosity of the sands. However there is extensive calcite cementation into these created pore spaces thereby diminishing the net increase in porosity. The main product of this alteration is kaolin, which occurs as vermicular pore-filling cements. The kaolin is deposited in the pore space thus reducing primary intergranular porosity. The alteration of feldspar into kaolin is also accompanied by release of SiO_2 which is source of quartz cementation and this further reduces primary porosity.

A major contributor to secondary porosity in many types of sandstone is the resorption of feldspars. The two main means of creating porosity within feldspars are replacement of feldspars followed by the dissolution of the replacement mineral and by direct leaching of the feldspar grains. Replacement of feldspars by authigenic clays such as kaolin creates microporosity (Heald and Larese, 1973; Pittman, 1979; Schmidt and McDonald, 1979). Based on visual estimation from thin sections, overall porosity in the MSF ranges from a minimum of 5 % to a maximum of 20 %. The bulk of this constitutes primary intergranular porosity (2 to 20 %) while secondary (mainly intragranular, dissolution, grain corrosion and grain fracturing) contributes between 2 and 10 %. Grain corrosion and fracturing is a major source of secondary porosity while secondary intragranular and dissolution porosity contributes only minor amounts. Intragranular porosity results from the partial dissolution of unstable grains such as feldspars.

The effectiveness of primary intergranular porosity as judged from the interconnectedness of the pore spaces was interpreted to be moderate to good while that of the secondary porosity, especially the dissolution and intergranular porosity was found to be poor, due to the fact that most secondary intragranular and dissolution pores are isolated from one another and thus not interconnected.

The vertical distribution of this porosity is rather uniform throughout the stratigraphic section in the MSF; there is however a marked decrease in porosity towards the top of the formation which is associated with

predominantly quartzitic facies represented by samples MUR 71D/04 and MUR/71G04. Presence of abundant detrital clay (sample MUR 21/04) is accompanied with the lowest porosity of 5 % as would be expected. High percentages of other cement types (such as kaolin in samples MUR 01/04 and MUR 50/04) are also accompanied by low porosity values of 5 to 10 % respectively.

There appears to be a relationship between grain size and visual porosity distribution in the MSF where the finer grained facies (sample MUR 20/04 and MUR 21/04) are characterized by low porosities while coarser sections (MUR 26/04 and MUR 71A/04) are characterized by the highest porosity observed in the section (20 %). This is in general agreement with trends where pore diameters (are thus bulk porosity) increase with increasing grain sizes (North, 1985; Wardlaw, 1976).

5.5. Comparison with the Lapur Sandstone Formation

The MSF and Lapur Sandstone Formation (LSF) together form two of the most important surface exposures of potential reservoir sandstones in the northwestern part of the Turkana area. Of the two, the LSF forms a better surface outcrop, exposed in the Lapur Range area (Fig. 10 and 11) while the MSF outcrops only locally within a limited area in the vicinity of the Muruanachok Hills. The two formations have significant thicknesses exposed, though the LSF shows a bigger thickness at the measured type section (485 m) compared to about 100m for the MSF measured section at the Muruanachok Hills. Estimated total thickness for the MSF has however been reported as being in the excess of 350 m. In terms of depositional environments, the MSF has been interpreted as having been deposited within a sand-dominated braided stream environment while the LSF shows a varying depositional environments ranging from distal alluvial plains to sandy braided stream environments.

Both formations have sediments derived purely from basement, with absolutely no volcanic material. The only exception is in the top part of the LSF where due to the alternation of volcanic activity with deposition of sediment, some volcanic clasts ate incorporated within the topmost bed of the LSF, as a result of erosive activity. Cementation in the two formations follows a slightly different pattern in that whereas in the MSF there does not appear to be any clearly marked cementation zonation, there are distinct zones within the LSF where calcite, hematite and kaolin cements dominate. Maximum porosity values for the two formations are 25 % and 20 % for LSF and MSF, respectively, and based on this single factor, the LSF appears to have a better reservoir potential than the MSF.

6. Conclusions

The observed maximum porosity values of up to 20 % in the MSF represent good porosity while the minimum value of 5 % can be classified as poor (North, 1985). 12 out 15 samples have porosity values of over 10 % and the MSF can thus be classified as having fair to good porosity. If porosity will be effective and the sandstone permeable, the MSF can be expected to have fair to good reservoir potential. If the conditions at the surface can be preserved in the subsurface, the MSF would therefore be expected to have fair to good reservoir potential. Dissolution of carbonate cements which is possible at depth can enhance porosity and thus increase the value of the MSF as a potential reservoir. The extensive grain fracturing in the MSF can also

improve the permeability of the sandstone and hence increase its value as a potential reservoir. The gross thickness of more than 100 m constitutes a substantial potential reservoir thickness should the porosity and permeability observed at surface outcrop be maintained at depth.

Chapter 3

Hydrocarbon Prospectivity in Mesozoic and Early-Middle Cenozoic Rift Basins of Central and Northern Kenya

Chapter III

Hydrocarbon Prospectivity in Mesozoic and Early-Middle Cenozoic Rift Basins of Central and Northern Kenya

Potentiel en Hydrocarbures des Bassins de Rift d'âge Méso-Cénozoique du centre et du nord du Kenya

soumis (septembre 2009) pour publication dans un Mémoire Spécial de l'*American Association of Petroleum Geologists,* 2010 (sous une version simplifiée).
Auteurs : Jean-Jacques Tiercelin, Peter Thuo, Jean-Luc Potdevin, Thierry Nalpas

Abstract

Because they offer the oldest and longest-lived sedimentary basins and they are a cross-over area between Cenozoic and Cretaceous rifts, the Northern (NKR) and Central (CKR) Kenya Rifts are among the most important areas of the East African Rift for hydrocarbon prospecting. During the 70s and 80s, the interest of oil companies focussed in the Turkana depression and the northeastern region of Kenya. Seismic reflection surveys and several exploration wells allowed the identification of several deep buried basins: 1) In the NKR, 3 strings of N-S oriented half-grabens, the oldest known basins being of Cretaceous(?)-Paleogene to middle Miocene age; 2) In the CKR, two N-S half-grabens, the Baringo Basin (Paleogene-Present) and the Kerio Basin (Paleogene-upper Miocene). All basins are filled by up to 8-km thick of alluvial, fluvio-deltaic or lacustrine sediments and volcanics of late Eocene to Neogene age.

New studies have focussed on reservoir/source rock quality in several of these basins. In terms of hydrocarbon potential, arkosic sandstones in CKR/NKR demonstrate a good reservoir quality with porosity up to 25 %. Strong changes in terms of diagenetic alteration relate to deformation events (burial/uplift) or change in sediment source. High quality source rocks relate to freshwater lake environments under tropical climate. Such environments have been identified during Paleogene in the NKR and lower Neogene in the CKR and can be envisaged to occur in basins of same age that are highly under-explored

Keywords: Cretaceous; Eocene-Oligocene; Turkana Depression; south Sudan Rifts; East African Rift System; Lacustrine shale, Source rock, Fluvial sandstone; Diagenesis; Reservoir potential

Mots-clés : Crétacé; Eocène-Oligocène; Dépression du Turkana; Rifts du Sud Soudan; Système de rift est-africain; Argiles lacustres; Roche-mère; Grès fluviatiles; Diagenèse; Potentiel réservoir

1. Introduction

Because they offer the oldest and longest-lived sedimentary basins of the Cenozoic East African Rift System (EARS) and they are a cross-over area between rifts of Cretaceous and Cenozoic age, the northern and central segments of the Kenya Rift, NKR and CKR, respectively, are important areas for hydrocarbon prospecting in East Africa (Fig. 7). In this paper, we review the evidence of oil potential in a suite of Cretaceous(?) to middle Miocene basins identified in these two rift segments, in terms of source rock quality and reservoir properties. This study provides a necessary basic set of data for potential oil explorers in the Kenya Rift.

During the 70s and early 80s, the high oil prices led to major exploration activity in northern Kenya. The interest of the oil companies focussed mainly in the northeastern region, where fluvial sandstones, carbonates and shales of lacustrine and deepwater marine origin were investigated by seismic reflection surveys and several exploration wells. These deposits relate to the Anza Rift, a large multi-phase rift basin that has been demonstrated to have been active from lower Cretaceous up to Paleogene times (Winn et al., 1993; Morley et al., 1999b) and interpreted to be the eastern termination of the Central African Rift system (Schull, 1988) (Fig. 6b, c). In 1981-83, an extensive reflection seismic program was conducted by Project PROBE (Proto-Rifts and Ocean Basin Evolution; Duke University, USA) on the two largest lake basins of the western branch of the East African Rift System, Lake Malawi, and Lake Tanganyika (Rosendahl, 1987; Rosendahl et al., 1986, 1988, 1992). This program was followed by land and offshore seismic surveys acquired by the Amoco Company in the Tanganyika Rift (Morley and Wescott, 1999) and in the Rukwa Rift (Morley et al., 1999e). Four exploration wells were drilled: two in the northern part of the Tanganyika Rift (the Rusizi-1 and Buringa-1 wells), and two in the Rukwa Rift (the Ivuna-1 and Galula-1 wells).

In the mid 80s, following the discovery of large hydrocarbon accumulations in the Cretaceous-Paleogene rifts of southern Sudan (Peterson, 1986; Schull, 1988; Mohammed et al., 1999; Mohammed et al., 2002; Obaje et al., 2004), a phase of aggressive exploration was developed by Amoco and Shell companies in the western part of the Turkana depression of northern Kenya. An initial, academic seismic reflection acquisition campaign was first conducted in 1984 under the auspices of the PROBE Project (Rosendahl et al., 1986), covering the offshore areas of Lake Turkana (Dunkelman et al., 1988, 1989). Then, an intense onshore seismic reflection survey conducted to the immediate west and southwest of Lake Turkana (Amoco Kenya Petroleum Company (AKPC); 1985-1986) and two exploration wells (Loperot-1 and Eliye Springs-1; Shell E & P Kenya B.V; 1990-1991) contributed to image the geometry and lithostratigraphy of a suite of 5 buried half-graben basins (Fig. 6c). These basins, called the Lokichar, North Kerio, North Lokichar, Lothidok and Turkana Basins, are with up to 7 km of sedimentary fill among the oldest and deepest known basins in the East African Rift System, being of Cretaceous(?) to Paleogene-middle Miocene age. To the northwest of Lake Turkana, gravity data and 5 reflection seismic lines also acquired by AKPC (1985) indicated the presence of two other deep buried, north-south oriented sedimentary basins, the Lotikipi Basin to the west, and the smaller Gatome Basin to the east, separated by a structural high called the Lokwanamoru Range (Fig. 6c). Maximum depth to basement was interpreted to be 4 km for the Lotikipi Basin, and up to 6 km in the Gatome Basin (Wescott et al., 1999; Desprès, 2008). To the immediate east of the Gatome Basin is a small elongated, N-S oriented half-graben called the Kachoda Basin, that has been recently identified using magnetotelluric soundings (Abdelfetah, 2009). With 1.5 km of sedimentary fill, this basin opens north towards the wide Omo River delta plain (Fig. 7).

South of 2° latitude N is the Central Kenya Rift (Fig. 7), that extends up to 2° latitude S, and which is a particularly well known segment of the EARS in terms of rift formation and morphotectonic evolution. It

also hosts, together with the Northern Kenya Rift, several of the most important sites for hominin remnants (Hill et al., 1986; Andrews and Banham, 1999). This part of the rift has however not really been studied in terms of hydrocarbon potential. Between the equator and 2°N, the Central Kenya Rift today shows a set of two major parallel, N-S trending half-grabens: the Baringo-Bogoria Basin to the east, and the Kerio Basin to the west, separated by the Tugen Hills structural block (Chapman et al., 1978; Tiercelin and Vincens, 1987; Hill, 1999) (Fig. 7). Gravity and seismic reflection data were acquired in 1990 in the Kerio Basin by the National Oil Corporation of Kenya (NOCK) (Beicip, 1987; Pope, 1992; Ngenoh, 1993). This study was later completed by a magnetotelluric survey performed to the east, in the Baringo-Bogoria Basin (Marigat-Loboi Plain) within the framework of a research contract with Elf Petroleum Norge AS (1996-1997) (Hautot et al., 2000). Together with a re-interpretation of the gravity and seismic data from the Kerio Basin, this study resulted in a completely new interpretation of the age and development history of this part of the Central Kenya Rift (Hautot et al., 2000). The two half-grabens forming this segment have been shown to be 7-8 km deep and filled by alternating packages of sediment and lavas, the oldest sediments being possibly of Paleogene age. Although no exploration wells have been drilled in these two basins, it is hoped that since the basins occur within Block 12A which is currently licensed for oil exploration to Platform Resources of Canada, new geophysical data as well as deep wells will be drilled in the near future.

In early 2008, a huge surge in interest was shown by oil companies to acquire exploration acreage in the Kenya Rift. This could be attributed partly to the rising world crude oil prices which for the first time in history rose above US$ 147 a barrel in July 2008 and also to the recent discoveries in the Albertine Graben of Uganda, in the western arm of the EARS The two main companies operating in the Albertine Graben are Heritage Oil Corporation and Tullow Oil Plc. Heritage operates and holds 50 % working interests in Blocks 1 and 3A while Tullow holds exploration licences in Block 1, 2 and 3A. Blocks 1 and 3A are held by Tullow/Heritage (50/50 % interests) and are operated by Heritage while Block 2 is held 100 % by Tullow. The discoveries within the Albertine Graben in the recent years have been spectacular, in 2006/07, Heritage's Kingfisher-1 well in Block 3A produced from 4 zones at an overall cumulative flow rate of 13,900 barrels of oil per day (bopd). This was followed in 2008 by Kingfisher-2 well which flowed at 14,364 bopd from 3 zones. Other discoveries include Kingfisher-3 with a net oil column of 40 m, the Warthog-1 in Block 1 with a 46 m net hydrocarbon pay and the Giraffe-1 drilled in January 2009 with a net oil pay of 38 m (Tullow and Heritage corporate web sites www.heritageoilplc.com and www.tullowoil.com).

In northern Kenya, the exploration for oil and gas is at an all time high, with several companies at various stages of their exploration programmes in various exploration blocks. The companies that have current exploration production sharing contracts (PSCs) in the Turkana area of northern Kenya include Africa Oil Corp. which holds the contract for Block 10BB and CAMEC (Central Africa Mineral Exploration Company) which holds the PSC for Block 11. The PSC for Block 10BB, where the Loperot-1 well was drilled by Shell in 1992, was previously held by the Turkana Drilling Consortium which has since been bought out by the Africa Oil Corp. This company also holds the PSC for Block 10A in the northwestern part of the Anza Rift. Block 10BA in the Northern Kenya Rift remains vacant, as well as Block 14T in the South Kenya Rift in the Magadi area. Within the Central Kenya Rift, Blocks 13T and 12A are licensed to Platform Resources, a Canadian exploration company. In all these PSCs, minimum work programme obligations include the re-interpretation of existing data, acquisition of new seismic data and the drilling of exploration wells.

As a consequence of this renewal of interest for oil exploration in this region of the East African Rift, new stratigraphic and sedimentological/petrographical studies have been focussed on source rock quality and reservoir properties within the most important sedimentary basins identified in the northern and central segments of the Kenya Rift: a) in the NKR, with the Lotikipi, Gatome and Lokichar Basins; b) in the CKR, with

the Kerio and the Baringo Basins (Fig. 7). These respective sedimentary basins demonstrate a large number of structural and sedimentary aspects of hydrocarbon exploration in rifts (Lambiase and Morley, 1999; Morley, 1999e). Such different examples demonstrate the extreme variability between individual half-grabens, particularly in regions where volcanics and sediments are involved. Those studies contributed to discover favorable and unfavorable aspects of the hydrocarbon potential in this region of the East African Rift System.

2. The Northern Kenya Rift Basins

All the buried basins identified in the Northern Kenya Rift (Figs. 6 and 7) are known to be filled by 5-8-km thick fluvial or fluvio-lacustrine-type sediments of Cretaceous(?)-Paleogene to Neogene age (Morley et al., 1999b; Wescott et al., 1999; Tiercelin et al., 2004), locally associated with thick (up to 3.5 km) volcanics of Paleogene-Neogene age known as the "Turkana Volcanics" (Zanettin et al., 1983). Sediments of Neogene age outcrop widely east and west of the present-day Lake Turkana, and have been intensely investigated by multiple paleontological projects. Cretaceous(?)-Paleogene sediments are only known from subsurface data with the exception of some arkosic sandstone formations originally described as the "Turkana Grits", a term first created by Murray-Hughes (1933) to refer to packages of immature siliciclastic sediments directly resting on basement rocks in the northern and central parts of the Kenya Rift.

The proximity of these NKR basins to the southern Sudanese oil-producing fields and the similarity in the structural trends of the two regions (Schull, 1988; Salama, 1997; Wescott et al., 1999) makes these basins an important target for oil exploration. Also, the possibility for positive hydrocarbon potential in these basins was confirmed by the Loperot-1 exploration well drilled in the Lokichar Basin (Fig. 7), that encountered a well-established lacustrine source rock with high TOC, and significant oil shows (Wescott et al., 1999; Talbot et al., 2004). Such potential was a considerable incentive for continuing exploration in this area. Reservoir potential and source rock quality have been examined for each of three of the NKR basins – the Lotikipi, Gatome, and Lokichar Basins - then compared with other types of reservoir and source rocks encountered in the other Kenya Rift basins. Finally, each studied basin has tentatively interpreted and classified in terms of hydrocarbon prospectivity.

2.1. The Lotikipi and Gatome Basins

The Lotikipi and Gatome Basins have been shown from gravity and seismic data to lie below the 120 km wide Lotikipi Plain, which is located 80 km northwest of the present-day Lake Turkana (Figs. 6 and 7). Due to the poor quality of the seismic data occasioned by the presence of a thick pile of volcanics, the deep geometry of the Lotikipi and Gatome Basins as well as depth to basement are not clearly defined. The Lotikipi Basin was interpreted either as a thermal sag basin or a rift basin, with a better preference for the rift interpretation (Wescott et al., 1999), and the deep stratigraphy of the basin has been only deduced from seismic facies data and outcrop geology, no exploration well having been drilled in this basin. The upper part of the basin fill is formed by ~1 km thick Neogene sediments (undetermined facies; possibly fluvial to shallow lacustrine) that overly a thick pile (up to 3 km) of basaltic and rhyolitic rocks belonging to the "Turkana Volcanics" formation. New radiometric ages obtained at the base of this formation indicate a late Eocene-early Oligocene age. Sub-volcanic strata seen on TVK-4 seismic line are estimated to be arkosic (fluvial) sandstones equivalent to

the “Turkana Grits”, and lacustrine deposits forming one single sedimentary unit up to 700 m thick (Wescott et al., 1999). To the immediate east, the Gatome Basin shows a similar stratigraphic succession with a greater infill thickness at its northern part. A revised interpretation of the TVK-7 seismic line suggests the presence below the Turkana Volcanics of a sedimentary unit (“A”) with a thickness of about 500 m. The lowest part of this unit are seen as unconformably overlying a “tilted block” paleotopography resulting from normal faulting affecting a “stratified basement” that cannot be clearly identified (sedimentary formation or Precambrian basement?) (Fig. 17a).

2.1.1. Reservoir Rocks

Fifty km to the east of the Gatome Basin, a 500-m thick pile of sandstones outcrop above the Precambrian basement in an impressive cliff, and is overlain by the Turkana Volcanics (Figs. 8, 11 and 13). The so-called “**Lapur Sandstone Formation**” (LSF) is dated from Cenomanian(?) near its base (on the basis of the discovery of poorly preserved dinosaur bones; Arambourg and Wolff, 1969) up to late Eocene-early Oligocene (the uppermost parts of the LSF are locally interbedded within the first lava flows of the Turkana Volcanics dated 33-37 Ma) (Fig. 14). Considering its stratigraphic position below the Turkana Volcanics, the sedimentary unit visible on the TVK–7 seismic line in the Gatome Basin can be tentatively correlated to the mid-Cretaceous-late Eocene Lapur Sandstone Formation. The “tilted block” palaeotopography underlying this formation could be interpreted as relating to one of the lower-middle Cretaceous rifting events that affected Southern Sudan and Northern Kenya parts of Africa (Giedt, 1990; Genik, 1993; Salama, 1997; Wescott et al., 1999), and possibly controlled later the deposition of the Lapur Sandstone Formation on top of this palaeotopography (Winn et al., 1992; Bosworth and Morley, 1994; Morley et al., 1999b) (Fig. 17).

Thus, the presence of the LSF in the deepest part of the Gatome Basin can be suspected, and extension of this formation toward the west, in the Lotikipi Basin, is envisaged. Nevertheless, major changes in thickness along a S-N trend have been observed in the LSF. Such lateral variation may suggest the presence in the Gatome and Lotikipi Basins of other sedimentary packages in a similar stratigraphic position. Such a possibility is illustrated by the presence at the south end of the Gatome Basin of an arkosic sandstone formation known as the “**Muruanachok Sandstone Formation**” (Walsh and Dodson, 1969; Morley et al., 1992; Wescott et al., 1993; Morley et al., 1999b; Thuo et al., in prep.) (Figs. 7, 27 and 28). These sandstones crop out in several isolated small hills, where they are seen to overlie Precambrian basement, and are locally unconformably overlain by volcanics of late Oligocene to Miocene age (Morley et al., 1999b). There is no argument (no fossil to the exception of a few, not very well preserved prints of plant leaves) to determine the age of the Muruanachok sediments. They can be of late Oligocene age or older.

Despite this uncertainty that can only be resolved by deep drilling, the Lapur Sandstone Formation, because of its significant thickness and wide geographical distribution, may offer an interesting reservoir potential. This formation has an original detrital composition made predominantly of polycrystalline quartz grains and K-feldspars sourced from metamorphic basement (Thuo et al., in press) Arkosic sandstones such as the ones deposited in the LSF (Fig. 32a, b) tend to undergo marked reduction in permeability following the diagenetic breakdown of feldspars (Morley, 1999). The main control on reservoir quality is cementation by calcite (Zone I; lower 85 m), hematite (Zone II; middle 125 m) and kaolin (Zone III; upper 275 m) (See Figs. 10 and 24, chapter I). The initial depositional porosity of the LSF may have been as high as 40 % as is common with many sandstones during deposition (Selley, 1978; McBride et al., 1996), which has since been redu-

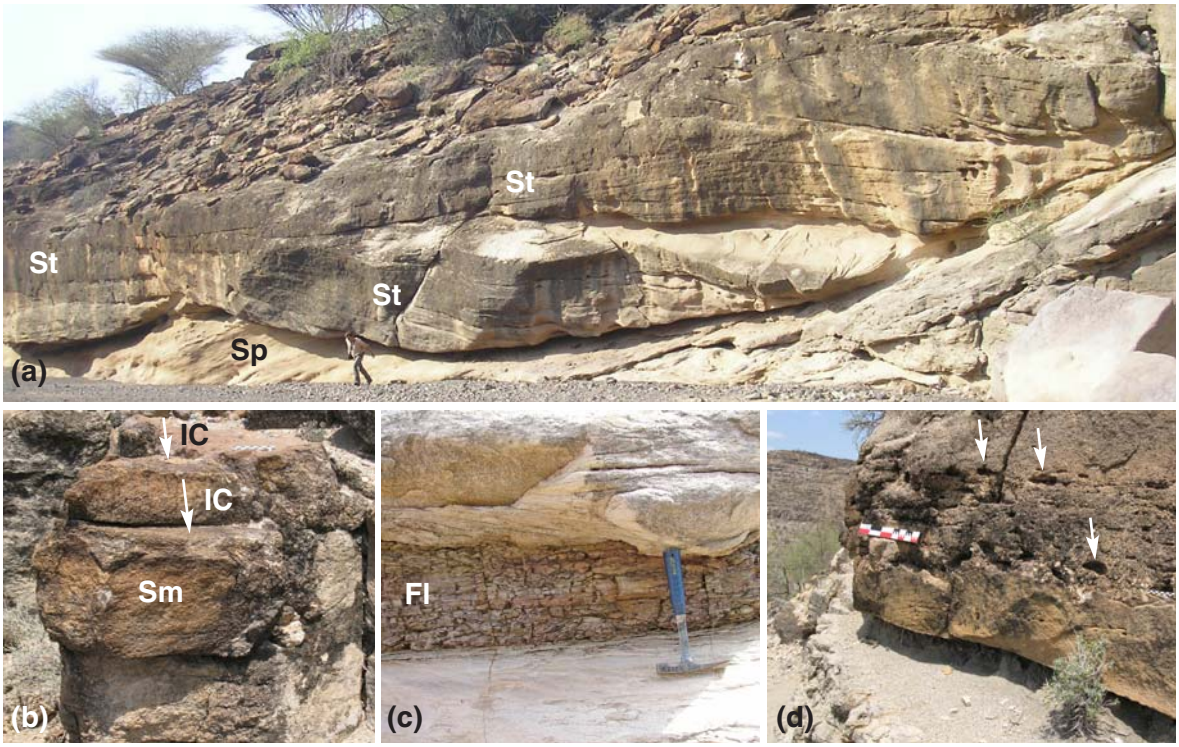

Figure 32. *A selection of sedimentary facies of the Lapur Sandstone Formation, in terms of reservoirs and source rocks. (a) Trough cross-laminated sandstone (facies St), middle part of the LSF. At the base of the unit, planar cross-stratified sandstone (facies Sp), very coarse-grained sandstone, with individual cross beds measuring 4-6 cm in thickness; (b) Iron crusts (made of hematite) are abundant in the middle part of the LSF (Zone II; see Figure 10). Such iron crusts may generate significant reservoir discontinuities. (c) Dark grey laminated silty mudstone (facies Fl) conformably overlying massive medium-grained sandstones, and unconformably overlain by planar and horizontally stratified medium-grained sandstone, upper part of the LSF. This type of facies possibly reflects flood plain or shallow lake environment. In the LSF, this facies shows a poor organic content, minimal thicknesses and limited lateral continuity, thus demonstrating poor source rock potential at outcrop level. (d) Major erosive discontinuities can be seen on top of mudstone beds, and the presence of mud clasts in overlying sandstone facies (marked in the photograph by holes in the sandstone – see white arrows) indicate strong erosive processes affecting such mudstone deposits.*

ced to values ranging from 3 to 25 % (Fig. 24). The initial mineralogic composition of quartz, feldspar and ferromagnesian minerals is composed of relatively high amounts of stable grains and the main agent of porosity reduction is cementation. In the lower part of the formation, cementation mainly by poikilotopic calcite has reduced porosity to between 7 and 11 %. The lowest porosity measured in the LSF is reported from the top of the formation (Fig. 24; Zone I) which is also cemented by poikilotopic calcite. In terms of hydrocarbon reservoir potential, the low porosity values and the corresponding low permeability values expected to be associated with lower part of the LSF make it a less prospective horizon. This would hold true unless there is, at depth, porosity enhancing processes such as dissolution of calcite or dolomitization which can improve reservoir potential. In terms of secondary or enhanced recovery from hydrocarbon reservoirs, carbonate cemented ones can benefit immensely from acid treatments resulting in increased permeability and hence in improved flows of produced fluids (Griffith and Nelson, 1988).

The middle 100 m of the LSF (Fig. 10; Zone II) is characterized by the abundance of hematite cements associated with locally abundant ferric crusts measuring up to 20 mm that occur at the tops of various beds (Fig. 32b). The effects of the abundant hematite has been to reduce the porosity of this section of LSF to

between 11 and 25 %. Kaolin cements are also present within the section where it occurs as a later cement after hematite. Though the measured porosity values are fair to good, the presence of iron crusts, if these are laterally continuous in reservoir scale, could create possible reservoir heterogeneities resulting in compartmentalization and hence production difficulties. In the top zone of the LSF (Fig. 10; Zone III), the most prominent cement is kaolin with subordinate amounts of hematite (except for the topmost calcite-cemented beds). Porosity in this zone has been relatively well-preserved, with values ranging from 12 to 22 %. Secondary dissolution porosity from the dissolution of feldspars and secondary intragranular porosity from partial dissolution of feldspars are important contributors to the total porosity. It has however been noted (Schmid et al., 2006) that secondary porosity is not in most cases of real benefit to reservoirs since it is redistributional in nature, where the material from dissolved minerals is re-precipitated as new cement elsewhere.

Microporosity is significant within the vermicular variety of the pore-filling kaolin. Due to its generally small size, however, the microporosity is unlikely to contribute significantly to permeability of the reservoir. Kaolin associated with kaolinization of detrital clays does not appear to produce significant amounts of microporosity. From a production point of view, the high amounts of microporosity associated with kaolin cements causes high residual water saturation and the small kaolin crystals can easily be moved from pore centers to pore throats by the moving fluids resulting in the clogging of pore throats and thus reducing the permeability of the reservoir (McBride et al., 1996). Overall, the top half of the LSF constitutes a more prospective reservoir zone than the lower half.

The Muruanachok Sandstone Formation (MSF) (Figs. 7, 27 and 28) is composed of conglomerates and sandstones deposited within a fluvial setting within alluvial plains and fluvial channels, with limited amounts of argillaceous matter. At the type locality, the thickness of the measured section is slightly over 110 m and this therefore represents a significant potential reservoir unit. The MSF is not a well-cemented formation. Total cement ranges in abundance between trace amounts to 30 %. The three main cements are, as it is in the LSF, kaolin, calcite and hematite. Iron oolites are concentrated near the middle part of the MSF containing abundant hematite cement. Porosity values based on visual estimation in thin sections studied throughout the vertical section of the MSF range from 5 to 20 %, mainly in the form of primary intergranular porosity as well as secondary intragranular and dissolution porosity resulting from the partial and occasionally total dissolution of feldspar grains. The formation contains fractures which are partially healed by the deposition of calcite cement and these could significantly enhance permeability thereby increasing the reservoir potential of the MSF.

2.1.2. Source Rocks

Potential source rock occurrence is also a major question within the Gatome and Lotikipi Basins. Good quality source rocks in continental rift basins are typically shales of lacustrine facies (Talbot, 1988), as it is for the Lokichar Basin (Morley et al. 1999b; Talbot et al., 2004). In the Gatome and Lotikipi Basins, there is no seismic evidence for thick accumulations of lacustrine shales. Only lenses of dark grey or black silty mudstones a few metres to few tens of m in thickness can be seen at the outcrop scale in the Lapur Sandstone Formation, where they may represent floodplain or shallow lake deposits (Thuo et al., in press) (Fig. 32c). Nevertheless, these mudstones do not demonstrate abundant organic content. Only few wood stems are found in the sandstone facies of LSF. Erosive discontinuities seen on top of mudstone beds and the presence of mud clasts in sandstone facies indicate strong erosive processes affecting such deposits (Fig. 32d). This also suggests that thicker piles of mudstones may be present in different environmental settings within the LSF. There is no source rock evidence from the Muruanachok Sandstone Formation. Only one metre-thick layer formed by grey and purple silty mudstone has been found containing small dark organic debris and prints of plant lea-

ves. This facies may represent a floodplain depositional environment (Khalifa and Catuneanu, 2008). It is however reasonable to expect, in conformity with common trends in continental rift basin characteristics, thick lacustrine shales which may have source rock potential may exist in the deeper parts of the basin (e.g. Morley, 1999). This will be confirmed through drilling, which can be expected as a culmination of the exploration activities currently taking place in northern Kenya.

2.2. The Lokichar, North Lokichar and North Kerio Basins

Located close to the southwest end of Lake Turkana (Figs. 6 and 7), the Lokichar Basin is a N-S trending, 60-km long and 30-km wide east-facing half-graben floored by Precambrian crystalline basement. The basin has been carefully described by Morley et al. (1999b). Its western boundary is a prominent east-dipping listric fault, the Lokichar Fault, which has no present-day topographic expression. As shown by reflection seismic data (TVK-12), the basin fill which is 7 km thick, consists of interbedded Paleogene to middle Miocene lacustrine and fluvio-deltaic sediments (Fig. 33). Capping the basin fill is a 300-m thick basaltic sequence - the Auwerwer Basalts - dated from 12.5 to 10.7 Ma (Fig. 33a). The 3-km deep Loperot-1 exploration well (Fig. 33) was drilled close to the Lokone Horst, a basement high which separates the Lokichar Basin from the North Kerio Basin, an other parallel half-graben, to the east. Alternating packages of coarse to fine sandstones tens to hundreds of meters thick were encountered in the well. These packages are divided into two main sedimentary units, from bottom to top: the Lokone Sandstone Formation, and the Auwerwer Sandstone Formation (Morley et al., 1999b) (Fig. 33b, c). The Lokone Sandstone Formation includes two major lacustrine shale intervals (the Lokone Shale Member, and the Loperot Shale Member) which are both several hundreds of meters thick in the well but may be as thick as 1.3 km to the west, when approaching the Lokichar boundary fault. Palynological data from the Loperot-1 well indicate a Paleogene to middle Miocene age for the whole formation. Mammal fauna discovery in sandstones overlaping the western side of the Lokone Horst indicate a late Oligocene age for this part of the basin infill (Ducrocq et al., 2009).

The North Lokichar Basin corresponds to a northern extension of the Lokichar Basin proper, consecutively to a northward propagation of the Lokichar Border Fault (Figs. 33 and 34) (Morley et al., 1999c). As there are no exploration wells in this basin, the nature of the basin infill has been identified in the area of southern Lothidok Hills. Approximately 1400 m of infill with 3 main units were defined by Boschetto et al. (1992): 1) The Kalakol Basalts (ranging from 28-18 Ma) at the base of the infill; 2) the Lothidok Formation; and 3) the Turkwell Beds of late Miocene-Pliocene age.

To the immediate east of the Lokichar Basin/Lokone Horst is the North Kerio Basin. This half-graben basin, imaged by the TVK-12 seismic line of AKPC (Fig. 35), is N-S oriented, parallel to the Lokichar Basin, but has been poorly studied compared to the Lokichar Basin. On the eastern side of Lake Turkana is the Mount Porr Basin, possibly representing an eastward prolongation of the North Kerio Basin. The structure of the Mt Porr Basin is influenced largely by the presence of a regional normal fault pattern striking N160°, and a few transverse faults striking N90° and N60°. The main Kajong lineament is expressed topographically by an escarpment, 10 km long, defined as the Kajong Fault Zone (Tiercelin et al, 2004) (Fig. 36). The sediment infill of this basin - the Sera Iltomia and Kajong Formations - are exposed mainly in a triangular lowland separated from the crystalline basement high to the north by two N90° trending features.

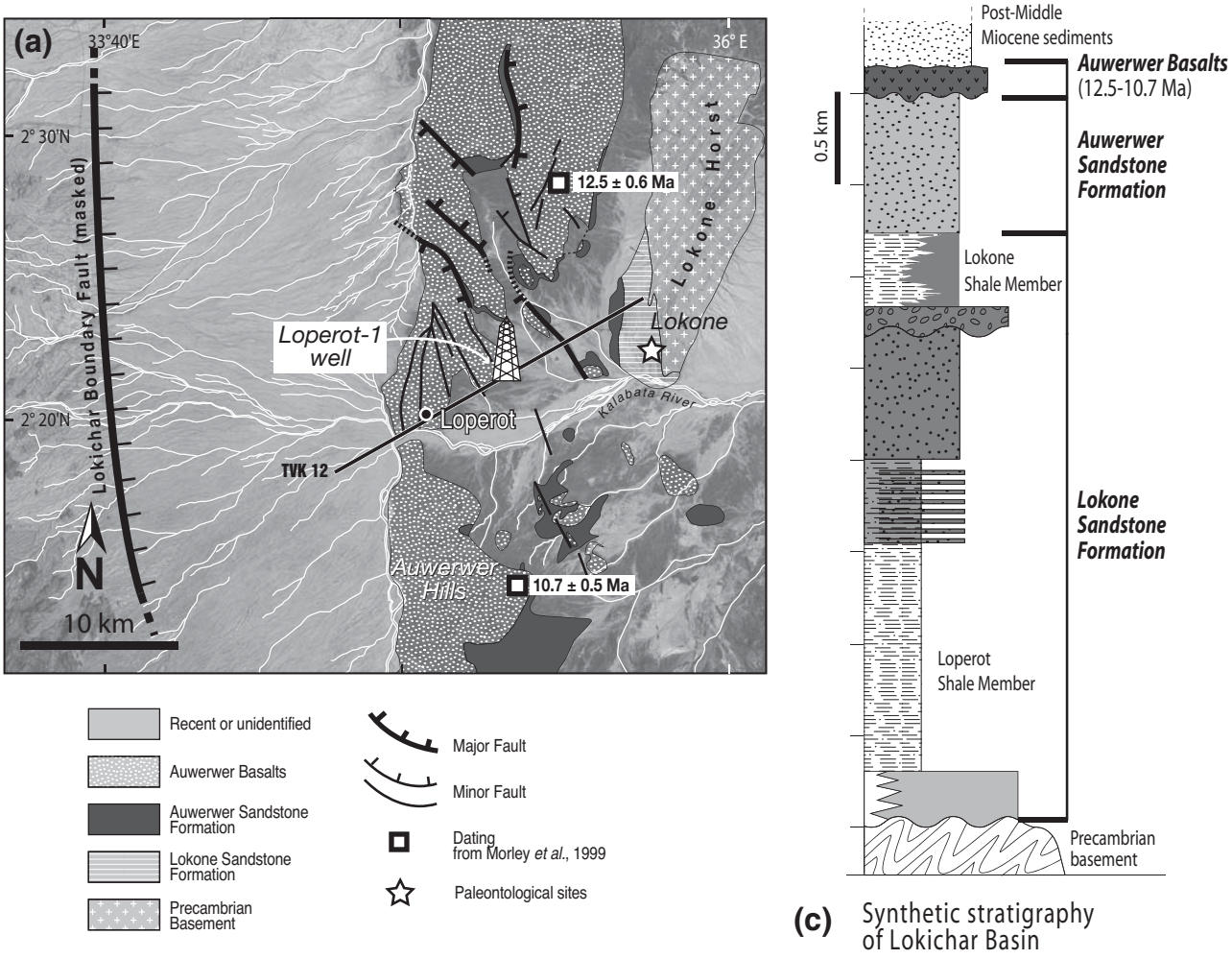
(a)
33°40'E
36° E
2° 30'N
2° 20'N
Lokichar Boundary Fault (masked)
12.5 ± 0.6 Ma
Lokone Horst
Loperot-1 well
Lokone
Loperot
Kalabata River
TVK 12
Auwerwer Hills
10.7 ± 0.5 Ma
N
10 km
Recent or unidentified
Auwerwer Basalts
Auwerwer Sandstone Formation
Lokone Sandstone Formation
Precambrian Basement
Major Fault
Minor Fault
Dating from Morley et al., 1999
Paleontological sites
Post-Middle Miocene sediments
0.5 km
Auwerwer Basalts (12.5-10.7 Ma)
Auwerwer Sandstone Formation
Lokone Shale Member
Lokone Sandstone Formation
Loperot Shale Member
Precambrian basement
(c) Synthetic stratigraphy of Lokichar Basin

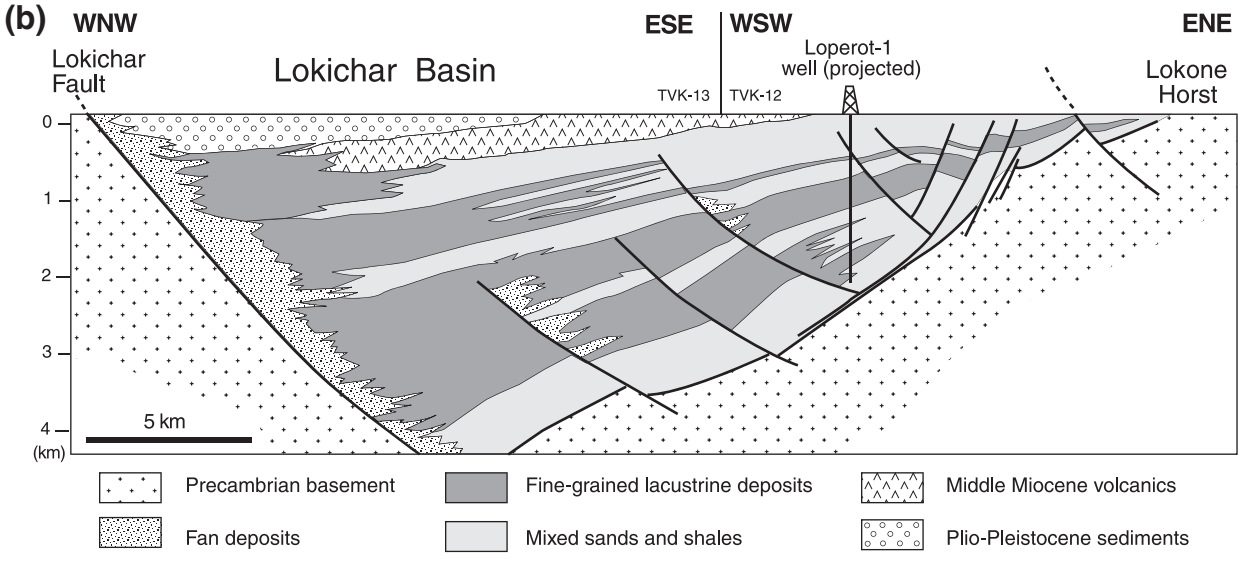
(b)
WNW
ESE
WSW
ENE
Lokichar Fault
Lokichar Basin
Loperot-1 well (projected)
TVK-13
TVK-12
Lokone Horst
0
1
2
3
4
(km)
5 km
Precambrian basement
Fan deposits
Fine-grained lacustrine deposits
Mixed sands and shales
Middle Miocene volcanics
Plio-Pleistocene sediments

← ***Figure 33.*** *(a) The Paleogene-middle Miocene Lokichar Basin, southwest Turkana. Location of the Loperot-1 well and seismic line TVK 12. The white star indicates the Lokone vertebrate locality, of late Oligocene age (Ducrocq et al., 2009). (b) Basin structure and stratigraphy based on reflection seismic data (TVK-12 line) (modified from Morley et al. (1999b). (c) Synthetic stratigraphy of the Lokichar Basin infill showing the vertical distribution of the potential source rocks (Loperot and Lokone Shale Members) and reservoirs (Lokone Sandstone Formation, and Auwerwer Sandstone Formation).*

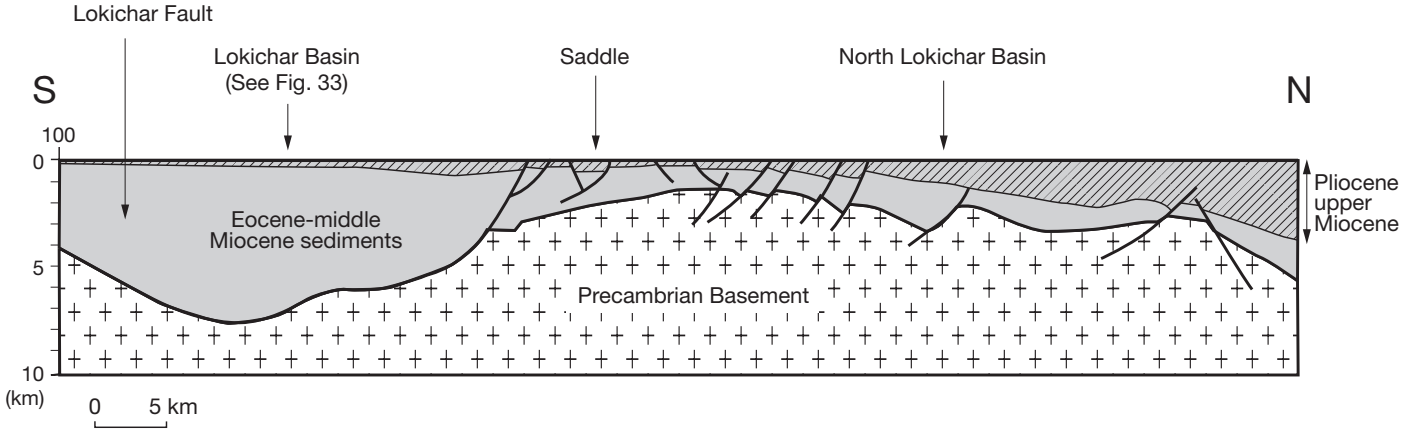

Figure 34. *South-North oriented geological cross-section based on the interpretation of the seismic line TVK-100, showing the position of the North Lokichar Basin, that results of the northward migration of tectonic activity along the major Lokichar Fault (See Fig. 33a, b). The North Lokichar Basin is of late Miocene to Pliocene age, while the Lokichar Basin is of Paleogene-middle Miocene age (modified from Morley et al., 1999b).*

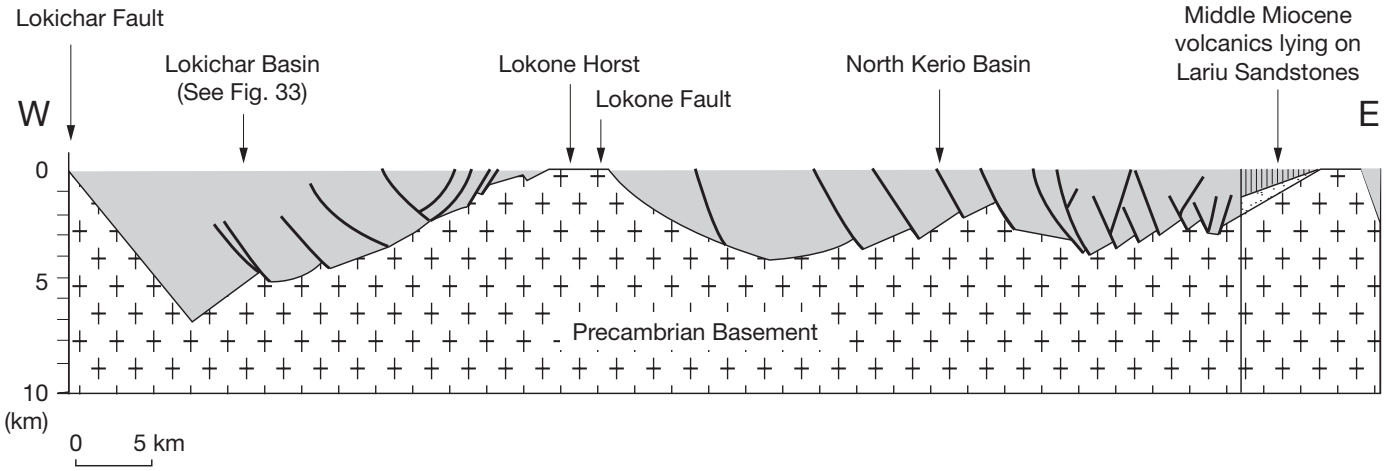

Figure 35. *West-East oriented regional geological cross-section (interpreted from the TVK-12 seismic line) through the Lokichar Basin to the west and the North Kerio Basin to the east, separated by the Lokone Horst (See Fig. 33) (from Morley et al., 1999b).*

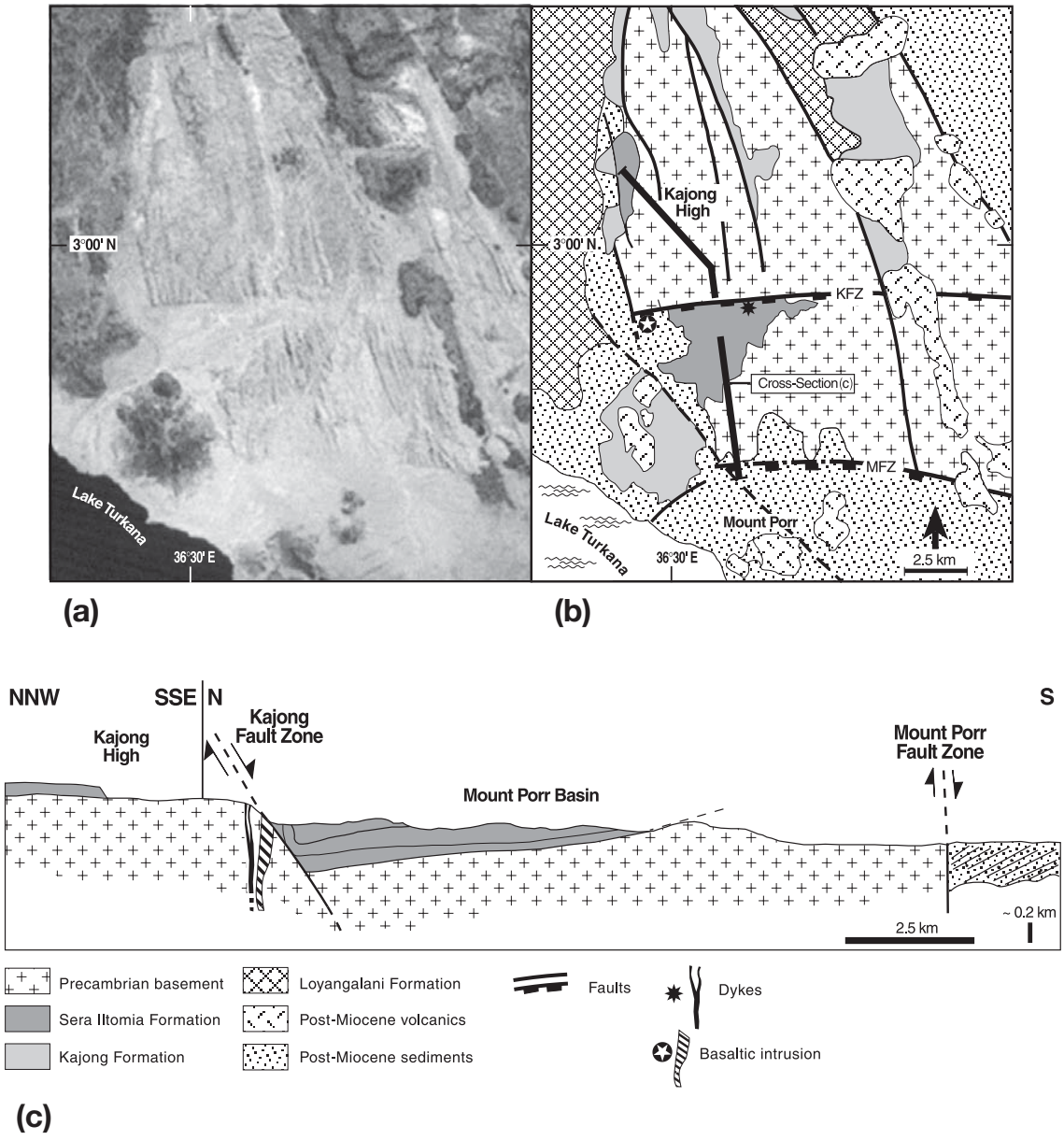

Figure 36. *(a) Satellite imagery of the Mount Porr area (from Landsat MSS 5; Mount Kulal, northern Kenya. (b) Geological map of the Mount Porr-Kajong area, south-east Turkana (from Williamson and Savage, 1986; Tiercelin et al., 2004). (c) Composite geological cross-section through the Kajong High, the Kajong Fault Zone (KFZ) and the Mount Porr Basin.*

2.2.1. Reservoir Rocks

In the Lokichar Basin, as due to low relief, sediment exposures are poor and only represent the flexural basin margin sediments. Pebbly sandstones and minor conglomerates of fluvio-deltaic facies onlap the gneissic basement of the Lokone Horst (Fig. 37a-c). Quartz, K-feldspar, biotite and muscovite are the dominant minerals, and demonstrate a sediment source from basement outcrops located to the south of the basin.

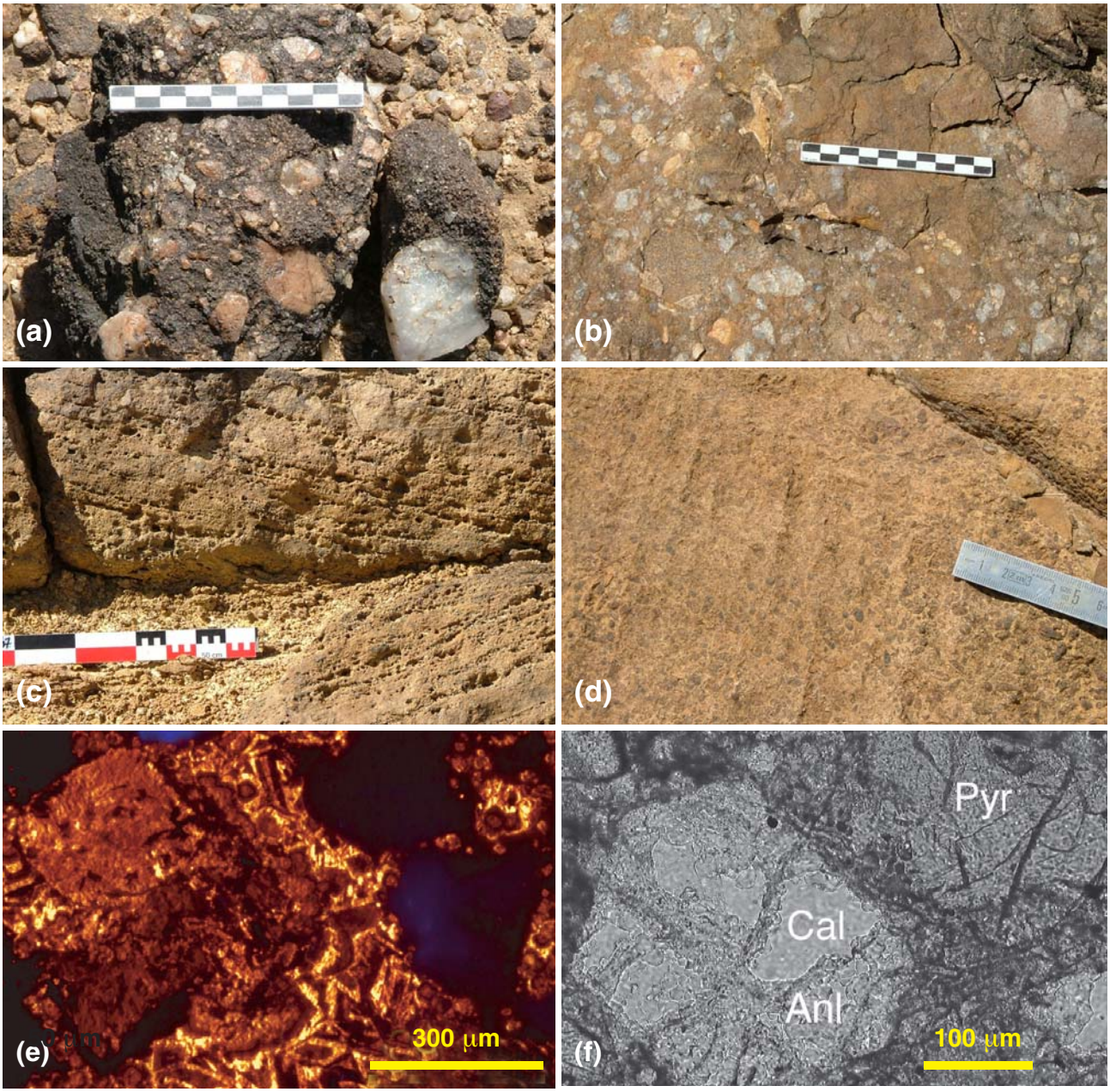

Figure 37. *A selection of sedimentary facies and cements of the Lokone Sandstone Formation, Lokichar Basin, in terms of reservoirs. (a), (b) Arkosic, pebbly sandstones onlapping the Lokone Horst, upper part of the Lokone Sandstone Formation. These basement-derived, strongly cemented sediments offer poor porosity. (c) Coarse-grained, cross-bedded sandstone of fluvial of fluvio-deltaic type. Ghosts of clay pebbles are abundant in this coarse facies that locally overlie claystones, perhaps as rip up clasts indicating erosion of floodplain deposits accompanied by sediment bypass. (d) Carbonate beds made of gastropod shells accumulations in shallow, freshwater, lacustrine shoreline environment, upper part of the Lokone Sandstone Formation. These carbonate facies are closely associated with the organic-rich shales (Lokone Shale Member) that accumulated in the deepest part of the basin. (e) Carbonate cement. The sandstones in the Lokone Formation show homogeneous, orange-luminescent cement. (f) Calcite-analcite pseudomorphs after pyroxene (Pyr). Analcite (Anl) forms microcrystalline ribbons which preserve the initial shape of the detrital minerals.Calcite (Cal) fills the pores remaining between the analcite ribbons. The calcite-anacilte cement is characteristic of sandstones containing significant amounts of fresh volcaniclastic materials (amphibole, pyroxene).*

The upper part of the Lokone Sandstone Formation and the Auwerwer Sandstone Formation show minerals such as quartz, feldspars, biotite, muscovite, but with significant amounts (more than 50 % of the detrital material) of fresh volcaniclastic material, amphibole, pyroxene, and plagioclase. The presence of volcanic components indicate a major change in the sediment source, from basement outcrops for the lower part of the Lokone Sandstone Formation, to an alkaline volcanic source, possibly basaltic flows occurring to the south of the Lokichar Basin, linked to the widespread lower Miocene Samburu Basalts (Tiercelin et al., 2004). Carbonate beds are locally present in the Lokone Formation, mainly made of gastropod shells accumulations and these could present interesting potential reservoir. However, only minimal thicknesses have been observed at the outcrop scale (Fig. 37d).

Diagenetic changes in the upper Lokone and Auwerwer Formations are marked by calcite or by analcite/calcite precipitation (Fig. 37e, f), resulting in a rather low porosity (values of 1-15 %; Tiercelin et al., 2004). Analcite and calcite precipitated from Na/Ca-rich fluids related to the dissolution of the volcanic material (Fig. 37f). Data from the Loperot-1 well (Visser, 1993) indicates that the dominant grain type in the main reservoir horizons is made up of fine to medium grained sandstone, poorly to very poorly sorted with a few moderately sorted exceptions. The main detrital components are quartz (predominantly monocrystalline) and feldspars (mainly plagioclase with lesser amounts of alkali feldspars), with significant amounts of lithic fragments and clay matrix. The lithic fragments are comprised mainly of argillaceous sedimentary fragments with lesser amounts of altered quartzofeldspathic metamorphic fragments and rare volcanic fragments. Authigenic minerals with the Loperot reservoirs include quartz and feldspar overgrowths, carbonate cements, zeolites, authigenic clays and opaque minerals. The quartz overgrowths, which generally form a minor component in the sandstones, occur as small syntaxial overgrowths that partially occlude adjacent pore spaces. The authigenic feldspars occur as overgrowths on detrital feldspar grains as well as albitization of plagioclase and neomorphism of albite. Carbonate cements are represented mainly by coarsely crystalline to locally poikilotopic pore-filling ferroan calcite, with minor amounts of non-ferroan calcite and siderite. Zeolites present in the sandstones include analcite, which occurs as very small subspherical crystals intermixed with pore-filling clay and laumontite, which occurs as coarsely crystalline pore-filling patches and as a product of partial replacement of framework grains. Authigenic clays occur as grain-coating rims, pore-filling clays and as pore-filling and grain-replacive patches of kaolinite. Opaques are represented by leucoxene and pyrite. The reservoir properties for the studied reservoir section are poor to very poor, with the point-counted porosity never exceeding around 5 %. The main agent responsible for the reduction in porosity are a combination of sediment compaction and cementation by laumontite and quartz overgrowths. There appears however to be a discrepancy between point count porosity and log-calculated porosity, which indicates values of 10-20 % for the same section. This can be explained by the abundance of detrital and authigenic clays which contain abundant microporosity which cannot be quantified by point counting but which would be detected on log calculated porosity. Porosities calculated from wireline logs are significantly higher because they represent total porosity including microporosity (Shell, 1993).

The **Lothidok Formation** is essentially characteristic of the North Lokichar Basin infill (Fig. 34), as it has been defined by Boschetto et al. (1992) . It is a series of volcaniclastic sandstones, arkosic sandstones, lava flows and pyroclastics that overly Oligocene or Miocene basalts, that are themselves overlain by Miocene-Pleistocene volcanics and sediments. The name Lothidok is derived from the Lothidok Range located between Lodwar and Kalakol where typical section of the formation outcrops. It includes all strata lying between the upper contact of the Kalakol Basalts and the lower contact of the Loperi Basalts. The Lothidok Formation is well exposed in the Lothidok Range (Fig. 7) and reaches a total thickness of 580 m consisting mainly of volcaniclastic sedimentary rocks, altered mafic tuffs and trachytic tuffs. The K-Ar dating of the

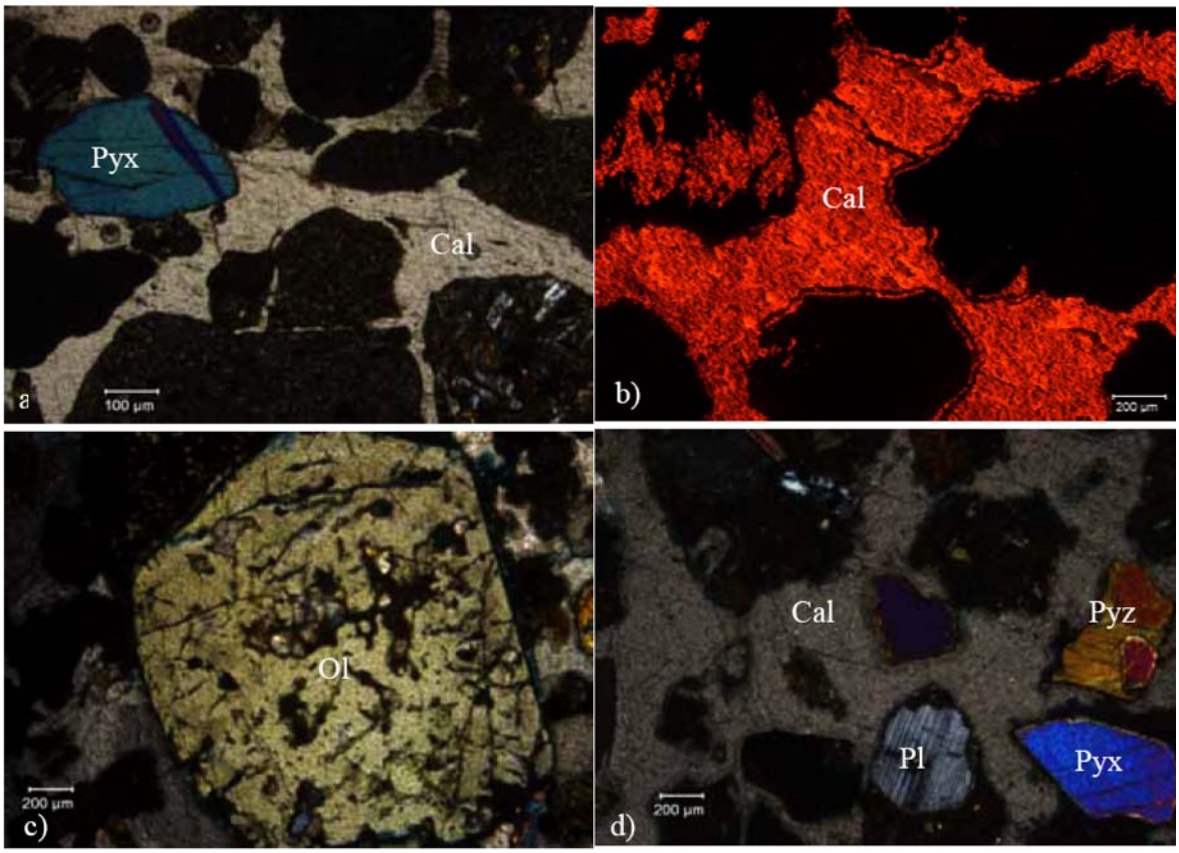

Figure 38. Petrographic characteristics of the Lothidok Sandstones. The main features include volcaniclastic detrital grains, cementation by calcite and the almost total absence of porosity. (a) detrital grains include volcanic grains, sedimentary rock fragments (srf), amphiboles and pyroxenes (Pyx). Cementation by calcite (cal) is pervasive, with poikilotopic textures. (b) Under cathodoluminescence, three zones of calcite are observed. The earliest is a very thin zone of brightly luminescent calcite, succeeded by a dark non-luminescent zone which is followed by a later brightly luminescent zone filling the pore spaces. (c) Olivine mineral (Ol) is a common detrital constituent of the Lothidok sandstones. (d) Plagioclase (Pyx), relatively unaltered is also common in the sandstones but in small percentages.

Kalakol Basalts immediately below the Lothidok Formation gives the ages between 28 and 18 Ma. The Kalakol Basalts contain dominant lava flows with intercalated volcaniclastic and pyroclastics units while the Lothidok Formation has less lava and more volcaniclastic and pyroclastics (Boschetto et al., 1992; Morley et al., 1999). Mammalian fossils were discovered in the area by Arambourg (1933) and Savage and Williamson (1978). Bivalves, gastropods and reptile fossils have also been reported from the area. The lowest fossiliferous beds within the Lothidok hills are in the Kalakol Basalts and thus the maximum age of the fossil fauna of the Lothidok Formation has been established by K-Ar dating of the underlying Kalakol Basalts at average age of 19.9 Ma.

Petrographically, the Lothidok sandstones are composed of medium to coarse-grained volcaniclastic sandstones. The framework grains consist predominantly of volcanic rock fragments which are well rounded with elongate volcanic minerals including plagioclase feldspar randomly distributed and oriented, dark grey to black, occasionally brownish and green, amphiboles and pyroxenes sometimes present (Fig. 38a-d). Plagioclase feldspars occur in relatively well-preserved state as both framework grains and constituents of volcanic rock fragments, mostly as small elongate crystals. Amphiboles, pyroxenes and olivine (Fig. 38c) are fairly common both as independent framework grains and as constituents of volcanic rock fragments, in sub-

hedral occasionally elongate grains, showing traces of cleavage. Biotite and Quartz occur in trace amounts. Matrix of dark brown material, containing elongate micaceous mineral and dark brown to black iron oxides is common. Cement is exclusively by poikilotopic and drusy calcite (Fig. 38a). There are three generations of cement which are clearly visible on cathodoluminescence microscopy, an early rim of brightly luminescent grain-coating calcite, followed by a thin zone of dark non-luminescent calcite and finally a pore-filling late generation brightly luminescent calcite (Fig. 38b). Porosity in the Lothidok sandstones is barely present, as a consequent of the pervasive nature of calcite cementation. There are however traces of secondary porosity resulting from the partial dissolution of rock fragments.

Possible equivalents of the lower part of the Lokone Sandstone Formation (arkosic sandstones) are know to outcrop at the eastern end of the North Kerio Basin (Fig. 35). Wescott et al. (1993) described at the Lariu Range (Fig. 7), along the western shore of Lake Turkana, coarse-grained arkosic pebbly sandstones with thin, discontinous red and grey siltstone-mudstone units up to 610 m thick, named the **Lariu Formation**. A thick sequence of volcanic flows overlie the sandstones, which are in places heavily intruded by dykes. Ages of 15.7 ± 0.7 Ma, for the lowest lava flow overlying the sandstones, and 14.7 ± 0.17 Ma, for one of the intruding dykes, were obtained (Wescott et al., 1993). Dyke intrusions of similar age (16.9 to 12.6 Ma) have been described in the Lokichar Basin (Tiercelin et al., 2004). Two distinct types of strata are exposed in the Lariu Formation. The lower portion of the section consists of well indurated cross-bedded sandstones and conglomerates, similar in appearance to the Lapur Sandstone Formation. The sediments, which are basement-derived, are characterized by large quartz pebbles and subangular metamorphic rock fragments near the base of the section. The upper part of the section is characterized by generally finer grained sandstones with colours that alternate from red to white (McGuirre et al., 1985). Petrographically, the Lariu sandstones are composed of arkoses, arkosic arenites and granule conglomerates. The conglomerates are composed predominantly of polycrystalline quartz with lesser amounts of microcline and orthoclase as the framework grains, while the cement is a combination of quartz overgrowths, authigenic kaolinite, calcite and hematite. The arkosic arenites consist predominantly of quartz and feldspar, with minor amounts of altered volcanic rock fragments. Plagioclase grains occur as relatively unaltered and highly altered grains, the alteration mainly involving replacement by calcite with minor amounts of sericitization. All framework grains show secondary dissolution where quartz grains show embayment, calcite-replaced plagioclase grains are almost completely dissolved forming moldic and intragranular secondary porosity while the relatively unaltered plagioclase commonly shows intragranular porosity along twin lamellae. Potassium feldspars (microcline and orthoclase) are abundant and are relatively unaltered, while volcanic rock fragments which occur in trace amounts have been largely replaced by clays and hematite. Cement material consists mostly of authigenic kaolinite, with minor amounts of clays and grain-replacement calcite. Porosity, which is estimated to be a maximum of 20 %, is mainly of primary intergranular with sufficient secondary intragranular to form an interconnected pore network capable of producing an effective permeable potential reservoir unit (Dunn, 1985).

Other sandstones similar to the Lariu and Lokichar sandstones can also be found at Mount Porr on the southeastern side of Lake Turkana (Williamson and Savage, 1986; Wescott et al., 1993; Tiercelin et al., 2004) (Fig. 7). As the Lokichar and Lariu sandstones, the **Mount Porr Sandstone**s (the Sera Iltomia Formation of Savage and Williamson, 1978) overlie the Precambrian basement and in turn are overlain by volcanics dated 18.5 ± 0.45 Ma. No precise age can be presented for the Mount Porr Sandstones. They could be Cretaceous in age (as the base of the Lapur Sandstone Formation) or Paleogene as the sandstones of the lower Lokone Formation. They possibly represent part of the infill of a basin developed east of the North Kerio Basin (Figs. 34 and 36) a part of it being intersected and downwarped by the recent(?) South Turkana Basin. The Mount Porr Sandstones are composed mainly of quartz and feldspars (microcline, albite and oligoclase), indi-

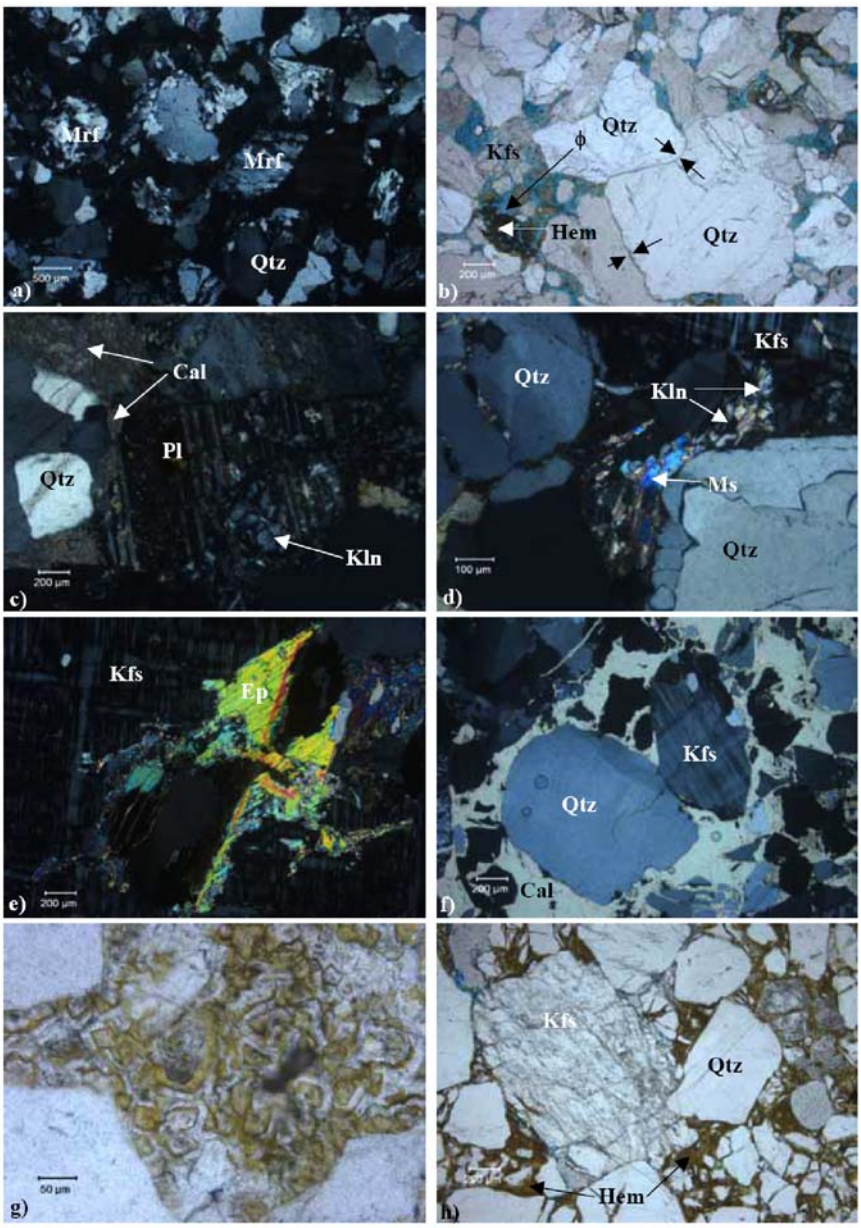

Figure 39. *(a) Grains of metamorphic origin as well as metamorphic rock fragments (mrf) are an important detrital grains component within the Mt. Porr Formation. Polycrystalline quartz (Qtz) grains are also very common (LPA photo). (b) Hematite (Hem) is an early generation cement, mechanical compaction has resulted in dissolution of grains at their contacts. Substantial amounts of residual primary intergranular porosity (Ê) has been preserved within the sandstones (LPNA photo). (c) Plagioclase feldspar (pl) dissolution is accompanied by precipitation of kaolin (Kln) (LPA photo). (d) Bent, broken and partially kaolinized muscovite grains (Ms) are good evidence for sediment mechanical compaction and chemical diagenetic alteration (LPA photo). (e) Intergrowths of feldspars and epidote (Ep) are common phenomena within the sandstones (LPA photo). (f) Early calcite (Cal) cementation was predated by some mechanical compaction of sediment, resulting in the dissolution of quartz and feldspar grains at contacts (LPA photo). (g) Pseudomorphs of dolomite have retained distinctive euhedral rhombic textures and zoning (LPNA photo). (h) Hematitic cements are post-compaction and they also postdate grain-to-grain pressure solution (LPNA photo). (LPA = polarized analysed light; LPNA= non polarized analysed light).*

cating a regional metamorphic source (Tiercelin et al., 2004). Diagenetic events are recorded by calcite, quartz or kaolin cements. Some of these events may relate to migration of fluids originating from igneous intrusions of Miocene age. The first detailed geological report of the area was reported by Savage and Williamson (1978) and later by Williamson and Savage (1986) who suggested that the lowermost grits in the area were Cretaceous in age. The Sera Iltomia Formation which rests unconformably on crystalline basement is the lower and the older one of the two grit horizons while the upper younger horizon is represented by the Kajong Formation which is overlain by volcanics dated at 18.5 + 0.45 Ma. The thicknesses of these two formations are 220 m for the Sera Iltomia Fm. and 200 m for the Kajong Fm. (Savage and Williamson, 1978). Wescott et al. (1993) have suggested an inferred age of Oligo-Miocene in the absence of direct paleontological evidence in the Sera Iltomia Fm. and the existence of Miocene vertebrates in sub-volcanic grits 30 km to the north of Mount Porr.

	STUR98-07		STUR98-08		STUR98-12		STUR98-13		STUR98-14		STUR98-15		STUR98-40		STUR98-44		STUR98-55	
	Count	%	Count	%	Count	%	Count	%	Count	%	Count	%	Count	%	Count	%	Count	%
Quartz	147	42,00	210	60,00	236	67,43	211	42,20	254	50,80	275	55,00	208	41,60	199	39,80	247	49,40
K-feldspar	11	3,14	12	3,43	45	12,86	20	4,00	21	4,20	13	2,60	11	2,20	24	4,80	9	1,80
Plagioclase	11	3,14	0	0,00	6	1,71	7	1,40	3	0,60	1	0,20	23	4,60	11	2,20	15	3,00
Unidentified	14	4,00	11	3,14	4	1,14	6	1,20	15	3,00	15	3,00	25	5,00	19	3,80	21	4,20
Clay matrix	77	22,00	7	2,00	22	6,29	145	29,00	174	34,80	49	9,80	13	2,60	6	1,20	4	0,80
Oxides	41	11,71	15	4,29	1	0,29	0	0,00	0	0,00	0	0,00	65	13,00	75	15,00	58	11,60
Calcite	4	1,14	0	0,00	0	0,00	0	0,00	0	0,00	0	0,00	79	15,80	130	26,00	111	22,20
Opaques	6	1,71	0	0,00	0	0,00	12	2,40	10,00	2,00	5	1,00	4	0,80	2	0,40	2,00	0,40
Porosity	39	11,14	95	27,14	36	10,29	99	19,80	23	4,60	142	28,40	72	14,40	34	6,80	33	6,60
Total	350	100	350	100	350	100	500	100	500	100	500	100	500	100	500	100	500	100
Grains	183	52,29	233	66,57	291	83,14	244	48,8	293	58,6	304	60,8	267	53,4	253	50,6	292	58,4
Matrix and																		
cements	128	36,57	22	6,29	23	6,57	157	31,4	184	36,8	54	10,8	161	32,2	213	42,6	175	35
Porosity	39	11,14	95	27,14	36	10,29	99	19,8	23	4,6	142	28,4	72	14,4	34	6,8	33	6,6

Table 12. *Point count data for samples from the Mount Porr Sandstones. The total number of points counted ranges from 350 to 500. Point-count porosity values were generally lower compared to actual figures in samples containing higher percentages of detrital and authigenic clays.*

The Sera Iltomia Formation is divided into four members composed of sequences of conglomerates, coarse to medium sandstones, fine sands and siltstones. On the footwall of the Kajong Fault Zone, the basal sandstone unit which rests horizontally on basement is composed of gravels and pebbles of quartz, with occasional basement-derived clasts. The sandstones here are horizontally stratified and locally show planar or trough cross-beds. To the south on the hanging wall of the KFZ, there is a 10 m well-bedded coarse pebbly sandstone exposure with alternating fine and conglomeratic beds. At this locality, the beds are almost vertical at an inclination of 75°. At the eastern tip of the KFZ outcrop well-bedded fine to very coarse sandstones measuring up to 45 m thick. To the south of the KFZ, on the distal part of the hanging wall, the exposure includes alternate beds of medium to coarse sandstones and silty mudstones and forms a 290 m section (Williamson and Savage, 1986; Wescott et al. 1993, Tiercelin et al., 2004) (Fig. 36).

The Mount Porr Formation is generally composed of very coarse sandstone with a bimodal grain size distribution where two sets of grains sizes are present; a coarser set of grains measuring between 4 mm and a maximum of 7.6 mm while the finer-grained matrix measures up to 0.4 mm in diameter. Occasionally there are samples that contain substantial amounts of metamorphic rock fragments (Fig. 39a) measuring up to 2 cm in long diameter. The detrital components include quartz, feldspars and metamorphic rock fragments while cementation is mainly by calcite, dolomite, kaolin, and hematite. Porosity is made up of fractures, residual intergranular porosity and intragranular porosity resulting from partial dissolution of grains such as feldspars. Point counting results (Table 12) give the abundances of the various components. Quartz is the main detrital component of the Mount Porr sandstone formation. Out of the 9 samples on which point counting was carried out, the amount of quartz ranges from a minimum of 41.6 % to a maximum of 67.43 %, with an average quartz content of 49.8 % (Table 12). The quartz grains are predominantly polycrystalline with trace monocrystalline grains. The monocrystalline variety has moderately to strongly undulose extinction. The grains are commonly subrounded to rounded and occasionally elongate. Grain fracturing, shattering and indentation (Fig. 39b) is common, with some of the fractures healed by calcite and hematite cements. Feldspars form the second most

abundant detrital grain in the Mount Porr Formation. Based on the point count data from 9 samples, the total feldspar composition ranges from 1.8 % to 12.86 %, with an average composition of 4.34 %. Both plagioclase (Fig. 39c) and K-feldspar (Fig. 39e-h) are present, with the latter being more abundant than the former, from visual observation rather than from actual point counting. The K-feldspar occurs in varying degrees of preservation, ranging from slight alteration by kaolinization to extensive alteration by replacement by both kaolin and calcite. There are also occasional intergrowths of both epidote and feldspar (Fig. 39e) observed within the sandstones. Plagioclase feldspars appear rather well preserved, having mainly suffered only grain fracturing as the only form of visible alteration with only slight partial kaolinization (Fig. 39c). Other detrital grains include metamorphic rock fragments, frequently broken and bent fragments of micas (biotite and muscovite). Muscovite flakes have undergone certain degree of kaolinization, especially at the edges where the flakes have parted and flayed. The total cement within the nine Mount Porr Formation samples that underwent point counting is in the range between 6.29 % and 42.6 %, with an average value of 26.47 % (Table 12). These numbers are however inclusive of the clay matrix. The main cementation materials in the sandstones are calcite, hematite, dolomite and kaolin.

Kaolin cement is not very abundant within the sandstones of the Mount Porr formation and where it occurs, it is mainly as the product of the partial alteration of feldspars, muscovite (Fig. 39c, d) and as a result of kaolinization of detrital clays. The kaolin occurs in vermicular textures within the partially replaced feldspars and within the flayed ends of partially altered muscovite flakes. Calcite cement constitutes between 0 % and 23 %, with an average of 7.23 % (Table 12). The calcite occurs primarily as poikilotopic textures where optically continuous crystals of calcite cement several grains together and occurring as pore-filling cement (Fig. 39f). Within the poikilotopic calcite-cemented sandstone, porosity has been severely reduced, with almost zero residual intergranular porosity. Some of the calcite has undergone dolomitization as evidenced by the presence of dolomite rhombs within the calcite. Later dedolomitization may have taken place since faint ghosts of dolomite rhombs are visible within some of the presently calcitic cement. Some of the calcite appears as replacive or as a product of feldspar alteration. Dolomitization of calcite cement is evidenced by the presence of rhombic shapes associated with the calcite cements. The dolomite cement appears cloudy and is commonly brown stained and zoned. The zones alternate from clear or slightly cloudy to brown stained (Fig. 39g). In some case, the rhombic shapes appear as ghost remaining within poikilotopic calcite cement, which could indicate reversion to calcite after dolomitization, in the process of dedolomitization. Hematite in many cases it occurs as early pore-lining cement which is followed by later generations of pore-filling cement. Rarely, the hematite occurs as brown pore-filling cement (Fig. 39h).

Of the 9 samples that were point-counted, porosity values range from 6.6 % to 27 %. The observed porosity is mainly residual primary intergranular porosity with minor amounts of secondary intragranular porosity resulting from partial dissolution of the feldspars. Microporosity associated with the vermicular kaolin cements is present though in minute amounts. Dolomitization, which is normally expected to enhance porosity, has not in this case resulted in any significant improvement in the porosity due to the fact that the process has been followed by subsequent dedolomitization and what remains are pseudomorphs of dolomite in calcite (Fig. 39g). Samples containing high amounts of clay matrix or high amounts of calcite cements (Fig. 39f) correspond to extremely low porosity values.

The main diagenetic events of the Mount Porr Sandstone formation can be summarised in Figure 40. The sedimentary facies observed in the Mount Porr Formation suggest depositional environments that range from high energy braided stream environments to channel and overbank deposits within a non-braided fluvial environments (Williamson and Savage, 1986; Tiercelin et al., 2004). The detrital mineral composition in the sandstones is indicative of purely metamorphic derivation with no volcanic input. In some cases, early calcite

Event	Early	Late
Mechanical compaction of sediment	———	
Cementation by hematite	———	
Cementation by calcite	——— ———	
Feldspar dissolution	———	
Kaolinization	———	
Dolomitization of calcite	———	
Dedolomitization	———	

Figure 40. *A summary of the main diagenetic events affecting sandstones of the Mount Porr Formation. Mechanical sediment compaction followed soon after sediment deposition while the latest diagenetic process is one of dedolomitization.*

cementation (Fig. 39f) results in almost total occlusion of original intergranular porosity; while in other cases, high detrital clay content had the effect of limiting effective depositional porosity and at the same time enhances mechanical compactibility of the sediment. Calcite cementation was, in certain instances, preceded by substantial sediment compaction (Fig. 39f). Late dolomitization is normally accompanied by an enhancement of porosity values but within the sandstones of Mount Porr Formation, subsequent dedolomitization (Fig. 39g) left only pseudomorphs of calcite after dolomite, recognized mainly base on the rhombic shapes and the zoning from remnants of insoluble matter. Feldspar dissolution (Fig. 39c) is accompanied by the precipitation of kaolin and it thus does not result in significant net increase in porosity values. Compaction of the sediment has in some instances resulted in grain-to-grain pressure solution (Fig. 39b). This dissolution along quartz grain contacts must have produced silica in solution and this must have in turn been deposited elsewhere as quartz overgrowths. Such overgrowths have been reported by Tiercelin et al. (2004), though none were observed in the present study. Bent micas are good indicators of mechanical sediment compaction (Fig. 39d); such micas have undergone insipient kaolinization at their edges. Though not volumetrically significant within the Mount Porr Formation, hematite cement was interpreted as the product of an early phase of cementation (Fig. 39b), most likely resulting from the alteration of ferromagnesian minerals derived from the source sediment.

2.2.2. Source Rocks

In terms of source rock potential, the presence of a source rock in the Lokichar Basin is not a critical question. The two black shale intervals encountered by the Loperot-1 well have been described as good quality source rocks (Morley, 1999e; Talbot et al., 2004) (Fig.33b, c). The upper shale interval (Lokone) is dated late Oligocene-early Miocene, while the lower interval (Loperot) is of possible Eocene to early Oligocene age (Morley et al., 1999b). Organic matter studies demonstrated a good source rock potential with high TOC values (1-17 %, average 2.4 %) (Morley et al., 1999b) and proved algal lacustrine origin for this organic matter (Talbot et al., 2004). Multicellular algae, *Botryococcus* spp., and *Pediastrum* spp. indicated fresh water conditions. HI values in the Loperot-1 well suggest a Type I/II composition for the productive kerogen. Similar source rocks characterized by the presence of botryococcanes derived from *Botryococcus brauni* and kerogen

of Type I and II, have been identified in the Paraa and Kibiro oil seeps in the Albertine Graben (Lirong et al., 2004).

Wide lateral extension of the Lokone shales into the North Kerio Basin is suspected from interpretation of seismic data across the Lokone Horst. These shales were deposited during a time when displacement on the main Lokichar boundary fault system was greater, and adjacent basins (the North Lokichar Basin to the north, and the North Kerio Basin to the east) had been established. Consequently, lacustrine conditions offering good source rock potential appear to have extended into these adjacent basins, thus allowing accumulation of high concentrations of organic matter in the basins. Pollen analyses have been conducted on the Lokone shale interval from the Loperot-1 well (Vincens et al., 2006). They demonstrate the presence in the Lokichar region of a mosaic environment of semi-deciduous forest and humid woodland presenting strong affinities with vegetation known today in the Guinea-Congolia/Zambezia phytogeographical zone. Rainfall of more than 1000 mm/yr characterized the Lokichar region during late Oligocene-lower/middle Miocene. The existence of a large, possibly deep fresh water lake is well supported by paleoclimatic data, and by the discovery of wide populations of fish, crocodiles, turtles in arkosic sandstones of late Oligocene age onlapping the basement at Lokone Horst (Ducrocq et al., 2009). The Eocene-middle Miocene Lokichar Lake could be interpreted as similar to some of the modern large lakes of the western branch of the EARS, such as the modern Lake Albert or Lake Edward. Such climatic conditions also support the possibility of high lake level conditions that, combined with tectonic displacements along the main boundary fault, induced the development of a large (possibly 100 km wide and more than 150 km long), highly productive fresh water lake covering the Lokichar, North Lokichar, and North Kerio Basins.

Evidence of oil generation from the Loperot shales was provided by traces of oil encountered at several levels in the Loperot-1 well (Shell Exploration and Production Kenya B.V., unpublished report). The upper Lokone Shale Member still has relatively high HI. It is thus probable that significant volumes of liquid hydrocarbons have already been generated from this unit, which still has considerable generative potential (Talbot et al., 2004).

3. The Central Kenya Rift Basins

3.1. The Kerio and Baringo Basins

The Kerio and Baringo Basins are located in the central segment of the Kenya Rift between 0°15’ and 0° 45’N, and are separated by the uplifted Tugen Hills fault-block (Fig. 7). The present-day Kerio Basin is occupied by the Kerio River valley, a semi-permanent river draining into Lake Turkana. This half-graben basin is considered today as tectonically quiescent while the Baringo Basin, which is today occupied by the freshwater Baringo Lake, and the saline alkaline Bogoria Lake, is considered as tectonically and volcanically active (Tiercelin and Vincens, 1987) (Fig. 41). Gravity and seismic investigations were conducted by the National Oil Corporation of Kenya in the Kerio Valley in 1989. A magnetotelluric survey conducted in 1996 in the Baringo Basin, associated to a re-interpretation of the Kerio seismic and gravity data demonstrated that the modern Kerio and Baringo Basins are superimposed on two deep sedimentary basins that possibly initiated during Paleogene. Today, the Kerio Basin is described as a >8 km deep typical half-graben, while the Baringo Basin is 7 km deep (Hautot et al., 2000; Tiercelin and Lezzar, 2002). Both basins are filled by alternating fluvial and lacustrine sediments and thick piles of volcanics (Fig. 41a).

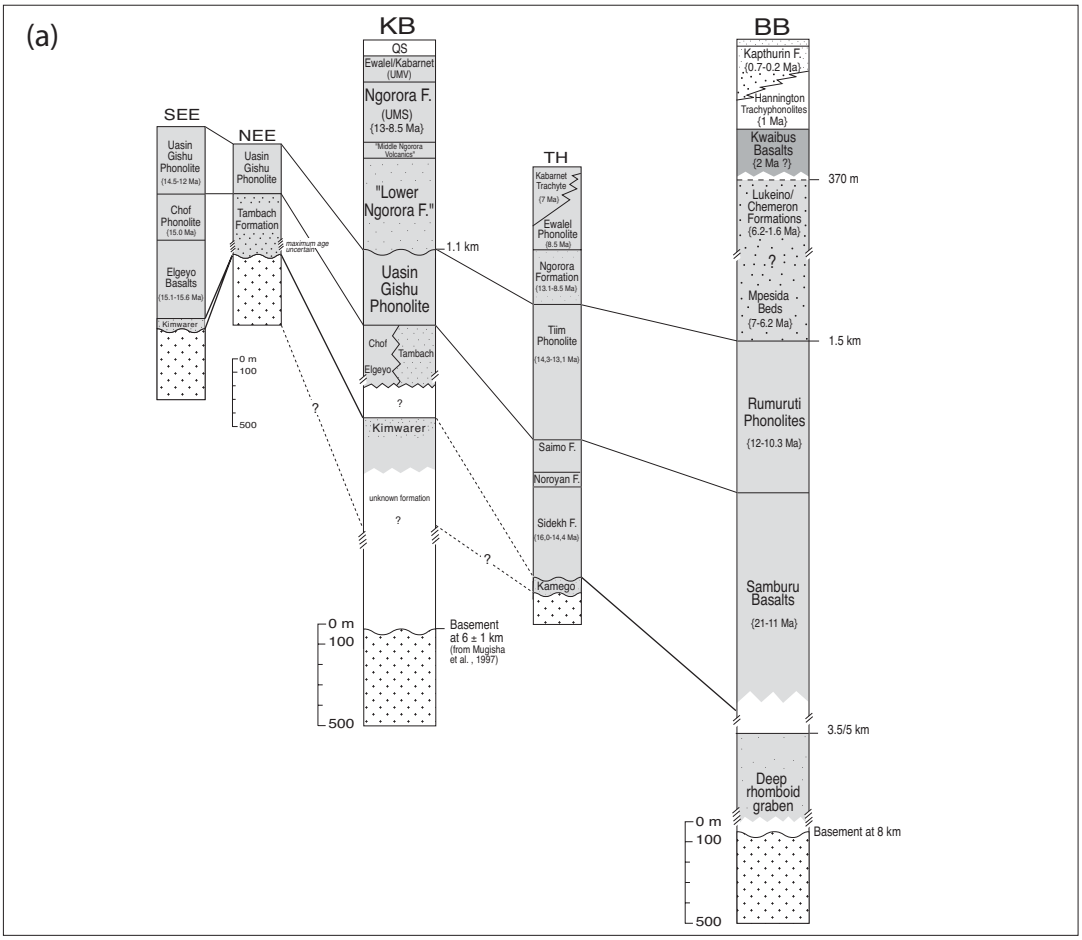
(a)
KB
BB
SEE
NEE
TH
QS
Ewalel/Kabarnet (UMV)
Ngorora F. (UMS) {13-8.5 Ma}
"Middle Ngorora Volcanics"
"Lower Ngorora F."
Uasin Gishu Phonolite
Chof
Tambach
Elgeyo
Kimwarer
unknown formation
Basement at 6 ± 1 km (from Mugisha et al., 1997)
1.1 km
Uasin Gishu Phonolite (14.5-12 Ma)
Chof Phonolite (15.0 Ma)
Elgeyo Basalts (15.1-15.6 Ma)
Kimwarer
Tambach Formation
maximum age uncertain
0 m
100
500
Kabarnet Trachyte (7 Ma)
Ewalel Phonolite (8.5 Ma)
Ngorora Formation (13.1-8.5 Ma)
Tiim Phonolite (14,3-13,1 Ma)
Saimo F.
Noroyan F.
Sidekh F. (16,0-14,4 Ma)
Kamego
Kapthurin F. (0.7-0.2 Ma)
Hannington Trachyphonolites (1 Ma)
Kwaibus Basalts (2 Ma ?)
Lukeino/ Chemeron Formations (6.2-1.6 Ma)
Mpesida Beds (7-6.2 Ma)
Rumuruti Phonolites (12-10.3 Ma)
Samburu Basalts (21-11 Ma)
Deep rhomboid graben
370 m
1.5 km
3.5/5 km
Basement at 8 km

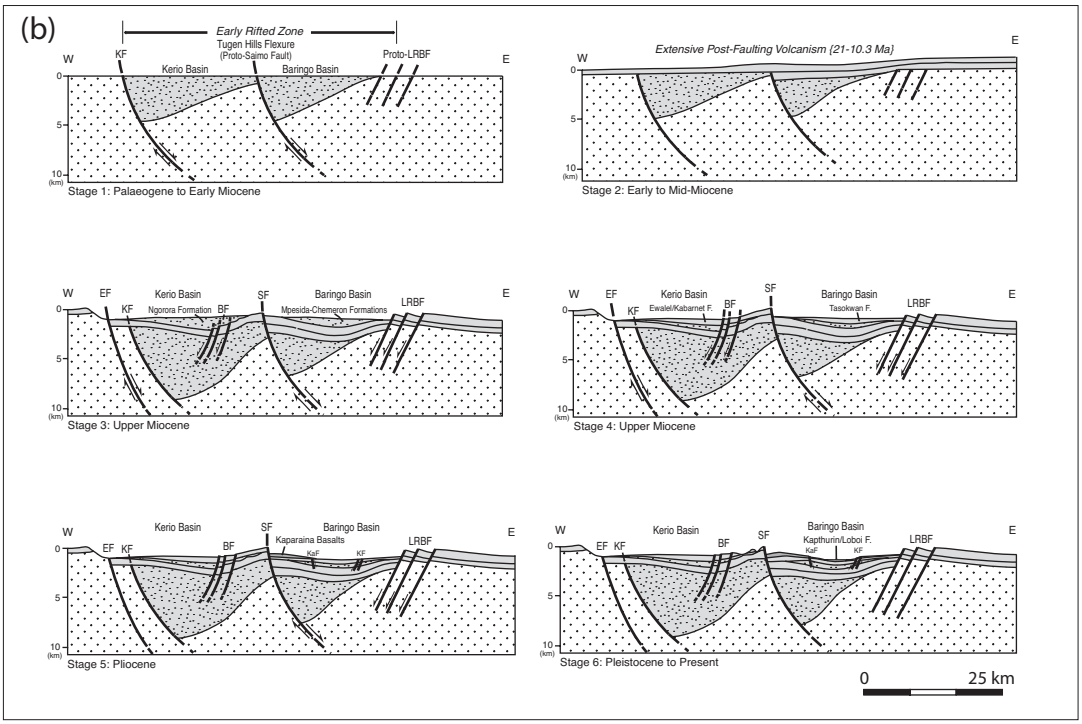
(b)
Early Rifted Zone
Tugen Hills Flexure (Proto-Saimo Fault)
Proto-LRBF
Kerio Basin
Baringo Basin
KF
W
E
Stage 1: Palaeogene to Early Miocene
Extensive Post-Faulting Volcanism (21-10.3 Ma)
Stage 2: Early to Mid-Miocene
EF
SF
BF
LRBF
Ngorora Formation
Mpesida-Chemeron Formations
Stage 3: Upper Miocene
Ewalel/Kabarnet F.
Tasokwan F.
Stage 4: Upper Miocene
Kaparainia Basalts
KaF
Stage 5: Pliocene
Kapthurin/Lobol F.
Stage 6: Pleistocene to Present
0
25 km

3.1.1. Reservoir Rocks

The lowest part of the Kerio Basin infill is of sedimentary origin and possibly of Paleogene age. At the southern end of the Kerio Basin, arkosic sandstones known as the "**Kimwarer Formation**" outcrop along the footwall of the western faulted margin of the basin - the Elgeyo Border Fault, where they overlie the Precambrian basement. Renaut et al. (1999) describe green, waxy, laminated tuffaceous shales associated to these sandstones. To the east, in the Baringo Basin, the oldest sediments exposed along the western faulted side of the basin – the Saimo Border Fault - are known as the "**Kamego Formation**" (Fig. 7). They are mainly arkosic fluviatile sandstones sourced from Precambrian rocks (Chapman et al., 1978; Renaut et al., 1999). These Kimwarer and Kamego sediments represent the earliest sections of the Kerio and Baringo Basins infill, possibly indicating fluvial and lacustrine environments similar to the ones found to the north in the Lokichar and North Kerio Basins. Fluvial networks of Paleogene age draining the basement floor of the Kerio and Baringo Basins are interpreted as flowing northward, feeding the Lokichar-North Kerio Basins (Morley and Wescott, 1999; Tiercelin et al., 2004). The Paleogene history of the Kerio and Baringo Basins is unfortunately poorly known because outcrops are scarce and poorly exposed and due to the absence of sufficient seismic data and exploration wells. Nevertheless, possible similarity between the Kimwarer-Kamego Formations and the Lokichar-North Kerio sediments may encourage oil exploration in Blocks 13T and 12A (presently licensed to Platform Resources).

The Miocene history of the Kerio-Baringo half-grabens is much better documented by sediments and lavas outcropping along the Elgeyo Border Fault and the western flank of the Tugen Hills fault block (Saimo Border Fault) (Fig. 41). Thick sedimentary deposits are found interbedded between the volcanic units and relate to the existence of at least two wide lacustrine domains known as the Tambach Lake and the Ngorora Lake, both dated middle Miocene. In the Kerio Basin, more than 2 km of volcanic rocks fill have been deposited between 23 and 15 Ma, then between 14 and 7 Ma (Chapman et al., 1978) (Fig. 41a). The oldest sequence of Neogene age is the **Tambach Formation**. Up to 400 m of colluvial, fluvial and lacustrine sediments are exposed discontinuously along the Elgeyo Border Fault, and lie upon an irregular topography of basement rocks (Ego, 1994; Renaut et al., 1999). The upper limit of the Tambach Formation is provided by the overlying Uasin Gishu Phonolite Formation (described by Lippard, 1973), that is dated from 14.5-12 Ma. The overall Tambach depositional sequence is formed by alluvial fan and gravelly braided stream deposits near the base of the sequence, followed by sandy braided deposits, to shallow deltaic and lacustrine sediments at the top part of the sequence (Renaut et al., 1999).

The **Ngorora Formation** is of Miocene age but younger than the Tambach Formation (Bishop and Chapman, 1970) (Fig. 41). The 400-m thick Ngorora sediments lie upon lavas of the Tiim Phonolite Formation dated 13.1 Ma and are unconformably overlain by the Ewalel Phonolite Formation dated 8.5 Ma (Hill, 1999). Clastic sediments in the Ngorora Formation are mainly fluvial sediments and lahar deposits, and have been

Figure 41. *(a) Interpreted stratigraphic series of the Central Kenya Rift, from the Kerio Basin to the west, to the Baringo Basin to the east. The logs for the Kerio Basin (SEE; South Elgeyo Escarpment; NEE, North Elgeyo Escarpment; KB, Kerio Basin; TH, Tugen Hills, eastern flank of the Kerio Basin) show the stratigraphic position of the Paleogene(?) old Kimwarer and Kamego Formations, of unknown thickness but presenting an interesting reservoir potential (see KB and TH logs), and the Neogene Tambach and Ngorora Formations. To the east, the Baringo Basin (BB) log shows the deep structure of the basin below the 2 km-thick Samburu Basalts (21-11 Ma). This deep part of the basin can offer potential source rocks and reservoirs of Paleogene age, but this can only be confirmed by deep drilling. (b) Simplified diagram of the Central Kenya Rift (Kerio-Baringo Basins) evolution from Paleogene times to present Central Kenya Rift. The early stages of rifting are contemporaneous of the Lokichar-North Kerio rifting events in the Northern Kenya Rift. But, contrary to the case of the Lokichar Basin, basin evolution in the Kerio Basin has continued until upper Miocene, and up to present in the Baringo Basin (modified from Hautot et al., 2000; Tiercelin and Lezzar, 2002).*

poorly studied. In terms of reservoir rocks, arkosic sandstones near the base of the Tambach Formation are quartz-rich and well sorted, and reflect dominant basement provenance. Cements are calcite and iron oxides, as it is in the Lapur Sandstone Formation in Northern Kenya Rift. Quartz and albite overgrowths are locally present. Near the top of the formation, the sandstone composition is characterized by an increase in volcanic grains as a consequence of the occurrence of regional volcanic activity (Ego, 1994).

3.1.2. Source Rocks

The main component of the Ngorora Formation is formed by lacustrine shales that were described by Pickford (1978) as being petroliferous and thus, the Tambach and Ngorora Formations were considered as attractive for hydrocarbon exploration. The lacustrine facies in the Tambach Formation are dominated by pale green, grey and white shales. Some are waxy in feel and appearance or show a “paper shale” facies (Renaut et al., 1999). They are interpreted as accumulated in fresh to slightly brackish waters. Of the two lacustrine members of the Ngorora Formation, one (Member C) shows interest in terms of source rock/hydrocarbon potential. Both members represent a succession of lake environments from shallow, freshwater lakes to small saline, alkaline lakes resembling the present-day Lake Baringo, or Lake Bogoria, respectively (Tiercelin and Vincens, 1987; Renaut and Tiercelin, 1994). Petroliferous shales with up to 4.3 % TOC have been described at Poi locality on the western flank of the Tugen Hills. The shales are dark green or dark grey in colour, and contain very well preserved fossil fish and leaf fragments. Presence of abundant zeolites such as analcite and clinoptilolite associated with other authigenic minerals indicate a saline, alkaline lacustrine domain, certainly hydrologically closed and submitted to frequent fluctuations in lake level as well as in salinity. An analogue can be found in the Central Kenya Rift with the modern lakes Nakuru and Elmenteita, or with Lake Bogoria, a meromictic lake with an anoxic monimolimnion, preserving the accumulation of organic-rich (up to 12 % TOC) zeolitic muds in the deeper parts of the lake (Tiercelin and Vincens, 1987). The Poi shales can also be compared to the Oligo-Miocene shales found in the Lokichar Basin.

Conclusions

Although the rift basins of Northern and Central Kenya Rifts have not attracted a lot of interest from oil exploration companies in the past, recent oil discoveries in the Albertine Graben in Uganda has shifted the focus of many oil companies to such rift basins. If the occurrence of hydrocarbons in rift basins is strongly controlled by the style of post-rift tectonics, it is also controlled by the nature of the basin-fill stratigraphy. Sedimentological, petrological and geochemical studies conducted on the reservoir and source rock potential in the major basins belonging to the Northern and Central Kenya Rifts have permitted the establishment of a provisional classification of these basins, that can be used as a predictive tool for evaluating every half-graben for source rock quality and quantity, and for reservoir potential:

1) In terms of source rocks:

Lacustrine source rocks are widespread in the East African Rift System, and have been particularly encountered in areas with well developed natural oil seeps. The best example in the EARS is the Lake Albert Rift where oil seeps are numerous and where major oil discoveries have recently been made. Other natural oil seeps are known in the northern basin of Lake Tanganyika (Pemba and Cape Kalamba), where asphaltic oil is generated from recent organic-rich muds associated to hydrothermal systems (Tiercelin et al., 1993; Simoneit et al., 2000). In the Northern Kenya Rift, the best known source rocks (qualified as good to high quality source rocks) have been identified in the Lokichar Basin, particularly in the Lokone Shale Member. According to Morley (1999e) calculations, 1 km in thickness can be expected for the Lokone shales near the major Lokichar boundary fault, and important volumes (about 16 billion of barrels) of hydrocarbons could be generated from the Lokichar Basin. The Poi source rocks found in the Ngorora Formation of the Kerio-Baringo Basins, Central Kenya Rift, can be also classified as good quality source rocks and comparable to the Lokone source rocks. In terms of oil potential, the main questions for the Ngorora Formation are 1) the quantity of source rock that is dependent on the basin size and the depositional setting of the shales. Minimum thickness is evaluated at outcrop scale, and paleogeographical reconstructions indicate a small lake basin (Pickford, 1978). Nevertheless, such data have been deduced from two-dimensional observations along the Elgeyo and Saimo fault escarpments. A dense seismic reflection coverage of the Kerio Basin will probably help to obtain a better description of the Ngorora Basin paleogeography.

No other source rocks of good quality have been identified in the Central or Northern Kenya Rifts, to the exception of modern organic-rich muds found in saline-alkaline lakes such as Lake Bogoria. Only dark grey silty mudstones have been described at outcrop scale within the Lapur Sandstone Formation at the northwest end of the Lake Turkana Basin. Poor organic content, minimal thicknesses and limited lateral continuity characterize these sediments. In addition, suspected depositional environments (floodplains or shallow lakes) suggest a minimal source rock potential. Nevertheless, thicker accumulations of similar dark shales can be expected in the deeper parts of Gatome Basin. But only acquisition of new good quality seismic and subsequent deep drilling will permit to solve this question.

2) In terms of reservoir rocks:

The different basins observed in the Northern and Central Kenya Rifts – Lotikipi/Gatome, Lokichar/North Kerio, Kerio and Baringo – all offer a good to very good reservoir potential. Sandstone quality in this part of the East African Rift is highly dependent upon the source area, and the transport distance (Morley, 1999e). Early stages of development for the older basins in Northern Kenya (Mid-Cretaceous to

Paleogene; Lotikipi/Gatome, Lokichar) are all characterized by alluvial, fluvial or fluvio-deltaic environments. Sandstones associated to these early stages of basin development and specific depositional environments are most commonly basement-derived arkoses (mainly quartz- and feldspar-rich). The better examples are provided by the Lapur and Muruanachok Formations, as well as the lowest parts of the Lokichar Basin infill (Loperot Sandstone Formation). Such arkosic sandstones are characterized by marked reduction of porosity mainly because of diagenetic evolution of feldspars. In the Cretaceous-Paleogene Anza Rift of northeastern Kenya, quality of reservoirs is locally deeply modified by diagenetic growth of zeolites (Winn et al., 1993). No zeolitic cementation has been encountered in the arkosic sandstones belonging to the Lapur, Muruanachok, and Mount Porr Formations, to the exception of the Lokichar Formation. Major cements are calcite, kaolinite and hematite, some of these cements being strongly associated to climatic changes prevailing in Central-Eastern Africa from middle Cretaceous. Results of porosity measurements in the Lapur Sandstone Formation yielded values ranging from a minimum of 3 % to a maximum of 25 % (Thuo et al., in press). These values compare well with other observed porosity values in sandstones of similar depositional environments in the southern Sudanese basins where porosities values ranging from 8 to 38 % have been reported (Schull, 1988; Giedt, 1990). In the Lokichar Basin, arkosic sandstones show calcitic and zeolitic cements, and porosities between 1-15 %. In the Loperot-1 well, reservoir levels show quartz and feldspar overgrowths, carbonate cements, zeolites, authigenic clays and opaque minerals, particularly in levels (Auwerwer Sandstone Formation) where sandstones contain large quantities of volcanic-derived material which are prone to diagenetic alteration. Good porosity values of 12-30 % have been obtained at different intervals in the Loperot-1 well (Morley, 1999e).

In the Central Kenya Rift, potential reservoirs may be expected from the Kimwarer and Kamego arkosic sandstones. Unfortunately, poor sedimentological/petrological studies have been conducted on these formations. Nevertheless, they may represent deep targets within the context of Paleogene-old deep Kerio and Baringo Basins. Sandstone units associated with the Miocene-old Tambach and Ngorora Formations show similar characteristics with the upper part of the Lokichar Basin infill (Auwerwer Sandstone Formation), as large quantities of volcanic minerals are directly derived from a volcanically-delineated basin watershed. Low porosities can be expected from these formations.

To conclude in terms of hydrocarbon prospectivity classification for the Northern and Central Kenya Rifts:

- **The Lokichar/North Kerio Basins** (NKR) can be classified on **Rank 1** as it offers a quite interesting ratio between source rock quality and quantity and reservoir potential;

- Rank 2 can be attributed to the **Gatome Basin** (NKR) because of its thick infill and the proximity of good potential reservoirs represented by the Lapur and Muruanachok Sandstone Formations. Nevertheless, no good source rock have been identified in this basin but there is a strong possibility to encounter such source rock at depth;

- Rank 3 can be attributed to the Miocene old **Kerio and Baringo Basins**, that offer a good source rock, but low quality potential reservoir rocks. Nevertheless, in similar conditions, reservoir quality sandstones can be encountered in wells at depths of at least 3 km.

With the increased oil exploration activity within Kenya rift basins, it will only be a matter of time before deep exploration wells are drilled in these basins providing a better understanding of the evolution of basin architecture and sedimentary fill.

References

References

References

Abdelfettah, Y., 2009. Inversion conjointe des données magnétotelluriques et gravimétriques: Application à l'imagerie géophysique crustale et mantellique. Thèse. Université de Bretagne Occidentale, 171 p.

Alconsult International., 1997. Hydrocarbon potential of Kenya. East Africa Regional Hydrocarbon Study. Calgary, Canada. 175 p.

Andrews, P., Banham, P., (Eds.), 1999. Late Cenozoic Environments and Hominid Evolution: a tribute to Bill Bishop. Journal of the Geological Society of London. 276 p.

Arambourg, C., 1935. Esquisse géologique de la bordure occidentale du Lac Rodolphe. Mission scientifique de l'Omo. 1932-33. Vol. 1 (1), Bulletin Muséum National d'Histoire Naturelle, Paris. 55 p.

Arambourg, C., 1943. Contribution à l'étude géologique et paléontologique du Bassin du lac Rodolphe et de Basse Vallée de l'Omo. Bulletin Muséum National d'Histoire Naturelle, Paris. Vol 1 (2), 157 – 230.

Arambourg, C., Wolf, R.G., 1969. Nouvelles données paléontologiques sur l'âge des grès de Lubur (Turkana Grits) à l'Ouest du lac Rodolphe. Comptes Rendus Société géologique de France 6, 190 – 202.

Beauchamp, J., 1977. La série sédimentaire en Ethiopie centrale et orientale. Thèse, No. 7749, Université de Lyon, 419p.

Beauchamp, J. 1988. Cadre géodynamique de la sédimentation détritique Crétacée en Afrique orientale. Annales Société Géologique Nord CVII, 89 – 94.

Beicip., 1987. Kenya Tertiary Rift Study: unpublished. Report to National Oil Corporation of Kenya 324p.

Bellieni, G., Justin Visentin, E., Zanettin, B., Piccirillo, E.M., Radicati di Brozolo, F., Rita, F., 1981. Oligocene transitional-tholeiitic magmatism in northern Turkana (Kenya). Comparison with the coeval Ethiopian volcanism. Bulletin of Volcanology 44, 411 – 427.

Bellieni, G., Justin Visentin, E., Piccirillo, E. M Zanettin, B., 1987. Volcanic cycles and magmatic evolution in northern Turkana (Kenya). Tectonophysics 143, 161 – 168.

Bishop, W.W., Chapman, G.R., 1970. Early Pliocene sediments and fossils from the northern Kenya Rift Valley. Nature 226, 914 – 918.

Bjørkum, P.A., Gjelsvik, N., 1988. Isochemical model for the formation of authigenic kaolinite, K-feldspar and illite in sediments. Journal of Sedimentary Petrology 58, 506 – 511.

Blatt, H., 1979. Diagenetic processes in sandstones. In: Scholle, P.A., Schluger, P.R. (Eds). Aspects of diagenesis. Society of Economic Paleontologists and Mineralogists Special Publication 26, 141 – 157.

Boschetto, H.B., Brown, F.H., McDougall, I.M., 1992. Stratigraphy of the Lothidok Range, Northern Kenya, and K-Ar ages of its Miocene primates. Journal of Human Evolution 22, 47 – 71.

Bosellini, A., Russo, A., Assefa, G., 2001. The Mesozoic succession of Dire Dawa, Harar Province, Ethiopia. Journal of African Earth Sciences 32, 403 – 417.

Bosworth W., 1992. Mesozoic and early Tertiary rift tectonics in East Africa. Tectonophysics 209, 115 – 137.

Bosworth, W., Morley, C.K., 1994. Structural and stratigraphic evolution of the Anza rift, Kenya. Tectonophysics, 236, 93 – 115.

Beitler, B., Parry, W.T., Chan, M.A., 2005. Fingerprints of fluid flow: chemical diagenetic history of the Jurassic Navajo Sandstone, southern Utah, USA. Journal of Sedimentary Research 75, 547 – 561.

References

Buatier, M.D., Travé, A., Labaume, P., Potdevin, J.L., 1997. Dickite related to fluid-sediment interaction and deformation in the Pyrenean thrust fault zones. European Journal of Mineralogy 9, 875 – 888.

Buatier, M.D., Deneele, D., Dubois, M., Potdevin, J.L., Lopez, M., 2000. Nacrite in the Lodève Permian Basin: a TEM and fluid inclusion study. European Journal of Mineralogy 12, 329 – 340.

Bussert, R., 1993. Evolution of Cretaceous continental basins in northern Sudan. In: Thorweihe, U., Schandelmeier, H., (Eds.), Geoscientific Research in Northwest Africa. Balkeema, Rotterdam., 776p.

Burgoyne, P.M., van Wyk, A.E., Anderson, J.M., Schrire, B.D., 2005. Phanerozoic evolution of plants on the African plate. Journal of African Earth Sciences 43, 13 – 52.

Burke, K., 1996. The African plate. South African Journal of Geology 99, 339 – 410.

Burke, K., Gunnel, Y., 2006. The African erosion surface: a continental-scale synthesis of geomorphology, tectonics, and environmental change over the past 180 million years. Geological Society of America Memoir 201, 64p.

Burke, K., MacGregor, D.S., Cameron, N.R., 2003. Africa's petroleum systems: four tectonic 'aces' in the past 600 million years. In: Arthur, T.J., MacGregor, D.S., Cameron, N.R., (Eds.) Petroleum geology of Africa: new themes and developing technologies. Geological Society, London, Special publications 207, 21 – 60.

Chan, M.A., Parry, W.T., Bowman, J.R., 2000. Diagenetic hematite and manganese oxides and fault-related fluid flow in Jurassic sandstones, southeastern Utah. American Association of Petroleum Geologists Bulletin 84, 1281 – 1310.

Chapman, G.R., Lippard, S. J., Martyn, J. E., 1978. The stratigraphy and structure of the Kamasia Range, Kenya Rift Valley. Journal of the Geological Society of London 135, 265 – 281.

Collinson, J.D., 1996. Alluvial sediments. In: Reading, H.G. (Ed.), Sedimentary environments: processes, facies and stratigraphy (3rd edition). Blackwell, Oxford. 688p.

Cotten, J., Le Dez, A., Bau, M., Caroff, M., Maury, R.C., Dulski, P., Fourcade, S., Bohn, M., Brusse, R. 1995. Origin of anomalous rare-earth element and yttrium enrichment in subearially exposed basalts: Evidence from French Polynesia. Chemical Geology 119, 115 – 138.

Crowley, S.F., 1991. Diagenetic modification of detrital muscovite: an example from the Great Limestone Cyclothem (Carboniferous) of Co. Durham, UK. Clay Minerals 26, 91 – 103.

Desprès, A., 2008. Evolution tectono-sédimentaire des bassins de rift Crétacé-Paléogène du Nord du Kenya. Master 2, Université de Rennes 1, France.

Dodson, R.G., 1971. Geology of the area south of Lodwar. Geological Survey of Kenya Report 87, 36p.

Donnadieu, Y., Pierrehumbert, R., Jacob, R., Fluteau, F. 2006. Modelling the primary control of paleogeography on Cretaceous climate. Earth and Planetary Science Letters 248, 426 – 437.

Ducrocq, S., Boisserie, J. R., Tiercelin, J.-J., Delmer, C., Garcia, G., Kyalo, M. F., Leakey, M. G., Marivaux, L., Otero, O., Peigné, S., Tassy, P., Lihoreau, F., 2009. New Oligocene vertebrate localities from Northern Kenya (Turkana Basin). Journal of Vertebrate Paleontology (in press).

Dunkelman, T.J., Karson, J.A., Rosendahl, B.R. 1988. Structural style of the Turkana Rift, Kenya. Geology 16, 258 – 261.

Dunkelman, T.J., Rosendahl, B.R., Karson J.A., 1989. Structure and stratigraphy of the Turkana rift from seismic

reflection data. Journal of African Earth Sciences 8, 489 – 510.

Dunn, J. L., 1985, Petrography of selected samples from the Lake Turkana area, Northwestern Kenya: Unpublished report prepared by NL Erco/NL Industries, Inc. for Amoco Production Company. 23p.

Ebinger, C.J., Ibrahim, A., 1994. Multiple episodes of rifting in Central and East Africa: A re-evaluation of gravity data. Geologische Rundschau, 83, 689 – 702.

Edwards, W.N., 1926. Fossil plants from the Nubian Sandstone of Eastern Darfur. Quarterly Journal of the Geological Society of London 84, 94 – 100.

Ego, J. K., 1994. Sedimentology and diagenesis of Neogene sediments in the central Kenya Rift Valley. M.Sc. thesis (unpublished), University of Saskatchewan, 148p.

EIA., 2007. Energy Information Administration. Official Energy Statistics from the US Government.

Eisawi, A., Schrank, E., 2009. Terrestrial palynology and age assessment of the Gedaref Formation (Eastern Sudan). Journal of African Earth Sciences 54, 22 – 30.

Einsele, G., 2000. Sedimentary basins: evolution, facies and sediment budget. 2nd edition. Springer, Heidelberg. 792p.

El-Ghali M.A.K., Tajori K. G., Mansurbeg, H., 2006. The influence of transgression and regression on the spatial and temporal distribution of diagenetic kaolin in the Upper Ordovician glaciogenic sandstones within a sequence stratigraphic framework, Murzuq Basin, SW Libya. Journal of Geochemical Exploration 89, 87 – 91.

Fairhead, J.D. 1986. Geophysical controls on sedimentation within the African rift systems.In: Frostick, L.E., Renaut, R.W. Reid, I., Tiercelin, J.J. (Eds.), Sedimentation in the African rifts. Geological Society of London Special Publication 25, 19 – 27.

Fuchs, 1939. The geological history of the Lake Rudolf basin, Kenya Colony. Philosophical Transactions of the Royal Society London 229, 219 – 274.

Garland, C.R., 1980. Geology of the Adigrat area. Geological Survey of Ethiopia Memoir 1, 51p.

Gdrniak, K., 1997. The role of diagenesis in the formation of kaolinite raw materials in the Santonian sediments of the North-Sudetic Trough (Lower Silesia, Poland). Applied Clay Science 12, 313 – 328.

Genik, G.J., 1993. Petroleum Geology of the Cretaceous-Tertiary Rift Basins in Niger, Chad and Central African Republic. American Association of Petroleum Geologists Bulletin 77, 1405 – 1434.

Getaneh, W., 2002. Geochemistry provenance and depositional tectonic setting of the Adigrat Sandstone of northern Ethiopia. Journal of African Earth Sciences 35, 185 – 198.

Ghibaudo, G., 1992. Subaqueous sediment gravity flow deposits: practical criteria for their description and classification. Sedimentology 39, 423 – 454.

Ghosh, P., Sarkar, S., Maulik, P., 2006. Sedimentology of a muddy alluvial deposit: Triassic Denwa Formation, India. Sedimentary Geology 191, 3 – 36.

Giedt, N.R., 1990. Unity Field - Sudan, Muglad Rift Basin, Upper Nile Province. Structural traps III. American Association of Petroleum Geologists Treatise of Petroleum Geology. Atlas of oil and gas fields. pp. 177 – 197.

Griffith, L. A., Nelson, M. R., 1988. The effect of acid (HCl) on the permeability of selected Cardium Formation

sandstones and conglomerates: Paper no. 88-39-50 presented at the 39th annual technical meeting of the Petroleum Society of CIM, June, pp. 50, 1 – 50, 13.

Guiraud, R., Bosworth, W., Thierry, J., Delplanque, A., 2005. Phanerozoic geologic evolution of Northern and Central Africa: an overview. Journal of African Earth Sciences 43, 83 – 143.

Handford, C.R., 1987. Turkana Grits: a Cretaceous braided alluvial system in northern Kenya. American Association of Petroleum Geologists Bulletin 71, 564.

Harms, J.C., Southard, J.B., Spearing, D.R., Walker, R.G., 1995. Depositional environment interpreted from primary sedimentary and stratification sequences. Society of Economic Paleontologists and Mineralogists Short Course 2, 161p.

Hassouta, L., Buatier, M.D., Potdevin, J.L., Liewig, N., 1999. Clay diagenesis in the sandstone reservoir of the Ellon field (Alwyn, North Sea). Clays and Clay Minerals 47, 269 – 285.

Hautot, S., Tarits, P., Whaler, K., Le Gall, B., Tiercelin, J.-J., Le Turdu, C., 2000. Deep structure of the Baringo Rift Basin (Central Kenya) from three-dimensional magnetotelluric imaging: Implications for rift evolution. Journal of Geophysical Research 105 (B10), 23, 493 – 23, 518.

Hayes, J.B., 1979., Sandstone diagenesis – The hole truth. In: Scholle, P.A., Schluger, P.R. (Eds). Aspects of diagenesis. Society of Economic Paleontologists and Mineralogists Special Publication 26, 127 – 139.

Heald, M.T., Larese, R.E., 1973. The significance of the dissolution of feldspars in porosity development. Journal of Sedimentary Petrology, 43, 458 – 460.

de Heinzelin, J. Haesaertes, P. 1983. The Shungura Formation. In: de Heinzelin, J. (Ed.), The Omo Group: Archives of the Internal Omo Research expedition. Musee Royal de L'Afrique centrale. Tervulen, pp. 25 – 127.

Hendrie D.B., Kusznir N.J., Morley C.K., Ebinger C.J., 1994. Cenozoic extension in northern Kenya: a quantitative model of rift basin development in the Turkana region. In: Prodehl C., Keller G. R., Khan M. A. (Eds.), Crustal and Upper Mantle Structure of the Kenya Rift. Tectonophysics 236, 409 – 438.

Hill, A., Curtis, G., Drake, R., 1986. Sedimentary stratigraphy of the Tugen Hills, Baringo District, Kenya. In : L. E. Frostick, R. W. Renaut, I. Reid, and J.-J. Tiercelin, (Eds.), Sedimentation in the African Rifts. Geological Society of London Special Publication 25, 285 – 295.

Hill, A., 1999. The Baringo Basin, Kenya: from Bill Bishop to BPRP. In: Andrews, P., Banham, P., (Eds.), Late Cenozoic Environments and Hominid Evolution: a tribute to Bill Bishop. Geological Society, London, pp. 85 – 97.

Hjellbakk, A., 1997. Facies and fluvial architecture of a high-energy braided river: the Upper Proterozoic Seglodden Member, Varanger Peninsula, northern Norway. Sedimentary Geology 114, 131 – 161.

Horton, B.K., Schmitt, J.G., 1996. Sedimentology of a lacustrine fan-delta system, Miocene Horse Camp Formation, Nevada, USA. Sedimentology, 43, 133 – 155.

Jorgensen, G.J., Bosworth, W., 1989. Gravity modelling in the central African rift system, Sudan: rift geometries and tectonic significance. Journal of African Earth Sciences 8, 231 – 249.

Jones, G.P., 1965. Red beds in Eastern Nigeria. Sedimentology 5, 235 – 247.

Joubert, P., 1966. Geology of the Loperot area. Geological Survey of Kenya Report 74, 52 pp.

References

Kasande, R. 2007. Developments in oil and gas exploration in the Albertine Graben of Uganda. Proceedings of the 3rd East Africa Petroleum Conference. Arusha, Tanzania.

Kenya National Bureau of Statistics. 2007. Kenya facts and figures. Government Printer, Nairobi. 90p.

Khalifa, M.A., Catuneanu, O., 2008. Sedimentology of the fluvial and fluvio-marine facies of the Bahariya Formation (Early Cenomanian), Bahariya Oasis, Western Desert, Egypt. Journal of African Earth Sciences 51, 89 – 103.

Klitzsch, E.H., Squiyres, C.H., 1990. Paleozoic and Mesozoic geological history of northeastern Africa based upon new interpretation of Nubian strata. American Association of Petroleum Geologists Bulletin 74, 1203 – 1211.

Kretz, R., 1983. Symbols for rock-forming minerals. American mineralogist 68, 277 – 279.

Lambiase, J. J., Morley, C. K., 1999. Hydrocarbons in rift basins: the role of stratigraphy. Philosophical Transactions of the Royal Society of London 357, 877 – 900.

Levandowski, D.W., Kaley, M.E., Silverman, S.R., Smalley, R.G., 1973. Cementation in Lyons Sandstone and its role in oil accumulation, Denver Basin, Colorado. American Association of Petroleum Geologists Bulletin 57, 2217 – 2244.

Lippard, S. J., 1973. The petrology of phonolites from the Kenya Rift. Lithos 6, 217 – 234.

Lirong, D., Dingsheng, C., Jianjung, W., Rubondo, E. N. T., Kasande, R., Byakagaba, A., Mugisha, F., 2004. Geochemical significance of seepage oils and bituminous sandstones in the Albertine Graben, Uganda. Journal of Petroleum Geology 27, 299 – 312.

Markwick, P.J., 1998. Fossil crocodilians as indicators of Late Cretaceous and Cenozoic climates: implications for using palaeontological data in reconstructing palaeoclimate. Palaeogeography, Palaeoclimatology, Palaeoecoclogy 137, 205 – 271.

Mateer, N. J., Wycisk, P., Jacobs, L. L., Brunet, M., Luger, P., Arush, M.A., Hendriks, F., Weissbrod, T., Gvirtzman, G., Mbede, E., Dina, A., Moody, R. T. J., Weigelt, G., El-Nakhal, H. A., 1992. Correlation of nonmarine Cretaceous strata of Africa and the Middle East. Cretaceous Research 13, 273 – 318.

McBride, E.F., Abdel-Wahab, A., Salem, A.M.K., 1996. The influence of diagenesis on the reservoir quality of Cambrian and Carboniferous sandstones, southwest Sinai, Egypt. Journal of African Earth sciences 22, 285 – 300.

McGuire, M., Serra, S. Day, R., 1985. Surface geological evaluation Block 10 concession, NW Kenya. Unpublished report for Amoco Production Company.

Mead, J.G., 1975. A fossil beaked whale (Cretacea: Ziphiidae) from the Miocene of Kenya. Journal of paleontology 49, 745 – 751.

Miall, A.D., 1977. A review of the braided river depositional environment. Earth science reviews 13, 1 – 62.

Miall, A.D., 1978. Lithofacies types and vertical profile models in braided river deposits: a summary. In: Miall, A.D. (Ed.), Fluvial Sedimentology. Canadian Society of Petroleum Geologist, Memoir 5, 597 – 604.

Miall, A.D., 1996. The Geology of Fluvial Deposits. Springer-Verlag. Berlin, 582 pp.

Middlemost, E.A.K., 1989. Iron oxidation ratios, norms and the classification of volcanic rocks. Chemical Geology 77, 19 – 26.

Mohammed, A.Y., Pearson, M.J., Ashcroft, W.A., Iliffe, J.E., Whiteman, A.J., 1999. Modeling petroleum genera-

tion in southern Muglad Rift Basin, Sudan. American Association of Petroleum Geologists Bulletin 83, 1943 – 1964.

Mohamed, A.Y., Pearson, M.J., Ashcroft, W.A., Iliffe, J.E., Whiteman, A.J., 2002. Petroleum maturation modelling, Abu Gabra-Sharaf area, Muglad Basin, Sudan. Journal of African Earth Sciences 35, 331 – 344.

Morad, S., 1998. Carbonate cementation in sandstones: distribution patterns and geochemical evolution. International Association of Sedimentologists Special Publication 26, 1 – 26.

Morley, C.K., 1999. Comparison of hydrocarbon prospectivity in rift systems. In: C.K. Morley (Ed.), Geoscience of rift systems-evolution of East Africa. American Association of Petroleum Geologists Studies in Geology 44, 233 – 242.

Morley, C.K., Wescott, W.A., Harper, R.M. Cunningham, S.M., 1999. Geology and geophysics of the Rukwa Rift. In: Morley, C.K. (Ed.), Geoscience of Rift systems- Evolution of East Africa. American Association of Petroleum Geologists Studies in Geology 44, 91 – 110.

Morley, C.K., Day, R.A., Lauck, R., Bosher, R., Stone, D.M., Wigger, S.T., Wescott, W.A., Haun, D., Bassett, N., Bosworth, W., 1999. Geology and Geophysics of the Anza Basin. In: Morley, C.K. (Ed.), Geoscience of rift systems-evolution of East Africa. American Association of Petroleum Geologists Studies in Geology 44, 19 – 54.

Morley, C.K., Ngenoh, D.K., Ego, J.K., 1999. An introduction to the East African Rift System. In: Morley, C.K. (Ed.), Geoscience of rift systems-evolution of East Africa, American Association of Petroleum Geologists Studies in Geology 44, 1 – 18.

Morley, C.K., Wescott, W.A., Stone, D.M., Harper, R.M., Wigger, S.T., Day, R.A. Karanja, F.M., 1999. Geology and Geophysics of the Western Turkana Basins, Kenya. In: Morley, C.K. (Ed.), Geoscience of rift systems-evolution of East Africa, American Association of Petroleum Geologists Studies in Geology 44, 19 – 54.

Morley, C.K., Wescott, W.A., Stone, D.M., Harper, R.M., Wigger, S.T., Karanja, F.M., 1992. Tectonic evolution of the northern Kenya Rift. Journal of the Geological Society, London 149, 333 – 348.

Mugisha, F., Ebinger, C. J., Strecker, M., Pope, D., 1997. Two-stage rifting in the Kenya rift: implications for half-graben models. Tectonophysics 278, 63 – 81.

Murray-Hughes, R., 1933. Notes on the geological succession, tectonics and economic geology of the western half of the Kenya colony. Report Geological Survey of Kenya 3, 8p.

Nemec, W., Steel, R.J., 1984. Alluvial and coastal conglomerates: their significant features and some comments on gravelly mass-flow deposits. In: Koster, E.H., Steel, R.J. (Eds.), Sedimentology of Gravels and Conglomerates. Canadian Society of Petroleum Geologists Memoir 10, 1 – 31.

Neves, M.A., Morales, N., Saad, A.R., 2005. Facies analysis of tertiary alluvial fan deposits in the Jundiaí region, São Paulo, southeastern Brazil Journal of South American Earth Sciences 19, 513 – 524.

Ngenoh, D. K. A., 1993. Hydrocarbon potential of South Kerio Trough basin (Kenya) from seismic reflection data. M.Sc. thesis (unpublished), University of Western Ontario, London, Canada, 126p.

Nilsen, T.H, 1982. Alluvial fan deposits. In: Sholle, P.A., Spearing, D. (Eds), Sandstone depositional environments. American Association of Petroleum Geologists Memoir 31, 49 – 86.

NOCK, 2009. Oil exploration opportunities in Kenya. Promotional brochures. National Oil Corporation of Kenya.

References

North, F.K., 1985. Petroleum geology. Allen and Unwin, Boston. 607p.

Obaje, N.G., Wehner, H., Hamza, H., Scheeder, G., 2004. New geochemical data from the Nigerian sector of the Chad basin: implications on the hydrocarbon prospectivity. Journal of African Earth Sciences 38, 477 – 487.

Parry, W.T., Chan, M.A., Nash, B.P., 2009. Diagenetic characteristics of the Jurassic Navajo Sandstone in the covenant oil field, Central Utah thrust belt. American Association of Petroleum Geologists Bulletin 93, 1039 – 1061.

PEPD., 2005. The hydrocarbon potential of the Albertine Graben, Uganda. Petroleum Exploration and Production Department, Ministry of Energy and Mineral Development, Republic of Uganda, unpublished internal reports.

PEPD., 2007. Well location map. Petroleum Exploration and Production Department, Ministry of Energy and Mineral Development, Republic of Uganda, unpublished internal reports.

PEPD., 2009. Petroleum potential of the Albertine graben, Uganda. Petroleum Exploration and Production Department, Ministry of Energy and Mineral development, Republic of Uganda. Unpublished internal reports.

Peterson, J.A. 1986. Geology and petroleum resources of central and east-central Africa. Modern Geology 10, 329 – 364.

Pettijohn, F.J., Potter, P.E., Siever, R., 1973. Sand and sandstone. Springer – Verlag, New York, 618 p.

Pickford, M. H., 1978. Geology, palaeoenvironment and vertebrate faunas of the mid-Miocene Ngorora Formation, Kenya. In: W. W. Bishop, (Ed.), Geological background to fossil man. Scottish Academic Press, Edinburgh, pp. 263 – 278.

Pope, D. A., 1992. Analyses and interpretation of seismic reflection profiles from the Kerio Valley, Kenya Rift. M.Sc. thesis (unpublished), University of Leeds, England, 133p.

Pierce, J., Lipkov, L., 1988. Structural interpretation of the Rukwa Rift, Tanzania. Geophysics 53, 824 – 836.

Pittman, E.D., 1979. Porosity, diagenesis and productive capability of sandstone reservoirs. In: Scholle, P.A., Schluger, P.R. (Eds). Aspects of diagenesis. Society of Economic Paleontologists and Mineralogists Special publication 26, 159 – 173.

Postma, G., 1990. Depositional architecture and facies of river and fan deltas: a synthesis. In: Colella, A., Prior, D. B., (Eds.), Coarse-grained Deltas. of International Association Sedimentologists Special Publication 10, 13 – 28.

Potdevin, J.L., Hassouta, L., 1997. Bilan de matière des processus d'illitization et de surcroissance de quartz dans un réservoir pétrolier du champ d'Ellon (zone d'Alwyn, Mer du Nord). Bulletin de la Société Géologique de France 168, 219 – 229.

Prasad, G. 1971. Nubian sandstone paleoenvironment Sudan: discussion. Bulletin American Association of Petroleum Geologists 55, pp. 883.

Renaut, R. W., Tiercelin, J.-J., 1994. Lake Bogoria, Kenya Rift Valley: a sedimentological overview. In: R.W. Renaut, and W.M. Last, (Eds.), Sedimentology and geochemistry of modern and ancient saline lakes. Special Publication of the Society of Sedimentary Geology (SEPM) 50, 101 – 123.

Renaut, R.W., Ego, J.K. Tiercelin, J-J., Le Turdu, C., Owen, R.B., 1999. Saline, alkaline palaeolakes of the Tugen

Hills-Kerio Valley region, Kenya Rift Valley. In: Andrews, P., Banham, P., (Eds.), Late Cenozoic Environments and Hominid Evolution: A Tribute to Bill Bishop. Geological Society, London pp. 41 – 58.

Rohais, S., Eschard, R., Guillocheau, F., 2008. Depositional model and stratigraphic architecture of rift climax Gilbert-type fan deltas (Gulf of Corinth, Greece). Sedimentary Geology 210, 132 – 145.

Rosendahl, B. R., 1987. Architecture of continental rifts with special reference to East Africa. Annual Reviews. Earth Planetary Sciences 15, 445 – 503.

Rosendahl, B. R., Reynolds, D. J., Lorber, P. M., Burgess, C. F., McGill, J., Scott, D., Lambiase, J.-J., Derksen, S. J., 1986. Structural expressions of rifting: lessons from Lake Tanganyika, Africa. In : L. E. Frostick, R. W. Renaut, I. Reid, and J.-J. Tiercelin, (Eds.), Sedimentation in the African Rifts. Geological Society London, Special Publication 25, 29 – 43.

Rosendahl, B. R., Versfelt, J. W., Scholz, C. A., Buck, J. E., Woods, L. D., 1988. Seismic atlas of Lake Tanganyika, East Africa. Project PROBE Geophysical Atlas Series, folio 1, Durham, North Carolina, Duke University.

Rosendahl, B. R., Kilembe, E. Kaczmarick, K., 1992. Comparison of the Tanganyika, Malawi, Rukwa and Turkana Rift zones from analyses of seismic reflection data. In: P. A. Ziegler, (Ed.). Geodynamics of Rifting, Volume II. Case History Studies on Rifts: North and South America and Africa. Tectonophysics 213, 235 – 256.

Rubondo, E.N.T., 2003. An overview of the petroleum provinces and prospective basins of East Africa. Proceedings of the 1st East Africa Petroleum Conference. Nairobi, Kenya.

Rubondo, E.N.T. 2005. The potential and developments in Uganda's upstream petroleum sector. Proceedings of the 2nd East Africa Petroleum Conference, 2 – 4 March 2005, Entebbe, Uganda.

Salama, R.B. 1997. Rift basins in the Sudan. In: Selley, R.C., (Ed.), African Basins. Sedimentary basins of the world. Vol. 3. Elsevier Amsterdam. pp. 105 – 149.

Salem A.M.K., Abdel-Wahab. A, McBride, E. F., 1998 Diagenesis of shallowly buried cratonic sandstones, south-west Sinai, Egypt. Sedimentary Geology 119, 311 – 335.

Savage, R.J.G., Williamson, P.G., 1978. The early history of the Turkana Depression. In: W.W. Bishop (Ed.), Geological background to fossil man. Scottish Academic Press, Edinburgh, pp. 375 – 394.

Schmid, S., Worden, R.H., Fisher, Q.J. 2006. Sedimentary facies and the context of dolocrete in the Lower Triassic Sherwood Sandstone group: Corrib Field west of Ireland. Sedimentary Geology 187, 205 – 227.

Schmidt, V., McDonald, D.A., 1979. The role of secondary porosity in the course of sandstone diagenesis. In: Scholle, P.A., Schluger, P.R. (Eds). Aspects of diagenesis. Society of Economic Paleontologists and Mineralogists Special publication 26, 175 – 208.

Schull, T.J., 1988. Rift basins of interior Sudan: Petroleum exploration and discovery. American Association of Petroleum Geologists Bulletin 72, 1128 – 1142.

Selley, R.C. 1978. Porosity gradients in the North Sea oil-bearing sandstones. Journal of the geological society, London 135, 119 – 132.

Sellwood, B.W., Price, G.D., 1993. Sedimentary facies as indicators of Mesozoic paleoclimates. Philosophical transactions of the Royal Society of London B341, 225 – 233.

Sellwood, B.W., Price, G.D., 1994. Sedimentary facies as indicators of Mesozoic palaeoclimate. In: Allen, J.R.L.,

Hoskins, B.J., Sellwood, B.W., Spicer, R.A., Valdes, P.J.,(Eds.), Palaeoclimates and Their Modelling: With Special Reference to the Mesozoic Era. Chapman and Hall, London, pp. 17 – 26.

Sellwood, B.W., Valdes, P.J., 2006. Mesozoic climates: General circulation model and the rock record. Sedimentary geology 190, 269 – 287.

Shackleton, R.M., 1946. Geology of the country between Nanyuki and Maralal. Geological Survey of Kenya Report 11, 54p.

Simoneit, B. R. T., Aboul-Kassim, T. A. T., Tiercelin, J.-J., 2000. Hydrothermal Petroleum from Lacustrine Sedimentary Organic Matter in the East African Rift. Applied Geochemistry 15, 355 – 368.

Shell Exploration and Production Kenya BV. 1993. Well resume Loperot-1. Block 10B, Lodwar South sub-basin, Kenya. Unpublished reports.

Steiger, R.H., Jäger, E., 1977. Subcommission on geochronology: convention on the use of decay constants in geo- and cosmochronology. Earth and Planetary Science Letters 36, 359 – 362.

Talbot, M. R., 1988. The origins of lacustrine oil source rocks: evidence from the lakes of tropical Africa, In: Fleet, A. J., Kelts, K., Talbot, M.R., (Eds.), Lacustrine Petroleum Source Rocks, Geological Society of London Special Publication 40, 29 – 43.

Talbot, M.R., Morley, C.K., Tiercelin, J.J., Le Hérissé, A., Potdevin, J.L., Le Gall, B., 2004. Hydrocarbon potential of the Meso-Cenozoic Turkana Depression, northern Kenya. I Source rocks: quality, maturation, depositional environments and structural control. Marine and Petroleum Geology 21, 63 – 78.

Thuo, P., Potdevin, J.L., Tiercelin, J.-J., Schuster, M., Bourquin, S., Clément, J.P., Bellon, H., Guillou, H., Ruffet, G. The Lapur Sandstone Formation of northern Kenya: Chronological setting, sediment characteristics and diagenetic evolution. Importance in terms of oil exploration of the Meso-Cenozoic Turkana Depression. Journal of African Earth Sciences (in press).

Tiercelin, J.-J., Vincens, A. (Eds.), 1987. Le demi-graben de Baringo – Bogoria, Rift Gregory, Kenya. 30.000 ans d'histoire hydrologique et sédimentaire. Bulletin des Centres de Recherches Exploration - Production Elf-Aquitaine 11, 249 – 540.

Tiercelin J.-J., Pflumio, C., Castrec, M., Boulègue, J., Gente, P., Rolet, J., Coussement, C., Stetter, K. O., Huber, R., Buku, S. Mifundu, W., 1993. Hydrothermal vents in Lake Tanganyika, East African Rift system. Geology 21, 499 – 502.

Tiercelin, J.J., Lezzar, K.E., 2002. A 300 millions years history of rift lakes in Central and East Africa: an updated broad review. In: E. Odada, and D. Olago (Eds.), The East African Great Lakes: Limnology, Palaeolimnology and Biodiversity. Advances in Global Change Research. Kluwer Publishers, Amsterdam pp. 3 – 60.

Tiercelin, J.J., Potdevin, J.L., Morley, C.K., Talbot, M.R., Bellon, H., Rio, A., Le Gall, B., Vétel, W., 2004. Hydrocarbon potential of the Meso-Cenozoic Turkana Depression, northern Kenya. I. Reservoirs: depositional environments, diagenetic characteristics, and source rock- reservoir relationships. Marine and Petroleum Geology 21, 41 – 62.

TPDC, 2009. Tanzania Petroleum Development Corporation promotional Brochure. Unpublished Internal reports, 50p.

Tucker, M.E., 2001. Sedimentary petrology: an introduction to the origin of sedimentary rocks. Wiley-Blackwell, 262p.

References

Vail, J.R., 1974. Distribution of Nubian Sandstone Formation in Sudan and vicinity. American Association of Petroleum Geologists Bulletin 58, 1025 – 1036.

Vail, J.R., 1982. Distribution and tectonic setting of post-kinematic igneous complexes in the Red Sea Hills of Sudan and the Arabian-Nubian Shield. Pre-Cambrian Research 16, Abstracts A41.

Vincens, A., Tiercelin, J.-J., Buchet, G., 2006. New Oligocene-early Miocene microflora from the southwestern Turkana Basin. Palaeoenvironmental implications in the northern Kenya Rift. Palaeogeography, Palaeoclimatology, Palaeoecology 239, 470 – 486.

Visser, C., 1993, Petrographic analysis of thirteen percussion sidewall samples from well Loperot-1, Kenya. Unpublished report prepared by Core Laboratories for Shell Internationale Petroleum Maatschappij, B.V.

Walsh, J., Dodson, R.G., 1969. Geology of northern Turkana. Report Geological Survey of Kenya, 82p.

Wardlaw, N.C., 1976. Pore geometry of carbonate rocks as revealed by pore casts and capillary pressure. American Association of Petroleum Geologists Bulletin 60, 245 – 257.

Wayland, E.J. 1925. Oil in Uganda. Geological survey of Uganda memoir, 1, (unpublished) 66p.

Weissert, H., Lini, A., Folmi, K.B., Kuhn, O. 1998. Correlation of Early Cretaceous carbon isotope stratigraphy and platform drowning events: a possible link? Palaeogeography, Palaeoclimatology, Palaeoecology 137, 189 – 203.

Wescott, W.A., Morley, C.K., Karanja, F.M., 1993. Geology of the Turkana Grits in the Lariu Range and Mt Porr areas, southern Lake Turkana, Northwestern Kenya. Journal of African Earth Sciences 16, 425 – 435.

Wescott, W.A., Wigger, S.T., Stone, D.M., Morley, C.K. 1999. Geology and Geophysics of the Lotikipi Plain. In: Morley, C.K. (Ed.), Geoscience of Rift Systems-Evolution of East Africa, American Association of Petroleum Geologists Studies in Geology 44, pp. 55 – 65.

Whiteman, A. J., 1970. Nubian Group: origin and status. American Association of Petroleum Geologists Bulletin 54, 526 – 529.

Whiteman, A.J., 1971. The geology of the Sudan republic. Oxford: Oxford Clarendon Press, 290p.

Williamson, P. G., Savage, R. J. G., 1986. Early sedimentation in the Turkana Basin, northern Kenya. In: L. E. Frostick, R. W. Renaut, I. Reid, J.-J. Tiercelin (Eds.), Sedimentation in the African Rifts. Geological Society London, Special Publication 25, 267 – 283.

Winn, R.D., Steinmetz, J.C., Kerekgyarto, W.L., 1993. Stratigraphy and rifting history of the Anza Rift. American Association of Petroleum Geologists Bulletin 77, 1989 – 2005.

Wolela, A., 2008. Sedimentation of the Triassic-Jurassic Adigrat Sandstone Formation, Blue Nile (Abay) Basin, Ethiopia. Journal of African Earth Sciences 52, 30 – 42.

Worden, R.H., Morad, S., 2000. Quartz cementation in oilfield sandstones: A review of the key controversies. International Association of Sedimentologists Special Publication 29, 1 – 20.

Wycisk, P., Klitzsch, E., Jos, C., Reynolds, O., 1990. Intracratonal sequence development and structural control of Phanerozoic strata in Sudan. Berliner Geowissenschaftliche Abhandlungen, Reihe A120, 45 – 86.

Zanettin, B., Justin Visentin, E., Bellieni, G., Piccirillo, E.M., Rita, F., 1983. Le volcanisme du Bassin du Nord-Turkana (Kenya) : Age, succession et évolution structurale. In: Popoff, M., Tiercelin, J.J., (Eds.), Rifts et Fossés anciens. Bulletin des Centres de Recherches Exploration - Production Elf - Aquitaine 7, 249 – 255.